ECOPHYSIOLOGY AND DIVERSITY OF *ANAEROMYXOBACTER* SPP. AND IMPLICATIONS FOR URANIUM BIOREMEDIATION

A Thesis
Presented to
The Academic Faculty

By

Sara Henry Thomas

In Partial Fulfillment
Of the Requirements for the Degree
Doctor of Philosophy in Environmental Engineering
School of Civil and Environmental Engineering

Georgia Institute of Technology

May, 2009

ECOPHYSIOLOGY AND DIVERSITY OF *ANAEROMYXOBACTER* SPP. AND IMPLICATIONS FOR URANIUM BIOREMEDIATION

Approved by:

Dr. Frank E. Löffler, Advisor
School of Civil and Environmental Engineering
Georgia Institute of Technology

Dr. Joseph B. Hughes
School of Civil and Environmental Engineering
Georgia Institute of Technology

Dr. Kurt D. Pennell
School of Civil and Environmental Engineering
Georgia Institute of Technology

Dr. Lawrence J. Shimkets
Microbiology Department
University of Georgia

Dr. Robert A. Sanford
Department of Geology
University of Illinois

Dr. Thomas DiChristina
School of Biology
Georgia Institute of Technology

Date Approved: March 23, 2009

In Memory of

Dr. Jane Bingham Henry

ACKNOWLEDGEMENTS

As I finish with what has been an incredible journey in so many ways, I would like to acknowledge the people who have come into my life, as well as those who have gone, and those who have always been with me. So many things have changed since I began. I start by thanking Kevin, my good and sweet husband. We were married during the second year of my PhD and I have been so fortunate and blessed to have him in my life. He is my partner and my greatest friend and advocate. I have always been so grateful for my wonderful family, now with Lily and Fox Angeline, the first children I've ever watched come into existence, coming into the world during my time here at Georgia Tech. I am grateful to their mother, Beth Henry Angeline, my constant friend and ally for life, my sister, who always carries half of my heart, and their father, Curtis Angeline, the first brother I've ever had. We have all changed so much, especially since we lost my mother. Dr. Jane Bingham Henry was the wisest person I have ever known, with the peace that passes understanding down in the depths of her soul. I miss her every day, more than I can say, but I see her in myself and I'm grateful for that. Finally, the rock and anchor for all of us, Andrew Henry, my dad. From teaching me how to laugh to teaching my how to think, to teaching me how to love, and be loved by, God and my family, my dad is my hero. I would also like to thank my new family, the Thomases and Reynoldses. Ellen and Russ have taught me how to live with abandon, how to love every minute of it, and how to take full advantage of everything life has to offer.

I'd like to thank Dr. Frank E. Löffler, my advisor. Frank's ideas and energy are endless. His willingness to try new things, and to trust me to try new things, has provided me with many incredible opportunities. I appreciate the trust he has granted me to go off

on my own, even when it wasn't, maybe, the best idea. On the other side of the coin, I was also given the opportunity to benefit from Frank's many collaborations and his extensive scientific network. I read that one should be careful about choosing one's advisor because you will find yourself doing science, and running your laboratory, just like him/her. I am pleased to have Frank's influence in my life. I look forward to being such an enthusiastic, innovative, and versatile scientist, with so many wonderful collaborators. I would also like to specially thank Drs. Rob Sanford and Joanne Chee Sanford for so much encouragement. Rob trusted me to work with his organism and allowed me to be a member of the World *Anaeromyxobacter* Union, for which I will be eternally grateful. If I could get an *Anaeromyxobacter* tattoo that made sense, I would. Finally, I would like to thank Dr. John Kirby, who was my co-advisor for the first three years of my degree before his move to Iowa. No one in the world is as enthusiastic and optimistic as John. We had a great time working together and I hope to have more time to work with him in the future.

To my committee: I have known Dr. Kurt Pennell longer than I've known my husband. Without his help and guidance, there is no doubt that I never would have ended up in graduate school. Kurt gives so much of his time and energy to his students, and I appreciate his influence very much. Dr. Larry Shimkets was one of the first myxobacteria scientists to embrace *Anaeromyxobacter*. It was his enthusiasm and thoughtful input at "myxobacteria meetings" that caused me to ask him to work with me on the genome manuscript and to be part of my committee. I am grateful that he consented to both. Dr. Joe Hughes is my own personal science idol. When I first saw his presentation on the global needs that can be met by Civil and Environmental Engineers, I

knew that I wanted his influence in my work, and that I wanted his council. I feel fortunate and, frankly, a little giddy and star-struck, every time I have an opportunity to meet with Dr. Hughes and I thank him for taking time to be on my committee. Last, but certainly never least, Dr. Tom DiChristina is a much-needed voice from the *Shewanella* and metal-reduction community. His input is invaluable and I am fortunate to have him nearby. He probably doesn't remember me but he also knew me when I was about 18 and I took his Biology for Engineers class. I think I've come a long way since then.

There isn't room here for me to adequately thank each member of the Löffler lab as they deserve. You know who you are. We make a terrific team. You are my friends, my confidants, and, so often, my inspiration. Dr. Benjamin Amos, your sympathetic ear and your wise council have been invaluable. Dr. Kirsti Ritalahti, I can't thank you enough for your energy and your patience. It's hard to believe that, when you taught me my first PCR (my Civil Engineering degree offered very little in this regard), you took a deep breath and said, "You're going to need to know the difference between transcription and translation." Dr. Claribel Cruz-Garcia, as I've said before, you brought sunshine with you when you came to our lab. We needed you so much. I hope that we gave you something back. There are so many others. I hope I have said, "Thank you" to each one of you: Dr. Janet Hatt, Kelly Fletcher (see below), Audrey Thorp, Shandra Justicia Leon, Elizabeth Padilla Crespo (I teach and learn at the same time), Kerry Holland, Dr. Youlboong Sung, Ryoung Sung, Ryan Wagner, Ivy Thomson, Courtney Phillips, Alan Nevins, et al. Thank you. Also, the other members of the EnvE department who came before me: Drs. Dave Himmelheber, Rebecca Deprato, Jackie Tront, Eric Suchomel, Gayle Hagler. Thank you, thank you, thank you.

Next, I would like to thank my mentors Dr. Mark Hay and Dr. Julia Kubanek, the IGERT fellowship, and the other IGERT instructors. You introduced me to Ecology, the love of my life. I was absolutely thrilled day after day in the IGERT program and, not only my scientific training, but my life-long friends have come from IGERT. This is where I try to express my gratitude to each of you, my greatest friends: Dr. Emily Prince and Dr. Amisha Shah, you know, I hope, how much you have meant to me. Your incredible minds and your kind hearts, I know this sort of thing makes Emily uncomfortable so I'll just say "thank you." Dr. Kimberly Catton (and Dr. Thomas Bradley), Kelly Fletcher, Wendy Morrison, Liliana Lettieri, thank you for allowing me to be part of your IGERT group. I love you all so much. Dr. Sara Edge, what would I do without having known you? You are strength incarnate. And to the rest of my IGERT group: Jason Landrum, Gary Dobbs, Zach Hallinan, Ryan Cantor, Doug Rudolf, Terry Watt, Ejae John, it was a good ride. I have been forever influenced by all of you. I am looking forward to seeing what everyone does next. I know it will be great.

TABLE OF CONTENTS

LIST OF TABLES

LIST OF FIGURES

LIST OF SYMBOLS AND ABBREVIATIONS

ABI	Applied Biosystems
ANOVA	Analysis of variance
ARDRA	16S rDNA restriction analysis
ATCC	American Type Culture Collection
BLAST	Basic local alignment tool
bgs	Below ground surface
bp	Base pair
CAI	Codon adaptation index
CDS	Coding sequence
DIRB	Dissimilatory iron-reducing bacteria
DMRB	Dissimilatory metal-reducing bacteria
DNA	Deoxyribonucleic acid
dNTP	Deoxyribonucleotide triphosphate
DOE	U.S. Department of Energy
e^-	Electron
EPS	Extracellular polysaccharides
E value	Expectation value
FBR	Fluidized bed reactor
f_e	Fraction of electrons used for e^- acceptor reduction
Fe-S	Iron-sulfur
FRC	Field research center
f_s	Fraction of electrons used for biomass production
G+C	Guanine + cytosine
GC	Gas chromatograph
HEPES	4-(2-hydroxyethyl)-1-piperazineethanesulfonic acid

HGT	Horizontal gene transfer
HPLC	High-performance liquid chromatography
IFC	Integrated field-scale subsurface research challenge
ITS-RFLP	Intergenic spacer-restriction fragment length polymorphism
JGI	Joint Genome Institute
MCAI	Minimum codon adaptation index
MES	2-(N-morpholino)ethanesulfonic acid
MLEE	Multilocus enzyme electrophoresis
mqPCR	Multiplex qPCR
mRNA	Messenger RNA
NADH	Nicotinamide adenine dinucleotide
ND	Not determined
NFQ	Non-fluorescent quencher
nosZ	Nitrous oxide reductase gene
NTA	Nitrilotriacetic acid
PCE	Perchloroethene
PCR	Polymerase chain reaction
PNNL	Pacific Northwest National Laboratory
pO_2	Partial pressure of oxygen
qPCR	Real-time quantitative PCR
rdhA	Reductive dehalogenase gene
Redox	Oxidation-reduction
REP-PCR	Repetitive extragenic palindromic PCR
R_n	Reported fluorescent signal
RNA	Ribonucleic acid
ROS	Reactive oxygen species
rRNA	Ribosomal ribonucleic acid

spp.	Species (plural)
SRB	Sulfate-reducing bacteria
t	Time
TCD	Thermal conductivity detector
TIGR	The Institute for Genome Research
T_m	Melting temperature
tRNA	Transfer RNA
TSB	Tryptic soy broth
vol/vol	Volume per volume
wt/vol	Weight per volume
XANES	X-ray absorption near edge structure
XPS	X-ray photoelectron spectroscopy

SUMMARY

Uranium has been released into the environment due to improper practices associated with mining and refinement for energy and weapons production. Soluble U(VI) species such as uranyl carbonate can be reduced to form the insoluble U(IV) mineral uraninite (UO_2) via microbial respiratory processes. Formation of UO_2 diminishes uranium mobility and prevents uranium-laden groundwater from being discharged into surface water; however, oxygen and other oxidants re-solubilize UO_2. Many organisms have been shown to reduce uranium, but variations in microbial physiology (e.g., growth rate, oxygen sensitivity, the range of substrates that are utilized, and electron donor availability) change the dynamics of microbial uranium reduction *in situ* and affect uraninite stability. Determining the physiology and prevalence of relevant uranium-reducing organisms is critical to adequately monitor and optimize the microbial uranium reduction process for bioremediation applications.

Anaeromyxobacter dehalogenans is a metal-reducing delta-Proteobacterium in the myxobacteria family that displays remarkable respiratory versatility and efficiently reduces U(VI). The approach of this research was to enhance characterization of *A. dehalogenans* by identifying unique genetic traits, describing variability within the species, and examining the environmental distribution of *A. dehalogenans* strains. Genome analysis revealed that *A. dehalogenans* shares many traits with the myxobacteria including type IV pilus-based motility and an aerobic-like electron transport chain, including NADH dehydrogenase and cytochrome oxidase subunits with sequence similarity to the aerobic myxobacteria. In addition, the genome revealed genes that share sequence similarity with strict anaerobes and other metal-reducing organisms, consistent

with observed respiratory versatility in *A. dehalogenans*. Physiological examination of microaerophilism in *A. dehalogenans* strain 2CP-C reveal growth at sub-atmospheric oxygen partial pressure. Experimental evidence is also presented that verifies surface motility in *A. dehalogenans* strain 2CP-C. Isolation efforts yielded several *A. dehalogenans* strains native to uranium-contaminated environments. Physiological characterization of the novel isolates demonstrated that strain-level variation in the 16S rRNA gene coincides with metabolic changes that can be linked to the loss of specific gene homologs. *Anaeromyxobacter* spp. were present at the Oak Ridge Integrated Field-scale Subsurface Research Challenge (IFC) site and multiplex qPCR tools designed using a minor-groove binding probe gave insights into strain and species differences in the community. *Anaeromyxobacter* spp. at the Oak Ridge IFC site appear to be primarily attached to the solid substrate *in situ*, consistent with surface motility mechanisms. Further, oxygen intrusion at the Oak Ridge IFC site corresponded to an increase in the sediment-associated *Anaeromyxobacter* community. Finally, 16S rRNA gene sequences were identified which suggest a novel *Anaeromyxobacter* species that is responsible for uranium reduction at the Oak Ridge IFC site. This research contributes new knowledge of the ecophysiology of a widely distributed, metal-reducing bacterial group capable of uranium immobilization. The characterization of *Anaeromyxobacter* spp. helps to elucidate the dynamics of biological cycling of metals at oxic-anoxic interfaces, like those at the Oak Ridge IFC, and contributes to the broader study of microbial ecology in groundwater and sediment environments.

CHAPTER 1: Introduction

1.1 Background

Uranium is released into the environment during mining and improper disposal of nuclear wastes [1]. In addition, uranium ore mining and processing [2] and production of nuclear weapons [3] have generated uranium waste streams that pose risks to human health and the environment [1]. The Cold War left a legacy of waste that includes large amounts of metal and radionuclide contamination on U.S. Department of Energy (DOE) lands [4]. Biological approaches are thought to be the most cost-effective method for remediation of large-scale subsurface metal and radionuclide contamination *in situ* [5]. Consequently, the DOE has targeted bioremediation as a viable and cost-effective treatment option and has recognized the need for additional research aimed toward mechanisms of microbial processes related to metals and radionuclides [3]. One of the main ways that microorganisms play a role in uranium remediation is via reductive immobilization of soluble U(VI) to relatively insoluble U(IV), primarily as the mineral uraninite [6].

Microbial reduction of metals and radionuclides is an ancient form of respiration [7]. As a result, many bacteria are able to metabolically reduce metals, but only a small handful is currently considered relevant to uranium reduction applications [6]. Four groups frequently implicated in environmental metal reduction, including uranium immobilization *in situ*; include the genera *Anaeromyxobacter* [8,9,10], *Shewanella* [11,12], and *Geobacter* [13,14,15,16], as well as sulfate-reducing bacteria, which reduce metals and radionuclides co-metabolically [6]. Clone libraries and other culture-independent techniques are often used to determine the potential for bioremediation in a

uranium-contaminated subsurface system and often depend on the presence of the key genera [17,18]. Culture-independent tools offer great insight into biological reduction of metal contamination when the most relevant organisms in a community have been characterized, but, culture-dependent methods are still needed to characterize physiology and metabolism of bacteria that play critical roles in environmental systems. Culture-based techniques are needed particularly when systems behave differently than expected [19]. While all of the metal-reducing genera are described as organisms occupying the same niche, ecological exclusion theory asserts that some ecotypic variation must exist in organisms that co-exist [20]. Characterization of each of the metal-reducing genera is needed to determine the variations in niche and make implications about the dominant genus in a given environment. Environmental bacterial population variation may be linked to strain variation within species as well. The conceptual approach used in this work is based on characterizing, using genomic and physiological techniques, the unique environmental niche of *Anaeromyxobacter dehalognenans*, a versaphilic metal-reducing organism that has been implicated in uranium-reduction at multiple uranium-contaminated DOE sites [8,9,18]. In addition, using isolates from the specific environments of interest, the species description is refined to include areas of variability among strains.

1.2 Research Hypotheses

1.2.1 Hypothesis 1: Traits common to the Myxobacteria will be observed in **Anaeromyxobacter** *physiology.*

Task 1—Evolutionary Context: Determine experimentally and in silico the presence/absence of various myxobacterial traits in A. dehalogenans strain 2CP-C that influence metal-reduction and cell-transport dynamics in the subsurface.

Rationale: While many characterization experiments for a newly isolated organism can be conducted based on comparisons to organisms with similar physiology (i.e., metal-reducing or dechlorinating organisms), additional information can be obtained by comparisons to organisms that are phylogenetically related. Since the phylogeny of *A. dehalogenans* is unlike other dechlorinating and metal-reducing organisms, novel pathways and physiological traits are expected that will influence *A. dehalogenans'* ecological role in contaminated groundwater environments. Genomic analysis was coupled to physiological studies to confirm characterized traits and as a predictive tool to help in investigations of traits that are novel among metal-reducing organisms (Chapter 3).

1.2.2 Hypothesis 2: Closely related **A. dehalogenans** *occurring in the same environments will demonstrate variable traits which correspond to different ecological niches.*

Task 2—Strain Diversity: Investigate respiration with and detoxification of oxygen in A. dehalogenans strain 2CP-C, and determine the potential implications of aerobic respiration on its metabolism in situ

Rationale: Despite the fact that small evolutionary steps can result in environmentally relevant physiological differences, culture-independent tools for investigating microbial community composition in the environment rarely distinguish free-living bacteria at the strain level. Isolation, culturing, and characterization must be utilized to fully understand the role of specific organisms in the environment. *A. dehalogenans* strains were isolated from a contaminated groundwater site and strain-specific tools were used to monitor their *in situ* distribution (Chapters 4 and 7). In addition, isolates derived from contaminated aquifer materials were compared, using genetic and physiological approaches, to isolates derived from pristine soils (Chapters 6 and 7).

1.2.3 Hypothesis 3: **A. dehalogenans** *respires and/or detoxifies oxygen differently than strictly anaerobic organisms but, as a metal reducing organism, oxygen metabolism is also expected to have a different pathway from its aerobic relatives.*

Task 3—Microaerophilism in A. dehalogenans: Evaluate ecological niches of A. dehalogenans strains via isolation and characterization and design tools to screen environmental and laboratory samples for strain-level dynamics

Rationale: Phylogeny, genomic evidence for aerobic respiration, and the variable redox environments occupied by *A. dehalogenans* (i.e., vadose zone, wetlands, rice paddies) suggest that this organism is microaerophilic. Microaerophilism may be widespread in the environment, but has been primarily studied in pathogenic bacteria. Investigation of respiration and defense against spatially or temporally changing oxygen concentrations in *A. dehalogenans* elucidates a novel environmental role of microaerophilism (Chapter 5).

1.2.4 Hypothesis 4: The physiology of **A. dehalogenans** *is unique among metal-reducing bacteria and it will, thus, have a unique role in uranium bioremediation.*

Task 4—Assess the role of A. dehalogenans at a Department of Energy uranium- and nitrate-contaminated groundwater site.

Rationale: Physiological and genomic characterizations demonstrate a unique ecological niche for *A. dehalogenans*. Studies applied to aquifer materials obtained from the Oak Ridge IFC site elucidate the relevance of various physiological traits to bioremediation of uranium in the groundwater environment. Oak Ridge IFC site materials were analyzed to determine the distribution of *A. dehalogenans* isolates *in situ* (Chapter 4) and the impact of oxygen intrusion into the groundwater (Chapter 5).

1.3 References

1. WHO (2001) Depleted uranium: sources, exposure, and health effects. World Health Organization, WHO/SDE/PHE/011.

2. Elias DA, Krumholz LR, Wong D, Long PE, Suflita JM (2003) Characterization of microbial activities and U reduction in a shallow aquifer contaminated by uranium mill tailings. Microbial Ecology 46: 83-91.

3. Fendorf S, Konopka A, Kostka JE, Lovley DR, Metting B, et al. (2003) Bioremediation of metals and radionuclides...what it is and how it works. U.S. Department of Energy LBNL-42595.

4. Riley RG, Zachara JM, Wobber FJ (1992) Chemical Contaminants on DOE Lands and Selection of Contaminant Mixtures for Subsurface Science Research. DOE/ER-0547T, US Department of Energy, Washington, DC.

5. Lloyd JR, Lovley DR (2001) Microbial detoxification of metals and radionuclides. Current Opinion in Biotechnology 12: 248-253.

6. Wall JD, Krumholz LR (2006) Uranium reduction. Annual Review of Microbiology 60: 149-166.

7. Vargas M, Kashefi K, Blunt-Harris EL, Lovley DR (1998) Microbiological evidence for Fe(III) reduction on early Earth. Nature 395: 65-67.

8. North NN, Dollhopf SL, Petrie L, Istok JD, Balkwill DL, et al. (2004) Change in bacterial community structure during in situ biostimulation of subsurface sediment cocontaminated with uranium and nitrate. Applied and Environmental Microbiology 70: 4911-4920.

9. Petrie L, North NN, Dollhopf SL, Balkwill DL, Kostka JE (2003) Enumeration and characterization of iron(III)-reducing microbial communities from acidic subsurface sediments contaminated with uranium(VI). Applied and Environmental Microbiology 69: 7467-7479.

10. Wu Q, Sanford RA, Löffler FE (2006) Uranium(VI) reduction by *Anaeromyxobacter dehalogenans* strain 2CP-C. Applied and Environmental Microbiology 72: 3608-3614.

11. Nealson KH, Belz A, McKee B (2002) Breathing metals as a way of life: geobiology in action. Antonie Van Leeuwenhoek International Journal of General and Molecular Microbiology 81: 215-222.

12. Wade R, DiChristina TJ (2000) Isolation of U(VI) reduction-deficient mutants of *Shewanella putrefaciens*. FEMS Microbiology Letters 184: 143-148.

13. Sanford RA, Wu Q, Sung Y, Thomas SH, Amos BK, et al. (2007) Hexavalent uranium supports growth of *Anaeromyxobacter dehalogenans* and *Geobacter* spp. with lower than predicted biomass yields. Environmental Microbiology 9: 2885-2893.

14. Sung Y, Fletcher KF, Ritalaliti KM, Apkarian RP, Ramos-Hernandez N, et al. (2006) *Geobacter lovleyi* sp nov strain SZ, a novel metal-reducing and tetrachloroethene-dechlorinating bacterium. Applied and Environmental Microbiology 72: 2775-2782.

15. Lovley DR, Phillips EJP, Gorby YA, Landa ER (1991) Microbial Reduction of Uranium. Nature 350: 413-416.

16. Amos BK, Sung Y, Fletcher KE, Gentry TJ, Wu WM, et al. (2007) Detection and quantification of *Geobacter lovleyi* strain SZ: Implications for bioremediation at tetrachloroethene- and uranium-impacted sites. Applied and Environmental Microbiology 73: 6898-6904.

17. Anderson RT, Vrionis HA, Ortiz-Bernad I, Resch CT, Long PE, et al. (2003) Stimulating the in situ activity of *Geobacter* species to remove uranium from the groundwater of a uranium-contaminated aquifer. Applied and Environmental Microbiology 69: 5884-5891.

18. Cardenas E, Wu WM, Leigh MB, Carley J, Carrol lS, et al. (2008) Microbial communities in contaminated sediments, associated with bioremediation of uranium to submicromolar levels. Applied and Environmental Microbiology 74: 3718-3729.

19. Wan JM, Tokunaga TK, Brodie E, Wang ZM, Zheng ZP, et al. (2005) Reoxidation of bioreduced uranium under reducing conditions. Environmental Science & Technology 39: 6162-6169.

20. Hutchinson GE (1961) The paradox of the plankton. American Naturalist 95: 137-145.

CHAPTER 2: Literature review

2.1 Isolation and characterization of *Anaeromyxobacter dehalogenans* strains.

2.1.1 Characterization of the first Anaeromyxobacter dehalogenans *isolates.*

The first *Anaeromyxobacter dehalogenans* isolate (strain 2CP-1) was derived from Michigan stream sediment via enrichment on 2-chlorophenol and described by Cole et al., in 1994 and represents the first representative in the myxobacteria family capable of anaerobic growth [1]. Characterization of five *A. dehalogenans* strains, including organisms derived from Michigan pond sediment and yard compost as well as Cameroon rain forest soil, and a description of the genus and species were provided subsequently by Sanford et al. [2]. *A. dehalogenans* was shown to use a range of respiratory substrates including fumarate, nitrate, and oxygen in addition to ortho-substituted chlorophenols (Figure 1; [3,4]. Cells are gram negative rods that are about 0.25 μm wide and 4-8 μm long (Figure 2). Doubling time on acetate and 2-chlorophenol is about 12 hours and the H_2 threshold concentration for this process is comparable to that required for denitrification. Anaerobically growing cells using fumarate as an electron acceptor are red in color while aerobically growing cells are color-less. In keeping with their phylogenetic classification as myxobacteria [5,6], *A. dehalogenans* colonies display gliding motility on solid surfaces. Colonies of *A. dehalogenans* can be seen on R2A plates in about 2-3 weeks when grown anaerobically with fumarate or with sub-atmospheric oxygen. In all cases, Sanford et al. observed that electron acceptor concentrations need to be kept low (1mM and lower in most cases) in order for *A. dehalogenans* to flourish.

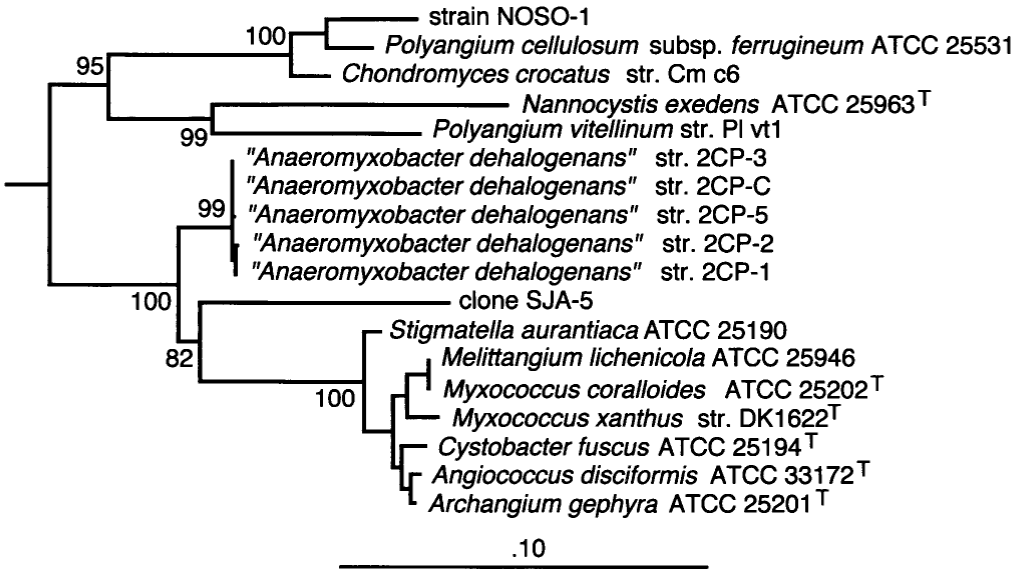

Figure 2.1. Phylogenetic tree based on 16S rRNA sequences of 2CP strains and representative myxobacteria [2].

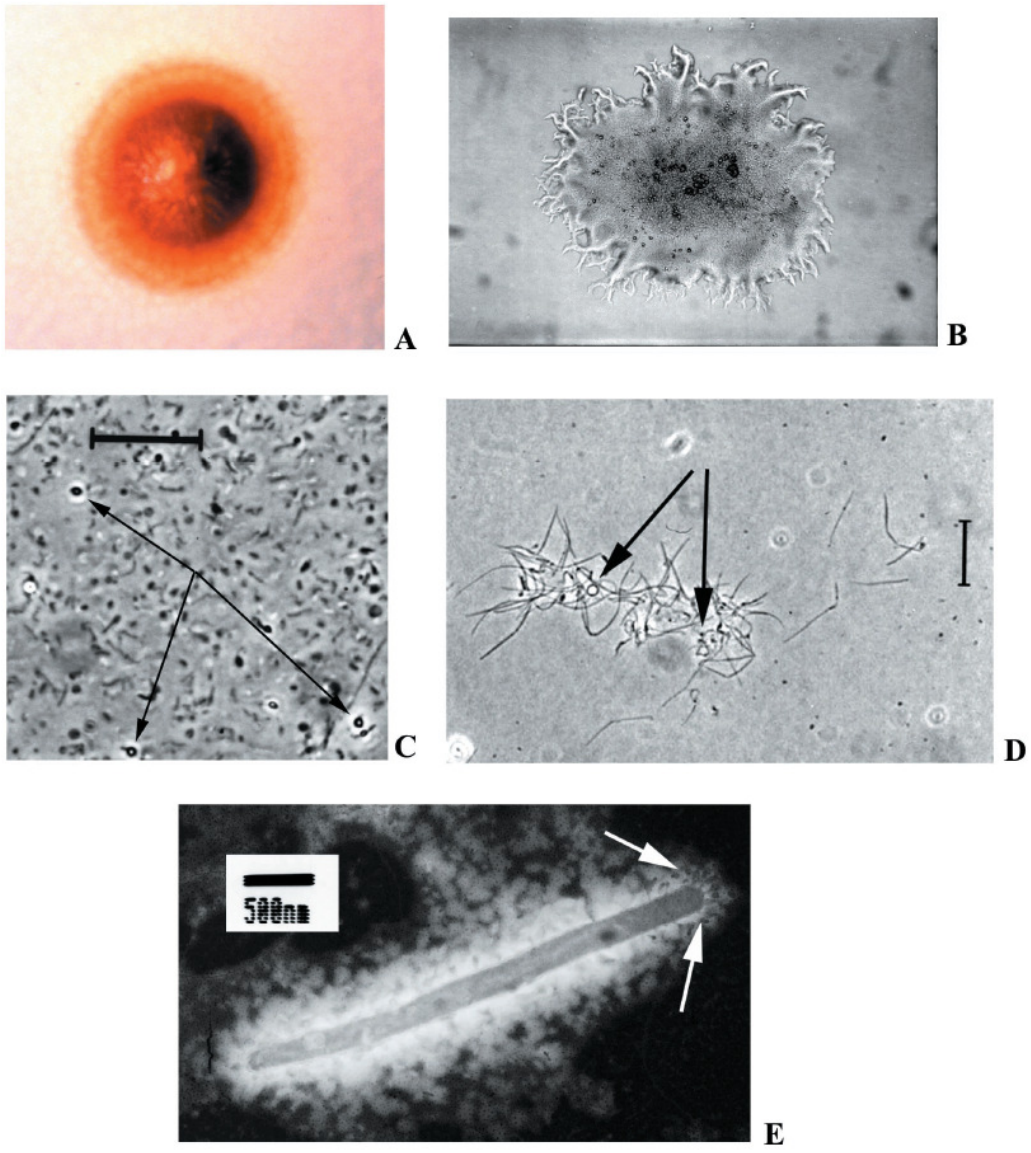

Figure 2.2. (A) Red colony formed by 2CP-C on anaerobic agar. (B) New 2CP-1 colony as it appears on agar surface. (C) Cells and refractile bodies from 2CP-C colony. Bar =13 µm. (D) Vegetative cells of strain 2CP-C shown by phase-contrast microscopy. Hook-like ends of cells and blebs are shown by arrows. (E) Transmission electron microscopy of strain 2CP-C showing pilus-like structures (arrows) [2].

A. dehalogenans strain 2CP-C was also included in a hydrogen threshold analysis designed to track the number of electrons transferred to various chlorinated electron acceptors [7]. Results from this analysis confirm that chlororespiratory processes, including 2-chlorophenol reduction by *A. dehalogenans*, consume H_2 to levels below threshold concentration for acetogens, methanogens, and sulfidogens.

2.1.2 Additional* Anaeromyxobacter *isolates. Concurrent with characterization of the 2-chlorophenol respiring strains of *A. dehalogenans*, several organisms were isolated by Coates et al. [8] based on their ability to utilize humic substances as electron donors when respiring nitrate. This ability is thought to give soil microorganisms more versatility in an environment where respiratory compounds are often limiting. Of the six organisms isolated, one long thin rod (0.3 μm by 5.3 μm) called strain KC was described as a novel genus of delta-Proteobacteria most closely related to *Stigmatella erecta*. This organism denitrified and was an anomaly in that it could not grow aerobically or with any electron acceptor tested other than nitrate, including simple aromatic hydrocarbons, Fe(III)-NTA, MnO_2, and sulfur. Strain KC has since been classified as an *Anaeromxyobacter* species. Another distinct strain, *A. dehalogenans* strain FAc12 was isolated from flooded rice field soils enriched with acetate and ferrihydrite by Treude et al. and described in 2003 [9]. This study was conducted at the Instituto Sperimentale per la Cerealicoltura near Vercelli (Po River Valley, Italy). Rice fields are flooded during most of the vegetation period but then drained for agricultural treatments and harvesting. Because of alternation between flooding and drainage, rice fields represent an environment that is characterized by spatial and temporal fluctuations between oxic and anoxic conditions. Since iron reduction has been estimated to account for up to 50% of

total carbon metabolism in paddy soils, and since little was known about microorganisms responsible for anaerobic iron respiration in rice fields, iron enrichments were utilized to characterize the community. Strain FAc12, which is 99.3-99.7% similar to previously described *A. dehalogenans* strains, was also grown under oxic conditions with acetate, glucose, or citrate as well as in complex medium. Gliding motility was not observed in strain FAc12. Also in the FAc12 characterization study, rice roots were examined using culture-independent 16S rRNA gene sequence analysis. Of 69 total environmental clone sequences, ten corresponded to *A. dehalogenans*-like organisms. The remaining sequences were alpha- and beta-Proteobacteria except for two clone sequences falling into *Desulfuromonadales*, the order which contains the *Geobacteraceae*. The characterization of FAc12 represents the first report of a non-*Geobacter* in the delta-Proteobacteria capable of dissimilatory iron reduction. The authors suggest that the original cluster of *A. dehalogenans* (2CP strains) have more myxobacterial traits than the cluster described by FAc12 and KC. However, they also suggest that FAc12 represents a unique ecotype due to its ability to reduce ferric iron.

2.1.3 Metal reduction by* Anaeromyxobacter *isolates. In response to characterization of iron-reduction in strain FAc12, He and Sanford [10] described iron-reduction in the chlororespiring strain 2CP-C, confounding the assertion that FAc12 represents an unique ecotype. In addition, He and Sanford demonstrated, using chloramphenicol, that Fe(III) reduction is constitutive while chlororespiration is induced. The constitutive versus induced descriptions of these different types of respiration point to two different mechanisms for respiratory versatility that make *A. dehalogenans* successful in its variable redox niche. In addition, when applied to questions of

bioremediation, description of these two methods for versatility helps elucidate metabolic processes that are important for mixed-waste site remediation. The study by He and Sanford described *A. dehalogenans* as a 'promising model organism for studying potential interferences between competing substrates that might be important in bioremediation.' Soluble Fe(III) was found to inhibit dechlorination while insoluble Fe(III) was reduced simultaneously with 2-chlorophenol. The authors also point out that microaerophilic growth by *A. dehalogenans* coupled with Fe(III) respiration gives it the ability to live at the oxic-anoxic interface, where iron cycling occurs, as in rice fields and contaminated groundwater environments. In order to further describe *A. dehalogenans* in the context of bioremediation applications, He and Sanford also characterized the acetate threshold concentration for chlororespiration, amorphous Fe(III) reduction and Fe(III) citrate reduction [11]. This analysis was targeted toward understanding the competitive interactions between different terminal electron-accepting processes in the environment. He and Sanford found that, while chlororespiration and amorphous Fe(III) reduction had acetate threshold concentrations of 69 ± 4 nM and 19 ± 8 nM, respectively, Fe(III) citrate-reducing cultures were able to use acetate until it dropped below the detection limit of 1 nM. This demonstrates the ability of *A. dehalogenans* to compete for nanomolar-level acetate as its electron donor. In addition, Fe(III) citrate-reduction was demonstrated to be a far more energetically favorable form of metabolism than the other two processes tested.

Recent characterization of *A. dehalogenans* strain 2CP-C has demonstrated that this versatile organism is also capable of uranium reduction [12]. The study by Wu et al. demonstrated conversion of U(VI) to U(IV) by *A. dehalogenans* and that the reduction

required hydrogen as electron donor. Since many uranium-impacted sites contain cocontaminants, such as nitrate and chloro-organic compounds, the effects of other oxidants on U(VI) reduction were also explored. Nitrate addition appeared to cause an increase in soluble U(VI) concentration which had previously been reduced by *A. dehalogenans* but following consumption of nitrate and nitrite, U(VI) reduction resumed. In the presence of ferric citrate, U(VI) reduction stopped, in favor of Fe(III) reduction and U(VI) reduction did not resume. However, this effect was also observed with citrate addition. Amorphous Fe(III) addition slowed U(VI) reduction but did not stop it. Finally, the effects of 2-chlorophenol and fumarate on U(VI) reduction were explored. Both of these organic electron acceptors were reduced concurrently with U(VI), suggesting that anaerobically grown cells of strain 2CP-C possess a constitutive pathway for U(VI) reduction. Further characterization of strain 2CP-C U(VI) reduction by Sanford et al. [13] demonstrated that *A. dehalogenans* and *Geobacter* spp. linked uranium reduction to growth; however, biomass yield was lower than expected based on the theoretical free energy calculation. Decreased biomass yield was thought to be due to inefficient (i.e., reduction to U(V) with spontaneous dismutaion to U(VI) and U(IV)) or costly metabolism of U(VI) (i.e., toxicity). Lower than predicted biomass yields were also determined for U(VI)-reducing cultures of *Geobacter lovleyi* and *Geobacter sulfurreducens*. Finally, U(VI)- and Tc(VII)-reduction by *A. dehalogenans* were examined in a study by Marshall et al. [14]. The impact of hydrogen versus acetate as electron donor was analyzed in terms of the effects on reduction rate and formation of nanoparticles. In addition, indirect Tc(VII) reduction was studied in conjunction with a Fe(II)-mediated mechanism. Fe(II) produced by *A. dehalogenans* metabolism of

ferrihydrite or DOE IFC Hanford site sediments rapidly removed $^{99}Tc(VII)O_4^-$ from solution. Thus, *A. dehalogenans* has the ability to efficiently affect mineralization of a variety of metals and radionuclides via metabolic and indirect methods.

2.2 Environmental distribution of *Anaeromyxobacter dehalogenans.*

2.2.1 **Anaeromyxobacter** ***sequences in pristine environments.*** In addition to isolations, clone libraries and PCR analysis in various environments can be used to describe the environmental distribution of *A. dehalogenans*. 16S rRNA gene clones that are derived from environmental samples and can be classified as *Anaeromyxobacter* species were identified in the NCBI non-redundant nucleotide sequence database in 11 studies from as early as 1997. These clones were derived from materials that can be placed into four categories: i) tropical forest soils, ii) wetland and river sediments, iii) rice field soils or rice roots, and iv) contaminated groundwater and groundwater sediments. No clones were identified from studies utilizing marine or saltwater materials and most were associated with areas expected to be subject to fluctuating redox conditions.

Borneman and Triplett conducted an experiment designed to examine soil microbial population shifts in response to deforestation in Eastern Amazonia [15]. Two eastern Amazonian soils were characterized using 100 SSU rDNA sequences. Five myxobacterial sequences were detected in 'reformed pasture' and 'mature forest' soils, including clones P45 (Accession number: U68672) and M36 (Accession number: U68621), which fall into the *Anaeromyxobacter* clade according to the 500 bases sequenced. The occurrence of *Anaeromyxobacter* sequences in the top 10 cm of these

Brazilian rain forest and deforested pasture soils is consistent with occurrence in the Cameroon rain forest from which strain 2CP-C was isolated.

Consistent with the role of *Anaeromyxobacter* as a metal reducer at the oxic/anoxic interface, additional clones indicating the presence of this organism were sequenced from freshwater ferromanganous micronodules [16]. Clone MNF2 (Accession number: AF293009) is an *Anaeromyxobacter* sequence derived from these ferromanganese-encrusted sediments collected from the bottom of Green Bay, WI. Since the organism was uncharacterized at the time of the micronodule study, the connection was not made but the presence of acetate and reduced metals is consistent with the expected niche based on the metabolism of characterized *Anaeromyxobacter* strains.

Before the organism was well characterized, another *Anaeromyxobacter* 16S rRNA gene clone (FW35) was sequenced in conjunction with a study by Brofft et al. at the Savanna River Site (Accession number: AF523970) [17]. This sequence was amplified from an acidic pine-dominated forested wetland that was adjacent to, but unaffected by, reject coal effluent. The forested wetland community analysis was used as a background for comparison to contaminated sediment samples.

In accordance with isolation of strain FAc12 from rice paddy soils and the multiple *Anaeromyxobacter* clones identified in association with rice roots by Treude et al. [9], additional studies of rice field soils have identified *Anaeromyxobacter* clones. A stable isotope probing study was conducted using material from the same region as the strain FAc12 study, Italian rice field soil near Vercelli [18]. In this study, Lueders et al. used ^{13}C-labelled substrate to identify methylotrophic organisms.

2.2.2 **Anaeromyxobacter** *sequences in contaminated groundwater.*

Multiple characterization studies have been conducted on the microbial communities involved in U(VI) and nitrate reduction at the U.S. Department of Energy (DOE) Oak Ridge Integrated Field-scale Subsurface Research Challenge (IFC) site (formerly known as the field research center [FRC]) (reviewed below). Petrie et al. [19] established iron(III)-reducing enrichment cultures from pristine and contaminated (high uranium, nitrate; low pH) subsurface sediments from the treatment zone designated Area 1. A range of carbon sources was utilized and two pH values were considered (pH 7 and pH 4-5). In addition, treatments were established in which nitrate was removed from the sediment by washing. Petrie et al. found that, while *Geobacteraceae* dominated in enrichments derived from background samples, *Anaeromyxobacter* species (and other organisms, at that point uncharacterized as metal reducers) dominated in the Fe(III)-reducing consortia derived from contaminated sediments. MPN-PCR of DNA extracted directly from IFC subsurface sediments reveals the same pattern, linking *Anaeromyxobacter* species more strongly with contaminated soils and organisms from *Geobacteraceae* with pristine soils. *Anaeromyxobacter* species grew in pH neutral contaminated-sediment enrichments with acetate, lactate, or glycerol as carbon source but, consistent with the Sanford et al. characterizations [2,10,11], acetate was the carbon source with the most *Anaeromyxobacter* clones (90% of the 152 clones total). Also, the fewest non-*Anaeromyxobacter* species are present in the acetate-amended contaminated sediment enrichments. Five different strains of *Anaeromyxobacter* are described in the IFC contaminated soil enrichments, three different strains in the acetate enrichments and two different strains in the glycerol enrichments. High nitrate concentrations inhibited

uranium reduction in all of the enrichment cultures. Low pH contaminated soil cultures were dominated by gram-positive organisms. The study by Petrie et al. reports the first evidence of *Anaeromyxobacter* sequences in a contaminated subsurface environment. A subsequent study of Area 1 at the DOE Oak Ridge IFC by North et al. [20] involved changes in bacterial community structure in response to *in situ* biostimulation of uranium- and nitrate-contaminated subsurface sediment. Based on the observation that U(VI)-reduction at the IFC was carbon substrate limited, biostimulation was conducted through carbon substrate addition and pH neutralization. Groundwater was aerobic prior to testing. Five additional *Anaeromyxobacter* sequences were reported from the biostimulation study, including two that were present before treatment and three that were detected after biostimulation. Twenty-five percent of the 16S rRNA gene sequences in the biostimulated clone libraries were 96% similar to *A. dehalogenans.* However, while *Anaeromyxobacter*-related gene sequences were more abundant than *Geobacter*-related sequences before biostimulation, *Geobacter* sequences increased and *Anaeromyxobacter*-related sequences remained stable or decreased. This observation suggests that *Anaeromyxobacter* may be considered a K-selected species that constitutively operates at carrying capacity, rather than quickly responding to nutrient inputs (r-selection strategy). Finally, a clone library study by Cardenas et al. [21] revealed the presence of *Anaeromyxobacter* in the subsurface uranium (VI) treatment zone was designated Area 3. The Area 3 study was conducted in conjunction with a uranium re-oxidation study by Wu et al. [22].

2.3 DOE Oak Ridge IFC.

2.3.1 Overview of the Oak Ridge IFC. Activities such as enrichment and production of nuclear materials, development of nuclear weapons, and construction and testing of nuclear reactors have left a substantial legacy of subsurface contamination on DOE lands [23]. Metals and radionuclides dominate subsurface contaminants, existing at more than 60% of DOE facilities and at 50% of DOE waste sites [23]. Bioremediation has been identified as a viable and cost-effective solution for addressing the problem of metal and radionuclide contamination on DOE lands [24]. The Oak Ridge site is one of three sites designated by the DOE Environmental Remediation Sciences Program IFC initiative for multidisciplinary field scale research intended to support DOE's cleanup mission and long-term stewardship responsibilities (http://www.esd.ornl.gov/orifrc/). Major facilities and waste disposal units at the 98 hectare Oak Ridge IFC include the former S-3 waste disposal ponds (the S-3 Ponds; four unlined surface impoundments that are currently covered with a parking lot), two reactive barrier demonstration projects associated with S-3 Pond groundwater contamination pathways, the west end treatment facility, the boneyard/burnyard, and a hazardous chemical disposal area built over the burnyard [25]. S-3 Pond effluent has very low pH and high contaminant concentrations which include nitrate, technetium, uranium, manganese, magnesium, aluminum, and volatile organic compounds [26]. Three contaminant migration pathways from the S-3 Ponds have been described and the contaminated area at the Oak Ridge IFC encompasses five field research areas (Table 2.1; Figure 2.3). Area 1 is just south and down dip of the S-3 Ponds, which means that since the primary direction of contaminant transport is strike

Table 2.1. Geochemistry of the five Oak Ridge IFC site treatment areas [26,27].

	pH	Nitrate (mg/L)	Uranium (mg/L)	Technetium (pCi/L)
Area 1	3.25 to 6.5	48 to 10,400	0.01 to 7.5	66 to 31,000
Area 2	6 to 7	< 100 to 1,000	0.01 to 1.3	< 600
Area 3	< 4.0	9,000	as high as 60	as high as 40,000
Area 4	5 to 7	up to 25,000	as high as 28	not reported
Area 5	3 to 7	6,100	as high as 44	not reported

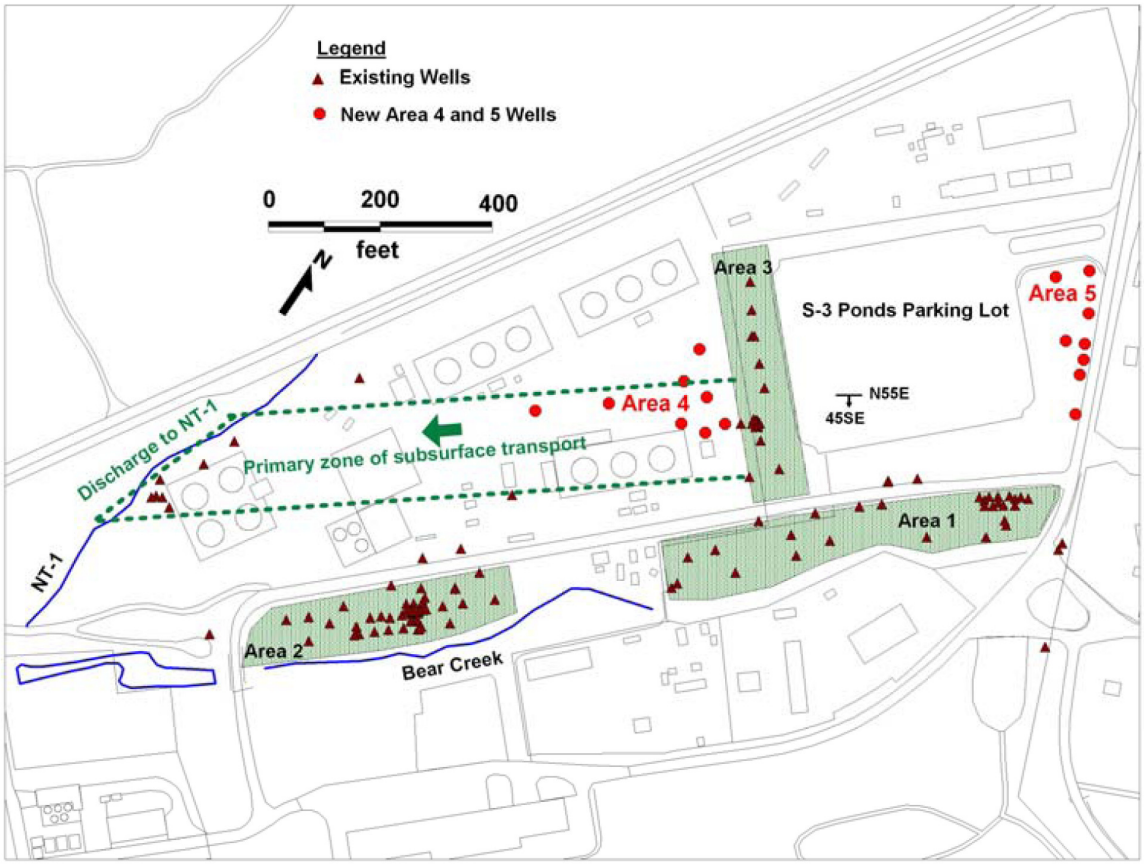

Figure 2.3. Map of Oak Ridge IFC treatment areas [25].

parallel, Area 1 receives only a fraction of the contamination that moves in groundwater from the S-3 Ponds. Area 2 is located several hundred feet to the southwest of the S-3 Ponds. Contaminants in Area 2 are thought to have been deposited there due to a historic stream channel of Bear Creek, which is located adjacent to the site. Area 3 is just west of the S-3 Ponds and directly down strike, in the direction of primary groundwater flow, which means that most of the contaminants moving from the S-3 Ponds via groundwater flow through Area 3. Area 3 is the most contaminated of the five research areas. Oak Ridge IFC site treatment areas 4 and 5 are the newest of the treatment areas. Area 4 is located west of Area 3, further downstream of the S-3 Ponds. Area 5 is east of the S-3 Ponds, upstream of the primary groundwater flow path.

2.3.2 Treatment and microbial characterization activities at the Oak Ridge IFC. Only a few of the many studies conducted at the Oak Ridge IFC, those which focus primarily on biological processes, will be described here. Compared to other treatment zones, the Area 1 treatment zone has been most exhaustively characterized in terms of its microbial community, including the two studies mentioned previously that implicated *Anaeromyxobacter* spp. [19,20]. As described above, clone libraries established by Petrie et al. [19] indicated that *Geobacteraceae* sequences were more abundant in pristine compared to contaminated environments in Area 1, whereas *Anaeromyxobacter* species were more abundant in contaminated sediments. Additionally, *Peanibacillus* and *Brevibacillus* spp. were found to predominate in the Fe(III)-reducing consortia of contaminated Area 1 sediments, based on Fe(III)-enrichment cultures. Also found in Fe(III)-reducing enrichments were *Pseudomonas rhodesiae*, *Burkholderia graminis*, and *Pantoea agglomerans*. The enrichment-culture studies by Petrie et al. indicated that none

of the culturable organisms detected in contaminated sediment enrichments were closely related to the most commonly cultured Fe(III)-reducing bacteria, such as *Shewanella* and *Geobacter*, suggesting that low pH and high nitrate concentrations may prevent their survival. The authors conclude that other model metal-reducing organisms would be more appropriate for the development of bioremediation strategies at the Oak Ridge IFC site. A biostimulation experiment was conducted using single-well, push-pull tests and downwell microbial samplers to monitor the response of the indigenous Area 1 microbial community to electron donor additions, including acetate, ethanol, and glucose [28]. Data from the Oak Ridge IFC site push-pull experiment indicated that the subsurface microbial community in Area 1 was electron donor-limited and that *Geobacter* species were detectable only in wells with added electron donors [28]. North et al. conducted microbial community analyses of Area 1 sediments affected by the push-pull treatment, which included pH neutralization as well as electron donor addition [20]. Before biostimulation, almost one-fourth of sequenced organisms were related to organisms which were previously cultured from low-nutrient environments, including *Caulobacter leidyi* and *Brevundimonas vesicularis*. Sequences increased from 5% to 40% in organisms related to delta-Proteobacteria that have been characterized as metal-reducing organisms. Nearly 25% of the 16S rRNA gene sequences in "biostimulated" clone libraries were related to *A. dehalogenans* and organisms in the *Geobacteraceae* family were also detected. Almost 15% of the "biostimulated" clone libraries represented organisms that are capable of polycyclic aromatic hydrocarbon degradation (e.g., *Burkholderia* sp. strain N2P5 and *Sphingomonas paucimobilis*). Additional Area 1 clone libraries were established along geochemical gradients [29] and in microcosms

cocontaminated with radionuclides and nitrate [30]. These studies included analyses of total and metabolically active microbial communities by implementing DNA- as well as RNA-derived clones. Nitrate-reducing organisms were found to be among the most active bacteria in the Oak Ridge IFC site Area 1 treatment zone [29]. In addition, a citrate synthase gene which has been linked to the *Geobacteraceae* family [31] was utilized as a functional gene indicator of metal-reduction activity [30]. Finally, a *Castellaniella* species was isolated from Oak Ridge IFC site Area 1 sediments that is thought to be important for nitrate removal at the Oak Ridge IFC site [32].

The microbial community in Area 2 is different from the other treatment areas and similar to the background area, with *Acidovorax* spp. making up most of the isolates from enrichment cultures and *Rhizobium* spp. predominating clone library sequences [25]. Differences are thought to be due to the low contaminant concentrations and circumneutral pH in Area 2 (Table 2.1). Nitrate-reducing enrichment cultures, established with methanol or glycerol and pH 5.7-6.2, were derived from Area 2 site materials [33]. *Clostridium*-like organisms were most dominant in nitrate-reducing enrichment cultures from the Oak Ridge IFC site Area 2 but *Paenibacillus graminis*, *Aeromonas* spp., and sequences within the phylum *Bacteroidetes* were also recovered. The Area 2 nitrate enrichment study found that uranium-reduction in microcosms was "nitrate-indifferent," suggesting that, counter to previous reports, nitrate concentrations did not inhibit uranium-reduction in Oak Ridge IFC microbial communities. Treatment activities in Area 2 include a zero-valent iron reactive barrier that was constructed in late November 1997 [34]. Evaluation of the microbial population and community composition in the reducing zone, over the course of three years, was performed using

phospholipid fatty acid and DNA analyses. The microbial community was stimulated by the reactive barrier in Area 2 but authors suggest that the guar gum used in trench excavation may have played a role in enrichment. Sulfate-reducing bacteria and denitrifying bacteria were found in and around the barrier while methanogens were low in Area 2 samples. Ethanol additions were assessed in column studies using Oak Ridge IFC site Area 2 sediment [35]. A combined lipid- and nucleic acid-based microbial community characterization indicated that biomass increased and that community composition changed in response to ethanol addition. *Geobacteraceae* increased significantly near the stimulated-column outlet, where soluble electron acceptors had been largely depleted, but no *Anaeromyxobacter* sequences were detected in the Area 2 sediment column experiment.

The Area 3 treatment zone contains perhaps the most long-term and large-scale treatment study at the Oak Ridge IFC site. Extensive flow modeling and well-design went into establishing the combination above- and below-ground treatment system in Area 3 [36,37,38]. The pilot test facility at the Oak Ridge IFC site in Area 3 included a four well recirculation system parallel to geologic strike, with an inner loop nested within an outer loop, and three perpendicular boreholes drilled for monitoring purposes [39]. In addition, a denitrifying fluidized bed reactor (FBR) was established aboveground [40]. Authors found that denitrifying and sulfate-reducing bacteria (SRB) in the aboveground FBR contributed to uranium reduction, including *Desulfovibrio vulgaris*. Biostimulation *in situ* was also effective, as a result of ethanol addition and conditioning (i.e., pH adjustment, calcium removal, nitrate reduction) [41]. Denitrifiers, SRB, and iron-reducing bacteria were detected in groundwater samples, including *Acidovorax*,

Desulfovibrio-like, and *Geobacter*-like species. A subsequent study of the stability of reduced uranium in the oxidized subsurface [22] indicated that the predominant bacterial community members in low-uranium wells included *Desulfovibrio, Geobacter, Geothrix, Ferribacterium, Acidovorax, Sphingomonas, Thiobacillus,* and others. But further characterization of the microbial communities involved in Area 3 bioremediation indicated that *Anaeromyxobacter* and *Desulfosporosinus* species were also present [21].

2.4 Microbial uranium mineralization.

Many studies have shown successful microbial uranium mineralization by bacteria in groundwater and in aquifer sediments [35,42,43,44,45,46]. The fate of uranium in a natural environment is governed by several factors which include reduction/oxidation reactions and complexation reactions, as well as sorption/desorption and precipitation/dissolution reactions. One major mechanism for bacterial uranium mineralization is reduction and subsequent complexation. The soluble, oxidized form of uranium, U(VI), can be transformed to insoluble U(IV) by biological processes, which then precipitates to uraninite (UO_2) [47]. Crude extracts of *Micrococcus lactilyticus* (renamed *Veillonella alcalescens*) were shown to reduce U(VI) in 1962 [48] but another 30 years elapsed before metabolism of live cells was correlated to uranium reduction [49,50,51]. The first study by Lovley et al. demonstrated uranium (VI) reduction by two dissimilatory metal reducing bacteria (DMRB), *Shewanella oneidensis* strain MR-1 and *Geobacter metallireducens* and established a link between U(VI) reduction and the metabolism of organisms that respire iron and other metals [51]. Many authors describing the distribution and diversity of potential uranium-reducing microorganisms at

contaminated sites have focused on DMRB present at the site like *Shewanella*, *Geobacter* and *Anaeromyxobacter* spp. [19,20,21,22] despite the fact that "the only common factor evident [among uranium-reducing bacteria] is the ability of all bacteria to grow anaerobically where a redox potential sufficiently low for U(VI) reduction would be established [47]." A list of organisms that have been shown to reduce U(VI) is in Table 2.2.

2.4.1 Uranium immobilization by aerobic organisms. As described by Wall and Krumholz [47], the only feature shared among uranium-reducing microorganisms is the ability to survive at redox potentials low enough for U(VI)-reduction to be thermodynamically favorable (Figures 2.4 and 2.5). However, biomineralization is also possible without uranium reduction [52,53,54,55]. Therefore, a range of organisms, with different levels of oxygen tolerance/utilization are able to convert soluble uranium to insoluble uranium minerals. Since redox plays a significant role in the metabolic processes that occur in the subsurface [56], the most relevant population for uranium biomineralization may be determined by the organisms' most favorable redox environment.

Because of the tendency of uranium to complex with phosphate [57], aerobic organisms have been shown to mineralize soluble U(VI) to an insoluble autunite/meta-autunite group mineral as a result of constitutive phosphatase activity [55,58]. *Myxococcus xanthus* is a common soil microorganism [59] that has never been shown to have any capacity for anaerobic metabolism. *M. xanthus* cell suspensions at pH 2 and 4.5

Table 2.2. Bacteria shown to reduce U(VI) to U(IV). Adapted from [47].

Anaeromyxobacter dehalogenans strain 2CP-C	*Desulfovibrio sulfodismutans* DSM 3696
Cellulomonas flaigena ATCC 482[a]	*Desulfovibrio vulgaris* Hildenborough ATCC 29579
Cellulomonas sp. WS01[a]	*Geobacter lovleyi* strain SZ [13,60]
Cellulomonas sp. WS18[a]	*Geobacter metallireducens* GS-15
Cellulomonas sp. ES5[a]	*Geobacter sulfurreducens*
Clostridium sp.	*Pseudomonas putida*
Clostridium sphenoides ATCC 19403	*Pseudomonas* sp.
Deinococcus radiodurans R1	*Pseudomonas* sp. CRB5
Desulfitobacterium hafniense strain JH-1[b]	*Pyrobaculum islandicum*
Desulfomicrobium norvegicum (formerly*Desulfovibrio baculatus*) DSM 1741	*Salmonella subterranea* sp. nov. strain FRC1
Desulfotomaculum reducens	*Shewanella alga* BrY
Desulfosporosinus orientis DSM 765	*Shewanella oneidensis* MR-1 (formerly *Alteromonas putrefaciens*, then *Shewanella putrefaciens* MR-1)
Desulfosporosinus spp. P3 91	*Shewanella putrefaciens* strain 200 11
Desulfovibrio baarsii DSM 2075	*Veillonella alcalescens* (formerly *Micrococcus lactilyticus*)
Desulfovibrio desulfuricans ATCC 29577	*Thermoanaerobacter* sp.
Desulfovibrio desulfuricans strain G20 (to be renamed *Desulfovibrio alaskensis*)	*Thermus scotoductus*
Desulfovibrio sp. UFZ B 490	*Thermoterrabacterium ferrireducens*

[a] Data for reduction by *Cellulomonas* strains has now been questioned, and evidence for precipitation by phosphate has been obtained [61].
[b] Fletcher et al., unpublished data

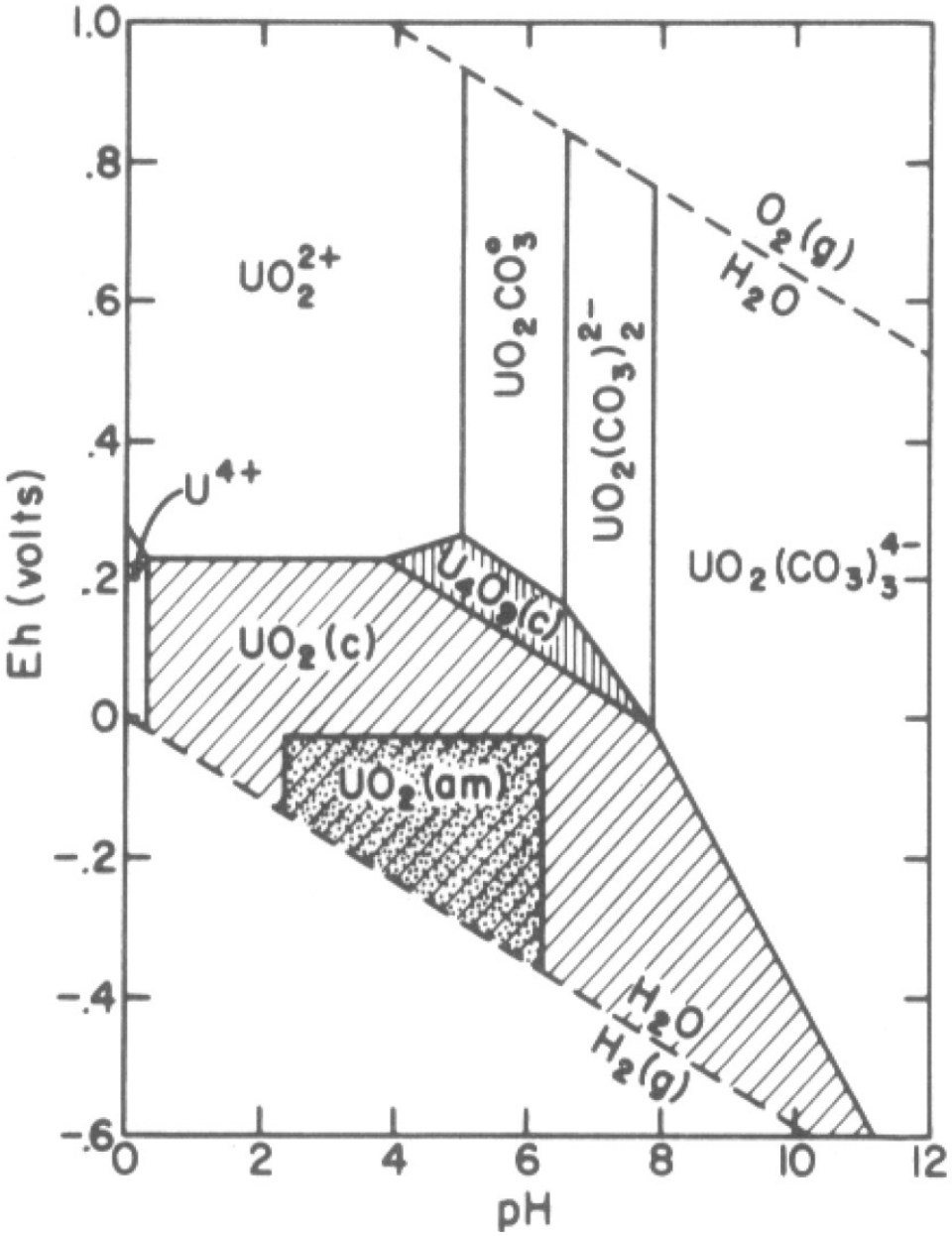

Figure 2.4. Eh-pH diagram in the U-O_2-CO_2-H_2O system at 25°C for pCO_2 = 0.01 atm, showing the stability fields of amorphous UO_2 [UO_2 (am)], ideal uraninite [UO_2 (c)] and U_40_9 (c). Solid-solution boundaries are drawn at 10^{-6}M (0.24p pm) dissolved uranium species [62].

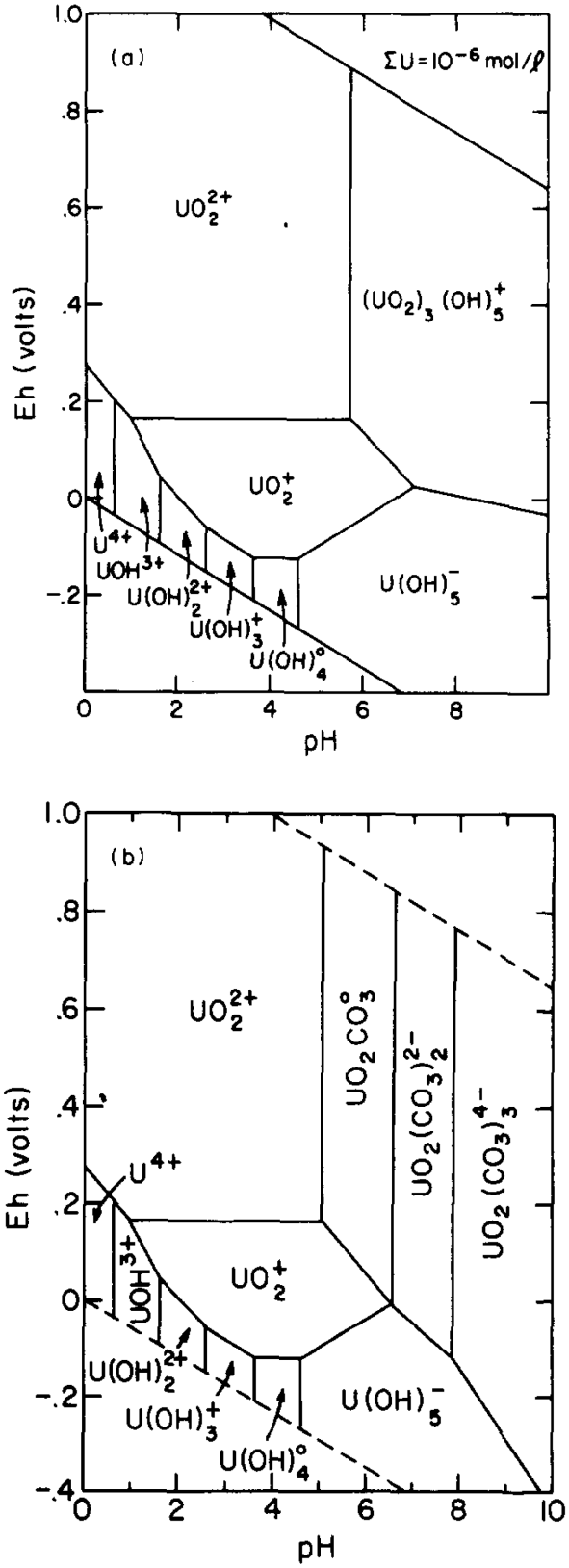

Figure 2.5. (taken from [62]) Eh-pH diagrams showing relative importance of U(IV), U(V), and U(VI) at 25°C; for [U_{Total}] = 1.0 μM (Figure 2a), and for [U_{Total}] = 1.0 μM at CO_2 partial pressure of 0.01 atm [62].

were treated with uranium and shown to be capable of precipitating U(VI) as the phosphate containing mineral m-autunite [53]. The shift in pH from 2 to 4.5 changed the localization of uranium pricipitates from the cell surface to extracellular precipitates within the extracellular polysaccharides (EPS). In response to uranium stress, the stalk-forming aerobic soil microorganism *Caulobacter crescentus* was shown to accumulate uranyl phosphate materials that were identified as autunite [52]. These data suggest that many bacterial species have adaptations for resisting toxic metals. Sorption of uranium complexes onto bacterial cell surfaces may also be a feasible mechanism for groundwater uranium remediation. Other aerobic organisms shown to precipitate U(VI) via phosphatase activity include *Bacillus* and *Rahnella* spp. that were isolated from the Oak Ridge IFC site [54,55]. In an experiment using synthetic groundwater medium with glycerol-3-phosphate as the sole carbon and phosphorus source and 200 μM U(VI), *Bacillus* and *Rahnella* spp., which had demonstrated phosphatase activity, removed 95% and 73%, respectively, of the U(VI) from solution. *Arthrobacter* spp., which did not demonstrate phosphatase activity, were not able to precipitate U(VI) [54]. Geochemical analyses confirmed that the biotically precipitated uranium mineral was part of the autinite/meta-autinite group [55]. As pH increased, uranium hydroxide minerals were formed as well. Genetically modified subsurface *Pseudomonas* isolates that were engineered to overexpress a plasmid-expressed *phoA* gene have been investigated as possible candidates for enhanced biomineralization of uranium in contaminated groundwater [58]. Finally, uranyl sorption onto cell surfaces has been recognized as a factor in the fate and transport of uranium and has been demonstrated in the gram-positive aerobic soil bacterium *Bacillus subtilis* [63,64].

2.4.2 Uranium immobilization by facultative organisms. *Cellulomonas* spp. are gram-positive facultative anaerobes that have been shown to reduce heavy metals including Cr(VI), Fe(III), and U(VI) [65]. As a facultative organism, capable of living in aerobic and anaerobic conditions, two mechanisms for uranium immobilization have been reported for *Cellulomonas* sp. ES6 [61]. Geochemical conditions dictated whether uranium reduction or phosphate precipitation occurred in *Cellulomonas* sp. ES6. In the presence of AQDS, U(VI) was completely reduced to U(IV) but in PIPES-buffered medium, phosphate precipitates were the primary uranium precipitate [61]. *Pseudomonas* species CRB5 is a facultative organisms which was isolated from a chromate-contaminated wood preservation site and shown to precipitate uranium both aerobically and anaerobically [66]. Uranium precipitates were shown to be associated with the cell envelope but phosphate was included in the medium and mineralogical analyses were not performed to confirm that uranium was reduced in either case. A facultatively anaerobic *Thermus* isolate capable of dissimilatory iron reduction as well as growth with oxygen and nitrate, was characterized for its ability perform dissimilatory reduction of U(VI) [67]. In the following year, U(VI) reduction was demonstrated, via AQDS, in the closely related organism *Deinococcus radiodurans*, the most radiation-resistant organism described to date [68]. *Salmonella subterranea* is a facultative anaerobic, acid-resistant bacterium that was isolated from the Oak Ridge IFC site (Area 1) and shown to reduce U(VI) in a washed cell suspension [69]. Experiments testing for phosphatase activity in any of these three facultative uranium-reducers were not reported. Finally, *Shewanella* spp. are facultative anaerobes which have been frequently implicated in environmental uranium reduction [49,51,70,71]. Respiratory processes involving c-

type cytochromes have been shown to be essential for U(VI) reduction in *S. oneidensis* MR-1 [72,73,74] and UO_2 has been shown to precipitate as extracellular nanoparticles [70]. Three *Shewanella* spp. (*S. alga* strain BrY, *S. putrefaciens* strain CN32, and *S. oneidensis* strain MR-1) were compared in a metal-reduction rate study by Liu et al. [75]. *S. putrefaciens* strain CN32 was isolated from an anaerobic aquifer in northwestern New Mexico, *S. oneidensis* strain MR-1 was isolated from anaerobic sediments of Oneida Lake [76], and *S. alga* strain BrY was isolated from the Great Bay estuary in New Hampshire [77]. Precipitates of U and Tc in association with the outer cell membrane and in the periplasm were associated with slow reduction rates of those to metals, when compared to Fe and Co precipitation. *S. putrefaciens* strain CN32 had the slowest U(VI) reduction rates in the study by Liu et al [75] but all *Shewanella* spp. demonstrated faster U(VI) reduction than *Geobacter metallireducens* strain GS-15, which was also included in the study. Since aerobic growth by *Shewanella* spp. is common, it is notable that *Shewanella putrefaciens* strain 200R has also been tested for U(VI) sorption under oxidative conditions, with pH titration tests for reversibility [78]. Results of *S. putrefaciens* sorption experiments indicated that U sorption onto *Shewanella* spp. is significant at environmentally relevant densities and pH values.

2.4.3 Uranium immobilization by anaerobic organisms.

Geobacter spp. are among the most commonly discussed U(VI)-reducing bacteria. As described above, *Geobacter metallireducens* strain GS-15 was included with *S. oneidensis* strain MR-1 in the first description of uranium-reduction by live bacteria [51]. A 2004 study of microbial reduction of U(VI) at the solid-water interface [79] investigated U(VI) reduction by another *Geobacter* species, *G. sulfurreducens.* Finally,

G. lovleyi strain SZ was isolated and characterized in 2006 [60] with a description of its ability to grow at the expense of U(VI) in 2007 [13]. These *Geobacter* spp. have demonstrated different levels of oxygen tolerance [80] but its U(VI)-reduction capability has been described under strictly anaerobic conditions. Another well-characterized group of anaerobic U(VI)-reducing organisms is the sulfate-reducing bacteria (SRB) [81,82,83]. *Desulfovibrio desulfuricans* was characterized for U(VI)-reduction during the same year as *G. metallireducens* and *S. oneidensis* with rates similar to those Fe(III)-reducing microorganisms [50]. Typically, cytochrome c_3 is implicated in U(VI)-reduction by *Desulfovibrio* spp. [84,85] but *Desulfosporosinus* is a U(VI)-reducing SRB that does not contain cytochrome c_3 [86]. The ability to obtain energy for growth by reducing U(VI) by a *Desulfotomaculum* strain has been the only one reported in a sulfate-reducing strain [87]. SRB are not completely anaerobic, as a group, but have many are strict anaerobes and all were classically characterized as anaerobic [88,89,90,91].

Another group of anaerobic bacteria with many characterized U(VI)-reducing strains is the gram-positive, spore-forming Clostridia [92]. The mechanism for U(VI) reduction is unclear but results suggest that the reducing power generated from glucose fermentation is responsible [19,92]. XPS and XANES studies showed that U(VI) was indeed reduced to U(IV) [93] so phosphatase activity can be ruled out. Several novel anaerobic genera and species have been added to the list of uranium-reducing organisms, indicating that uranium-reduction is not exclusive to any bacterial group. *Thermo-terrabacterium ferrireducens* is a thermophilic, gram-positive, anaerobic bacterium that has been shown to couple organtrophic growth to the reduction of U(VI) phosphate [94]. *Pyrobaculum islandicum* is an anaerobic hyperthermophilic *Archaean* that was initially

isolated from hydrothermal groundwater [95] and was shown to reduce U(VI) in cell suspensions with H_2 as electron donor [96]. Finally, uranium-reduction was demonstrated in *Termoanaerobacter* strains from deep subsurface environments of the Piceance Basin, Colorado [97].

2.5 Molecular mechanisms for bacterial metal reduction

Anaerobic metal-reduction, including reduction of uranium, is an energetically favorable reaction, which has been widely exploited for respiration by bacterial species, particularly in the case of Mn and Fe [98,99]. In fact, iron-reduction may have been one of the first forms of respiration on earth [100]. Redox-stratified environments such as those found in aquifer, rice paddy, and river sediments present a particularly conducive environment for organisms that are able to derive energy from the reduction of many oxidized metal species [101,102]. Many physiological and genetic studies investigating bacterial metal reduction have been conducted using model organisms from the *Shewanella* and *Geobacter* genera [Reviewed by; [98,101,103,104]]. Thus, the current molecular model for bacterial metal reduction is based primarily on data collected from *Shewanella* and *Geobacter* spp.

One major challenge associated with bacterial metal reduction pertains to the insoluble nature of many metal species [101]. The spatial requirements of insoluble metal reduction thus present many questions about how large numbers of individual cells are able to gain energy from minerals with limited surface area. Currently, three main mechanisms have been proposed to explain the insoluble metal reduction phenomenon [101]: (1) Direct electron transfer between cytochromes and metal surfaces occurs, at

the cell surface in some cases and facilitated by extracellular matrices in other cases, (2) Electron shuttles allow insoluble metals to be reduced extracellularly by redox-active compounds that can be transported across the cell membrane, and (3) Metals are solubilized extracellularly by chelating compounds that can be transported across the cell membrane. The first of the three explanations will be the primary focus of this discussion.

2.5.1 Membrane-bound respiratory components. Unlike respiration of soluble electron acceptors like oxygen, nitrate, and sulfate, which involves direct reduction of oxidized species by terminal reductases within the inner membrane, respiring solid electron acceptors requires some transfer of electrons to the outside of the cell. In many cases, metal oxides are thought to be reduced with the help of multiheme *c*-type cytochromes [105]. One of the proposed roles of the multiple hemes in these proteins is as an extracytoplasmic electron sink, which is thought to function as capacitors in environments with variable electron acceptor abundance [106]. In the case of *S. oneidensis*, a 21 kDa tetraheme cytochrome *c* (CymA) oxidizes menaquinol in the inner membrane [107] and then is thought to transfer electrons to an outer membrane decaheme cyotochrome *c* such as MtrA [108]. Another outer membrane decaheme c-type cytochrome involved in insoluble metal reduction by *S. oneidensis* is OmcA [109]. In fact, MtrA and OmcA are thought to form a complex that enhances metal reduction [110]. MtrA and OmcA have been identified in association with flexible extracellular structures [70].

Early studies in *Geobacter metallireducens* revealed that Fe(III) reduction was localized in the membrane [111]. Several multiheme *c*-type cytochromes have since been

implicated in metal oxide reduction by *G. sulfurreducens* [112,113,114]. OmcB was identified, via genome analysis, with another c-type cytochrome (OmcC) located at the end of a 10-kb chromosomal duplication consisting of two tandem three-gene clusters [113]. Both proteins were disrupted but only OmcB was shown to play a major role in Fe(III) reduction. OmcS, OmcT, OmcE are three outer-membrane c-type cytochromes, two of which were easily sheared from the outer surface of *G. sulfurreducens* and all of which seem to have important roles for reducing metal oxides but not chelated metal species [112]. OmpJ is not a cytochrome but a membrane-associated putative porin protein that was shown to be required for metal respiration [114]. Hence, *Geobacter* data are consistent with *Shewanella* data indicating that outer membrane multi-heme cytochromes, as well as other membrane-associated components, are critical for metal reduction by these two phylogenetically divergent organisms.

2.5.2 Nanowires. Recent modeling predictions have indicated that the maximum electron transfer distance between *S. oneidensis* OmcA and a surface covered with a monolayer of water is 9 Angstroms [115]. According to scanning tunneling and tunneling microscopy studies by Wigginton et al., electron transfer to hematite through small tetraheme cytochromes from *S. oneidensis* may occur over longer distances than those predicted by models [116,117,118]. Electron transfer distance, in any case, is shorter than the thickness of many biofilms. Thus, some mechanism must be employed in order to enable electron transfer through the thickness of several cells. One of the prevailing hypotheses for long-distance electron transfer is the nanowire. Two types of nanowires have been proposed [119,120]. In the case of *Shewanella oneidensis*, the proposed nanowire involves Type II secretion and appendages that range from 50 to >150

nm in diameter and are tens of microns long [120]. Along the length of the pilus-like appendages, *c*-type decaheme cytochromes MtrC and OmcA are positioned external to the cell. In contrast, the *G. sulfurreducens* nanowire involves flexible conductive proteins, free of cytochrome decoration [119]. The *Geobacter* nanowires are still similar to pili but, in this case, the proteins have much smaller diameter (less than 0.05 nm) [119]. Thus, while both models describe mechanisms for transferring electrons through biofilms [120,121], the nature of the extracellular structure is very different. Studies which explore further the role of conductive bacterial nanowires is warranted since many bacteria are expected to use this mechanisms for coordinating 3-dimensionally complex communities like biofilms [120].

2.6 Phenotypic differences among closely-related bacterial strains.

Historically, the term "strain" referred to "descendants of a single [bacterial] colony [122]." However, since the concept of "a single colony" is difficult to interpret from an ecological perspective, different "strains" have come to be determined by phenotypic or genotypic characteristics [123]." The modern definition of a "strain" refers to "a descriptive subdivision of a species [123]." In the current age of gene and genome sequences, the translation of the strain definition has become an issue of genetic variability, either genomic or 16S rRNA gene phylogeny, wherein a "strain" refers to different organisms within the same species (i.e., >94% different 16S rRNA gene sequence, >70% DNA-DNA hybridization, 95-96% amino acid identity) [124,125,126]. The concept of "strain" refers to the changing nature of bacteria over time [122], and the

concept that even closely related bacteria (i.e., within the same species) typically possess some genetic and, hence, phenotypic variation.

2.6.1 Population analyses in pathogenic bacteria. Strain-to-strain variations in phenotype have been frequently studied in pathogenic organisms, based particularly on pathogenicity phenotypes and can be used for epidemiological studies [127,128,129,130,131,132,133]. *Staphylococcus aureus,* for example, demonstrates a great deal of variability in short evolutionary time due to mobile genetic elements and clones differ substantially in their disease-evoking potentials [134]. *Salmonella* serovars have been compared between those which cause enteric fevers like typhoid, and those which cause gastroenteritis [135]. In addition, different *Salmonella enterica* serovars are associated with typhoidal diseases in cows, as opposed to fowl, mice, or humans [136]. Different *Mycobacterium tuberculosis* strains are associated with differential transmissibility, virulence, and clinical manifestations as well [137]. Changes in strain also dictate virulence of *Vibrio cholerae* outbreaks [138]. *Escherichia coli* isolates are pathogenic species that have frequently been studied in the environment, historically as indicators of faecal pollution [139] but, more recently, studies have shown that some strains of *E. coli* reproduce and persist outside animal hosts [140]. Walk et al. [140] demonstrated that particular *E. coli* genotypes are dominant in freshwater beaches and that they cluster together phylogenetically, representing an autochthonous clade of *E. coli* separate from the pathogenic strains.

Burkholderia cepacia complex bacteria are both opportunistic pathogens responsible for infections, particularly in cystic fibrosis patients, and organisms of ecological importance that break down pollutants and enhance crop growth [141,142]. In

some cases, clonally identical *B. cepacia* complex strains have been found both in the natural environment and in infected individuals, however, the majority of strains have been associated with either one or the other and the diversity of *B. cepacia* complex habitats is attributed to large genomes and huge genetic capacity [141]. Due to their prevalence in both medical and agricultural applications, environmental *Burkholderia* spp. are perhaps the most frequently studied environmental organisms when it comes to population biology and strain variability [142]. *Burkholderia* spp. are also interesting because of the discrepancy between DNA-DNA hybridization values and gene sequence similarity [143], indicative of frequent gene transfer/modification. Mulitlocus enzyme electrophoresis (MLEE) was used to study *B. cepacia* population isolated from a southeastern blackwater stream in 1995 and revealed extensive genetic mixing among strains and contributing preliminary data to the current understanding of horizontal gene transfer [144]. An environmental study of plant-associated *B. cepacia* complex species used a colony hybridization assay based on the variable V3 region of the 16S rRNA gene sequence combined with *recA*-targeted PCR [143]. The V3-targeted assay was able to distinguish strains sufficiently to examine strain distribution among individual maize plant rhizospheres and showed that strains varied both between plants and within a single plant's *B. cepacia* community. A study that compared *B. cepacia* communities between different crops (rice and maize) determined that crop-to-crop comparisons did uncover major changes in the community composition [145]. Based on *recA* sequences, Jacobs et

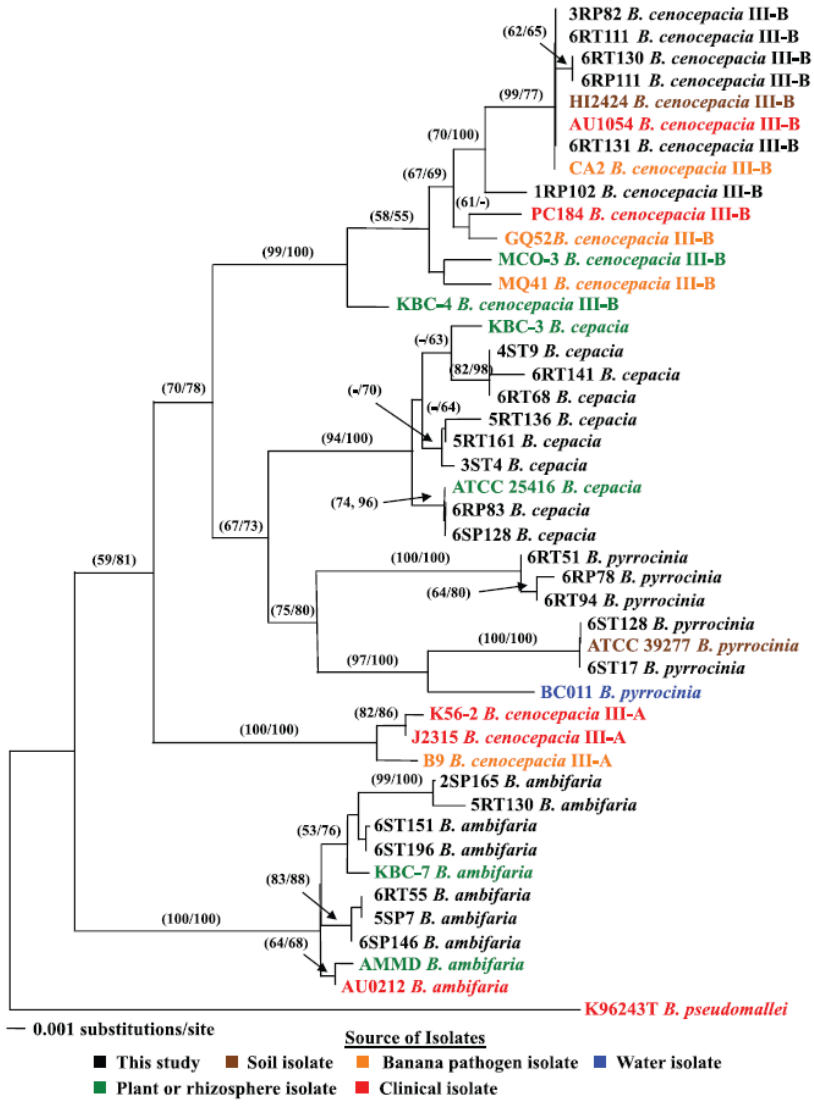

Figure 2.6. Phylogenetic analysis of *recA* gene sequences from 45 *B. cepacia* complex strains [146].

al. [146] grouped *B. cepacia* complex isolates to determine if a phylogenetic origin could be linked to ecotype but results suggest that pathogenicity and plant specificity are not reflected in *recA* gene phylogeny (Figure 2.6). Authors concluded that *B. cepacia* onion-associated strains are potential human pathogens [146]. Thus, in the case of *B. cepacia* complex strains, phylogeny is not a good indicator of phenotype.

2.6.2 Population analyses in environmentally relevant bacteria. While epidemiology has provided incentive for many studies of population genetics among pathogenic organisms, fewer studies have been conducted for environmentally relevant organisms, particularly those which are involved in bioremediation applications. *Anabaenopsis* strains isolated from Kenyan, Mexican, and Ugandan water bodies were compared phylogenetically and morphologically [147]. According to 16S rRNA gene sequence analysis, all fifteen of the studied isolates would fall into one species (>97.5%) but, according to morphology, and phylogenetic clustering, two species were proposed, *A. abijatae* and *A. elenkinii*. Several investigations of diversity within *Rhodopseudomonas palustris* isolates have also been reported [148,149,150]. Initially, 128 strains of purple nonsulfur bacteria were isolated from freshwater marsh sediments. Strong endemicity was implied by the data in this study, as well as a difference in benzoate degradation capacity [149]. More detailed examination of the *R. palustris* isolates specifically revealed a gradual decrease in 16S rRNA gene sequence similarity as a function of distance with phenotypic differences noted among strains. A follow-up study by Bent et al. [150] suggested that the distribution of *R. palustris* ecotypes was patchy, utilizing only strains which could grow on benzoate. Again, high levels of diversity were noted on a small spatial scale but genetic distance was not correlated with physical distance.

Cho and Tiedje [151] described biogeography of fluorescent *Pseudomonas* strains in soils using three molecular typing methods (16S rDNA restriction analysis [ARDRA], 16S-23S rDNA intergenic spacer-restriction fragment length polymorphism [ITS-RFLP], and repetitive extra-genic palindromic PCR genomic fingerprinting with a BOX primer set [BOX-PCR]). Data suggested that fluorescent *Pseudomonas* strains are strongly endemic (i.e., not globally mixed). A biological application which has seen the importance of phenotypic variation among strains is in the waste water treatment industry. *Candidatus* Accumulibacter strains, implicated in intracellular accumulation of inorganic phosphate in activated sludge, were analyzed for their natural distribution [152]. The *ppk1*gene was used as a phylogenetic marker to determine that habitats with similar characteristics were more likely to harbor similar Accumulibacter lineages than habitats that were geographically clustered. These data suggest that phenotypic differences play a role in the selection that governs distribution in closely related *Candidatus* Accumulibacter strains. *Dehalococcoides* 16S rRNA genes from chloroethene-contaminated sites were analyzed and authors conclude that members of three subgroups of the dechlorinating genus appear to be associated with specific sites [153]. The 16S rRNA gene for *Dehalococcoides* species is insufficient for describing function [154]. Instead, for determining the dechlorinating potential of *Dehalococcoides* strains, it is necessary to utilize genes which code for specific dechlorination capabilities (i.e., reductive dehalogenases genes) [155,156]. Thus, phenotypic variation at the strain level is critical in bioremediation capacity among *Dehalococcoides* spp. Among metal-reducing species, strain-to-strain variability is rarely described; however, the three closely related (>99% 16S rRNA gene sequence similarity) *Thermoanaerobacter* strains from

deep subsurface environments of the Piceance Basin, Colorado demonstrated metabolic variability in terms of electron donor utilization [97]. Strain-comparisons within *Geobacter* spp. and *Shewanella* spp. have not been conducted to our knowledge. Phenotypic comparisons between strains relevant for uranium-reduction are warranted to add credence to conclusions drawn from clone library data. In addition, strain characterization contributes to the overall body of scientific knowledge regarding the universality of traits in metal-reducing organisms.

2.7 References

1. Cole JR, Cascarelli AL, Mohn WW, Tiedje JM (1994) Isolation and characterization of a novel bacterium growing via reductive dehalogenation of 2-chlorophenol. Applied and Environmental Microbiology 60: 3536-3542.

2. Sanford RA, Cole JR, Tiedje JM (2002) Characterization and description of *Anaeromyxobacter dehalogenans* gen. nov., sp. nov., an aryl halorespiring facultative anaerobic Myxobacterium. Applied and Environmental Microbiology 68: 893-900.

3. Reichenbach H (1999) The ecology of the myxobacteria. Environmental Microbiology 1: 15-21.

4. Reichenbach H (2001) Myxobacteria, producers of novel bioactive substances. Journal of Industrial Microbiology & Biotechnology 27: 149-156.

5. Dworkin M (1996) Recent advances in the social and developmental biology of the myxobacteria. Microbiological Reviews 60: 70-102.

6. Shimkets L, Woese CR (1992) A phylogenetic analysis of the myxobacteria - Basis for their classification. Proceedings of the National Academy of Sciences of the United States of America 89: 9459-9463.

7. Löffler FE, Tiedje JM, Sanford RA (1999) Fraction of electrons consumed in electron acceptor reduction and hydrogen thresholds as indicators of halorepiratory physiology. Applied and Environmental Microbiology 65: 4049-4056.

8. Coates JD, Cole KA, Chakraborty R, O'Connor SM, Achenbach LA (2002) Diversity and ubiquity of bacteria capable of utilizing humic substances as electron donors for anaerobic respiration. Applied and Environmental Microbiology 68: 2445-2452.

9. Treude N, Rosencrantz D, Liesack W, Schnell S (2003) Strain FAc12, a dissimilatory iron-reducing member of the *Anaeromyxobacter* subgroup of Myxococcales. FEMS Microbiology Ecology 44: 261-269.

10. He Q, Sanford RA (2003) Characterization of Fe(III) reduction by chlororespiring *Anaeromyxobacter dehalogenans*. Applied and Environmental Microbiology 69: 2712-2718.

11. He Q, Sanford RA (2004) Acetate threshold concentrations suggest varying energy requirements during anaerobic respiration by *Anaeromyxobacter dehalogenans*. Applied and Environmental Microbiology 70: 6940-6943.

12. Wu Q, Sanford RA, Löffler FE (2006) Uranium(VI) reduction by *Anaeromyxobacter dehalogenans* strain 2CP-C. Applied and Environmental Microbiology 72: 3608-3614.

13. Sanford RA, Wu Q, Sung Y, Thomas SH, Amos BK, et al. (2007) Hexavalent uranium supports growth of *Anaeromyxobacter dehalogenans* and *Geobacter* spp. with lower than predicted biomass yields. Environmental Microbiology 9: 2885-2893.

14. Marshall MJ, Dohnalkova AC, Kennedy DW, Plymale AE, Thomas SH, et al. (2008) Electron donor-dependent radionuclide reduction and nanoparticle formation by *Anaeromyxobacter dehalogenans* strain 2CP-C. Environmental Microbiology 11: 534-543.

15. Borneman J, Triplett EW (1997) Molecular microbial diversity in soils from eastern Amazonia: Evidence for unusual microorganisms and microbial population shifts associated with deforestation. Applied and Environmental Microbiology 63: 2647-2653.

16. Stein LY, La Duc MT, Grundl TJ, Nealson KH (2001) Bacterial and archaeal populations associated with freshwater ferromanganous micronodules and sediments. Environmental Microbiology 3: 10-18.

17. Brofft JE, McArthur JV, Shimkets LJ (2002) Recovery of novel bacterial diversity from a forested wetland impacted by reject coal. Environmental Microbiology 4: 764-769.

18. Lueders T, Wagner B, Claus P, Friedrich MW (2004) Stable isotope probing of rRNA and DNA reveals a dynamic methylotroph community and trophic interactions with fungi and protozoa in oxic rice field soil. Environmental Microbiology 6: 60-72.

19. Petrie L, North NN, Dollhopf SL, Balkwill DL, Kostka JE (2003) Enumeration and characterization of iron(III)-reducing microbial communities from acidic subsurface sediments contaminated with uranium(VI). Applied and Environmental Microbiology 69: 7467-7479.

20. North NN, Dollhopf SL, Petrie L, Istok JD, Balkwill DL, et al. (2004) Change in bacterial community structure during *in situ* biostimulation of subsurface sediment cocontaminated with uranium and nitrate. Applied and Environmental Microbiology 70: 4911-4920.

21. Cardenas E, Wu WM, Leigh MB, Carley J, Carrol lS, et al. (2008) Microbial communities in contaminated sediments, associated with bioremediation of uranium to submicromolar levels. Applied and Environmental Microbiology 74: 3718-3729.

22. Wu W-M, Carley J, Luo J, Ginder-Vogel MA, Cardenas E, et al. (2007) *In situ* bioreduction of uranium (VI) to submicromolar levels and reoxidation by dissolved oxygen. Environmental Science & Technology 41: 5716-5723.

23. Riley RG, Zachara JM, Wobber FJ (1992) Chemical Contaminants on DOE Lands and Selection of Contaminant Mixtures for Subsurface Science Research. DOE/ER-0547T, US Department of Energy, Washington, DC.

24. Fendorf S, Konopka A, Kostka JE, Lovley DR, Metting B, et al. (2003) Bioremediation of metals and radionuclides...what it is and how it works. U.S. Department of Energy LBNL-42595.

25. Watson DB, Kostka JE, Fields MW, Jardine PM (2004) The Oak Ridge Field Research Center conceptual model. http://www.esd.ornl.gov/orifrc/: U.S. Department of Energy.

26. Brooks SC (2001) Waste characteristics of the former S-3 ponds and outline of uranium chemistry relevant to NABIR Field Research Center studies. Oak Ridge, TN: U.S. Department of Energy ORNL/TM-2001/27.

27. Watson DB, Roh Y (2004) Natural and Accelerated Bioremediation Research (NABIR) Field Research Center (FRC) Site Characterization Plan Addendum 1. US Department of Energy ORNL/TM-2004/56.

28. Istok JD, Senko JM, Krumholz LR, Watson D, Bogle MA, et al. (2004) In situ bioreduction of technetium and uranium in a nitrate-contaminated aquifer. Environmental Science & Technology 38: 468-475.

29. Akob DM, Mills HJ, Kostka JE (2007) Metabolically active microbial communities in uranium-contaminated subsurface sediments. FEMS Microbiology Ecology 59: 95-107.

30. Akob DM, Mills HJ, Gihring TM, Kerkhof L, Stucki JW, et al. (2008) Functional diversity and electron donor dependence of microbial populations capable of U(VI) reduction in radionuclide-contaminated subsurface sediments. Applied and Environmental Microbiology 74: 3159-3170.

31. Bond DR, Mester T, Nesbo CL, Izquierdo-Lopez AV, Collart FL, et al. (2005) Characterization of citrate synthase from *Geobacter sulfurreducens* and evidence for a family of citrate synthases similar to those of eukaryotes throughout the *Geobacteraceae*. Applied and Environmental Microbiology 71: 3858-3865.

32. Spain AM, Peacock AD, Istok JD, Elshahed MS, Najar FZ, et al. (2007) Identification and isolation of a *Castellaniella* species important during

biostimulation of an acidic nitrate- and uranium-contaminated aquifer. Applied and Environmental Microbiology 73: 4892-4904.

33. Madden AS, Smith AC, Balkwill DL, Fagan LA, Phelps TJ (2007) Microbial uranium immobilization independent of nitrate reduction. Environmental Microbiology 9: 2321-2330.

34. Gu BH, Watson DB, Wu LY, Phillips DH, White DC, et al. (2002) Microbiological characteristics in a zero-valent iron reactive barrier. Environmental Monitoring and Assessment 77: 293-309.

35. Michalsen MM, Peacock AD, Spain AM, Smithgal AN, White DC, et al. (2007) Changes in microbial community composition and geochemistry during uranium and technetium bioimmobilization. Applied and Environmental Microbiology 73: 5885-5896.

36. Luo J, Cirpka OA, Fienen MN, Wu WM, Mehlhorn TL, et al. (2006) A parametric transfer function methodology for analyzing reactive transport in nonuniform flow. Journal of Contaminant Hydrology 83: 27-41.

37. Luo J, Weber F-A, Cirpka OA, Wu W-M, Nyman JL, et al. (2007) Modeling *in situ* uranium(VI) bioreduction by sulfate-reducing bacteria. Journal of Contaminant Hydrology 92 129–148.

38. Luo J, Wu WM, Fienen MN, Jardine PM, Mehlhorn TL, et al. (2006) A nested-cell approach for in situ remediation. Ground Water 44: 266-274.

39. Wu W-M, Carley J, Fienen M, Mehlhorn T, Lowe K, et al. (2006) Pilot-scale *in situ* bioremediation of uranium in a highly contaminated aquifer. 1. Conditioning of a treatment zone. Environmental Science & Technology 40: 3978-3985.

40. Wu W-M, Gu B, Fields MW, Gentile M, Ku Y-K, et al. (2005) Uranium (VI) reduction by denitrifying biomass. Bioremediation Journal 9: 49-61.

41. Wu WM, Carley J, Gentry T, Ginder-Vogel MA, Fienen M, et al. (2006) Pilot-scale *in situ* bioremedation of uranium in a highly contaminated aquifer. 2. Reduction of U(VI) and geochemical control of U(VI) bioavailability. Environmental Science & Technology 40: 3986-3995.

42. Anderson RT, Vrionis HA, Ortiz-Bernad I, Resch CT, Long PE, et al. (2003) Stimulating the in situ activity of *Geobacter* species to remove uranium from the groundwater of a uranium-contaminated aquifer. Applied and Environmental Microbiology 69: 5884-5891.

43. Elias DA, Krumholz LR, Wong D, Long PE, Suflita JM (2003) Characterization of microbial activities and U reduction in a shallow aquifer contaminated by uranium mill tailings. Microbial Ecology 46: 83-91.

44. Yabusaki SB, Fang Y, Long PE, Resch CT, Peacock AD, et al. (2007) Uranium removal from groundwater via *in situ* biostimulation: Field-scale modeling of transport and biological processes. Journal of Contaminant Hydrology 93: 216-235.

45. Suzuki Y, Kelly SD, Kemner KA, Banfield JF (2003) Microbial populations stimulated for hexavalent uranium reduction in uranium mine sediment. Applied and Environmental Microbiology 69: 1337-1346.

46. Lloyd JR, Renshaw JC (2005) Bioremediation of radioactive waste: radionuclide-microbe interactions in laboratory and field-scale studies. Current Opinion in Biotechnology 16: 254-260.

47. Wall JD, Krumholz LR (2006) Uranium reduction. Annual Review of Microbiology 60: 149-166.

48. Woolfolk CA, Whiteley HR (1962) Reduction of Inorganic Compounds with Molecular Hydrogen by *Micrococcus lactilyticus*.1. Stoichiometry Compounds of Arsenic, Selenium, Tellurium, Transition and Other Elements. Journal of Bacteriology 84: 647-&.

49. Gorby YA, Lovley DR (1992) Enzymatic Uranium Precipitation. Environmental Science & Technology 26: 205-207.

50. Lovley DR, Phillips EJP (1992) Reduction of Uranium by *Desulfovibrio desulfuricans*. Applied and Environmental Microbiology 58: 850-856.

51. Lovley DR, Phillips EJP, Gorby YA, Landa ER (1991) Microbial Reduction of Uranium. Nature 350: 413-416.

52. Hu P, Brodie EL, Suzuki Y, McAdams HH, Andersen GL (2005) Whole-genome transcriptional analysis of heavy metal stresses in *Caulobacter crescentus*. Journal of Bacteriology 187: 8437-8449.

53. Jroundi F, Merroun ML, Arias JM, Rossberg A, Selenska-Pobell S, et al. (2007) Spectroscopic and microscopic characterization of uranium biomineralization in *Myxococcus xanthus*. Geomicrobiology Journal 24: 441-449.

54. Martinez RJ, Beazley MJ, Taillefert M, Arakaki AK, Skolnick J, et al. (2007) Aerobic uranium (VI) bioprecipitation by metal-resistant bacteria isolated from radionuclide- and metal-contaminated subsurface soils. Environmental Microbiology 9: 3122-3133.

55. Beazley MJ, Martinez RJ, Sobecky PA, Webb SM, Taillefert M (2007) Uranium biomineralization as a result of bacterial phosphatase activity: Insights from bacterial isolates from a contaminated subsurface. Environmental Science & Technology 41: 5701-5707.

56. Lovley DR, Chapelle FH, Woodward JC (1994) Use of Dissolved H_2 Concentrations to Determine the Distribution of Microbially Catalyzed Redox Reactions in Anoxic Groundwater Environmental Science & Technology 28: 1205-1211.

57. Jerden JL, Sinha AK (2003) Phosphate based immobilization of uranium in an oxidizing bedrock aquifer. Applied Geochemistry 18: 823-843.

58. Powers LG, Mills HJ, Palumbo AV, Zhang CL, Delaney K, et al. (2002) Introduction of a plasmid-encoded phoA gene for constitutive overproduction of alkaline phosphatase in three subsurface *Pseudomonas* isolates. FEMS Microbiology Ecology 41: 115-123.

59. Dawid W (2000) Biology and global distribution of myxobacteria in soils. FEMS Microbiology Reviews 24: 403-427.

60. Sung Y, Fletcher KF, Ritalaliti KM, Apkarian RP, Ramos-Hernandez N, et al. (2006) *Geobacter lovleyi* sp nov strain SZ, a novel metal-reducing and tetrachloroethene-dechlorinating bacterium. Applied and Environmental Microbiology 72: 2775-2782.

61. Sivaswamy V (2005) Uranium immobilization by *Cellulomonas* sp. ES6: Washington State University. 96 p.

62. Langmuir D (1978) Uranium solution-mineral equilibria at low temperatures with applications to sedimentary ore deposits. Geochimica Et Cosmochimica Acta 42: 547-569.

63. Fowle DA, Fein JB, Martin AM (2000) Experimental study of uranyl adsorption onto *Bacillus subtilis*. Environmental Science & Technology 34: 3737-3741.

64. Fowle DA, Fein JB (2000) Experimental measurements of the reversibility of metal-bacteria adsorption reactions. Chemical Geology 168: 27-36.

65. Sani RK, Peyton BM, Smith WA, Apel WA, Peterson JN (2002) Dissimilatory reduction of Cr(VI), Fe(III), and U(VI) by *Cellulomonas* isolates. Applied Microbiology and Biotechnology 60: 192-199.

66. McLean J, Beveridge TJ (2001) Chromate Reduction by a Pseudomonad Isolated from a Site Contaminated with Chromated Copper Arsenate. Applied and Environmental Microbiology 67: 1076-1084.

67. Kieft TL, Fredrickson JK, Onstott TC, Gorby YA, Kostandarithes HM, et al. (1999) Dissimilatory reduction of Fe(III) and other electron acceptors by a *Thermus* isolate. Applied and Environmental Microbiology 65: 1214-1221.

68. Fredrickson JK, Kostandarithes HM, Li SW, Plymale AE, Daly MJ (2000) Reduction of Fe(III), Cr(VI), U(VI), and Tc(VII) by *Deinococcus radiodurans* R1. Applied and Environmental Microbiology 66: 2006-2011.

69. Shelobolina ES, Sullivan SA, O'Neill KR, Nevin KP, Lovley DR (2004) Isolation, characterization, and U(VI)-reducing potential of a facultatively anaerobic, acid-resistent bacterium from low-pH, nitrate- and U(VI)-contaminated subsurface sediment description of *Salmonella subterranea* sp. nov. Applied and Environmental Microbiology 70: 2959-2965.

70. Marshall MJ, Beliaev AS, Dohnalkova AC, Kennedy DW, Shi L, et al. (2006) *c*-Type cytochrome-dependent formation of U(VI) nanoparticles by *Shewanella oneidensis*. PLoS Biology 4: e268.

71. Wade R, DiChristina TJ (2000) Isolation of U(VI) reduction-deficient mutants of *Shewanella putrefaciens*. FEMS Microbiology Letters 184: 143-148.

72. Beliaev AS, Saffarini DA (1998) *Shewanella putrefaciens mtrB* Encodes an Outer Membrane Protein Required for Fe(III) and Mn(IV) Reduction. Journal of Bacteriology 180: 6292-6297.

73. Dale JR, Wade R, Dichristina TJ (2007) A conserved histidine in cytochrome c maturation permease CcmB of *Shewanella putrefaciens* is required for anaerobic growth below a threshold standard redox potential. Journal of Bacteriology 189: 1036-1043.

74. Beliaev AS, Saffarini DA, McLaughlin JL, Hunnicutt D (2001) MtrC, an outer membrane decahaem *c* cytochrome required for metal reduction in *Shewanella putrefaciens* MR-1. Molecular Microbiology 39: 722-730.

75. Liu C, Gorby YA, Zachara JM, Fredrickson JK, Brown CF (2002) Reduction kinetics of Fe(III), Co(III), U(VI), Cr(VI), and Tc(VII) in cultures of dissimilatory metal-reducing bacteria. Biotechnology and Bioengineering 80: 637-649.

76. Myers CR, Nealson KH (1988) Bacterial manganese reduction and growth with manganese oxide as the sole electron acceptor. Science 240: 1319-1321.

77. Caccavo F, Blakemore RP, Lovley DR (1992) A hydrogen-oxidizing, Fe(III)-reducing microorganism from the Great Bay estuary, New Hampshire. Applied and Environmental Microbiology 58: 3211-3216.

78. Haas JR, Dichristina TJ, Wade R (2001) Thermodynamics of U(VI) sorption onto *Shewanella putrefaciens*. Chemical Geology 180: 33-54.

79. Jeon B-H, Kelly SD, Kemner KM, Barnett MO, Burgos WD, et al. (2004) Microbial reduction of U(VI) at the solid-water interface. Environmental Science & Technology 38: 5649-5655.

80. Lin WC, Coppi MV, Lovley DR (2004) *Geobacter sulfurreducens* can grow with oxygen as a terminal electron acceptor. Applied and Environmental Microbiology 70: 2525-2528.

81. Pietzsch K, Babel W (2003) A sulfate-reducing bacterium that can detoxify U(VI) and obtain energy via nitrate reduction. Journal of Basic Microbiology 43: 348-361.

82. Lovley DR, Roden EE, Phillips EJP, Woodward JC (1993) Enzymatic iron and uranium reduction by sulfate-reducing bacteria. Marine Geology 113: 41-53.

83. Ganesh R, Robinson KG, Reed GD, Sayler GS (1997) Reduction of hexavalent uranium from organic complexes by sulfate- and iron-reducing bacteria. Applied and Environmental Microbiology 63: 4385-4391.

84. Lovley DR, Widman PK, Woodward JC, Phillips EJP (1993) Reduction of uranium by cytochrome-c(3) of *Desulfovibrio vulgaris*. Applied and Environmental Microbiology 59: 3572-3576.

85. Payne RB, Gentry DM, Rapp-Giles BJ, Casalot L, Wall JD (2002) Uranium reduction by *Desulfovibrio desulfuricans* strain G20 and a cytochrome c_3 mutant. Applied and Environmental Microbiology 68: 3129-3132.

86. Suzuki Y, Kelly SD, Kemner KM, Banfield JF (2004) Enzymatic U(VI) reduction by *Desulfosporosinus* species. Radiochimica Acta 92: 11-16.

87. Tebo BM, Obraztsova AY (1998) Sulfate-reducing bacterium grows with Cr(VI), U(VI), Mn(IV), and Fe(II) as electron acceptors. FEMS Microbiology Letters 162: 193-198.

88. Brune A, Frenzel P, Cypionka H (2000) Life at the oxic-anoxic interface: Microbial activities and adaptations. FEMS Microbiology Reviews 24: 691-710.

89. Cypionka H (2000) Oxygen respiration by *Desulfovibrio* species. Annual Review of Microbiology 54: 827-848.

90. Krekeler D, Teske A, Cypionka H (1998) Strategies of sulfate-reducing bacteria to escape oxygen stress in a cyanobacterial mat. FEMS Microbiology Ecology 25: 89-96.

91. Marschall C, Frenzel P, Cypionka H (1993) Influence of Oxygen on Sulfate Reduction and Growth of Sulfate-Reducing Bacteria. Archives of Microbiology 159: 168-173.

92. Gao W, Francis AJ (2008) Reduction of uranium(VI) to uranium(IV) by Clostridia. Applied and Environmental Microbiology 74: 4580-4584.

93. Francis AJ, Dodge CJ, Lu F, Halada GP, Clayton CR (1994) XPS and XANES studies of uranium reduction by *Clostridium* spp. Environmental Science & Technology 28: 636-639.

94. Khijniak TV, Slobodkin AI, Coker V, Renshaw JC, Livens FR, et al. (2005) Reduction of uranium(VI) phosphate during growth of the thermophilic bacterium *Thermoterrabacterium ferrireducens*. Applied and Environmental Microbiology 71: 6423-6426.

95. Huber R, Kristjansson JK, Stetter KO (1987) *Pyrobaculum* gen. nov., a new genus of neutrophilic, rod-shaped archaebacteria from continental solfataras growing optimally at 100°C. Archives of Microbiology 149: 95-101.

96. Kashefi K, Lovley DR (2000) Reduction of Fe(III), Mn(IV), and toxic metals at 100°C by *Pyrobaculum islandicum*. Applied and Environmental Microbiology 66: 1050-1056.

97. Roh Y, Liu SV, Li G, Huang H, Phelps TJ, et al. (2002) Isolation and characterization of metal-reducing *Thermoanaerobacter* strains from deep subsurface environments of the Piceance Basin, Colorado. Applied and Environmental Microbiology 68: 6013-6020.

98. Lovley DR, Holmes DE, Nevin KP (2004) Dissimilatory Fe(III) and Mn(IV) reduction. Advances in Microbial Physiology, Vol 49 49: 219-286.

99. Lovley DR (1991) Dissimilatory Fe(III) and Mn(Iv) Reduction. Microbiological Reviews 55: 259-287.

100. Vargas M, Kashefi K, Blunt-Harris EL, Lovley DR (1998) Microbiological evidence for Fe(III) reduction on early Earth. Nature 395: 65-67.

101. Dichristina TJ, Fredrickson JK, Zachara JM (2005) Enzymology of electron transport: Energy generation with geochemical consequences. Reviews in Mineralogy and Geochemistry 59: 27-52.

102. Himmelheber DW, Thomas SH, Loeffler FE, Taillefert M, Hughes JB (2009) Microbial Colonization of an *In Situ* Sediment Cap and Correlation to Stratified Redox Zones. Environmental Science & Technology 43: 66-74.

103. Fredrickson JK, Romine MF, Beliaev AS, Auchtung JM, Driscoll ME, et al. (2008) Towards environmental systems biology of *Shewanella*. Nature Reviews Microbiology 6: 592-603.

104. Fredrickson JK, Zachara JM (2008) Electron transfer at the microbe-mineral interface: a grand challenge in biogeochemistry. Geobiology 6: 245-253.

105. Shi L, Squier TC, Zachara JM, Fredrickson JK (2007) Respiration of metal (hydr)oxides by *Shewanella* and *Geobacter*: a key role for multihaem c-type cytochromes. Molecular Microbiology 65: 12-20.

106. Esteve-Nunez A, Sosnik J, Visconti P, Lovley DR (2008) Fluorescent properties of *c*-type cytochromes reveal their potential role as an extracytoplasmic electron sink in *Geobacter sulfurreducens*. Environmental Microbiology 10: 497-505.

107. Myers JM, Myers CR (2000) Role of the tetraheme cytochrome CymA in anaerobic electron transport in cells of *Shewanella putrefaciens* MR-1 with normal levels of menaquinone. Journal of Bacteriology 182: 67-75.

108. Beliaev A, Saffarini DA, McLaughlin JL, Hunnicutt D (2001) MtrC, an outer membrane decahaem *c* cytochrome required for metal reduction in *Shewanella putrefaciens* MR-1. Molecular Microbiology 39: 722-730.

109. Myers JM, Myers CR (2001) Role for outer membrane cytochromes OmcA and OmcB of *Shewanella putrefaciens* MR-1 in reduction of manganese dioxide. Applied and Environmental Microbiology 67: 260-269.

110. Shi L, Chen BW, Wang ZM, Elias DA, Mayer MU, et al. (2006) Isolation of a high-affinity functional protein complex between OmcA and MtrC: Two outer membrane decaheme c-type cytochromes of Shewanella oneidensis MR-1. Journal of Bacteriology 188: 4705-4714.

111. Gorby YA, Lovley DR (1991) Electron-transport in the dissimilatory iron reducer, GS-15. Applied and Environmental Microbiology 57: 867-870.

112. Mehta T, Coppi MV, Childers SE, Lovley DR (2005) Outer membrane *c*-type cytochromes required for Fe(III) and Mn(IV) oxide reduction in *Geobacter sulfurreducens*. Applied and Environmental Microbiology 71: 8634-8641.

113. Leang C, Coppi MV, Lovley DR (2003) OmcB, a *c*-type polyheme cytochrome, involved in Fe(III) reduction in *Geobacter sulfurreducens*. Journal of Bacteriology 185: 2096-2103.

114. Afkar E, Reguera G, Schiffer M, Lovley DR (2005) A novel *Geobacteraceae*-specific outer membrane protein J (OmpJ) is essential for electron transport to Fe (III) and Mn (IV) oxides in *Geobacter sulfurreducens*. BMC Microbiology 5.

115. Neal AL, Rosso KM, Geesey GG, Gorby YA, Little BJ (2003) Surface structure effects on direct reduction of iron oxides by Shewanella oneidensis. Geochimica Et Cosmochimica Acta 67: 4489-4503.

116. Wigginton NS, Rosso KM, Stack AG, Hochella MF (2009) Long-Range Electron Transfer across Cytochrome-Hematite (alpha-Fe2O3) Interfaces. Journal of Physical Chemistry C 113: 2096-2103.

117. Wigginton NS, Rosso KM, Hochella MF (2007) Mechanisms of electron transfer in two decaheme cytochromes from a metal-reducing bacterium. Journal of Physical Chemistry B 111: 12857-12864.

118. Wigginton NS, Rosso KM, Lower BH, Shi L, Hochella MF (2007) Electron tunneling properties of outer-membrane decaheme cytochromes from Shewanella oneidensis. Geochimica Et Cosmochimica Acta 71: 543-555.

119. Reguera G, McCarthy KD, Mehta T, Nicoll JS, Tuominen MT, et al. (2005) Extracellular electron tranfer via microbial nanowires. Nature 435: 1098-1101.

120. Gorby YA, Yanina S, McLean JS, Rosso KM, Moyles D, et al. (2006) Electrically conductive bacterial nanowires produced by *Shewanella oneidensis* strain MR-1 and other microorganisms. Proceedings of the National Academy of Sciences of the United States of America 103: 11358-11363.

121. Reguera G, Nevin KP, Nicoll JS, Covalla SF, Woodard TL, et al. (2006) Biofilm and nanowire production leads to increased current in *Geobacter sulfurreducens* fuel cells. Applied and Environmental Microbiology 72: 7345-7348.

122. Dijkshoorn L, Ursing BM, Ursing JB (2000) Strain, clone and species: comments on three basic concepts of bacteriology. Journal of Medical Microbiology 49: 397-401.

123. Tenover F, Arbeit R, Goering R, Mickelsen P, Murray B, et al. (1995) Interpreting chromosomal DNA restriction patterns produced by pulsed- field gel electrophoresis: criteria for bacterial strain typing. J Clin Microbiol 33: 2233-2239.

124. Konstantinidis KT, Tiedje JM (2005) Genomic insights that advance the species definition for prokaryotes. Proceedings of the National Academy of Sciences of the United States of America 102: 2567-2572.

125. Konstantinidis KT, Tiedje JM (2005) Towards a genome-based taxonomy for prokaryotes. Journal of Bacteriology 187: 6258-6264.

126. Stackebrandt E, Frederiksen W, Garrity GM, Grimont PAD, Kampfer P, et al. (2002) Report of the ad hoc committee for the re-evaluation of the species definition in bacteriology. International Journal of Systematic and Evolutionary Microbiology 52: 1043-1047.

127. Musser JM, Schlievert PM, Chow AW, Ewan P, Kreiswirth BN, et al. (1990) A Single Clone of *Staphylococcus aureus* Causes the Majority of Cases of Toxic Shock Syndrome. Proceedings of the National Academy of Sciences of the United States of America 87: 225-229.

128. Selander RK, Levin BR (1980) Genetic Diversity and Structure in *Escherichia coli* Populations. Science 210: 545-547.

129. Ochman H, Whittam TS, Caugant DA, Selander RK (1983) Enzyme Polymorphism and Genetic Population-Structure in *Escherichia coli* and *Shigella*. Journal of General Microbiology 129: 2715-2726.

130. Whittam TS, Ochman H, Selander RK (1983) Multilocus Genetic-Structure in Natural-Populations of *Escherichia coli*. Proceedings of the National Academy of Sciences of the United States of America-Biological Sciences 80: 1751-1755.

131. Caugant DA, Mocca LF, Frasch CE, Froholm LO, Zollinger WD, et al. (1987) Genetic Structure of *Neisseria meningitidis* Populations in Relation to Serogroup, Serotype, and Outer-Membrane Protein Pattern. Journal of Bacteriology 169: 2781-2792.

132. Caugant DA, Zollinger WD, Mocca LF, Frasch CE, Whittam TS, et al. (1987) Genetic Relationships and Clonal Population Structure of Serotype-2 Strains of *Neisseria meningitidis*. Infection and Immunity 55: 1503-1513.

133. Beltran P, Plock SA, Smith NH, Whittam TS, Old DC, et al. (1991) Reference collection of strains of the *Salmonella typhimurium* complex from natural populations. Journal of General Microbiology 137: 601-606.

134. Holtfreter S, Grumann D, Schmudde M, Nguyen HTT, Eichler P, et al. (2007) Clonal distribution of superantigen genes in clinical *Staphylococcus aureus* isolates. Journal of Clinical Microbiology 45: 2669-2680.

135. Selander RK, Beltran P, Smith NH, Helmuth R, Rubin FA, et al. (1990) Evolutionary Genetic Relationships of Clones of *Salmonella* Serovars That Cause Human Typhoid and Other Enteric Fevers. Infection and Immunity 58: 2262-2275.

136. Pullinger GD, Dziva F, Charleston B, Wallis TS, Stevens MP (2008) Identification of *Salmonella enterica* Serovar Dublin Specific Sequences by Subtractive Hybridization and Analysis of Their Role in Intestinal Colonization and Systemic Translocation in Cattle. Infection and Immunity 76: 5310-5321.

137. Mathema B, Kurepina N, Fallows D, Kreiswirth BN (2008) Lessons from molecular epidemiology and comparative genomics. Seminars in Respiratory and Critical Care Medicine 29: 467-480.

138. Chokesajjawatee N, Zo YG, Colwell RR (2008) Determination of clonality and relatedness of *Vibrio cholerae* isolates by genomic fingerprinting, using long-range repetitive element sequence-based PCR. Applied and Environmental Microbiology 74: 5392-5401.

139. Yang HH, Vinopal RT, Grasso D, Smets BF (2004) High diversity among environmental *Escherichia coli* isolates from a bovine feedlot. Applied and Environmental Microbiology 70: 1528-1536.

140. Walk ST, Alm EW, Calhoun LM, Mladonicky JM, Whittam TS (2007) Genetic diversity and population structure of *Escherichia coli* isolated from freshwater beaches. Environmental Microbiology 9: 2274-2288.

141. Mahenthiralingam E, Baldwin A, Dowson CG (2008) *Burkholderia cepacia* complex bacteria: opportunistic pathogens with important natural biology. Journal of Applied Microbiology 104: 1539-1551.

142. Compant S, Nowak J, Coenye T, Clement C, Barka EA (2008) Diversity and occurrence of *Burkholderia* spp. in the natural environment. FEMS Microbiology Reviews 32: 607-626.

143. Ramette A, LiPuma JJ, Tiedje JM (2005) Species abundance and diversity of *Burkholderia cepacia* complex in the environment. Applied and Environmental Microbiology 71: 1193-1201.

144. Wise MG, Shimkets LJ, Mcarthur JV (1995) Genetic Structure of a Lotic Population of *Burkholderia* (*Pseudomonas*) *cepacia*. Applied and Environmental Microbiology 61: 1791-1798.

145. Zhang LX, Xie GL (2007) Diversity and distribution of *Burkholderia cepacia* complex in the rhizosphere of rice and maize. FEMS Microbiology Letters 266: 231-235.

146. Jacobs JL, Fasi AC, Ramette A, Smith JJ, Hammerschmidt R, et al. (2008) Identification and onion pathogenicity of *Burkholderia cepacia* complex isolates from the onion rhizosphere and onion field soil. Applied and Environmental Microbiology 74: 3121-3129.

147. Ballot A, Dadheech PK, Haande S, Krienitz L (2008) Morphological and phylogenetic analysis of *Anabaenopsis abijatae* and *Anabaenopsis elenkinii* (Nostocales, Cyanobacteria) from tropical inland water bodies. Microbial Ecology 55: 608-618.

148. Oda Y, Star B, Huisman LA, Gottschal JC, Forney LJ (2003) Biogeography of the purple nonsulfur bacterium *Rhodopseudomonas palustris*. Applied and Environmental Microbiology 69: 5186-5191.

149. Oda Y, Wanders W, Huisman LA, Meijer WG, Gottschal JC, et al. (2002) Genotypic and phenotypic diversity within species of purple nonsulfur bacteria isolated from aquatic sediments. Applied and Environmental Microbiology 68: 3467-3477.

150. Bent SJ, Gucker CL, Oda Y, Forney LJ (2003) Spatial distribution of *Rhodopseudomonas palustris* ecotypes on a local scale. Applied and Environmental Microbiology 69: 5192-5197.

151. Cho JC, Tiedje JM (2000) Biogeography and degree of endemicity of fluorescent *Pseudomonas* strains in soil. Applied and Environmental Microbiology 66: 5448-5456.

152. Peterson SB, Warnecke F, Madejska J, McMahon KD, Hugenholtz P (2008) Environmental distribution and population biology of *Candidatus* Accumulibacter, a primary agent of biological phosphorus removal. Environmental Microbiology 10: 2692-2703.

153. Hendrickson ER, Payne JA, Young RM, Starr MG, Perry MP, et al. (2002) Molecular analysis of Dehalococcoides 16S ribosomal DNA from chloroethene-contaminated sites throughout north America and Europe. Applied and Environmental Microbiology 68: 485-495.

154. He JZ, Ritalahti KM, Yang KL, Koenigsberg SS, Löffler FE (2003) Detoxification of vinyl chloride to ethene coupled to growth of an anaerobic bacterium. Nature 424: 62-65.

155. Ritalahti KM, Amos BK, Sung Y, Wu QZ, Koenigsberg SS, et al. (2006) Quantitative PCR targeting 16S rRNA and reductive dehalogenase genes simultaneously monitors multiple *Dehalococcoides* strains. Applied and Environmental Microbiology 72: 2765-2774.

156. Holmes VF, He JZ, Lee PKH, Alvarez-Cohen L (2006) Discrimination of multiple *Dehalococcoides* strains in a trichloroethene enrichment by quantification of their reductive dehalogenase genes. Applied and Environmental Microbiology 72: 5877-5883.

CHAPTER 3: The mosaic genome of *Anaeromyxobacter dehalogenans* strain 2CP-C suggests an aerobic common ancestor to the delta-Proteobacteria

Abstract

Anaeromyxobacter dehalogenans strain 2CP-C is a versaphilic delta-Proteobacterium distributed throughout many diverse soil and sediment environments. 16S rRNA gene phylogenetic analysis groups *A. dehalogenans* together with the myxobacteria, which have distinguishing characteristics including strictly aerobic metabolism, sporulation, fruiting body formation, and surface motility. Analysis of the 5.01 Mb strain 2CP-C genome substantiated that this organism is a myxobacterium but shares genotypic traits with the anaerobic majority of the delta-Proteobacteria (i.e., the *Desulfuromonadales*). Reflective of its respiratory versatility, strain 2CP-C possesses 68 genes coding for putative c-type cytochromes, including one gene with 40 heme binding motifs. Consistent with its relatedness to the myxobacteria, surface motility was observed in strain 2CP-C and multiple types of motility genes are present, including 28 genes for gliding, adventurous (A-) motility and 17 genes for type IV pilus-based motility (i.e., social (S-) motility) that all have homologs in *Myxococcus xanthus*. Although *A. dehalogenans* shares many metabolic traits with the anaerobic majority of the delta-Proteobacteria, strain 2CP-C grows under microaerophilic conditions and possesses detoxification systems for reactive oxygen species. Accordingly, two gene clusters coding for NADH dehydrogenase subunits and two cytochrome oxidase gene clusters in strain 2CP-C are similar to those in *M. xanthus.* Remarkably, strain 2CP-C possesses a

third NADH dehydrogenase gene cluster and a cytochrome cbb_3 oxidase gene cluster, apparently acquired through ancient horizontal gene transfer from a strictly anaerobic green sulfur bacterium. The mosaic nature of the *A. dehalogenans* strain 2CP-C genome suggests that the metabolically versatile, anaerobic members of the delta-Proteobacteria may have descended from aerobic ancestors with complex lifestyles.

3.1 Introduction

Classification of the eubacterial domain remains a major challenge in prokaryotic taxonomy. Lateral gene transfer events introduce complexity that current classification methods rarely capture [1,2]. 16S rRNA gene phylogeny is unreliable for predicting physiology but this analysis does typically provide information about an organism's evolutionary history [3,4]. When applied to genomic analyses, phylogeny deduced from the 16S rRNA gene sequence provides a framework for using genomic information to interpret evolution by distinguishing derived traits from those of a common ancestor. *Anaeromyxobacter dehalogenans* strains were initially isolated from pristine soils based on their ability to derive energy from reductive dechlorination of chlorophenols [5,6]. Characteristic for *A. dehalogenans* strains is great respiratory versatility including metal and radionuclide reduction and recent efforts have yielded additional isolates from contaminated subsurface environments and agricultural soils [7-10]. *Anaeromyxobacter* spp. are the first anaerobes that group with the order *Myxococcales* (traditionally called 'myxobacteria') according to 16S rRNA gene phylogeny.

Despite the dominance of anaerobes in the delta-Proteobacteria class, bacteria designated as myxobacteria have been unified as strict aerobes (reviewed in [11]).

Myxobacteria are adapted to aerobic soil environments with changing nutrient availability. Myxobacteria form spores and fruiting bodies in response to unfavorable conditions, and use gliding motility and communal wolf pack behavior for predatory lifestyle [11,12]. Many myxobacteria species are able to feed on and defend against other microorganisms using exoenzymes (e.g., proteases, nucleases, lipases, glucanases). Myxobacteria also produce secondary metabolites such as stigmatellin, saframycin, and myxovirescin with antifungal and antibacterial activities [13]. A common feature of myxobacteria is their extraordinary ability to sense and respond to complex environmental stimuli. For example, a multi-input signal transduction cascade tightly regulates fruiting body development and sporulation [14-16]. Additional characteristics that have been used to describe myxobacteria include large genome sizes around 10 Mb and high G+C contents in the range of 66-72% [11,12]. Members of the *Myxococcales* include *Sorangium cellulosum*, *Stigmatella aurantiaca*, and the most extensively studied laboratory organism of this group, *Myxococcus xanthus*, which was the first to have a sequenced genome [17,18]. Research on the nonpathogenic, free-living soil bacterium *M. xanthus* has led to the elucidation of many phenomena that were previously not known to exist in the prokaryotic domain such as coordinated social behavior, complex signal transduction networks, unique and complex motility mechanisms, and contact signaling [19]. Many of these complex and costly traits are lost in the absence of evolutionary pressure (e.g., following repeated transfers in rich medium) indicating their importance for survival in the soil environment [20]. Based on these unique observable traits, the myxobacteria were expected to constitute a distinct bacterial taxonomic domain [21]. When 16S rRNA gene classification placed the myxobacteria within the delta-

Proteobacteria comprising bacteria whose primary distinction was anaerobic respiratory versatility rather than morphological and behavioral ingenuity, questions arose as to how such diversity originated within a coherent phylogenetic group (i.e., the delta-Proteobacteria) [22].

We used the genome sequence of *A. dehalogenans* strain 2CP-C (Accession number: CP000251) for comparative analysis with delta-Proteobacteria that share similar physiology (i.e., *Geobacteraceae*) and two phylogenetically closely related, aerobic myxobacteria. The genome analysis demonstrated that strain 2CP-C shares traits with strictly aerobic myxobacteria and anaerobic delta-Proteobacteria. The analysis provides evidence for ancient horizontal gene transfer from another bacterial domain and supports the hypothesis that respiratory versatility in *A. dehalogenans* is a derived trait, one that was gained after splitting from an aerobic ancestor that is common to the myxobacteria and possibly the entire delta-Proteobacteria class. We propose that the common ancestor of *M. xanthus* and *A. dehalogenans* was a facultative aerobe with an intermediate genome size of high G+C content that was capable of gliding motility, advanced signaling, sporulation, and flagellar motility.

3.2 Results and Discussion

3.2.1 Taxonomic classification. The contributions of horizontal gene transfer (HGT) to bacterial evolution and speciation are currently unclear and estimates range from minimal to very relevant [2,4]. Although the 16S rRNA gene is not immune from transfer between organisms [23], it is generally accepted that this gene is a phylogenetic marker that depicts evolutionary history in most

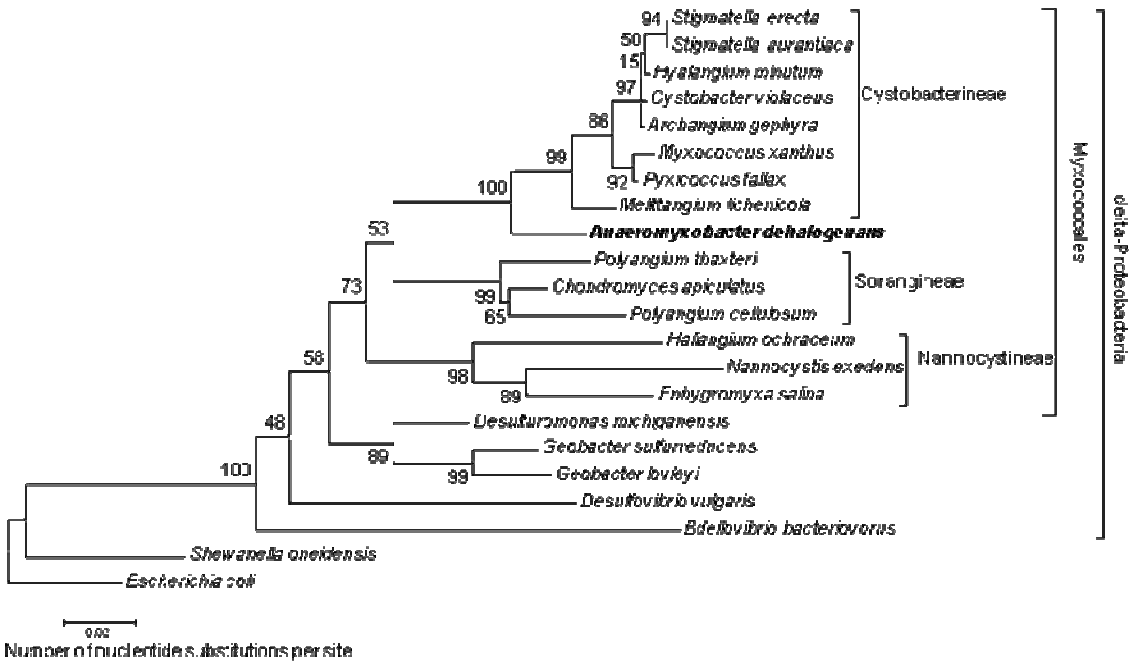

Figure 3.1. 16S rRNA gene-based phylogenetic tree of the delta-Proteobacteria indicates that *A. dehalogenans* strain 2CP-C is deeply nested in the order Myxococcales. Neighbor-joining bootstrap values (500 replicates) are indicated at each branch. Class, order, and suborder designations are indicated on the right side.

cases [3]. According to 16S rRNA gene phylogeny, *A. dehalogenans* is a delta-Proteobacterium that is deeply nested in the order Myxococcales (Figure 3.1). Surprisingly, the *Anaeromyxobacter* suborder falls between the *Cystobacterineae* and the other two suborders, *Sorangineae* and *Nannocystineae*, implying that *A. dehalogenans* bears more relation to *M. xanthus* than the other two myxobacteria suborders (Figure 3.1). In accordance with this phylogenetic placement, 24.3% of genes on the strain 2CP-C genome have their highest top non-paralogous similarities (i.e., *E* values $<10^{-4}$ based on the Bacterial Genome Subset, see Materials and Methods for details) to *M. xanthus* and 17.9% are most similar to genes in *Stigmatella aurantiaca* (Figure 3.2; Table 3.1). Only 6.4% of similar genes are shared between *A. dehalogenans* and the physiologically comparable delta-Proteobacterium *Geobacter sulfurreducens* (Figure 3.2; Table 3.1). About half of the total number of predicted genes had highest similarity to genes outside of the delta-Proteobacteria. No single organism outside the delta-Proteobacteria contributed more than 1.7% of the *Anaeromyxobacter* genome. For example, 1.7% of genes were similar to sequenced *Acidobacterium* genes, which make up an abundant but poorly understood phylum of acid-tolerant bacteria recently postulated to be a sister group to the delta-Proteobacteria [24-26]. Since the highest top non-paralogous similarity may not be statistically valid as the best estimate of closest relationship when there are several functional domains, 140 multi-domain proteins of particular functional

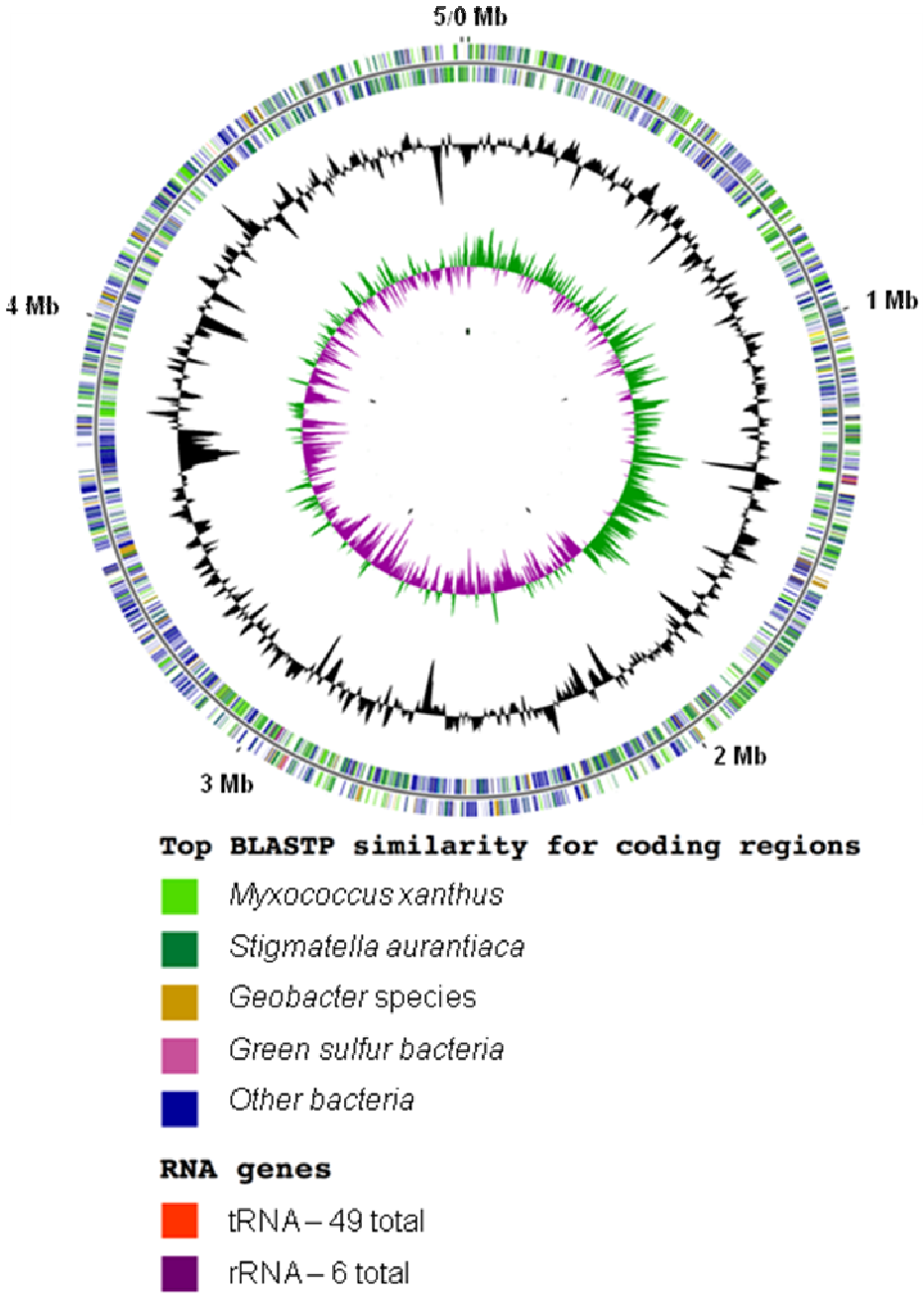

Figure 3.2. The *Anaeromyxobacter dehalogenans* strain 2CP-C complete genome with genes color-coded to indicate putative ancestry. Genome positions are indicated on the outside of the circle. The color legend refers to the two outer circles. The outer circle indicates predicted coding regions on the plus strand colored according to the organism that carries a gene with greatest sequence similarity. The second circle indicates predicted coding regions on the minus strand also color coded by gene similarity. The third circle (black) shows variation in G+C content with the average G+C value as the center line. The innermost circle (green and purple) depicts GC skew with the average GC skew as the center line.

Table 3.1. *Anaeromyxobacter dehalogenans* strain 2CP-C genome summary. Values indicated are based on both analyses from this study as well as automated annotation reflected in the NCBI genome database.

Species	***Anaeromyxobacter dehalogenans***
Strain	2CP-C
Taxonomic position	Myxococcales
Accession number	CP000251
Size, bp	5,013,479
G+C content	74.91%
G+C content in coding areas	74.82%
G+C content in areas outside putative phage regions	75.21%
Predicted number of open reading frames	4,346
Hypothetical proteins	1,236
CDS* with top BLAST hits to *Myxococcus xanthus*	1,057 (24.3%)
CDS with top BLAST hits to *Stigmatella aurantiaca*	737 (17.9%)
CDS with top BLAST hits to Myxobacteria	1,794 (41.2%)
CDS with top BLAST hits to *Geobacter* spp.	282 (6.4%)
CDS with top BLAST hits in *Acidobacteria* spp.	75 (1.7%)
Average CDS length	1050
% of genome coding	91
rRNA operons	2
rRNA genes	6
tRNA genes	49
Structural RNAs	58
Regions of deviating G+C content	15
Phage-related regions	10
rRNA or tRNA-coding regions	3
Low G+C regions of unknown origin	2

interest were analyzed for the potential for multiple origins. Only three of the analyzed proteins (2.1%) demonstrated mixed origin. Our multi-domain sequence analysis suggests that genes of mixed origin do not occur frequently enough in the *A. dehalogenans* genome to affect the results of our large-scale analysis (Figure 3.2; Table 3.1).

In order to use whole genome information to verify the remarkable evolutionary relationship between *A. dehalogenans* and the myxobacteria implied by 16S rRNA gene phylogeny, phenetic classification was performed based on the presence or absence of genes coding for enzymes with known function. Phenetic trees based on (putative) enzymatic capabilities have been used to classify organisms according to ecological niches occupied across all three domains of life [27]. This genome sequence-based classification divides the delta-Proteobacteria along the aerobic/anaerobic boundary and groups strain 2CP-C with the aerobes *M. xanthus* and *Bdellovibrio bacteriovorus* (Figure 3.3). The many genes associated with aerobic and predatory lifestyles present on the strain 2CP-C genome confirm the evolutionary relationship implied by 16S rRNA gene phylogeny and support classification of this organism as a member of the myxobacteria. Thus, phenetic classification puts forward the hypothesis that anaerobic metabolism is a derived trait in *A. dehalogenans*.

In order to test hypotheses regarding the evolutionary history in *A. dehalogenans,* we analyzed the strain 2CP-C genome for genes consistent with phylogeny as well as those consistent with physiology. Results indicate that the strain 2CP-C genome is made up of both, genes coding for known myxobacterial functions (i.e., predation, sporulation, motility, signaling) and genes that correspond to a versatile respiratory lifestyle.

3.2.2 Features of the **A. dehalogenans** *Strain 2CP-C Genome.*

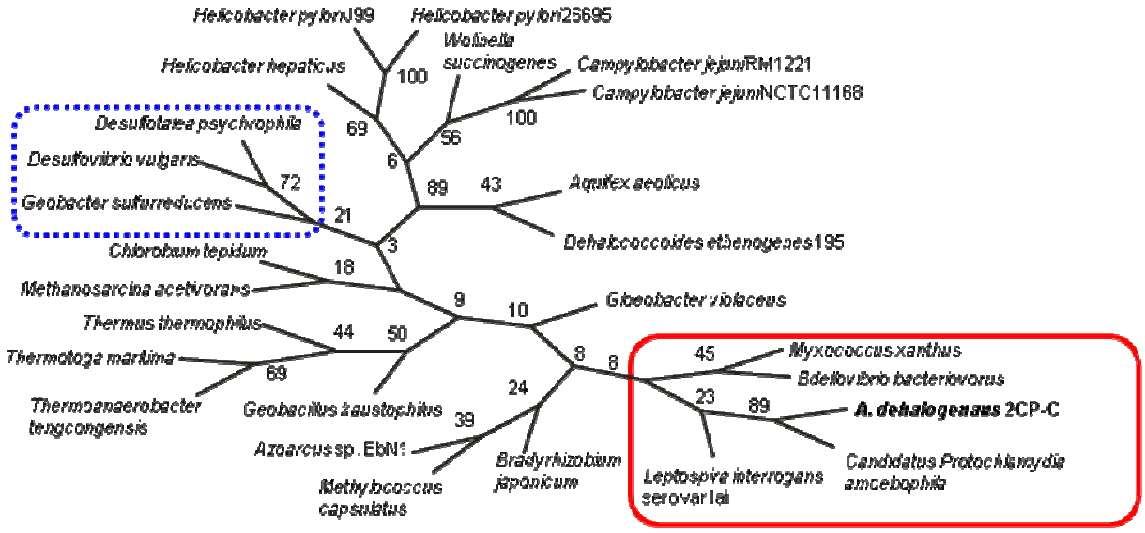

Figure 3.3. Phenetic, enzyme-based classification groups *A. dehalogenans* strain 2CP-C with aerobic organisms (red box). The blue dashed line box indicates the anaerobic delta-Proteobacteria included in the analysis. Bootstrap values are indicated at each node.

The *A. dehalogenans* strain 2CP-C genome consists of a single, closed circular chromosome with 5,013,482 base pairs encoding 4,287 candidate protein-encoding genes (Table 3.1; Figure 3.2). The genome includes two copies each of the rRNA genes in two paralogous gene clusters and 49 tRNA genes distributed throughout the genome.

The genome has a remarkably high G+C content of 74.9%, among the highest G+C percentage of any described organism. Organisms with similarly high G+C percentages, *Micrococcus luteus* (75%) and *Streptomyces griseus* (75%), are Gram-positive Actinobacteria. Among the Gram-negative bacteria, traditional myxobacteria are the only described organisms with high G+C content [11]. *M. xanthus* genomic DNA contains 68% G+C while the genomes of organisms in the suborders *Sorangineae* and *Cystobacterineae* range from 70-72% and 64-70%, respectively. Haywood-Farmer and Otto [28] recently presented a Brownian motion model to explain G+C content variation in closely related organisms, demonstrating that G+C content variation can be used to estimate the time lapsed since divergence from a common ancestor. Based on this model, G+C content suggests that *A. dehalogenans* is evolutionarily closer to the myxobacteria than to other delta-Proteobacteria families and that *A. dehalogenans* shares a common ancestor with the entire clade of myxobacteria, rather than representing an evolutionary intermediate (data not shown).

The higher than average G+C content facilitates the identification of recent gene acquisitions, as foreign DNA typically has lower G+C content. To begin HGT analysis, a total of 15 regions (including tRNA- and rRNA-coding regions) were identified having G+C contents below 70% (Figure 3.2, Table 3.2). Ten out of the 15 lower G+C regions contain genes with sequence similarities to phage- or transposon-related genes with *E*

Table 3.2. Putative Horizontal Gene Transfer (HGT) regions based on deviating G+C content and Minimum Codon Adaptation Index (MCAI)

HGT calculation was based on phylogenetic origin of lower G+C regions and regions of low codon adaptation index in the *A. dehalogenans* strain 2CP-C genome. Ten out of 15 G+C regions below 70% contain genes with sequence similarities to phage- or transposon-related genes with *E* values less than 0.01. Four additional putative HGT regions were identified by codon adaptation index. The genome average MCAI is 0.729.

Approximate position (bp included in total HGT)	G+C %	MCAI
651,423-657,132 (5,709 bp)	61.8	0.283 Adeh_0563
1,140,945-1,146,257 (5,310 bp)	75.2	0.698 Adeh_0991
1,193,693-1,196,312 (2,619 bp)	73.3	0.362 Adeh_1037
1,619,133-1,625,971 (6,838 bp)	65.4	0.253 Adeh_1408
1,684,675-1,687,653 (2,978 bp)	69.7	0.312 Adeh_1463
1,813070-1,829,454 Not included in total	67.0	0.673
1,997,218-200,1552 Not included in total	68.1	0.552
2,034,615-2,058,673 (24,058 bp)	74.9	0.228 Adeh_1794
2,097,739-2,111,883 (14,144 bp)	66.5	0.263 Adeh_1845
2,128,510-2,143,067 (14,557 bp)	70.5	0.356 Adeh_1876
2,168,208-2,174,240 Not included in total	69.5	0.690
2,177,427-2,204,940 Not included in total	69.5	0.689
2,619,127-2,632,994 (13,867 bp)	63.5	0.345 Adeh_2326
3,244,090-3,251,195 (7,105 bp)	69.2	0.436 Adeh_2868
3,661,055-3,733,532 (72,477 bp)	67.0	0.210 Adeh_3214
3,962,432-3,956,308 (6,124 bp)	67.5	0.269 Adeh_3442
4,064,430-4,090,399 (26,079 bp)	65.4	0.263 Adeh_3537
4,143,301-4,164,184 (20,883 bp)	69.9	0.231 Adeh_3618
4,437,523-4,447,517 (9,994 bp)	68.7	0.341 Adeh_3864
4,917,551-4,928,537 (10,986 bp)	62.4	0.205 Adeh_4278
Total HGT=243,728 bp		

values of less than 0.01 (NCBI non-redundant database). No significant dinucleotide compositional difference was detected between low G+C regions and average G+C regions, indicating long residence time of horizontally-acquired sequences within the host genome [29]. However, rare codon usage in low G+C regions supports the hypothesis that these regions were horizontally transferred (Table 3.2). Based on G+C content and codon usage as indicators of recent HGT events, our analyses suggest that less than 0.2 Mb (4%) of the strain 2CP-C genome is attributed to HGT. These methods will likely fail to identify ancient HGT events because it is impossible to trace these genes' ancestral history, especially in cases where they were not maintained in other delta-Proteobacteria. Interestingly, gene locus Adeh_1877 has a BLASTP hit with 29% sequence identity to a *Myxococcus* phage Mx8 gene (*E* value = 9×10^{-10}) suggesting that *A. dehalogenans* may be subject to infection by myxobacteria phages. In contrast to the limited HGT events in strain 2CP-C, HGT contributed at least 1.4 Mb of the 9.0 Mb (almost 16%) genome of *M. xanthus* (9). In addition to extensive HGT, frequent duplication events are manifested in the *M. xanthus* genome, which account for another 1.4 Mb [30]. The cause of the remaining 1.3 Mb genome size difference between *M. xanthus* and *A. dehalogenans* is documented in the GC skew of the strain 2CP-C genome.

In most eubacterial circular chromosomes, the excess of guanine relative to cytosine on the leading replicating strand (i.e., GC skew) aids in the detection of the origin and terminus of replication (23, 24). The origin and terminus are typically situated 180 degrees to each other on a circular chromosome [31]. However, the strain 2CP-C leading strand is about 1.5 Mb shorter than the lagging strand (Figure 3.2). This remarkable lack of symmetry may be a remnant of a large deletion event. An

approximately 1.5 Mb contiguous region on the *M. xanthus* genome (position 4,300,000-5,800,000) codes for enzyme systems involved in secondary metabolism [30]. Secondary metabolite production, a signature feature of myxobacteria, is lacking in known *A. dehalogenans* strains and represents one of the major physiological differences between *A. dehalogenans* and traditional myxobacteria. The presence of secondary metabolite gene clusters in the common ancestor, and subsequent loss in *A. dehalogenans*, would explain the asymmetry between leading and lagging strand, as well as the genome size discrepancy with traditional myxobacteria.

These findings suggest that a hypothetical common ancestor to *M. xanthus* and *A. dehalogenans* had a genome of intermediate size that was both expanded by HGT and duplication events to 9.0 Mb in *M. xanthus* and trimmed, by one or more deletions, to 5.0 Mb in *A. dehalogenans*. The remaining 5.0 Mb of the strain 2CP-C genome reflect both the evolutionary history and respiratory innovation characteristic for the delta-Proteobacteria.

3.3.3 Mosaic nature of the genome. Genes consistent with taxonomy together with those lacking counterparts in sequenced genomes of members of the Myxococcales order illustrate the mosaic nature of the strain 2CP-C genome. The sequence similarity of nearly half of the strain 2CP-C genes to myxobacterial genes roots *A. dehalogenans* in its taxonomic order while the foreign genes, which share highest similarities to genes from phylogenetically and physiologically diverse bacterial groups, elucidate the causes of functional diversity in this taxonomically coherent group.

3.3.3.1 Predation and sporulation. Predation and sporulation are common features of previously characterized myxobacteria and these functions were used as defining traits

for the taxon [32]. Unfortunately, the genes required for predation have been largely unexplored. Based on the knowledge available, the genes required for predation include *asgA*, *asgC*, *asgE*, *sdeK*, *csgA*, *frzABEFZ*, and the A motility system (specific genes tested include *aglB* and *cglB*) [33]. While predation has not been observed with *A. dehalogenans*, the *frz* genes and several A motility genes are present on the 2CP-C genome, and genes encoding chaperones and proteases implicated in predatory behavior in *M. xanthus* are present in multiple copies on the 2CP-C genome (Tables 3.3 and 3.4; [30]). Other predation genes including A- and C-signal genes were not found on the *A. dehalogenans* genome (e.g., *asgA, csgA*). Experimentally, predation has not been confirmed so it is unclear if *A. dehalogenans* is capable of a modified form of predation, if those genes have alternate functions, or if the genes are remnants of a formerly complete set of genes required for predatory lifestyle.

Like predation, sporulation has not been observed in *A. dehalogenans* under laboratory conditions. In contrast to the predation genes, of which the necessary complement is unknown, a known cadre of genes is required for sporulation in *M. xanthus.* Strain 2CP-C possesses putative gene homologs responsible for sporulation in *M. xanthus*, though essential genes for fruiting body development and sporulation in *M. xanthus* (e.g., *devRS* and *fruCD*) [34,35] are lacking in strain 2CP-C. The presence of sporulation genes implies that *A. dehalogenans* once possessed the ability to sporulate but the paucity of genes remaining, and the lack of experimental evidence for sporulation,

Table 3.3. Genes for adventurous motility proteins on the *A. dehalogenans* strain 2CP-C genome imply that this type of motility is present. *E* values and identities given refer to *M. xanthus* sequences. Many of the gliding motility genes identified in *M. xanthus* are present in *A. dehalogenans* strain 2CP-C but whether or not the genes present are sufficient to produce gliding motility is unknown.

Protein name	*E* value	Identity*
AglR	e-76	147/244 (60%)
AglS	e-34	76/168 (45%)
AglT	e-68	166/460 (66%)
AglU	e-47	171/536 (31%)
AglW	e-107	202/430 (46%)
AglX	e-72	135/238 (56%)
AglZ*	e-41	219/583 (37%)
AgmA	e-66	191/578 (33%)
AgmB	Sequence not available	
AgmC	e-37	90/185 (48%)
AgmD	e-48	125/346 (36%)
AgmE	e-108	196/315 (62%)
AgmF	e-78	155/262 (59%)
AgmG	No similar *A. dehalogenans* protein	
AgmH	e-60	123/277 (43%)
AgmI	e-37	112/288 (38%)
AgmJ	No similar *A. dehalogenans* protein	
AgmK	0	1119/2521 (44%)
AgmL	0	327/429 (76%)
AgmM	e-23	88/298 (29%)
AgmN	No similar *A. dehalogenans* protein	
AgmO	No similar *A. dehalogenans* protein	
AgmP	e-48	122/307 (39%)
AgmQ	No similar *A. dehalogenans* protein	
ArmR	e-96	191/370 (51%)
AgmS	e-37	101/250 (40%)
AgmT	e-18	83/304 (27%)
AgmU	0	474/1231 (38%)
AgmV	e-13	227/796 (28%)
AgmW	e-102	205/436 (47%)
AgmX	e-76	215/683 (31%)
AgmY	Sequence not available	
AgmZ	e-8	42/129 (32%)
CglB	No similar *A. dehalogenans* protein	
MglA	e-97	171/195 (87%)

* Percent identities represent the number of amino acids of the *A. dehalogenans* translated protein that are common with its *M. xanthus* protein counterpart divided by the total number of amino acids in the comparison.

Table 3.4. The *A. dehalogenans* strain 2CP-C genome contains multiple copies of protease and chaperone genes. The *E* values and identities refer to a comparison with *M. xanthus* genes. Of the 19 genes identified encoding proteolytic enyzmes in the strain 2CP-C genome, 14 have homologs in *M. xanthus*.

Protein name	*E* value	Identity*
LonB1	No *M. xanthus* homolog	
Lon2	0	674/803 (83%)
LonC3	No *M. xanthus* homolog	
Lon4	e-24	73/157 (46%)
FtsH1	0	423/634 (66%)
FtsH2	0	416/606 (68%)
FtsH3	*S. aurantiaca* homolog only (e-147)	
DnaJ1	e-38	93/218 (42%)
DnaJ2	No *M. xanthus* homolog	
DnaJ3	e-73	213/512 (41%)
DnaJ4	No *M. xanthus* homolog	
DnaJ5	e-14	42/68 (61%)
DnaJ6	e-37	92/176 (52%)
DnaJ7	No *M. xanthus* homolog	
DnaJ8	e-113	215/370 (58%)
ClpX1	0	344/424 (81%)
ClpX2	0	332/415 (80%)
DnaK1	0	484/635 (76%)
DnaK2	e-153	473/938 (50%)
DnaK3	0	474/606 (78%)

* Percent identities represent the number of amino acids of the *A. dehalogenans* translated protein that are common with its *M. xanthus* protein counterpart divided by the total number of amino acids in the comparison.

suggest that this behavior has been lost. Sporulation is a mechanism to survive unfavorable environmental conditions, which, in the case of the surface soil-dwelling myxobacteria, includes desiccation and rapidly changing nutritional conditions. Thus, differences in the genomes of two related organisms (i.e., presence versus absence of a complete set of sporulation genes) reflect a divergence in ecological niche speciation and survival strategy.

3.3.3.2 Surface motility. Motility in strain 2CP-C occurs on solid surfaces (Figure 3.4), resembling the pattern of social motility observed in *M. xanthus* [36]. Many of the adventurous (A-) motility genes identified in *M. xanthus* are present in strain 2CP-C (Table 3.3) but whether or not these genes are sufficient for A-motility is unclear. Type IV pilus-based social (S-) motility, encoded by *pil* genes, is also partially responsible for *M. xanthus*' ability to move along surfaces (such as soil particles) [37]. Synteny and homology for the *pil* genes is shared between *M. xanthus* and strain 2CP-C (Figure 3.5A). Additionally, at least eight other genes implicated in social motility in *M. xanthus* have sequence similarity to genes on the strain 2CP-C genome. Interestingly, these genes are located in the region of the *M. xanthus* genome (position 4,300,000-5,800,000) that is absent in *A. dehalogenans* suggesting that gene rearrangement prior to the deletion event or gene acquisition following the deletion event have occurred. In any case, motility gene synteny and homology imply that *M. xanthus* and *A. dehalogenans* share a common ancestor that used type-IV pilus-based S-motility.

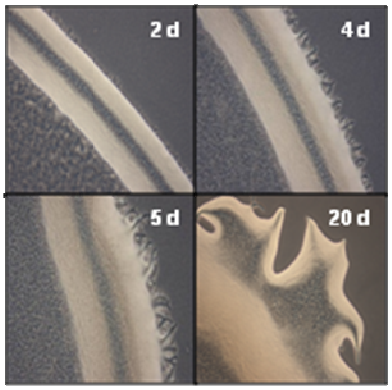

Figure 3.4. *A. dehalogena*ns strain 2CP-C colony edges magnified 100-fold bear evidence of gliding motility. Flares characteristic of gliding motility began forming after 2 days of incubation.

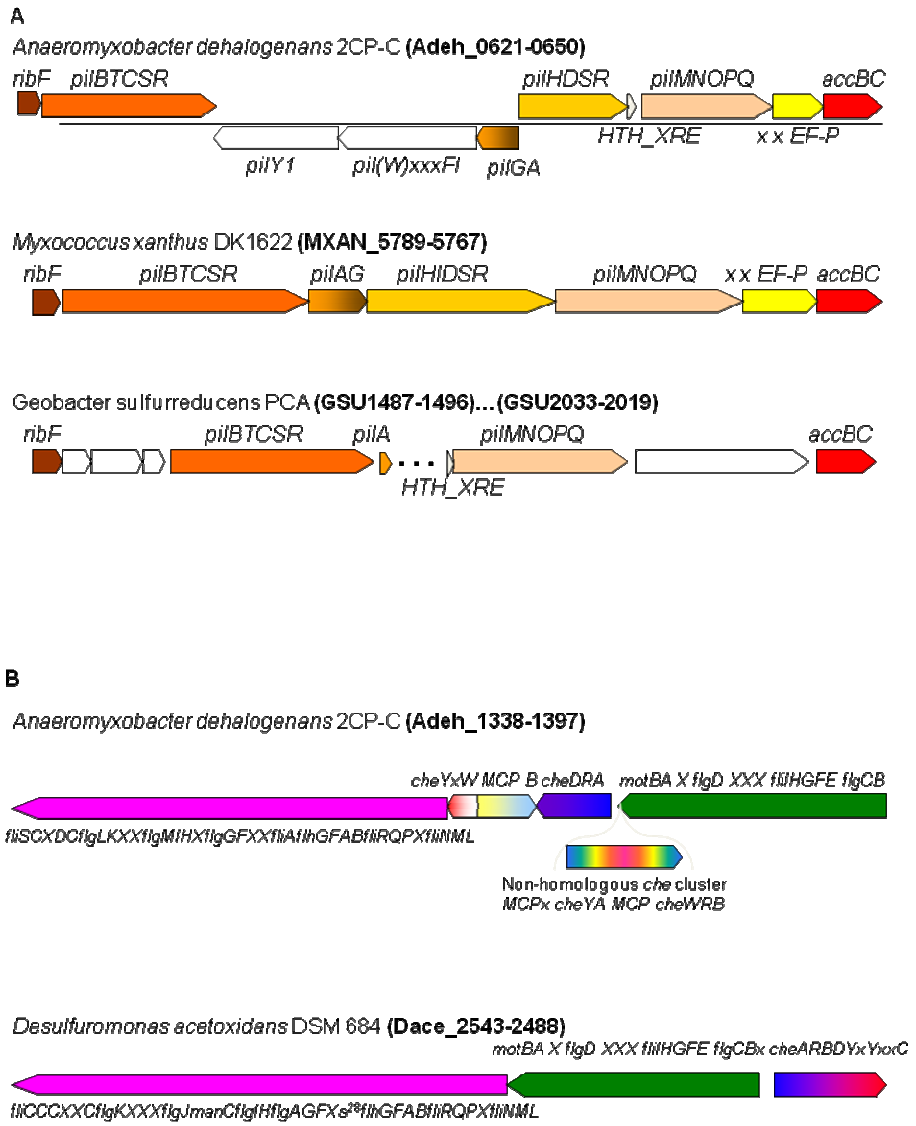

Figure 3.5. Gene orders of motility gene clusters of *A. dehalogenans* strain 2CP-C suggest diverse ancestry. Locus ID tags for the gene clusters are given in parentheses. Color-coding of bars indicates clusters with similar gene order. White, unlabelled genes/gene clusters are not conserved between the organisms.

(A) Type IV pilus-based motility clusters of A. *dehalogenans* strain 2CP-C are syntenous with *M. xanthus*, and *G. sulfurreducens*. The *G. sulfurreducens pil* genes are divided into two clusters that are missing several of the genes present in the myxobacteria clusters. Conserved non-*pil* genes include *accBC* and *ribF*.

(B) Flagellar motility clusters of *A. dehalogenans* strain 2CP-C and *Desulfuromonas acetoxidans* have conserved gene order. Embedded in the center of the *A. dehalogenans* flagellar cluster, between *motAB* and a cluster of *fli* genes, is a cluster of chemotaxis genes including two *cheA* genes, four mcp genes, and two response regulator *cheY* genes, whereas in *Desulfuromonas acetoxidans*, the complete flagellar gene cluster is downstream of a single chemotaxis gene cluster. Chemotaxis gene cluster bars are color-coded according to the genes present (see Figure 3.7).

Within the delta-Proteobacteria, type IV pilus-based motility has only been observed in the myxobacteria, despite the presence of type IV pilus genes on the genomes of both *Bdellovibrio bacteriovorus* and *G. sulfurreducens [38,39]*. The *G. sulfurreducens* pilin encoded by *pilA* was implicated in biofilm formation and electron transfer to insoluble iron oxides outside of the cell but has not been shown to be involved in motility [40,41]. *pil* gene synteny is shared between *M. xanthus,* strain 2CP-C*,* and *G. sulfurreducens* but sequence is not as well conserved in *G. sulfurreducens* (Figure 3.5A). For example, the 273 bp *pilA* gene in *G. sulfurreducens* is considerably smaller than *pilA* in *M. xanthus* (663 bp) or strain 2CP-C (711 bp). The *G. sulfurreducens pil* genes are divided into two clusters that lack several of the genes present in the myxobacteria clusters. However, some non-*pil* genes are conserved in the *pil* clusters in *M. xanthus*, strain 2CP-C and *G. sulfurreducens*. For example, the *accBC* genes are present in the *pil* clusters across genera suggesting that these genes play roles in pilus formation and function. The *accB* and *accC* genes are frequently located in a two-gene operon and regulated together to control biotin synthesis [42]. While a separate *accAB* cluster (Mxan_0081-0082) has been characterized in *M. xanthus* previously, the function of these two *acc* genes at the end of the pilus gene cluster (Mxan_5767-5768) are unclear [43]. Also conserved across all three genera is a *ribF* gene implicated in riboflavin biosynthesis that is located upstream of the *pil* cluster. The appearance of a conserved *ribF* gene upstream of a motility gene cluster in these three organisms reinforces the idea that riboflavin may have unexplored functions in the delta-Proteobacteria. There are no known interactions between *pil* genes and the *acc* or *rib* genes at this time. However, the presence of genes coding for type IV pili in all three organisms, arranged in syntenous clusters along with

other conserved genes, suggests that the ancestor to the delta-Proteobacteria contained a similar set of type-IV pilus genes (and other genes) that may or may not have been involved in motility.

3.3.3.3 Signal transduction. Like *M. xanthus*, strain 2CP-C possesses a large number of signal transduction genes to process information from its complex environment. Those organisms whose genomes contain multiple chemotaxis-like gene clusters have recently been shown to use chemosensory systems to regulate alternative functions. For example, transcription is regulated by one of the eight chemotaxis-like systems in *M. xanthus* [14,44]. The multitude of chemosensory systems capable of responding to concentration gradients is thought to be required for temporal regulation of many aspects of physiology, including behavior [14].

Four of the seven chemotaxis gene clusters in strain 2CP-C share a high degree of synteny with *M. xanthus* clusters including *frz*, *dif*, *che*6, and *che*8 (Figure 3.6) [45]. The *dif* and *frz* clusters in *M. xanthus* are involved in extracellular polymeric substance (EPS) production, gliding motility, and fruiting body formation [46-48], and these gene clusters may play a similar role in *A. dehalogenans*. Strain 2CP-C possesses homologs to gliding motility genes *aglR* and *aglS* within the *dif* cluster, suggesting that the relationship between *agl* and *dif* genes may hold for *A. dehalogenans* as well as for *M. xanthus* (Figure 3.6). While spatial correlation between motility and regulatory genes on the genome has not been identified for *M. xanthus,* the strain 2CP-C genome provides more than one example of this. The *mglA* gene, which regulates both the adventurous and gliding motility systems in *M. xanthus* [49,50], is associated with the *dif* cluster in strain

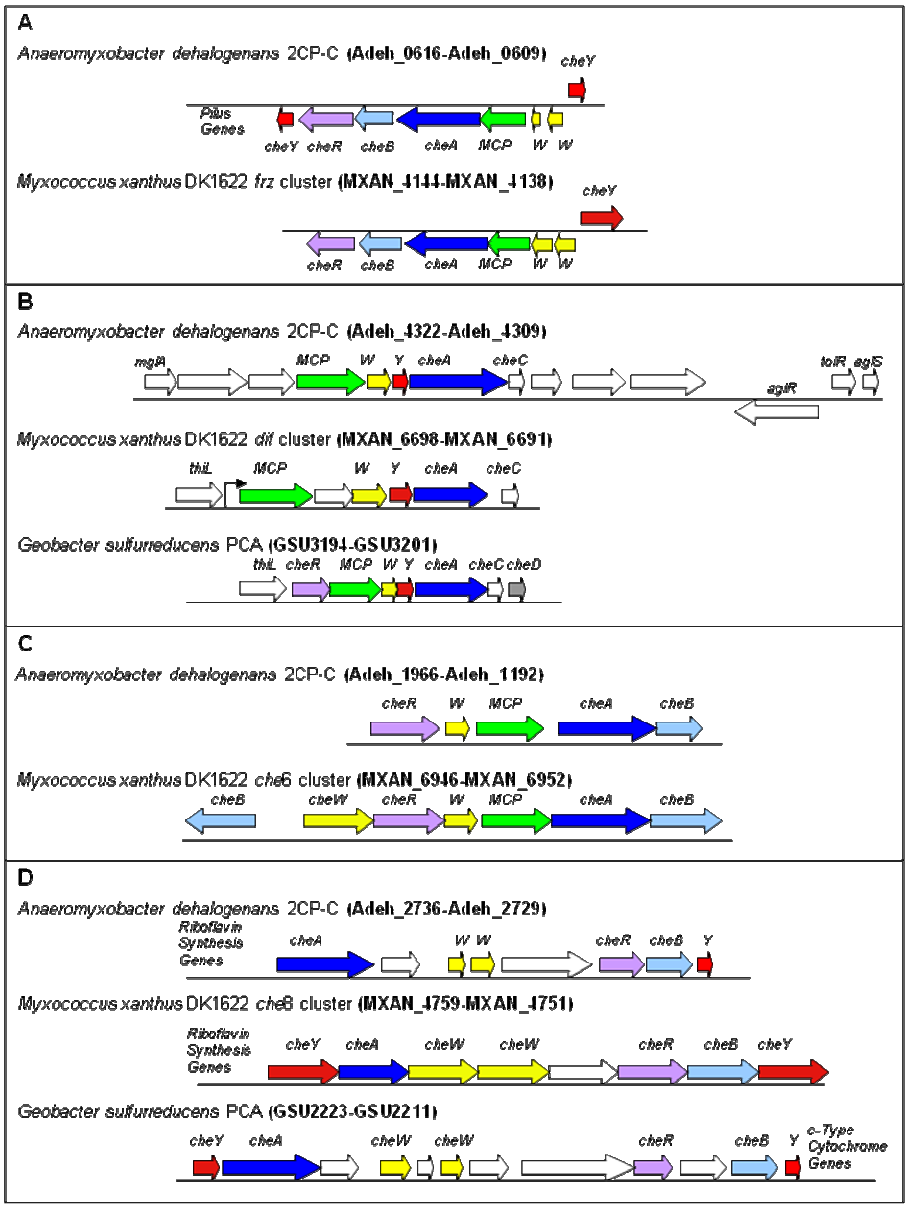

Figure 3.6. Four chemotaxis gene clusters in *A. dehalogenans* strain 2CP-C are highly syntenous with *M. xanthus* clusters. Two of those clusters also show conserved gene order with *G. sulfurreducens.* Locus tag designations are either as indicated in public databases (IMG or NCBI) or interpolated from adjacent loci (i.e., *M. xanthus frz* and *dif* clusters). Arrows represent individual genes. Non-*che* genes are indicated in white.(A) The *M. xanthus frz* gene cluster is conserved in strain 2CP-C but not in *G. sulfurreducens.* (B) The *M. xanthus dif* gene cluster is conserved in both strain 2CP-C and *G. sulfurreducens*.(C) The *M. xanthus che6* gene cluster is conserved in strain 2CP-C but not in *G. sulfurreducens.* (D) The *M. xanthus che8* gene cluster is conserved in both strain 2CP-C and *G. sulfurreducens.*

2CP-C. In addition, the *frz* cluster in strain 2CP-C is located upstream of genes coding for type IV pilus-based motility. A lack of proximity of genes with correlated functions in the *M. xanthus* genome in these two instances may be a result of the genome expansion that has taken place in *M. xanthus*. Thus, genome organization in strain 2CP-C assists in elucidating motility and regulatory pathways in *M. xanthus* by bringing to light possible protein interactions that have not been identified in the more complex *M. xanthus* genome.

3.3.3.4 Flagellar motility. While swimming motility is common among the known delta-Proteobacteria, previously characterized myxobacteria do not display flagellar motility [51]. Three published myxobacterial genomes, each of which does not contain flagellar genes, reflect visual observations regarding motility [30,52]. Surprisingly, the genome of strain 2CP-C includes a 55.7 kb cluster of genes coding for flagellar proteins including *motA, motB,* and *fliC* as well as more than 30 other genes with highest sequence similarities to genes implicated in flagellar motility [53] (Figure 3.5B). According to the currently accepted *Salmonella* and *Escherichia coli* models, almost all the genes necessary for flagellum synthesis and export are present in the strain 2CP-C cluster with the exception of the chaperone genes *fliJ*, *flgN*, *fliT*, and *flgA*, a rod capping protein *flgJ*, and a hook-length-control protein *fliK* (Table 3.5) [53]. Swimming motility has been observed in *A. dehalogenans* strain K cultures grown in liquid medium with nitrate as electron acceptor but this behavior is not commonly observed in strain 2CP-C. In order to determine whether flagellar motility in *A. dehalogenans* was retained from the delta-Proteobacterial ancestor or acquired after diversion from the myxobacteria, gene sequences and cluster

Table 3.5. Flagellar motility genes on the *A. dehalogenans* strain 2CP-C genome. According to the currently accepted *Salmonella* and *E. coli* models, almost all the genes necessary for flagellum synthesis and export are present in a coherent cluster on the *A. dehalogenans* genome with the exception of four chaperone genes (*fliJ*, *flgN*, *fliT*, *flgA*), a rod capping protein *flgJ*, and a hook-length-control protein *fliK*.

Gene name	Locus ID	Closest homolog	*E* value	Identity*
fliA	Adeh_1355	*Chromohalobacter salexigens*	e-21	89/197 (45%)
fliC	Adeh_1339; Adeh_1342	*Bdellovibrio bacteriovorus*	e-46	135/254 (53%)
fliD	Adeh_1341	*Geobacter sulfurreducens*	e-35	144/465 (30%)
fliE	Adeh_1395	*Syntrophus aciditrophicus*	e-5	21/39 (53%)
fliF	Adeh_1394	*Geobacter* sp. FRC-32	e-46	149/375 (39%)
fliG	Adeh_1393	*Thermotoga maritima*	e-32	109/312 (34%)
fliH	Adeh_1392	*Blastopirellula marina*	e-4	30/100 (30%)
fliI	Adeh_1391	*Desulfitobacterium hafniense*	e-90	217/401 (54%)
fliL	Adeh_1366	*Lawsonia intracellularis*	e-7	32/96 (33%)
fliM	Adeh_1365	*Nitrosospira multiformis*	e-20	79/259 (30%)
fliN	Adeh_1364	*Lawsonia intracellularis*	e-26	61/94 (64%)
fliO	Adeh_1363	*Geobacter metallireducens*	0.002	37/106 (34%)
fliP	Adeh_1362	delta-Proteobacterium MLMS-1	e-47	113/217 (52%)
fliQ	Adeh_1361	*Aquifex aeolicus*	0.35	16/38 (42%)
fliR	Adeh_1360	*Saccharophagus degradans*	e-15	62/220 (28%)
fliS	Adeh_1338	*Bdellovibrio bacteriovorus*	0.91	24/84 (28%)
flbD	Adeh_1386	*Desulfitobacterium hafniense*	0.001	21/35 (60%)
motA	Adeh_1385	*Chromobacterium violaceum*	e-54	112/222 (50%)
motB	Adeh_1384	*Geobacter sulfurreducens*	e-30	82/242 (33%)
flhA	Adeh_1358	*Pelobacter carbinolicus*	e-102	282/630 (44%)
flhB	Adeh_1359	*Ralstonia solanacearum*	e-28	70/135 (51%)
flhF	Adeh_1357	*Clostridium tetani*	e-31	73/196 (37%)
flhG	Adeh_1356	*Pelobacter carbinolicus*	e-54	124/291 (42%)
flgB	Adeh_1397	marine gamma-Proteobacterium	e-4	22/44 (50%)
flgC	Adeh_1396	*Desulfovibrio vulgaris*	e-28	68/145 (46%)
flgD	Adeh_1388	*Geobacter metallireducens*	e-31	78/192 (40%)
flgE	Adeh_1387	*Geobacter metallireducens*	e-61	185/422 (43%)
flgF	Adeh_1352	*Acidovorax avenae subsp. citrulli*	e-19	81/237 (34%)
flgG	Adeh_1351	*Halothermothrix orenii*	e-59	123/258 (47%)
flgH	Adeh_1349	*Syntrophus aciditrophicus*	e-30	71/185 (38%)
flgI	Adeh_1348	*Rhodopseudomonas palustris*	e-62	169/343 (49%)
flgK	Adeh_1344	*Geobacter metallireducens*	e-19	138/454 (30%)
flgL	Adeh_1343	*Geobacter sulfurreducens*	e-13	54/169 (31%)

* Percent identities represent the number of amino acids of the *A. dehalogenans* translated protein that are common with its closest homolog divided by the total number of amino acids in the comparison.

synteny of strain 2CP-C were examined to document these genes' ancestry. The highest similarity to genes in the strain 2CP-C flagellar cluster ranges throughout the Proteobacteria and Firmicutes including similarities with genes found in *Thermotogales*, *Planctomycetes*, and *Aquificae*. Since strain 2CP-C is the first member of the Myxococcales that possesses genes for flagellar motility, no known gene homolog exists in traditional myxobacteria while eight out of the 33 genes coding for components of the flagellum apparatus have sequence similarities to genes found in members of the *Geobacteraceae* (Table 3.5). The closest gene order to that of the *A. dehalogenans* strain 2CP-C flagellar genes is in the flagellar gene cluster of *Desulfuromonas acetoxidans* (Figure 3.5B). Synteny and sequence similarity among flagellar genes of delta-Proteobacteria suggest that the flagellar gene cluster in *A. dehalogenans* strain 2CP-C is more ancient than the splitting of the myxobacteria from the *Desulfuromonadales*, and that this gene cluster was not acquired by HGT. Gliding motility and a shift to a lifestyle in unsaturated media (e.g., soil) may have triggered the loss of flagellar genes or re-allocation of the flagellar machinery to other function(s) (e.g., non-flagellar type III secretion) in most myxobacteria. Retention or acquisition of the flagellar gene cluster in strain 2CP-C along with the ability for surface motility reflects an adaptation to the environments *Anaeromyxobacter* spp. occupy, which include surface soils, saturated and unsaturated subsurface environments, and freshwater sediments such as those associated with rice fields and wetlands.

3.3.3.5 Versatile energy metabolism. Additional variations between the traditional Myxobacteria and *A. dehalogenans* manifest in the genes responsible for the remarkable respiratory versatility of *A. dehalogenans.* c-type cytochromes carrying one or multiple

heme-binding sites are commonly involved in respiratory processes [54-56]. Accordingly, bacteria with low respiratory versatility possess a modest number of c-type cytochromes, which typically have fewer than five heme-binding motifs, whereas organisms with great respiratory versatility such as *Shewanella* spp., *Geobacter* spp., and *Anaeromyxobacter* spp. contain numerous c-type cytochrome genes, many of which have multiple heme binding motifs (Figure 3.7). The abundance of c-type cytochromes has consequences for the ecology of the host organism. *Shewanella* spp., *Geobacter* spp., and *Anaeromyxobacter* spp. occupy environments with variable redox conditions [57-61], whereas low numbers or the absence of c-type cytochromes limit an organism's environmental distribution. For example, *Dehalococcoides* strains lacking c-type cytochromes are restricted to low redox potential, anaerobic zones where reductive dechlorination is a feasible terminal electron accepting process [62]. The strain 2CP-C genome contains 68 putative c-type cytochrome genes with 57 containing multiple heme-binding motifs. In fact, the 40-heme cytochrome in strain 2CP-C has among the most putative heme binding sites of any described c-type cytochrome. Large numbers of hemes in c-type cytochromes may function as capacitors allowing organisms to store electrons during feast times to be used during famine and maintain the cell's metabolism under substrate-limiting conditions [56,63,64]. An analogous phenomenon is observed in eukaryotes where heme-containing ferritins store iron to outlast iron-shortages [65]. Strain 2CP-C possesses a gene for bacterioferritin, the prokaryotic corollary to ferritin [65,66]. If large c-type cytochromes function as electron capacitors or if a varied collection of c-type cytochromes imparts the ability to respire across a broad redox spectrum (i.e., respiratory versatility), then large

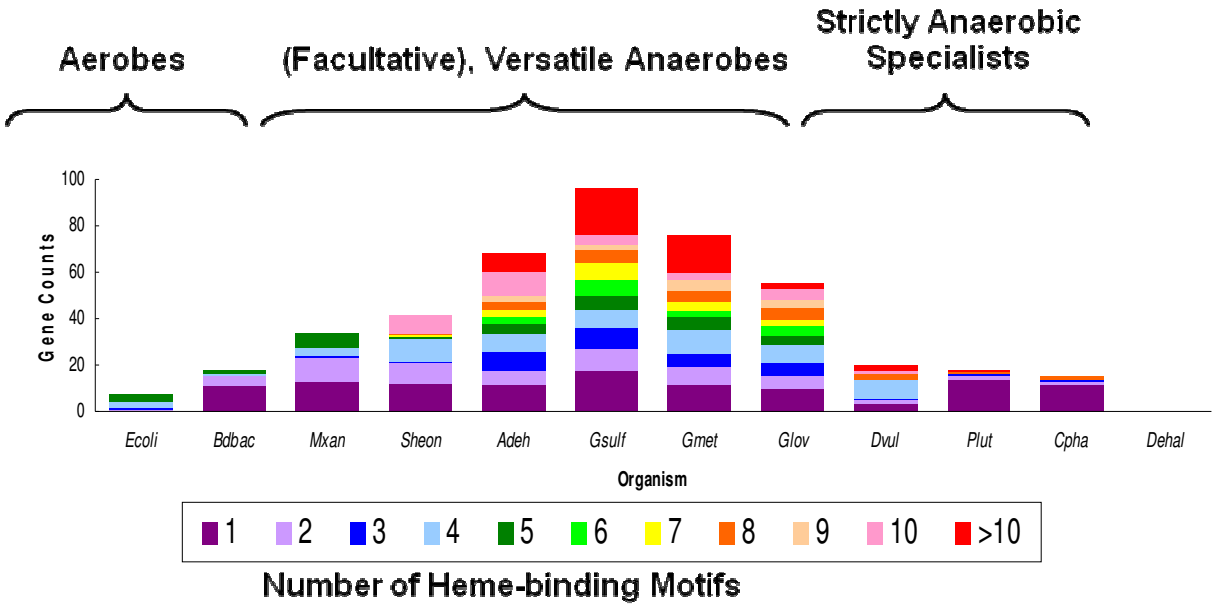

Figure 3.7. Distribution of heme-binding motifs in c-type cytochrome genes varies according to respiratory versatility and correlates with aerobic, facultative, or strict anaerobic lifestyle: aerobic bacteria, metal reducers, and obligate anaerobes. *Escherichia coli* (*Ecoli*), *Bdellovibrio bacteriovorus* (*Bdbac*), *Myxococcus xanthus* (*Mxan*), *Shewanella oneidensis* (*Sheon*), *Anaeromyxobacter dehalogenans* (*Adeh*), *Geobacter sulfurreducens* (*Gsulf*), *Geobacter metallireducens* (*Gmet*), *Geobacter lovleyi* (*Glov*), *Desulfovibrio vulgaris* (*Dvul*), *Pelodictyon luteolum* (*Plut*), *Chlorobium phaeobacteroides* (*Cpha*), and *Dehalococcoides* species strain BAV1 (*Dehal*).

numbers of c-type cytochrome genes with multiple heme-binding sites may represent an evolutionary adaptation to life in environments with variable redox and substrate conditions. Respiratory versatility is fueled by electrons derived from organic (e.g., acetate) or inorganic (e.g., hydrogen) electron donor oxidation. Strain 2CP-C possesses two Ni-Fe-type hydrogenases. One Ni-Fe hydrogenase large subunit gene (Adeh_0478) is highly similar in sequence to a gene in *G. sulfurreducens* (GSU0785) (*E* value of 0 and an amino acid similarity of 57%); this gene is included in the 1.7% of the genome most similar to the Acidobacterium *Solibacter usitatus* (*E* value of 0 and amino acid similarity of 64%). The other Ni-Fe hydrogenase large subunit gene (Adeh_4162) is an F420-reducing-type hydrogenase, which is located adjacent to a gene (Adeh_4163) coding for fused δ and γ Ni-Fe hydrogenase subunits. Adeh_4163 is one of three multi-domain proteins of mixed evolutionary origin that were found out of 140 multi-domain genes analyzed on the genome. The N-terminal domain of Adeh_4163 has its top non-*Anaeromyxobacter* blastp hit to FrhD, a methyl-viologen-reducing hydrogenase delta subunit in *Syntrophobacter fumaroxidans* MPOB (Sfum_1973; *E* value = 2e-34) [67] while the C-terminal domain aligns to an NADH ubiquinone oxidoreductase in *Candidatus Desulforudis audaxviator* MP104C (Accession number ACA60153; *E* value = 1e-62). Adeh_4162 is related to hydrogenase group 3 *vhuA* in strictly anaerobic, chlororespiring *Dehalococcoides* spp. (e.g., *Dehalococcoides* sp. strain BAV1 VhuA, *E* value of $3x10^{-105}$) [68]. These two types of hydrogenases may impart respiratory versatility under distinct environmental conditions (e.g., high versus low H_2 partial pressures).

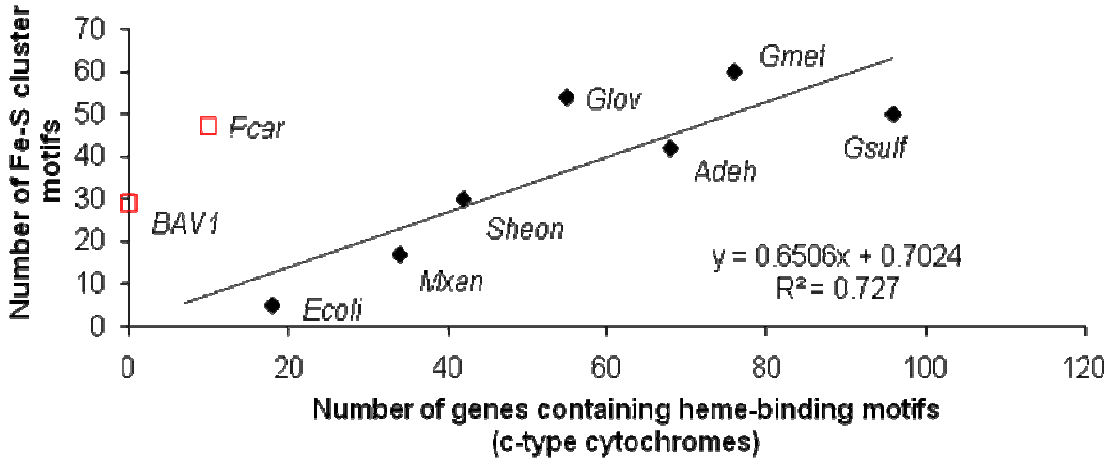

Figure 3.8. A correlation exists between the number of genes containing Fe-S cluster motifs and the number of genes containing heme binding motifs for selected aerobic and anaerobic organisms. Outliers not included in the regression analysis are shown in red, open symbols. *Escherichia coli* (Ecoli), *Myxococcus xanthus* (Mxan), *Shewanella oneidensis* (Sheon), *Anaeromyxobacter dehalogenans* (Adeh), *Geobacter sulfurreducens* (Gsulf), *Geobacter metallireducens* (Gmet), *Geobacter lovleyi* (Glov), *Pelobacter carbinolicus* (Pcar), and *Dehalococcoides* sp. strain BAV1 (BAV1).

Similar to mixed-valence Ni-Fe clusters, iron-sulfur (Fe-S) clusters are commonly involved in electron transfer proteins. The strain 2CP-C genome codes for 42 different Fe-S domains whereas the *M. xanthus* genome (which encodes 34 c-type cytochromes) contains only 17 Fe-S domains. Apparently, abundances of c-type cytochromes and proteins with Fe-S domains correlate and convey respiratory versatility (Figure 3.7). In accordance with its ability to perform respiratory reductive dechlorination (chlororespiration) [6], the strain 2CP-C genome contains two putative reductive dehalogenase (RDase) genes (Adeh_0329 and Adeh_0331), which have *E* values ranging from $2x10^{-22}$ (Adeh_0331) to $1x10^{-12}$ (Adeh_0329) compared to the *pceA* gene encoding the tetrachloroethene reductive dehalogenase of *D. hafniense* strain Y51 [69]. Each putative RDase contains an Fe_4-S_4 motif and a signal peptide characteristic for RDase genes (Figure 3.8, [70]). Distinguishing features of the putative RDases in strain 2CP-C are non-Tat signal peptides and internal transmembrane helices (Figure 3.8). In addition, while RDase genes are typically associated with an adjacent, downstream B gene encoding a small, hydrophobic protein with two or three transmembrane-spanning helices [71], the putative RDase genes Adeh_0329 and Adeh_0331 in the strain 2CP-C genome are associated with B genes that contain one and 10 transmembrane-spanning motifs, respectively. Linked with the strain 2CP-C RDase gene cluster is a gene (Adeh_0328) with five putative transmembrane-spanning motifs. Similar genes are associated with the putative tetrachloroethene RDase gene of *G. lovleyi* strain SZ and a putative RDase gene of *D. hafniense* strain DCB2; however, the genes of the latter two bacteria include an FMN binding domain, which is absent in strain 2CP-C (Figure 3.8) [72] . The function(s) of the transmembrane-spanning proteins including the RDase internal hydrophobic

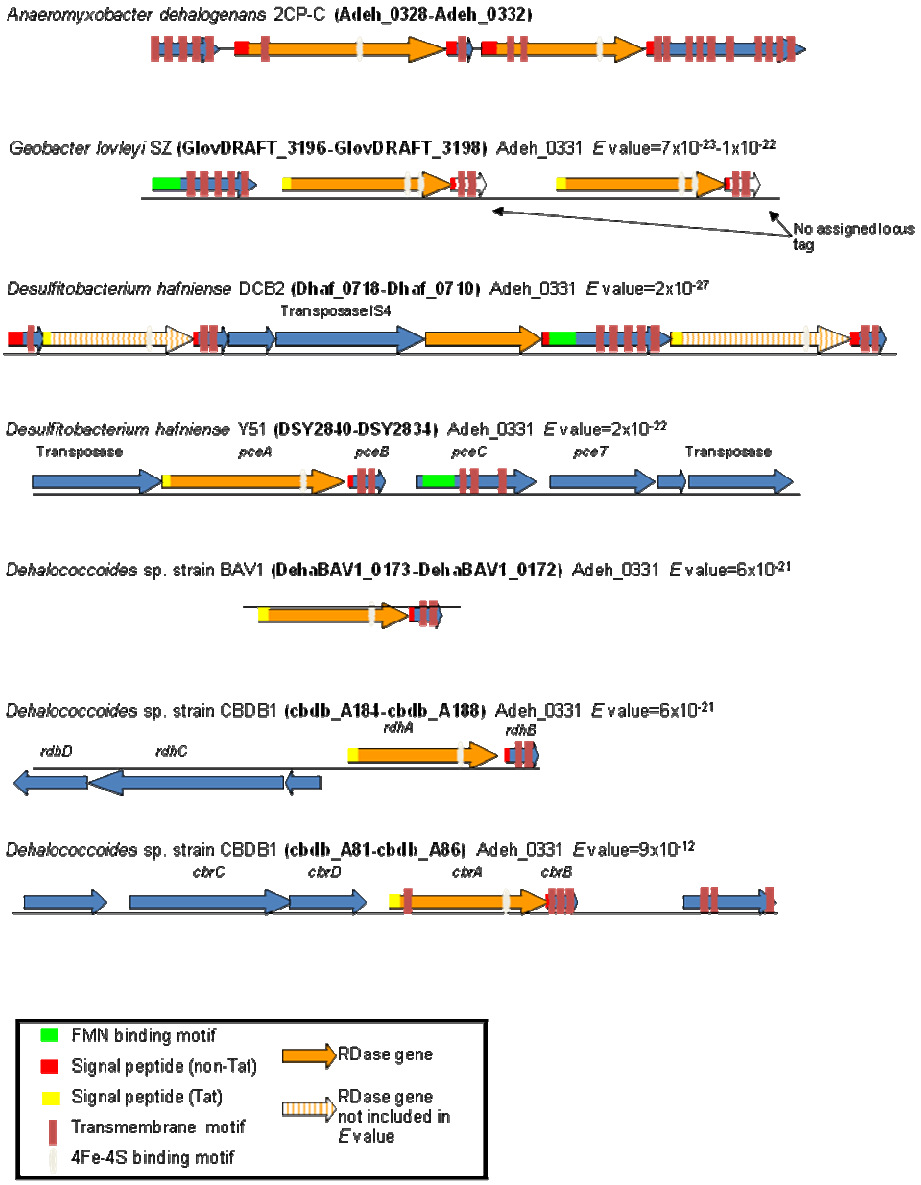

Figure 3.9. Gene order and domain structure of putative reductive dehalogenase gene clusters in *A. dehalogenans* strain 2CP-C are unique when compared to other putative reductive dehalogenase gene clusters. Locus tag designations are given in parentheses. Selected domains (determined by http://www.cbs.dtu.dk/services/TMHMM-2.0) are indicated according to the legend. Arrows represent individual genes.

domains have not been explored, though it has been speculated that these hydrophobic regions are required for RDase functionality, possibly by anchoring the RDase to the membrane. Adeh_0331 is most similar to an uncharacterized RDase gene of *Desulfitobacterium hafniense* strain DCB-2 (*E* value of $2x10^{-27}$ and an amino acid similarity of 39%). While convergent evolution cannot be excluded, the high RDase gene similarity points towards horizontal gene transfer between a gram-negative delta-proteobacterium and a gram-positive bacterium. Interestingly, *A. dehalogenans* strain 2CP-C also possesses four genes encoding hydrolytic dehalogenases, one predicted haloalkane dehydrogenase (Adeh_0522) and three predicted haloacid dehalogenases (Adeh_0672, Adeh_3811, and Adeh_1218), suggesting that this organism's dehalogenation functions are not limited to reductive dechlorination.

3.3.4 Oxygen utilization and detoxification. Due to its capacity for versatile anaerobic respiration, *A. dehalogenans* was hypothesized to bridge the evolutionary gap between delta-Proteobacteria with aerobic and anaerobic lifestyles [6]. However, *A. dehalogenans'* grouping within a subphylum inside the myxobacteria is inconsistent with this hypothesis (Figure 3.1). An alternative explanation is that the anaerobic versatile metabolism of *A. dehalogenans* is a result of convergent evolution arising from aerobic ancestry. The repertoire of respiratory genes and oxidative-stress-related genes in the strain 2CP-C genome includes genes characteristic for anaerobic and aerobic respiration, many of which have homologs in traditional myxobacteria (Figures 3.10-3.13, Table 3.6). The analysis of genes involved in oxidative phosphorylation and defense against reactive oxygen species support the hypothesis that *A. dehalogenans* has an aerobic ancestor.

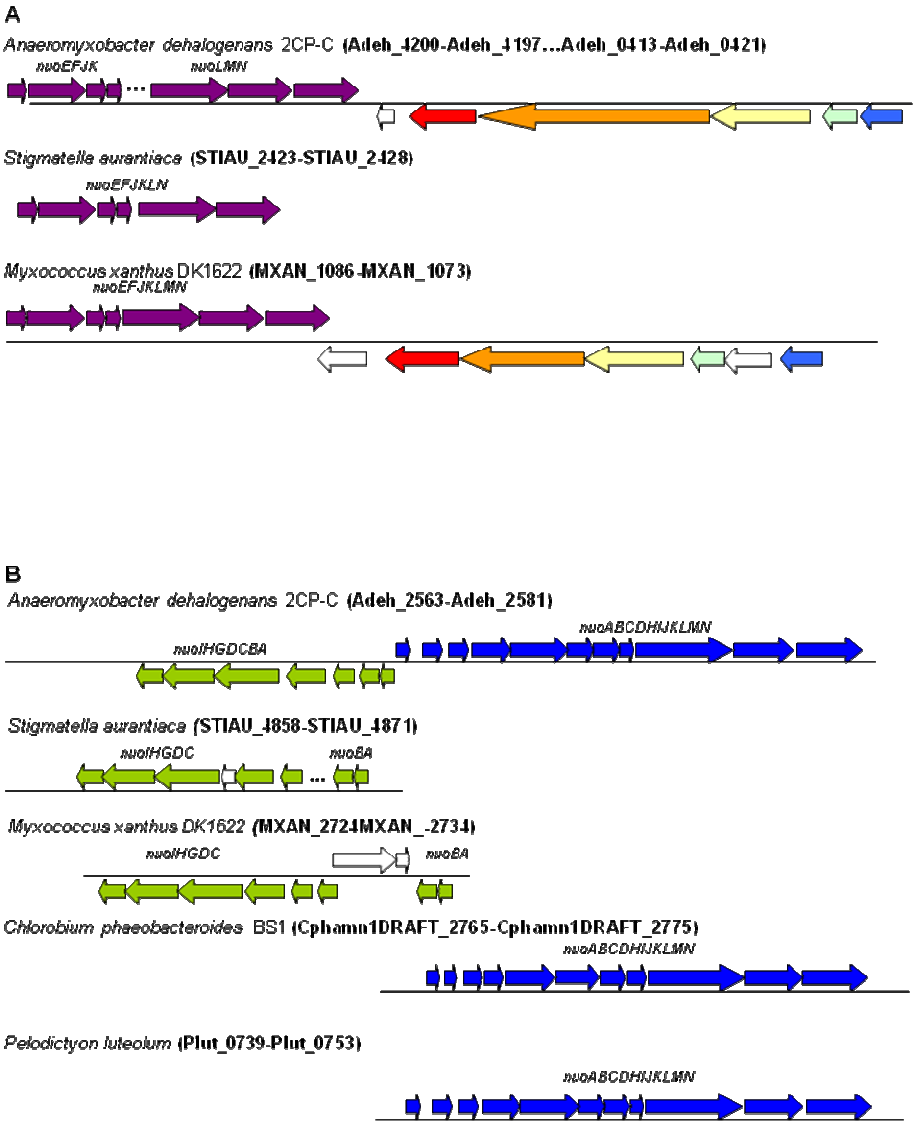

Figure 3.10. Gene order of NADH dehydrogenase gene clusters in *A. dehalogenans* strain 2CP-C indicates both phylogenetically consistent and foreign ancestry, representing aerobic and anaerobic organisms, respectively. Color-coding of arrows indicates clusters with similar gene order and genes with sequence similarity.

(A) One group of myxobacteria-like NADH dehydrogenase (*nuo*, ubiquinone oxidoreductase) subunit genes is split into two separate clusters on the *A. dehalogenans* strain 2CP-C genome but its gene sequences are conserved among myxobacteria.

(B) Two NADH dehydrogenase (*nuo*) gene clusters are located back-to-back on the *A. dehalogenans* strain 2PC-C genome. One of the coupled NADH dehydrogenase gene clusters is myxobacteria-like while the other has conserved sequence and gene order with green sulfur bacteria.

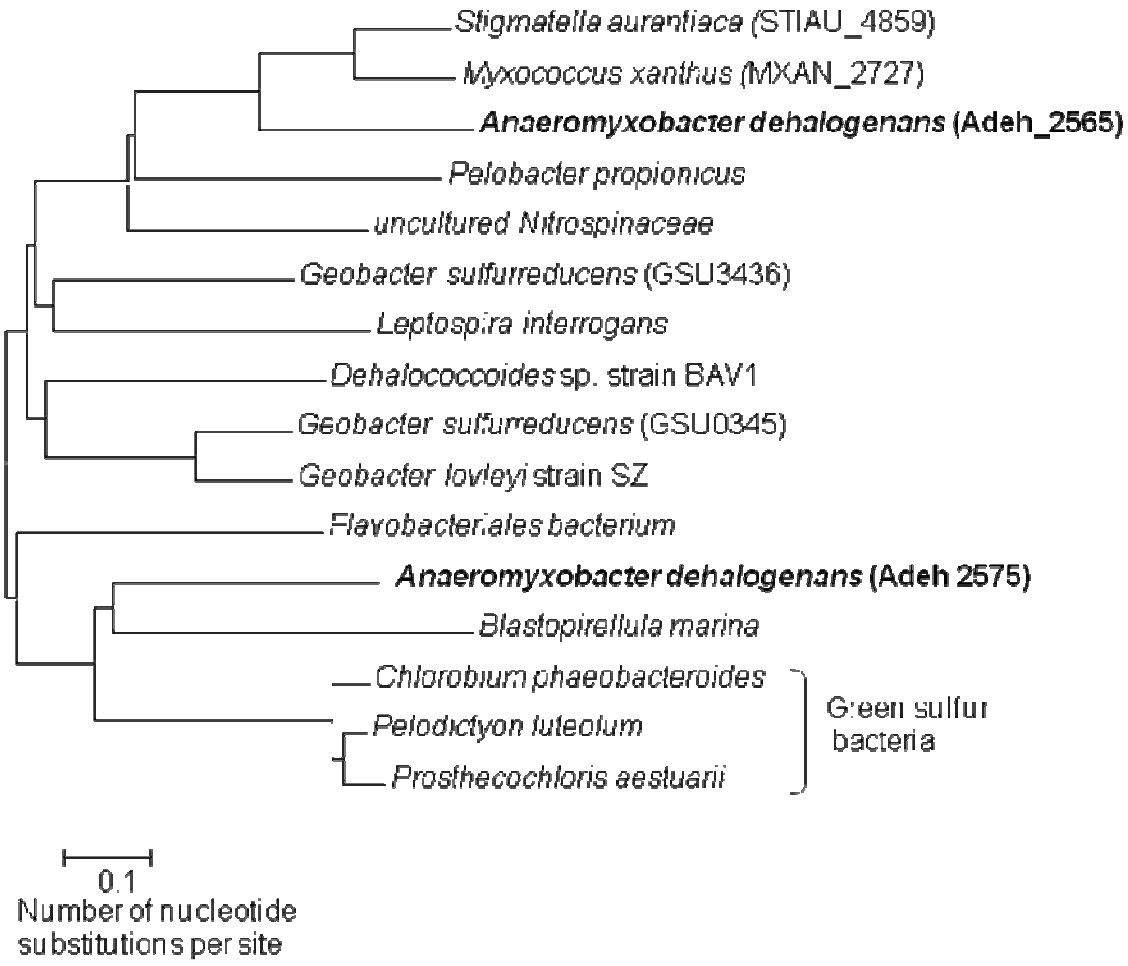

Figure 3.11. Multiple sequence alignment of *A. dehalogenans* strain 2CP-C NADH dehydrogenase subunit 1 genes (*nuoH*) indicates aerobic and anaerobic ancestry. Alignment was made with full-length genes (NCBI database). Locus ID tags for select organisms are indicated in parentheses.

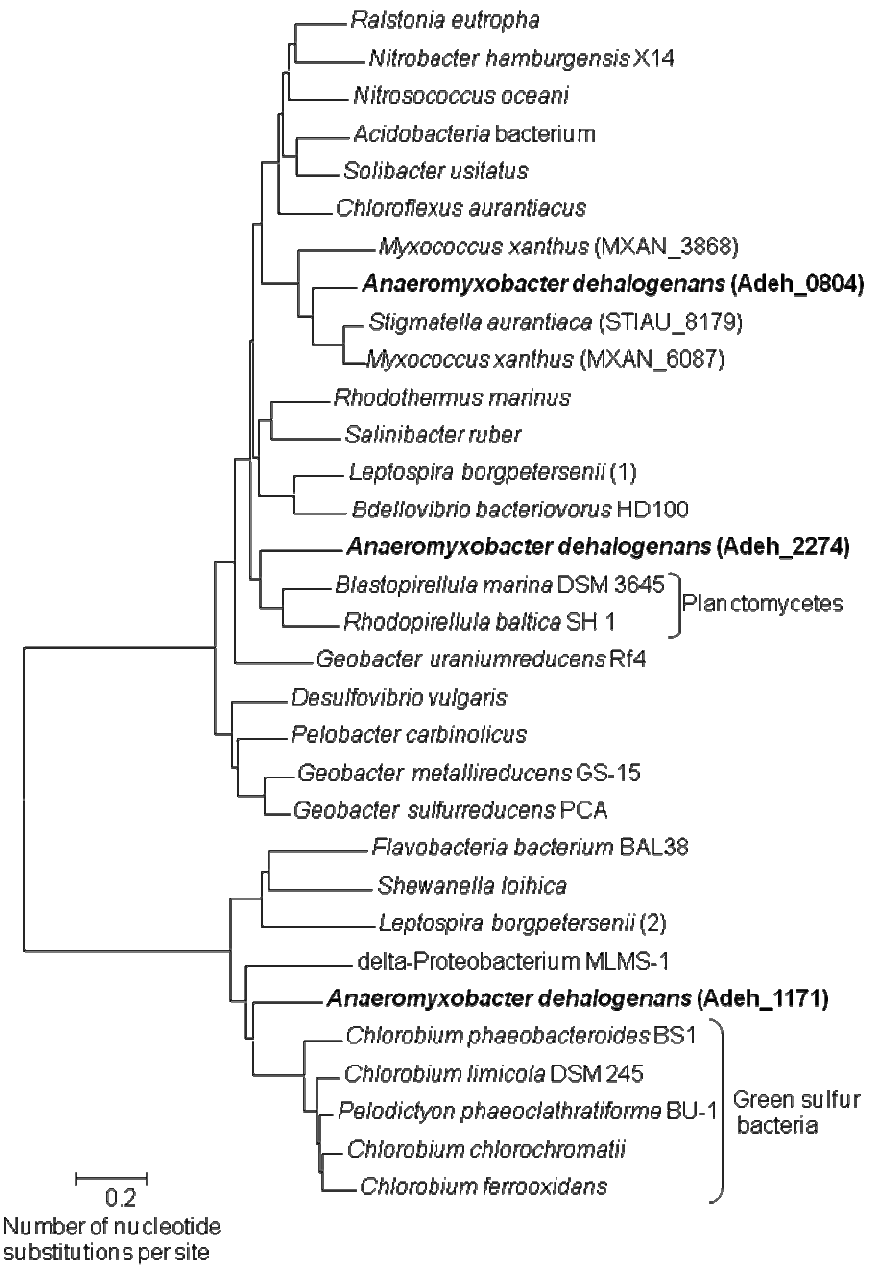

Figure 3.12. Multiple sequence alignment of *A. dehalogenans* strain 2CP-C cytochrome oxidase subunit I (*ctaD* or *fixN*) genes indicates aerobic and anaerobic ancestry. Alignment was made with full-length genes from the NCBI database. Locus ID tags for select organisms are indicated.

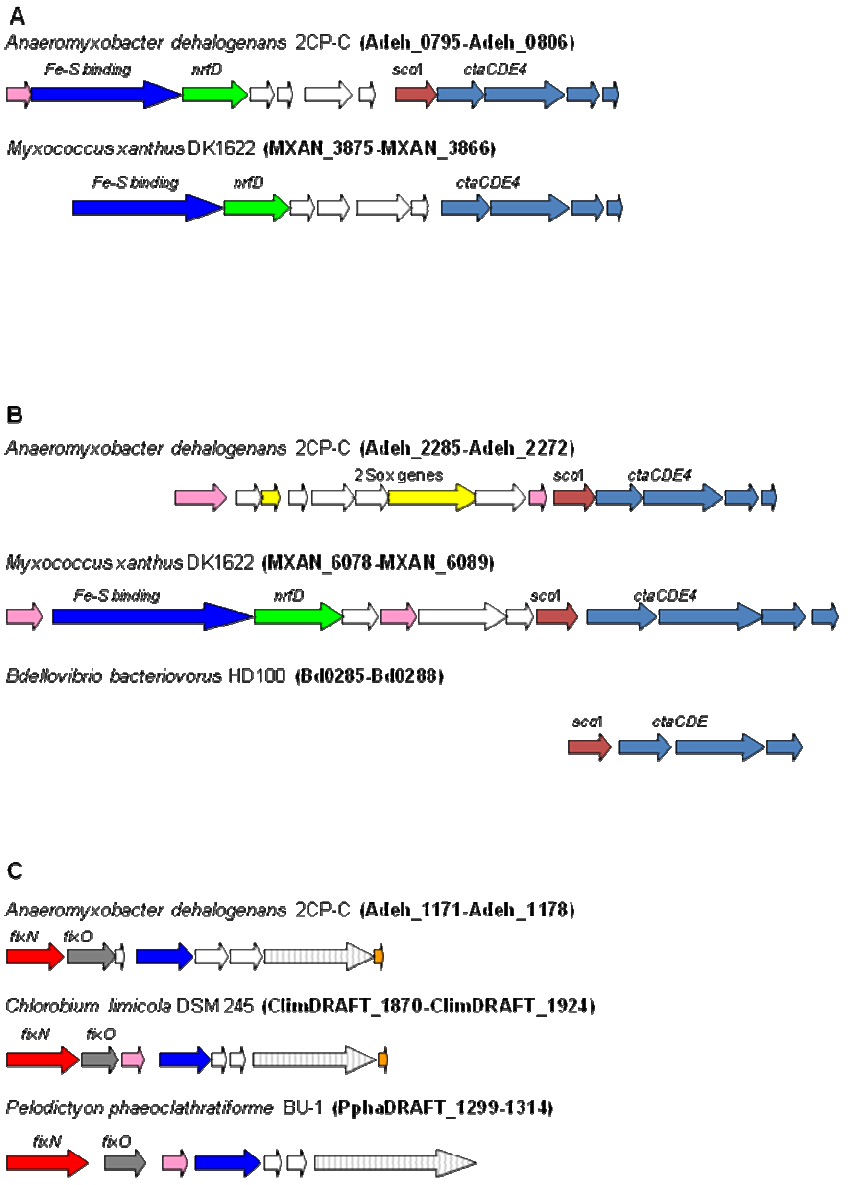

Figure 3.13. Gene order of cytochrome oxidase gene clusters of *A. dehalogenans* strain 2CP-C indicate diverse ancestry. Color-coding of arrows indicates clusters with similar gene order and genes with sequence similarity. Colors represent gene annotations as follows: teal-Fe-S binding motif-containing genes; green-polysulphide reductase genes (*nrfD*); dark blue-synthesis of cytochrome c oxidase genes (*sco1*); light blue-cytochrome c oxidase subunit genes; pink-c-type cytochrome genes; yellow-sox genes; red-cytochrome cbb3 oxidase subunit 1 genes (*fixN*); solid grey-cytochrome cbb3 oxidase mono-heme subunit genes (*fixO*); striped grey-copper-translocating P-type ATPase genes; Orange-cytochrome cbb3 oxidase maturation genes. Hypothetical or non-conserved genes are indicated in white. Locus ID tags are given in parentheses. (A and B) Cytochrome c oxidase clusters syntenous with aerobic organisms. (C) Cytochrome cbb3 oxidase clusters syntenous with anaerobic organisms.

Table 3.6. Reactive Oxygen Species (ROS)-detoxification gene comparison across selected delta-proteobacteria genomes (*Myxococcus xanthus* DK1622, *Anaeromyxobacter dehalogenans* 2CP-C, *Geobacter sulfurreducens* PCA, and *Desulfovibrio vulgaris* Hildenborough)

Enzyme	Reaction catalyzed	Locus ID tags			
		M. xanthus	*A. dehalogenans*	*G. sulfurreducens*	*D. vulgaris*
Catalases	$H_2O_2 + H_2O_2 \rightarrow 2\ H_2O + O_2$	MXAN_6188 MXAN_4389	Absent	GSU2100	DVUA0091
Superoxide dismutases	$O_2^- + O_2^- + 2H^+ \rightarrow H_2O_2 + O_2$	MXAN_5862 MXAN_4826	Adeh_1952	GSU1158	DVU2410
Superoxide reductases	$O_2^- + 2H^+ + \text{cyt } c_{reduced} \rightarrow H_2O_2 + \text{cyt } c_{oxidized}$	Absent	Absent	Absent	DVU3183
Alkylhydro-peroxidases	$H_2O_2 + NADH + H^+ \rightarrow 2\ H_2O + NAD^+$	MXAN_1564 MXAN_1563 MXAN_5223	Adeh_0313 Adeh_0314 Adeh_3128	GSU3246 GSU0893	Absent
Thiol peroxidase	$H_2O_2 + NADH + H^+ \rightarrow 2\ H_2O + NAD^+$	MXAN_6496	Adeh_1146 Adeh_1148 Adeh_0828	GSU0352	DVU1228
Cytochrome c peroxidases	$H_2O_2 + NADH + H^+ \rightarrow 2\ H_2O + NAD^+$	MXAN_0977 MXAN_7213 MXAN_5562 MXAN_5801	Absent	GSU2813 GSU0466	Absent
Rubrerythrin	$H_2O_2 + NADH + H^+ \rightarrow 2\ H_2O + NAD^+$	Absent	Adeh_0765 Adeh_2075 Adeh_3092* Adeh_2193*	GSU2814* GSU2612*	DVU3094 DVU2310 DVU0019
Rubredoxin	$\text{Polyglucose}^\dagger + NADH + H^+ \rightarrow \text{glucose}^\dagger + NAD^+$	Absent	Adeh_3092* Adeh_2193*	GSU2814* GSU2612* GSU0847 GSU3188	DVU3184
Rubredoxin:oxygen oxidoreductase	$O_2 + 4H^+ \rightarrow 2H_2O$ $NO \rightarrow N_2O$	Absent	Absent	GSU3294	DVU3185

*GSU2814, GSU2612, Adeh_3092, and Adeh_2193 encode rubrerythrin:rubredoxin fused proteins

†Polyglucose is the electron donor in the rubredoxin reaction of *D. vulgaris*; the donor is unknown in other organisms

3.3.4.1 Oxidative phosphorylation. In aerobic respiration, electron flow is initiated by an NADH dehydrogenase accepting electrons from an electron donor, and ends with cytochrome c oxidase, an enzyme system catalyzing the reduction of oxygen to water [73]. Fourteen genes encoding NADH dehydrogenase subunits in the strain 2CP-C genome produced closest BLAST hits to *M. xanthus* or *S. aurantiaca* homologs, and are located in two separate clusters, each of which is syntenous between all three organisms (Figure 3.10). Multiple sequence alignment of the first NADH dehydrogenase subunit (*nuoH*) suggest shared evolutionary history of this respiratory chain component between *A. dehalogenans*, *M. xanthus* and *S. aurantiaca* (Figure 3.10). Sequence similarities suggest further that many of the individual genes in these two myxobacterial NADH dehydrogenase gene clusters are homologous to those in the two large *G. sulfurreducens* NADH dehydrogenase gene clusters; however, the *G. sulfurreducens* clusters lack conserved gene order with the myxobacteria (gene order of both *G. sulfurreducens* clusters: *nuoABCDEFGHIJKLMN* compared to the separate *nuoEFJKLMN* and *nuoIHGDBA* clusters in the myxobacteria), suggesting more ancient divergence. Interestingly, the strain 2CP-C genome contains a third NADH dehydrogenase gene cluster located back-to-back with one of the conserved NADH dehydrogenase gene clusters characteristic for myxobacteria (Figure 3.10). This third cluster contains genes with sequence similarity and conserved synteny to *Chlorobium phaeobacteroides* and *Pelodictyon luteolum* (*nuoH E* values of $1x10^{-71}$ and $1x10^{-70}$, respectively), both of which are strictly anaerobic green-sulfur bacteria (Figures 3.10 and 3.11) [74-76]. The other sequenced myxobacteria genomes do not contain genes with homology to the genes in the green sulfur bacterial NADH dehydrogenase gene cluster. Thus, strain 2CP-C

possesses a unique assemblage of NADH dehydrogenase subunits including clusters that resemble those of both strict anaerobes and aerobes.

A cluster of cytochrome c oxidase genes is present in all of the sequenced delta-Proteobacteria even though many of these organisms are considered strict anaerobes. This observation suggests that aerobic, possibly microaerophilic growth has not been recognized, or that these enzyme systems fulfill a different function such as detoxification of oxygen and reactive oxygen species (ROS) [77]. *A. dehalogenans* strain 2CP-C possesses three gene clusters that code for the 3-4 subunits of cytochrome oxidases. The first gene cluster encoding cytochrome oxidase subunits is homologous and syntenous to two cytochrome c oxidase clusters in *M. xanthus* and one in *S. aurantiaca* (Figures 3.12 and 3.13A). A second cytochrome oxidase gene cluster shares highest sequence similarity with the cytochrome c oxidase genes in the *Bdellovibrio bacteriovorus* genome but the gene synteny is most similar to the *M. xanthus* and *S. aurantiaca* gene clusters (Figures 3.12 and 3.13B). The third strain 2CP-C cytochrome oxidase gene cluster codes for a cytochrome cbb_3 oxidase, a distinctive class of proton-pumping, respiratory heme-copper proteins reducing O_2 to water [78]. Like the genes for the anaerobic NADH dehydrogenase, the cytochrome cbb_3 oxidase genes are homologous and syntenous to genes in *Chlorobacteriaceae* (Figures 3.12 and 3.13C). These patterns of oxidative phosphorylation gene similarity imply that the myxobacteria have a common ancestor that reduced O_2 to water as an energy-yielding respiratory process involving electron transfer to oxidized nicotinamide adenine dinucleotide (NAD^+). Additionally, the oxidative phosphorylation gene clusters with sequence similarity to strict anaerobes explain the anaerobic respiratory versatility of *A. dehalogenans.* The synteny and

sequence similarity among oxidative phosphorylation genes imply that the delta-Proteobacteria, including the distantly related *B. bacteriovorus,* share a common ancestor capable of aerobic respiration. Further, the presence of a green sulfur bacteria-like cbb_3-type cytochrome oxidase gene cluster in *A. dehalogenans* strain 2CP-C that includes genes with sequence similarity to other anaerobic delta-Proteobacteria genes suggests that the respiratory versatility found in the extant delta-Proteobacteria is actually an innovation on aerobic respiration made possible by acquisition of foreign genes.

3.3.4.2 Defense against reactive oxygen species (ROS). Oxidative phosphorylation generates ROS, for which aerobic organisms developed defense mechanisms to avoid detrimental effects [79]. It is not uncommon for catalase and superoxide dismutase to occur in organisms described as strict anaerobes to protect the cells from ROS [80]. While the *A. dehalogenans* strain 2CP-C genome does not contain genes for catalase, superoxide reductase, or cytochrome c peroxidases, genes encoding superoxide dismutases of the Mn and Fe type are present (Table 3.11). The genome also contains four rubrerythrin homologs. Rubrerythrin is a non-heme containing iron enzyme system that catalyzes the conversion of hydrogen peroxide to water in *D. vulgaris* [81]. *A. dehalogenans* also possesses two alkylhydroperoxidases, which are responsible for hydrogen peroxide conversion to water in *M. xanthus*. Hence, *A. dehalogenans* has combined aerobic and anaerobic strategies for ROS detoxification. Neelaredoxin and desulfoferrodoxin superoxide reductases, both non-heme containing iron enzyme systems that couple cytochrome c oxidation to superoxide reduction, are common ROS detoxifying enzymes in anaerobic organisms [82-84] but, of the delta-Proteobacteria

surveyed, only *D. vulgaris* has superoxide reductase (Table 3.6). Interestingly, *G. sulfurreducens* seems to possess the full aerobe-type antioxidant enzymatic machinery, with genes encoding catalase, superoxide dismutase, and peroxidase in addition to the complete suite of genes required for oxidative phosphorylation and, yet, this organism is not able to grow with atmospheric oxygen concentrations. Many bacteria initially characterized as strict anaerobes, including *Geobacter sulfurreducens*, have subsequently been shown to consume oxygen at sub-atmospheric concentrations [84-86]. The presence of ROS detoxifying enzymes in the anaerobic delta-Proteobacteria support the hypothesis that the organisms classified as delta-Proteobacteria descended from an aerobic ancestor.

3.3.4 Conclusions.

The *A. dehalogenans* strain 2CP-C genome provides evidence that, contrary to the prevailing wisdom, aerobic organisms can be ancestral to anaerobes. While a duality is implied by the terms 'aerobic' versus 'anaerobic' environment, the soil rarely contains such definite distinctions. Soil-dwelling organisms are subject to frequently changing redox conditions, which govern their ecophysiology and consequently impact bioremediation practice [87,88]. The delta-Proteobacteria, being primarily sediment- and soil-dwelling, are the only class of Proteobacteria that is dominated by anaerobes. A unique evolutionary history involving an aerobic ancestor may explain why all of the sequenced delta-Proteobacteria genomes contain genes encoding the cytochrome c oxidase complex, implicated in O_2 reduction to water. *G. sulfurreducens*, a delta-Proteobacterium characterized by its anaerobic versatile lifestyle, has a genome that shares many characteristics with aerobes. The two recognized groups of aerobic delta-

Proteobacteria are *B. bacteriovorus* and the myxobacteria, which are only distantly related to one another but show homology in genes coding for aerobic respiratory pathways. Because aerobic organisms do not form a monophyletic clade, it is widely accepted that aerobic metabolism arose several times independently in evolutionary history [77]. However, the distribution of aerobic organisms in all three myxobacterial suborders belies independent evolution of aerobic metabolism among the myxobacteria. These findings, along with the phylogeny and genome characteristics of *A. dehalogenans* strain 2CP-C, point to an alternate evolutionary history for this major bacterial class. Contrary to the hypothesis that anaerobic metabolism in the *Desulfuromonadales* or *Desulfovibrionales* was the ancestral metabolism from which myxobacterial aerobic respiration evolved, the detailed analysis of the *A. dehalogenans* strain 2CP-C genome suggests that in respiratory diversification within the delta-Proteobacteria class, it was the versaphilic anaerobes that innovated and the aerobic *Myxococcales* and *Bdellovibrionales* that were conservative.

3.4 Materials and Methods

3.4.1 Genome sequencing. Genomic DNA of *A. dehalogenans* strain 2CP-C was extracted from whole cells grown anoxically in non-reduced liquid R2A (Difco) complex medium without shaking at 35°C. DNA was extracted using the Qiagen genomic DNA extraction kit (Qiagen, Hilden, Germany). Genome sequencing was performed by the Department of Energy's Joint Genome Institute (JGI). The *A. dehalogenans* strain 2CP-C genome sequence has been assigned EMBL accession number CP000251.

3.4.2 Gene prediction and annotation, phylogenetic and phenetic analyses. In addition to automated annotation provided by JGI, the high precision multi-genome scale annotation tool EFICAz was applied for refined annotation [89,90]. Phylogenetic and molecular evolutionary analyses based on 16S rRNA gene sequences comparisons were conducted using MEGA version 3.1 [91]. ClustalW was used for multiple alignments and trees and bootstrap values were calculated using the Neighbor-Joining algorithm with default settings. Phenetic analysis based on enzymes was carried out as follows: first, 26 organisms with fully sequenced genomes were selected, including all available Proteobacteria from the delta and epsilon subdivisions, and representative species of other phyla. Enzyme function annotations for these organisms in the KEGG database [92] were complemented with predictions made by EFICAz [89], a highly precise approach for enzyme function inference that significantly increases annotation coverage [90]. Then, for each organism, a binary character table was constructed encoding the presence/absence of 1,272 different enzymes classified according to the Enzyme Commission system [93]. This character matrix was used as input for the SEQBOOT, DOLLOP and CONSENSE programs from the PHYLIP v3.66 phylogenetic package to generate a majority-rule consensus tree based on the Dollo parsimony method. DOLLOP and CONSENSE were run using default settings; the number of bootstrap samples generated by SEQBOOT was 100.

3.4.3 Comparative genome analysis. A database of eubacterial protein sequences was compiled from the proteomes of fully sequenced bacterial genomes deposited in GenBank and the proteomes of draft bacterial genomes from JGI and The Institute for

Genomic Research (TIGR) (Bacterial Genome Subset). Each *A. dehalogenans* strain 2CP-C protein sequence was then compared against this database using the BLAST software package [94] using a cutoff *E* value of $1x10^{-5}$ and default settings for all other parameters. Resulting BLAST output files were parsed using perl scripts to obtain top hits outside of the *A. dehalogenans* genome. Using the top non-paralogous hits, each coding sequence (CDS) in the circular chromosome was colored according to closest phylogenetic similarity.

3.4.4 Survey of relevant genes having more than one functional domain. To detect putative chimeric genes coding for multi-domain proteins in strain 2CP-C, 140 amino acid sequences of proteins related to respiration, flagella assembly, pilus assembly, and signal-transduction were blasted against the NCBI non-redundant database at using default parameters and the conserved domains search option. Alignments of top blastp hits outside of *Anaeromyxobacter* spp. were viewed in the graphical output of NCBI blast and checked for correspondence to domains marked in the NCBI conserved domains output.

3.4.5 Identification of HGT regions. Analysis of the *A. dehalogenans* strain 2CP-C genome for evidence of gene acquisitions via HGT was based upon base composition and codon usage patterns [95,96]. Regions having a G+C content between the minimum of 57.5% and 70% were located on genome plots in Artemis and Cgview [97,98]. Duplicated ribosomal RNA loci with G+C contents of 57.5% were excluded from further analysis. Artemis was used to manually select protein-coding genes outside the low G+C

regions for codon counts and plot the Karlin signature, which compares local dinucleotide composition within a sliding window relative to dinucleotide composition of the entire genome [99]. Codon Adaptation Indices (CAI) for all protein-coding loci were computed with JCat using default parameters (www.jcat.de)[100]. The CAI measures codon usage deviation from average codon usage of the entire genome [101]. Occurrences of the codons $TTA_{Leucine}$ and $ATA_{Isoleucine}$ found in the strain 2CP-C genome only 52 times and 140 times, respectively, were manually tallied in Artemis. To determine the level of amino acid sequence similarity of translated gene sequences within and adjacent to low G+C regions, protein sequences were queried against a collection of phage proteomes and translated phage-related genes present in complete bacterial genomes from NCBI and IMG. Genes from low G+C regions not containing phage gene BLAST hits were then compared against the NCBI non-redundant database to confirm the absence of horizontally transferred sequences. The BLAST *E* value provides an estimate of the probability that the similarity of a random hit of a query sequence to a hit [94]. Two regions located between Adeh_1913 and Adeh_1963 with 69.5% G+C content contain ribosomal proteins, show no deviation in codon adaptation, and were excluded from further analysis.

3.4.6 Motility assays. *A. dehalogenans* was grown as described [6] and cells were harvested in mid-log phase. Cell suspensions (10 µL, ~10^6 cells) were transferred onto R2A solid medium (1.5% agar), allowed to dry, and incubated aerobically at 32°C.

3.4.7 Microscopy. Surface motility was observed using Nikon SMZ10000 dissecting and Nikon Eclipse E400 phase-contrast microscopes. Images were captured with a digital camera and manipulated using QImaging software.

3.5 Acknowledgments

We acknowledge the contributions by the U.S. Department of Energy Joint Genome Institute personnel to sequencing, genome closure, and automated annotation. Thanks to Soojin Yi for helpful discussion about G+C content in prokaryotes.

3.7 References

1. Gogarten JP, Townsend JP (2005) Horizontal gene transfer, genome innovation and evolution. Nature Reviews Microbiology 3: 679-687.

2. Brown JR (2003) Ancient horizontal gene transfer. Nature Reviews Genetics 4: 121-132.

3. Konstantinidis KT, Tiedje JM (2005) Genomic insights that advance the species definition for prokaryotes. Proceedings of the National Academy of Sciences of the United States of America 102: 2567-2572.

4. Dagan T, Martin W (2007) Ancestral genome sizes specify the minimum rate of lateral gene transfer during prokaryote evolution. Proceedings of the National Academy of Sciences of the United States of America 104: 870-875.

5. Cole JR, Cascarelli AL, Mohn WW, Tiedje JM (1994) Isolation and characterization of a novel bacterium growing via reductive dehalogenation of 2-chlorophenol. Applied and Environmental Microbiology 60: 3536-3542.

6. Sanford RA, Cole JR, Tiedje JM (2002) Characterization and description of *Anaeromyxobacter dehalogenans* gen. nov., sp. nov., an aryl halorespiring facultative anaerobic Myxobacterium. Applied and Environmental Microbiology 68: 893-900.

7. He Q, Sanford RA (2003) Characterization of Fe(III) reduction by chlororespiring *Anaeromxyobacter dehalogenans*. Applied and Environmental Microbiology 69: 2712-2718.

8. Sanford RA, Wu Q, Sung Y, Thomas SH, Amos BK, et al. (2007) Hexavalent uranium supports growth of Anaeromyxobacter dehalogenans and Geobacter spp. with lower than predicted biomass yields. Environmental Microbiology 9: 2885-2893.

9. Wu Q, Sanford RA, Löffler FE (2006) Uranium(VI) reduction by *Anaeromyxobacter dehalogenans* strain 2CP-C. Applied and Environmental Microbiology 72: 3608-3614.

10. Treude N, Rosencrantz D, Liesack W, Schnell S (2003) Strain FAc12, a dissimilatory iron-reducing member of the *Anaeromyxobacter* subgroup of Myxococcales. FEMS Microbiology Ecology 44: 261-269.

11. Dawid W (2000) Biology and global distribution of myxobacteria in soils. FEMS Microbiology Reviews 24: 403-427.

12. Reichenbach H (1999) The ecology of the myxobacteria. Environmental Microbiology 1: 15-21.

13. Reichenbach H (2001) Myxobacteria, producers of novel bioactive substances. Journal of Industrial Microbiology & Biotechnology 27: 149-156.

14. Kirby JR, Zusman DR (2003) Chemosensory regulation of developmental gene expression in *Myxococcus xanthus*. Proceedings of the National Academy of Sciences of the United States of America 100: 2008-2013.

15. Jelsbak L, Sogaard-Andersen L (2000) Pattern formation: fruiting body morphogenesis in *Myxococcus xanthus*. Current Opinion in Microbiology 3: 637-642.

16. Kaiser D (2004) Signaling in myxobacteria. Annual Review of Microbiology 58: 75-98.

17. Pradella S, Hans A, Sproer C, Reichenbach H, Gerth K, et al. (2002) Characterisation, genome size and genetic manipulation of the myxobacterium *Sorangium cellulosum* So ce56. Archives of Microbiology 178: 484-492.

18. Reichenbach H, Dworkin M (1969) Studies on *Stigmatella aurantiaca* (Myxobacterales). Journal of General Microbiology 58: 3.

19. Dworkin M (1996) Recent advances in the social and developmental biology of the myxobacteria. Microbiological Reviews 60: 70-102.

20. Velicer GJ, Stredwick KL (2002) Experimental social evolution with *Myxococcus xanthus*. Antonie Van Leeuwenhoek International Journal of General and Molecular Microbiology 81: 155-164.

21. Shimkets L, Woese CR (1992) A phylogenetic analysis of the myxobacteria - Basis for their classification. Proceedings of the National Academy of Sciences of the United States of America 89: 9459-9463.

22. Karlin S, Brocchieri L, Mrazek J, Kaiser D (2006) Distinguishing features of delta-proteobacterial genomes. Proceedings of the National Academy of Sciences of the United States of America 103: 11352-11357.

23. Gogarten JP, Doolittle WF, Lawrence JG (2002) Prokaryotic evolution in light of gene transfer. Molecular Biology and Evolution 19: 2226-2238.

24. Zhou J, Gu Y, Zou C, Mo M (2007) Phylogenetic diversity of bacteria in an earth-cave in Guizhou Province, Southwest of China. Journal of Microbiology 45: 105-112.

25. Sait M, Davis KER, Janssen PH (2006) Effect of pH on isolation and distribution of members of subdivision 1 of the phylum Acidobacteria occurring in soil. Applied and Environmental Microbiology 72: 1852–1857.

26. Ciccarelli FD, Doerks T, von Mering C, Creevey CJ, Snel B, et al. (2006) Toward automatic reconstruction of a highly resolved tree of life. Science 311: 1283-1287.

27. Aguilar D, Aviles FX, Enrique Q, Sternberg MJE (2004) Analysis of phenetic trees based on metabolic capabilities across the three domains of life. Journal of Molecular Biology 340: 491-512.

28. Haywood-Farmer E, Otto SP (2003) The evolution of genomic base composition in bacteria. Evolution 57: 1783-1792.

29. Blaisdell BE, Campbell AM, Karlin S (1996) Similarities and dissimilarities of phage genomes. Proceedings of the National Academy of Sciences of the United States of America 93: 5854-5859.

30. Goldman BS, Nierman WC, Kaiser D, Slater SC, Durkin AS, et al. (2006) Evolution of sensory complexity recorded in a myxobacterial genome. Proceedings of the National Academy of Sciences of the United States of America 103: 15200-15205.

31. Mrazek J, Karlin S (1998) Strand compositional asymmetry in bacterial and large viral genomes. Proceedings of the National Academy of Sciences of the United States of America 95: 3720-3725.

32. Boone DR, Castenholz RW, Garrity GM (2001) Bergey's manual of systematic bacteriology New York: Springer.

33. Pham VD, Shebelut CW, Diodati ME, Bull CT, Singer M (2005) Mutations affecting predation ability of the soil bacterium *Myxococcus xanthus*. Microbiology-Sgm 151: 1865-1874.

34. Akiyama T, Inouye S, Komano T (2003) Novel developmental genes, *fruCD*, of *Myxococcus xanthus*: Involvement of a cell division protein in multicellular development. Journal of Bacteriology 185: 3317-3324.

35. Thony-Meyer L, Kaiser D (1993) *devRS*, an autoregulated and essential genetic locus for fruiting body development in *Myxococcus xanthus*. Journal of Bacteriology 175: 7450-7462.

36. Berleman JE, Chumley T, Cheung P, Kirby JR (2006) Rippling is a predatory behavior in *Myxococcus xanthus*. Journal of Bacteriology 188: 5888-5895.

37. Jelsbak L, Kaiser D (2005) Regulating pilin expression reveals a threshold for S motility in *Myxococcus xanthus*. Journal of Bacteriology 187: 2105-2112.

38. Evans KJ, Lambert C, Sockett RE (2007) Predation by Bdellovibrio bacteriovorus HD100 requires type IV pili. Journal of Bacteriology 189: 4850-4859.

39. Reguera G, McCarthy KD, Mehta T, Nicoll JS, Tuominen MT, et al. (2005) Extracellular electron tranfer via microbial nanowires. Nature 435: 1098-1101.

40. Reguera G, Pollina RB, Nicoll JS, Lovley DR (2007) Possible nonconductive role of *Geobacter sulfurreducens* pilus nanowires in biofilm formation. Journal of Bacteriology 189: 2125-2127.

41. Afkar E, Reguera G, Schiffer M, Lovley DR (2005) A novel Geobacteraceae-specific outer membrane protein J (OmpJ) is essential for electron transport to Fe (III) and Mn (IV) oxides in *Geobacter sulfurreducens*. BMC Microbiology 5.

42. Abdel-Hamid AM, Cronan JE (2007) Coordinate expression of the acetyl coenzyme A carboxylase genes, *accB* and *accC*, is necessary for normal regulation of biotin synthesis in *Escherichia coli*. Journal of Bacteriology 189: 369-376.

43. Kimura Y, Miyake R, Tokumasu Y, Sato M (2000) Molecular cloning and characterization of two genes for the biotin carboxylase and carboxyltransferase subunits of acetyl coenzyme A carboxylase in *Myxococcus xanthus*. Journal of Bacteriology 182: 5462-5469.

44. Rao CV, Kirby JR, Arkin AP (2004) Design and diversity in bacterial chemotaxis: A comparative study in *Escherichia coli* and *Bacillus subtilis*. PLoS Biology 2: 239-252.

45. Ulrich L, Koonin E, Zhulin I (2005) One-component systems dominate signal transduction in prokaryotes. Trends in Microbiology 13: 52-56.

46. Bellenger K, Ma XY, Shi WY, Yang ZM (2002) A CheW homologue is required for *Myxococcus xanthus* fruiting body development, social gliding motility, and fibril biogenesis. Journal of Bacteriology 184: 5654-5660.

47. Bonner PJ, Xu Q, Black WP, Li Z, Yang ZM, et al. (2005) The Dif chemosensory pathway is directly involved in phosphatidylethanolamine sensory transduction in *Myxococcus xanthus*. Molecular Microbiology 57: 1499-1508.

48. Sun H, Zusman DR, Shi WY (2000) Type IV pilus of *Myxococcus xanthus* is a motility apparatus controlled by the *frz* chemosensory system. Current Biology 10: 1143-1146.

49. Kimura Y, Ishida S, Matoba H, Okahisa N (2004) RppA, a transducer homologue, and MmrA, a multidrug transporter homologue, are involved in the biogenesis and/or assembly of polysaccharide in *Myxococcus xanthus*. Microbiology 150: 631-639.

50. Mignot T, Shaevitz JW, Hartzell PL, Zusman DR (2007) Evidence that focal adhesion complexes power bacterial gliding motility. Science 315: 853-856.

51. Bohlendorf B, Herrmann M, Hecht HJ, Sasse F, Forche E, et al. (1999) Antibiotics from gliding bacteria, 85([not equivalent to]) - Melithiazols A-N: New antifungal beta-methoxyacrylates from myxobacteria. European Journal of Organic Chemistry: 2601-2608.

52. Schneiker S, Perlova O, Kaiser O, Gerth K, Alici A, et al. (2007) Complete genome sequence of the myxobacterium *Sorangium cellulosum*. Nature Biotechnology 25: 1281-1289.

53. Macnab RM (2003) How bacteria assemble flagella. Annual Review of Microbiology 57: 77-100.

54. Guiral M, Leroy G, Bianco P, Gallice P, Guigliarelli B, et al. (2005) Interaction and electron transfer between the high molecular weight cytochrome and cytochrome c(3) from *Desulfovibrio vulgaris* Hildenborough: Kinetic, microcalorimetric, EPR and electrochemical studies. Biochimica Et Biophysica Acta-General Subjects 1723: 45-54.

55. Lovley DR, Widman PK, Woodward JC, Phillips EJP (1993) Reduction of uranium by cytochrome-c(3) of *Desulfovibrio vulgaris*. Applied and Environmental Microbiology 59: 3572-3576.

56. Shi L, Squier TC, Zachara JM, Fredrickson JK (2007) Respiration of metal (hydr)oxides by *Shewanella* and *Geobacter*: a key role for multihaem c-type cytochromes. Molecular Microbiology 65: 12-20.

57. Dedysh SN, Pankratov TA, Belova SE, Kulichevskaya IS, Liesack W (2006) Phylogenetic analysis and *in situ* identification of bacteria community composition in an acidic *Sphagnum* peat bog. Applied and Environmental Microbiology 72: 2110-2117.

58. Todorova SG, Costello AM (2006) Design of *Shewanella*-specific 16S rRNA primers and application to analysis of *Shewanella* in a minerotrophic wetland. Environmental Microbiology 8: 426–432.

59. Methe BA, Nelson KE, Eisen JA, Paulsen IT, Nelson W, et al. (2003) Genome of *Geobacter sulfurreducens*: Metal reduction in subsurface environments. Science 302: 1967-1969.

60. Lovley DR, Giovannoni SJ, White DC, Champine JE, Phillips EJP, et al. (1993) *Geobacter metallireducens* Gen-Nov Sp-Nov, a microorganism capable of coupling the complete oxidation of organic-compounds to the reduction of iron and other metals. Archives of Microbiology 159: 336-344.

61. Lowe KL, Dichristina TJ (2000) Microbiological and geochemical characterization of microbial Fe(III) reduction in salt marsh sediments. Geomicrobiology Journal 17: 163–178.

62. He JZ, Ritalahti KM, Yang KL, Koenigsberg SS, Löffler FE (2003) Detoxification of vinyl chloride to ethene coupled to growth of an anaerobic bacterium. Nature 424: 62-65.

63. Rodrigues ML, Oliveira TF, Pereira IA, Archer M (2006) X-ray structure of the membrane-bound cytochrome c quinol dehydrogenase NrfH reveals novel haem coordination. EMBO Journal 25: 5951-5960.

64. Esteve-Nunez A, Sosnik J, Visconti P, Lovley DR (2008) Fluorescent properties of *c*-type cytochromes reveal their potential role as an extracytoplasmic electron sink in *Geobacter sulfurreducens*. Environmental Microbiology 10: 497-505.

65. Stiefel EI, Watt GD (1979) *Azotobacter* cytochrome-B557.5 is a bacterioferritin. Nature 279: 81-83.

66. van Eerde A, Wolternik-van Loo S, van der Oost J, Dijkstra BW (2006) Fortuitous structure determination of 'as-isolated' *Escherichia coli* bacterioferritin in a novel crystal form. Acta Crystallographica Section F-Structural Biology and Crystallization Communications 62: 1061-1066.

67. de Bok FAM, Roze EHA, Stams AJM (2002) Hydrogenases and formate dehydrogenases of Syntrophobacter fumaroxidans. Antonie Van Leeuwenhoek International Journal of General and Molecular Microbiology 81: 283-291.

68. Rahm BG, Morris RM, Richardson RE (2006) Temporal expression of respiratory genes in an enrichment culture containing *Dehalococcoides ethenogenes*. Applied and Environmental Microbiology 72: 5486-5491.

69. Suyama A, Yamashita M, Yoshino S, Furukawa K (2002) Molecular characterization of the PceA reductive dehalogenase of *Desulfitobacterium* sp strain Y51. Journal of Bacteriology 184: 3419-3425.

70. Krajmalnik-Brown R, Holscher T, Thomson IN, Saunders FM, Ritalahti KM, et al. (2004) Genetic identification of a putative vinyl chloride reductase in *Dehalococcoides* sp strain BAV1. Applied and Environmental Microbiology 70: 6347-6351.

71. Fung JM, Morris RM, Adrian L, Zinder SH (2007) Expression of reductive dehalogenase genes in *Dehalococcoides ethenogenes* strain 195 growing on tetrachloroethene, trichloroethene, or 2,3-dichlorophenol. Applied and Environmental Microbiology 73: 4439-4445.

72. Letunic I, Copley RR, Pils B, Pinkert S, Schultz J, et al. (2006) SMART 5: domains in the context of genomes and networks. Nucl Acids Res 34: D257-260.

73. Madigan MT, Martinko JM, Parker J (2003) Brock biology of microorganisms. Upper Saddle River, NJ: Pearson Education, Inc.

74. Pfennig N (1967) Photosynthetic bacteria. Annual Review of Microbiology 21: 285-&.

75. Pfennig N, Trüper H (1989) Anoxygenic phototrophic bacteria. In: Staley J, Pfennig N, Holt J, editors. Bergey's Manual of Systematic Bacteriology. Baltimore: Williams and Wilkins. pp. 1635–1709.

76. Gorlenko VM (2004) History of the study of biodiversity of photosynthetic bacteria. Microbiology 73: 541-550.

77. Castresana J, Lubben M, Saraste M, Higgins DG (1994) Evolution of cytochrome oxidase, an enzyme older than atmospheric oxygen. Embo Journal 13: 2516-2525.

78. Pitcher RS, Watmough NJ (2004) The bacterial cytochrome cbb_3 oxidases. Biochimica et Biophysica Acta 1655: 388-399.

79. Storz G, Imlay JA (1999) Oxidative stress. Current Opinion in Microbiology 2: 188-194.

80. Brioukhanov AL, Thauer RK, Netrusov AI (2002) Catalase and superoxide dismutase in the cells of strictly anaerobic microorganisms. Microbiology 71: 281-285.

81. Lumppio HL, Shenvi NV, Summers AO, Voordouw G, Donald M. Kurtz J (2001) Rubrerythrin and rubredoxin oxidoreductase in *Desulfovibrio vulgaris*: A novel oxidative stress protection system. Journal of Bacteriology 183: 101–108.

82. Jovanovic T, Ascenso C, Hazlett KRO, Sikkink R, Krebs C, et al. (2000) Neelaredoxin, an iron-binding protein from the syphilis spirochete, *Treponema pallidum*, is a superoxide reductase. Journal of Biological Chemistry 275: 28439-28448.

83. Lombard M, Touati Dl, Fontecave M, Nivie`re V (2000) Superoxide reductase as a unique defense system against superoxide stress in the microaerophile *Treponema pallidum*. Journal of Biological Chemistry 275: 27021–27026.

84. Dolla A, Fournier M, Dermoun Z (2006) Oxygen defense in sulfate-reducing bacteria. Journal of Biotechnology 126: 87-100.

85. Lin WC, Coppi MV, Lovley DR (2004) *Geobacter sulfurreducens* can grow with oxygen as a terminal electron acceptor. Applied and Environmental Microbiology 70: 2525-2528.

86. Baughn AD, Malamy MH (2004) The strict anaerobe *Bacteroides fragilis* grows in and benefits from nanomolar concentrations of oxygen. Nature 427: 441-444.

87. Löffler FE, Edwards EA (2006) Harnessing microbial activities for environmental cleanup. Current Opinion in Biotechnology 17: 274-284.

88. Pett-Ridge J, Firestone MK (2005) Redox fluctuation structures microbial communities in a wet tropical soil. Applied and Environmental Microbiology 71: 6998-7007.

89. Tian WD, Arakaki AK, Skolnick J (2004) EFICAz: a comprehensive approach for accurate genome-scale enzyme function inference. Nucleic Acids Research 32: 6226-6239.

90. Arakaki A, Tian W, Skolnick J (2006) High precision multi-genome scale reannotation of enzyme function by EFICAz. BMC Genomics 7: 315.

91. Kumar S, Tamura K, Nei M (2004) MEGA3: Integrated software for Molecular Evolutionary Genetics Analysis and sequence alignment. Briefings in Bioinformatics 5: 150-163.

92. Kanehisa M, Goto S, Hattori M, Aoki-Kinoshita KF, Itoh M, et al. (2006) From genomics to chemical genomics: new developments in KEGG. Nucleic Acids Research 34: D354-357.

93. International Union of Biochemistry and Molecular Biology. Nomenclature Committee., Webb EC (1992) Enzyme nomenclature 1992 : recommendations of the Nomenclature Committee of the International Union of Biochemistry and Molecular Biology on the nomenclature and classification of enzymes. San Diego: Published for the International Union of Biochemistry and Molecular Biology by Academic Press. xiii, 862 p. p.

94. Altschul SF, Gish W, Miller W, Myers EW, Lipman DJ (1990) Basic Local Alignment Search Tool. Journal of Molecular Biology 215: 403-410.

95. Lawrence JG, Ochman H (1998) Molecular archaeology of the *Escherichia coli* genome. Proceedings of the National Academy of Sciences of the United States of America 95: 9413-9417.

96. Shi SY, Cai XH, Ding DF (2005) Identification and categorization of horizontally transferred genes in prokaryotic genomes. Acta Biochimica Et Biophysica Sinica 37: 561-566.

97. Rutherford K, Parkhill J, Crook J, Horsnell T, Rice P, et al. (2000) Artemis: sequence visualization and annotation. Bioinformatics 16: 944-945.

98. Stothard P, Wishart DS (2005) Circular genome visualization and exploration using CGView. Bioinformatics 21: 537-539.

99. Karlin S, Campbell AM, Mrazek J (1998) Comparative DNA analysis across diverse genomes. Annual Review of Genetics 32: 185-225.

100. Grote A, Hiller K, Scheer M, Munch R, Nortemann B, et al. (2005) JCat: a novel tool to adapt codon usage of a target gene to its potential expression host. Nucleic Acids Research 33: W526-W531.

101. Sharp PM, Li WH (1987) The Codon Adaptation Index - a Measure of Directional Synonymous Codon Usage Bias, and Its Potential Applications. Nucleic Acids Research 15: 1281-1295.

CHAPTER 4: Diversity and distribution of *Anaeromyxobacter* strains in a uranium-contaminated subsurface environment with nonuniform flow

4.1 Abstract

Versaphilic *Anaeromyxobacter dehalogenans* strains implicated in hexavalent uranium reduction and immobilization are present in the fractured saprolite subsurface environment at the Department of Energy Integrated Field-Scale Subsurface Research Challenge (IFC) site near Oak Ridge, TN. To provide insight into the *in situ* distribution of *Anaeromyxobacter* in this nonuniform flow groundwater system, 16S rRNA gene-targeted primers and linear hybridization (TaqMan) probes were designed for Oak Ridge IFC *Anaeromyxobacter* isolates FRC-D1 and FRC-W along with an *Anaeromyxobacter* genus-targeted probe and primer set. Multiplex quantitative real-time PCR (mqPCR) was applied to samples collected from Oak Ridge IFC site Areas 1 and 3, which are not connected by the primary groundwater flow paths; however, transport between them through cross-plane fractures is hypothesized. Strain FRC-W accounted for more than 10% of the total quantifiable *Anaeromyxobacter* community in Area 1 soils, while strain FRC-D1 was not detected. In FeOOH-amended enrichment cultures derived from Area 1 site materials, strain FRC-D1 accounted for 30-90% of the total *Anaeromyxobacter* community, demonstrating that this strain was present *in situ* in Area 1. Area 3 total *Anaeromyxobacter* abundance exceeded that of Area 1 by three to five orders of magnitude, but neither strain FRC-W- or FRC-D1-like sequences were quantifiable in any of the 33 Area 3 groundwater or sediment samples tested. The *Anaeromyxobacter* community in Area 3 increased from below 10^5 cells/g sediment outside the ethanol biostimulation treatment zone to 10^8 cells/g sediment near the injection well and 16S rRNA gene clone library analysis revealed that representatives of a novel phylogenetic cluster dominated the Area 3 *Anaeromyxobacter* community inside the treatment loop. The combined applications of genus- and strain-level mqPCR along with clone libraries

provided novel information on patterns of microbial variability within a bacterial group relevant to uranium bioremediation.

4.2 Introduction

Molecular analyses enable specific detection of target organisms, providing insight into microbial biogeography and the factors controlling microbial community structure and function over temporal and spatial scales (reviewed in [1,2,3]. Spatial isolation in disconnected environments has been demonstrated in plant rhizospheres [4], saturated soils versus unsaturated soils [5,6], and undisturbed (pristine) top soils [7,8]. One unresolved issue of biogeography involves spatial distribution of distinct populations (of a given species) in physically connected environments such as heterogeneous subsurface media with nonuniform flow characteristics (e.g., fractured saprolite). A complex matrix of aged bedrock makes up the uranium contaminated subsurface environment at the U.S. Department of Energy Integrated Field-scale Subsurface Research Challenge (IFC) site near Oak Ridge, TN (formerly known as the Field Research Center [FRC]). Connectivity and transport between two distinct Oak Ridge IFC study areas (a near-source contaminant plume in Area 3 and farther-source plume in Area 1) have been hypothesized based on evidence of flow through fractured bedding planes that extend from the Area 3 vicinity (near the S3 waste disposal ponds) to Area 1 [9]. Whether microbes are transported between these two subsurface regimes is unclear, but the implications are important for understanding spatially-variable biogeochemical processes that control contaminant fate and migration at the site [9].

A. dehalogenans populations are relevant to bioremediation at the Oak Ridge IFC site due to their capacity to metabolically reduce soluble U(VI) to sparingly soluble, immobile U(IV) [10,11,12]. More than a dozen different *Anaeromyxobacter* 16S rRNA gene sequences have been identified in contaminated site materials derived from the Oak Ridge IFC site [13,14,15]. Distinct *A. dehalogenans* strains were isolated from IFC site materials from Area 1 (16S rRNA

gene Accession numbers FJ190048-FJ190062). Laboratory characterization of *A. dehalogenans* strains that are very closely related (>99.9% 16S rRNA gene similarity) demonstrate metabolic variability in terms of growth rates as well as substrate [16,17,18]. This is consistent with observations from other studies that have demonstrated that exploring diversity at the sub-species level is crucial for understanding microbial interactions and processes [8,19,20,21,22,23]. Tools that capture the distribution and abundance of *A. dehalogenans* strains in spatially and temporally heterogeneous subsurface environments are desirable to comprehensively describe biogeochemical processes controlling contaminant migration. Quantitative real-time PCR (qPCR) approaches using TaqMan probe detection chemistry offer high specificity (i.e., distinguish sequences that differ by only 1-2 bp) and allow the quantification of multiple targets in a single reaction [24,25]. The multiplex qPCR (mqPCR) technique reduces materials consumption, labor, and the probability for experimental errors, and has been successfully applied for discrimination of pathogenic bacteria, including *Listeria monocytogenes* strains [26] and *Brucella* isolates [27], as well as simultaneous identification of four bioterrorism agents [28]. Despite successful applications in the medical and biodefense fields, mqPCR approaches have had limited application to monitoring bioremediation processes. To demonstrate that strain-specific resolution of *Anaeromyxobacter* strains is feasible and provides relevant information about microbial distribution, we designed and applied a mqPCR approach to characterize and monitor the *Anaeromyxobacter* community at the Oak Ridge IFC site across Areas 1 and 3. The results from this study provide new information about microbial, and hence functional, heterogeneity in a uranium-contaminated, saturated subsurface environment with nonuniform flow.

4.3 Materials and Methods

4.3.1 Selection of strains. Oak Ridge IFC site isolates FRC-D1 and FRC-W were derived from Area 1 soil core samples collected from boreholes FW032 and FW034, respectively. Strain FRC-D1 was isolated via FeOOH enrichment [14] whereas strain FRC-W was obtained via enrichment with 2-chlorophenol, as were the first *Anaeromyxobacter* isolates [17]. Strains FRC-D1 and FRC-W share 99.99% 16S rRNA gene sequence similarity over a stretch of 1,550 bp and share >99% 16S rRNA gene sequence similarity with the previously characterized *Anaeromyxobacter* strains 2CP-1 and 2CP-C [17,29].

4.3.2 Culture conditions. *A. dehalogenans* strains were routinely grown at 25°C without shaking in 60 mL (nominal capacity) glass serum bottles (Wheaton, Millville, NJ) with 40 mL of reduced, 30 mM bicarbonate-buffered mineral salts medium and a N_2/CO_2 headspace (80:20, vol:vol) [30]. The bottles were sealed with butyl rubber stoppers (Geo-Microbial Technologies, Inc., Ochelata, OK) and aluminum crimp caps (Wheaton). Acetate (5 mM) (Sigma-Aldrich, St. Louis, MO) was provided as electron donor, and fumarate (10 mM) (Sigma-Aldrich) served as electron acceptor.

Co-culture experiments were initiated with 300 µL inocula of a FRC-W culture and 400 µL of FRC-D1 culture, which were both in late exponential phase (OD 600 nm of 0.20 and 0.15, respectively). Each inoculum contained 1.0-1.5 x 10^7 cells. Co-culture samples were removed periodically for 16S rRNA gene quantification and organic acid (i.e., acetate, fumarate and succinate) analysis.

4.3.3 Oak Ridge IFC site description. Subsurface soil cores and sediment slurries were acquired from the Oak Ridge IFC site, which is heavily contaminated with a mixture of metals, radionuclides, and ligands [31]. The site resides near the former S-3 Waste Disposal Ponds that were unlined surface impoundments used in the disposal of over 300 million liters of concentrated uranium and nitric acid waste during the period of 1951-1983 [32]. Infiltration was

the primary release mechanism to soils and groundwater, and vast subsurface domains have been contaminated, creating a massive legacy waste problem [31].

Contaminant fate and transport at the Oak Ridge IFC site are controlled by a complex, nonlinear, and transient hydrological, geochemical, and microbial processes [31]. Dynamics of these three interacting processes are controlled by the highly structured nature of the subsurface media that underlie the site [33,34]. Oak Ridge IFC site subsurface soils and sediments are acidic inceptisols consisting of highly fractured saprolites that have weathered from interbedded shale-limestone sequences. The limestone has been weathered to massive clay lenses that may contain residual carbonate, and the more resistant shale has weathered to an extensively fractured saprolite. Fractures are highly interconnected with densities in the range of 200 fractures per meter [35]. The fracture network consists of (i) fractures along bedding planes, (ii) two sets of orthogonal extensional fractures that are perpendicular to bedding planes, and (iii) shear fractures. Extensional fractures are either parallel or perpendicular to the strike of bedding planes, and form an orthogonal fracture network with the bedding plane fractures. Under saturated conditions, strike parallel fractures control the direction of groundwater and contaminant migration, but bedding plane fractures dominate the fracture network of the media and may also contribute, to a significantly lesser extent, to the migration tendency of contaminants.

Soil, sediment and groundwater samples were obtained from two spatially distinct Oak Ridge IFC site locations, Areas 1 and 3 [9]. Area 3 is near the S-3 Waste Disposal Ponds waste source. Materials in the Area 3 vicinity of the regime are up-dip from subsurface material residing in Area 1, which is tens of meters away. The two subsurface environments are not connected by the main groundwater flow path, which is strike parallel from the waste source, but they may be connected by less conductive bedding parallel and orthogonal extension fractures. Single-well, push-pull tests and downstream samplers have been utilized during biostimulation experiments using ethanol, acetate, and/or glucose in Area 1 [14,15,36]. Area 3 is the location of a pilot-scale

in situ uranium bioremediation study that involved groundwater conditioning and periodic ethanol (i.e, 88.12% ethanol, 4.65% methanol, 7.23% water) biostimulation [13,37,38,39].

4.3.4 Field samples, microcosms, and enrichment cultures. Soil core samples were collected from Area 1 boreholes as described (http://public.ornl.gov/orifc/map_area1_inset.cfm) [14,40]. Microcosms were established with homogenized soil core samples collected from six Area 1 wells and boreholes (FWB030, FWB302, FWB032, FB061, FWB027, and FWB034) by Petrie et al. [14], and FeOOH enrichment cultures were provided by Denise Akob and Joel Kostka, Florida State University. In addition, the Kostka group provided Area 1 soil core samples including multiple homogenized depth interval samples from boreholes FB074 (96, 115, 130, 132, 148, 168, 186, 188, 204, 228, 230, and 240 inches below ground surface [bgs]), FB089 (21, 27, and 33 inches bgs) and FB090 (17, 23, and 29 inches bgs) for DNA extraction and qPCR analysis. Soil cores included in molecular analysis were collected adjacent to those used for enrichment and isolation efforts [14,31].

Area 3 sediment samples were collected from wells FW024, FW026, FW100, FW101, FW102, FW103, and FW104 inside the pilot-scale U(VI) bioreduction demonstration plot (http://public.ornl.gov/orifc/map_area3_inset_a.cfm) [37,38,39]. Sediment samples were collected on October 5, 2005, during the ethanol biostimulation phase using a well surging procedure as described [13]. Groundwater samples were collected by Sue Carroll, Weimin Wu, Jack Carley, and Terry Gentry from wells FW104, FW101 and FW102 inside the Area 3 pilot-scale demonstration plot [37,38,39,41]. Area 3 microcosms were established by Youlboong Sung from site samples obtained on August 4, 2005 from well FW104 as described [41]. In an anoxic chamber filled with N_2/H_2 (97:3, vol:vol), 160-ml glass serum bottles received 15 mL of mineral salts medium and were amended with 2 g of sediment, 10 mM acetate, 5 mM fumarate and 5 mM nitrate.

4.3.5 DNA extraction. Aliquots (0.5 mL) from microcosms, enrichment cultures and co-cultures were removed with a syringe and transferred to 1.5-mL Eppendorf plastic tubes. Cells were collected by centrifugation at 16,000 x g for 3 minutes at room temperature, the supernatant was decanted and the pellets were frozen at -20ºC for at least 24 hours. To extract DNA, 0.2 mL Instagene Matrix solution (Bio-Rad Laboratories, Hercules, CA) was added to each frozen pellet, and DNA was prepared according to the manufacturer's specifications. The DNA was used immediately for qPCR analysis or stored at -20°C.

DNA from 14 Area 1 samples collected from boreholes FB074, FB089, and FB090 was extracted using the MoBio Power Soil DNA kit (MoBio, Carlsbad, CA) following the manufacturer's protocol. Additional DNA samples from 44 Area 1 enrichment cultures and 18 Area 3 sediment samples were provided by Denise Akob (Florida State University) and Mary Beth Leigh and Erick Cardenas (Michigan State University), respectively. Dry DNA pellets from Area 3 sediments were suspended in 100 µL of sterile, nuclease-free, deionized water to yield a DNA concentration of 1 ng μL^{-1}. Fifteen DNA samples from Area 3 groundwater collected from wells FW102 and FW101 were provided by Joy Van Nostrand and Jizhong Zhou (University of Oklahoma). Quantification of laboratory cultures, soil and sediment samples, and groundwater samples was normalized to mL of culture, g of soil or sediment, or L of groundwater, respectively.

4.3.6 Design of* A. dehalogenans *strain-specific primers and probes. Thirty one *Anaeromyxobacter*-like 16S rRNA gene sequences from the NCBI non-redundant database (GenBank accession numbers AJ504428-AJ504437, AF382396-AF382400, AF482687, AKYG1825, DQ451451, DQ145119, DQ145125, DQ110017, DQ110097, AY360608, AY527735, AY527764, AY527784, AY527785, AY527791, AY527798) were aligned using Clustal W (MegAlign, DNA Star Inc., Madison, WI). Included in the alignment were sequences of related delta-proteobacteria including several Myxobacteria (Accession numbers AJ233935,

AJ233908, AJ233897, CEX23393, AJ233913, M34114, and AF503460) and two *Geobacter* species (Accession numbers L07834 and U13928).

Linear hybridization (TaqMan) probes and primers were designed using Primer Express software (Applied Biosystems [ABI], Foster City, CA). All primer/probe sets were designed to meet the criteria for multiplex application (i.e., probes and primers share similar melting temperatures) (Table 4.1) [42]. qPCR reactions contained a forward primer, a reverse primer (Integrated DNA Technologies, Coralville, IA) , and a probe that carried FAM, NED, or VIC as a reporter dye on the 5' end and a non-fluorescent quencher with a minor-groove-binder on the 3' end (ABI). Two strain-specific TaqMan mqPCR probes targeting the variable V3 region of the 16S rRNA gene were designed for the same primer pair (Table 4.1). The specificity of all probes and primers was evaluated using BLAST for "short, nearly exact nucleotide" sequence matches [43]. To verify probe specificity, each strain-specific probe was used in reactions with target and/or non-target (i.e., the cloned 16S rRNA gene fragment of the other strain) plasmid DNA. The FAM-labeled FRC-W probe targets *A. dehalogenans* strains FRC-W, 2CP-C, 2CP-3, and 2CP-5. The NED-labeled FRC-D1 probe targets strains FRC-D1, 2CP-1, and 2CP-2. A VIC-labeled genus-specific Total *Anaeromyxobacter* (TAna) probe targets a separate region of the 16S rRNA gene with a different primer pair and was used to quantify the total *Anaeromyxobacter* community (Table 4.1). The optimal probe and primer concentrations were determined experimentally following the protocol provided in the ABI Chemistry Guide [42]. For enumeration of total bacterial 16S rRNA gene copies, primers Bac1055YF and Bac1392R combined with Bac1115Probe were used as described [22].

4.3.7 qPCR analysis. qPCR master mix (ABI), 2.5 μM of each probe (ABI), and 5 μM of each primer were combined in sterile, nuclease-free water prior to addition of any DNA template. Aliquots (18 μL) of the reaction mix were dispensed into an ABI MicroAmp™ Fast Optical 96-Well Reaction Plate held on ice. Template DNA (2 μL) was added to each well, contents were

Table 4.1. Probes and primers used for TaqMan mqPCR.

Primer/probe	Target group	Primer/probe sequence (5'-3')
Ade399 Fwd	*Anaeromyxobacter*	GCA ACG CCG CGT GTG T
Ade466 Rev	*Anaeromyxobacter*	TCC CTC GCG ACA GTG CTT
TAna VIC probe	*Anaeromyxobacter*	VIC–ATG AAG GTC TTC GGA TCG T–NFQ
2CP444 Fwd	2CP-like strains [a]	TCG CGA GGG ACG AAT AAG G
2CP513 Rev	2CP-like strains [a]	CGG TGC TTC CTC TCG AGG TA
FRC-D1 NED probe	2CP-1, 2CP-2, FRC-D1	NED–ACA GTC CGT TTC GAT GAC–NFQ [b]
FRC-W FAM probe	2CP-C, 2CP-5, FRC-W	FAM–ACA GTC CGT CAC GAT GA–NFQ [b]

[a] Includes all *Anaeromyxobacter* strains described by Sanford et al. (41).

[b] Strain-specific nucleotides are underlined

mixed, and the wells were sealed with an ABI Optical Adhesive Cover. An ABI 7500 Real-Time PCR System was used to detect FAM, VIC, and/or NED fluorescence either individually (singleplex) or simultaneously (multiplex). *Anaeromyxobacter*-targeted mqPCR reactions were carried out with the following thermal program: 50°C for 2 min (1 cycle); 95°C for 10 min (1 cycle); 95°C for 15 sec, 60°C for 1 min (40 cycles). Fluorescence data were collected at 60°C during each cycle. qPCR to enumerate total bacteria was carried out as described [22].

4.3.8 qPCR calibration curves. In order to obtain calibration standard curves (i.e., gene copy number versus the cycle number at which the fluorescence intensity reaches a set cycle threshold value), 16S rRNA genes of strains 2CP-1 and 2CP-C, which share identical primer and probe binding sites with strains FRC-D1 and FRC-W, respectively (Table 4.1), were cloned into plasmids using the Invitrogen TOPO TA Cloning kit (Invitrogen, Carlsbad, CA). A 10-fold dilution series of purified plasmid was used for each qPCR reaction plate, and copy numbers of unknown samples were calculated as described [22]. Samples and standards were run in triplicate qPCR reactions. Amplification efficiencies were calculated based on standard curve slope values as described [44]. If necessary, samples were diluted so that the copy number values fell within the quantification range of the calibration curve for each individual reaction plate. The lowest value in the linear calibration curve for each plate is reported as the quantification limit, which ranged from 1.0×10^1 to 3.0×10^1 gene copies per reaction (Table 4.2). Samples falling above the quantification limit produce fluorescence that crosses the threshold value within 38 PCR cycles in every replicate. Below detection limit (BDL) is reported when probe fluorescence did not exceed threshold fluorescence (i.e., delta $R_n = 0$) for any reaction cycle. "Detected but not quantified" is reported when fluorescence values cross the threshold value after more than 38 PCR cycles [42]. The quantification of 16S rRNA gene copies was utilized as an approximation of cell numbers. The four sequenced *Anaeromyxobacter* genomes (GenBank Accession numbers: CP001131, CP000769, CP000251, ABKC00000000) harbor duplicate rRNA operons [45] suggesting that members of the *Anaeromyxobacter* group contain two 16S rRNA gene copies.

Table 4.2. Linear regression results of multiplex and singleplex qPCR standard curves (see also Figure S1).

	Fluorophore					
	FAM		NED		VIC	
	Multiplex	Singleplex	Multiplex	Singleplex	Multiplex	Singleplex
Slope	-3.57 ± 0.01	-3.67 ± 0.16	-3.27 ± 0.10	-3.37 ± 0.08	-3.76 ± 0.12	-3.97 ± 0.23
P-value	0.67		0.62		0.56	
y-intercept	41.15 ± 0.57	42.26 ± 0.99	42.19 ± 0.61	42.20 ± 0.44	43.82 ± 0.71	45.83 ± 1.28
P-value	0.28		0.17		0.14	
R^2	0.86	0.93	0.81	0.97	0.83	0.89
n [a]	20	3	20	4	20	3
Amplification efficiency [b]	1.91	1.87	2.02	1.98	1.84	1.79
Quantification limit[c]	3×10^1	8×10^1	3×10^1	3×10^2	1×10^1	1×10^2

[a] *n* indicates the number of replicate, independent dilution series
[b] Amplification efficiency was calculated based on best fit slope for replicate data sets
[c] Reported in 16S rRNA gene copies per reacti

4.3.9 Clone libraries. Three 16S rRNA gene clone libraries were established using the *Anaeromyxobacter* 16S rRNA gene-specific forward primer 60F described previously [14] and the reverse primer 1450-1470 REV (5'-TTG GCG CGG CCA CTT CT-3'). The primer pair yielded 1,410 bp-long amplicons. One library was established with DNA extracted from biomass collected on a 0.2 µm membrane filter from 2 L of groundwater obtained from the Oak Ridge IFC site Area 3 injection well FW104 on August 4, 2005 (gro8 clones). Another library was generated with DNA extracted from microcosms established with materials collected from well FW104 (micA clones). A third library was established with DNA extracted from sediment collected from well FW104 at the end of the ethanol biostimulation phase before a U(IV) re-oxidation experiment was initiated [39] (sedO clones). The total volume of each PCR mixture was 25 µL and contained (final concentrations) 1 x reaction buffer, 2.5 mM $MgCl_2$ (GeneAmp PCR Kit, ABI), 50 nM of each primer, 250 µM concentrations of each deoxynucleoside triphosphate (Invitrogen), 13 mg mL^{-1} of bovine serum albumin (Invitrogen), 2.5 U of AmpliTaq polymerase (ABI), and 2 µl of 1:10 diluted template DNA (10-20 ng mL^{-1}). PCR reactions were carried out in 9600 GeneAmp PCR system (Perkin Elmer, Waltham, MA) with the following temperature program: 94°C for 2 min and 10 sec (1 cycle); 94°C for 30 sec, 57.5°C for 45 sec, and 72°C for 2 min and 10 sec (30 cycles); 72°C for 6 min. Fresh PCR products were cloned into the TOPO vector pCR 2.1 (TA Cloning Kit, Invitrogen) according to the manufacturer's instructions. Transformants from each of the three *Anaeromyxobacter* 16S rRNA gene clone libraries were selected and screened for the presence of the expected 16S rRNA gene insert using vector-targeted primers M13F and M13R [46] and the *Anaeromyxobacter* 16S rRNA gene-targeted primers 60F and 461R [14]. In order to detect distinct sequences, amplified fragments from 10 clones of each library were digested with the restriction endonucleases *MspI*, *HhaI* and *RsaI* (Gibco) at 37°C for 3 hours according to the manufacturer's recommendations. Restriction fragments were resolved in 3% (w:vol) Metaphor agarose (FMC Bioproducts, Rockland, ME) gels using fresh TAE buffer (40 mM Tris base in 20 mM acetic acid, 1 mM EDTA, pH 8.5) at

4°C and stained with ethidium bromide (1 µg mL^{-1}). Fragment sizes were estimated by comparison with the Invitrogen 1kb Plus DNA molecular weight markers.

4.3.10 Sequence and phylogenetic analysis. To obtain sequence information of cloned *Anaeromyxobacter* 16S rRNA gene fragments, plasmids were extracted with the QIAGEN Plasmid Mini Kit (QIAGEN Inc., Valencia, CA) according to the manufacturer's protocol. Plasmid templates (~270 ng of DNA) from representative clones were sequenced by Nevada Genomics Center (University of Nevada, Reno, NV). Sequences were aligned and analyzed with Clustal W and tested for possible chimera artifacts with the RDP CHIMERA CHECK tool [47]. Phylogenetic relationships of *Anaeromyxobacter* 16S rRNA gene sequences were inferred using the Neighbor-Joining method in MEGA4 [48,49]. The percentage of replicate trees in which the associated taxa clustered together in the bootstrap test (500 replicates) are shown at each branching point [50]. The evolutionary distances were calculated using the Maximum Composite Likelihood method [51] and are in the units of the number of base substitutions per site. All missing data and positions containing gaps were eliminated from the dataset (MEGA4; Complete deletion option).

4.3.11 Modeling spatial distribution of* Anaeromyxobacter *in Area 3. The Area 3 *Anaeromyxobacter* population distribution was visualized using the United States Department of Defense Groundwater Modeling System 3.1 (http://chl.erdc.usace.army.mil/Media/3/7/2/GMSFactSheet.pdf). Input parameters were *Anaeromyxobacter* abundance data measured in samples obtained from the hydraulically connected depths of each well sampled in Area 3 (well screen depth 12-14 m bgs for multi-level sampling wells [i.e., depth interval 2 [37]]. Interpolation of scatter point data was performed using the natural neighbor method and the software's default parameters.

4.3.12 Statistical analysis. The average slope and y-intercept of each qPCR calibration curve were determined by regression analysis and used to calculate the number of gene copies per

mL of culture or sample. All significance tests, regression analyses, and 95% confidence intervals were performed using GraphPad Prism 5 with default settings. ANOVA repeated measures test with Tukey post test (95% confidence) was used to determine whether the standard curves generated for the three primer/probe combinations were consistent with one another and between multiplex and singleplex experiments. Samples for qPCR analysis were run with three replicates per reaction. Co-culture experiments were performed in triplicate. The symbols and error bars for co-culture analyses, thus, represent the averages of nine qPCR data points and standard deviations of three replicate culture data points per time point.

4.3.13 Chemical analyses. Organic acids for co-culture experiments were quantified using a Waters 1525 high performance liquid chromatography (HPLC) system equipped with an Aminex HPX-87H ion exclusion column and a Waters 2487 dual wavelength absorbance detector as previously described [52].

4.4 Results

4.4.1 Sensitivity and specificity of the mqPCR approach. TaqMan detection chemistry enabled quantification of *Anaeromyxobacter* target 16S rRNA gene copies over a large dynamic range spanning eight orders of magnitude (i.e., 10^1 to 10^9 copies per reaction). The quantification limit was fewer than 10 copies of target genes per reaction in the strain- and the *Anaeromyxobacter* genus-specific assays. No cross-reactivity was observed between the strain FRC-W-specific probe and DNA from the closely related, non-target strain FRC-D1, or vice versa even though they share 99.99% 16S rRNA gene sequence identity. mqPCR analysis with FRC-W-FAM, FRC-D1-NED, and TAna-VIC TaqMan probes (all with a non-fluorescent quencher) produced results similar to singleplex analysis (Figure 4.1), thus validating the multiplex analysis. ANOVA comparisons of linear regression slopes and y-intercepts for multiple standard curves indicated that singleplex and multiplex qPCR results were not

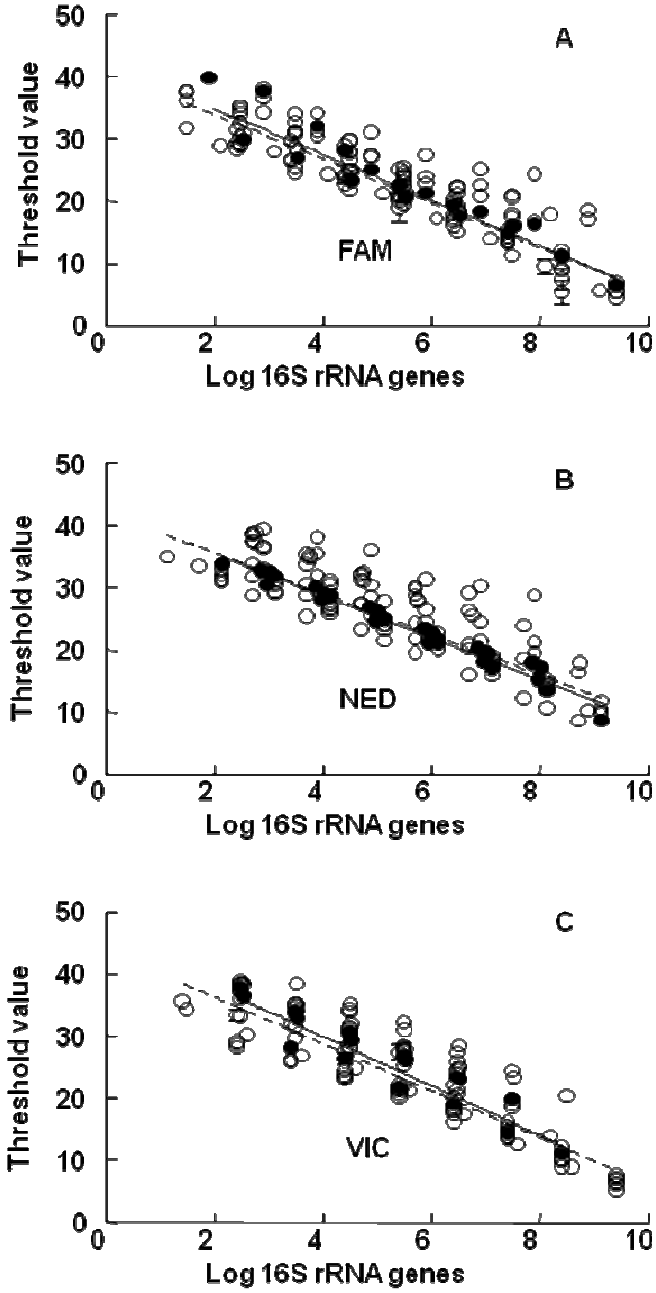

Figure 4.1. Threshold values for multiplex and singleplex qPCR assays of tenfold-diluted plasmid standards.

(A) FAM-labeled probe targeting the cloned 16S rRNA gene of strain 2CP-C.

(B) NED-labeled probe targeting the cloned 16S rRNA gene of strain 2CP-1.

(C) VIC-labeled probe targeting the cloned 16S rRNA gene sequences of both strains 2CP-C and 2CP-1.

Open symbols and dotted lines represent mqPCR values, closed symbols and solid lines represent singleplex qPCR values.

significantly different, with P-values ranging between 0.14 and 0.67 (Table 4.2). Regression analysis of multiplex data indicated a slope of -3.27 ± 0.10 for amplification with the NED-labeled FRC-D1 probe, which is close to the slope value of -3.32 corresponding to 100% amplification efficiency [42]. Amplification efficiencies were calculated based on the slope of the line describing cycle number versus log gene copy number for 20 multiplex standard curves and three singleplex standard curves per probe (Table 4.2). Amplification with the VIC-labeled TAna probe was less efficient, with a slope of -3.76 ± 0.12 and an efficiency value of 1.84, which is comparable to previously published qPCR efficiency values [22,44]. Standard curves obtained with the VIC-labeled probe had higher y-intercepts indicating that more gene copies were needed to achieve equivalent fluorescence intensity (i.e., lower sensitivity was achieved). Hence, the TAna primer/probe set provided slightly reduced sensitivity and efficiency than the strain-specific assays.

The analysis of strain FRC-W and strain FRC-D1 co-cultures verified that strain-specific and genus-level TAna TaqMan probes quantified both strains simultaneously, along with the total *Anaeromyxobacter* community, in multiplex format (Figure 4.2). Since co-culture experiments contained only strains FRC-D1 and FRC-W, the sum of cells enumerated using the strain-specific probes is expected to equal the enumeration by the TAna probe. Over the course of the experiment, the total *Anaeromyxobacter* cell numbers and the sum of copies enumerated with each strain-specific probe remained within one standard deviation of triplicate culture data (representative data points are shown in Figure 4.2). The agreement between the TAna probe data and the numbers generated with the strain-specific probes corroborated that all three assays were suitable for application in mqPCR format.

4.4.2 Application of the mqPCR approach to Oak Ridge IFC site-derived samples.

Upon validation of the mqPCR method in defined co-cultures, the approach was used to quantify *Anaeromyxobacter* 16S rRNA gene sequences in DNA derived from Oak Ridge IFC

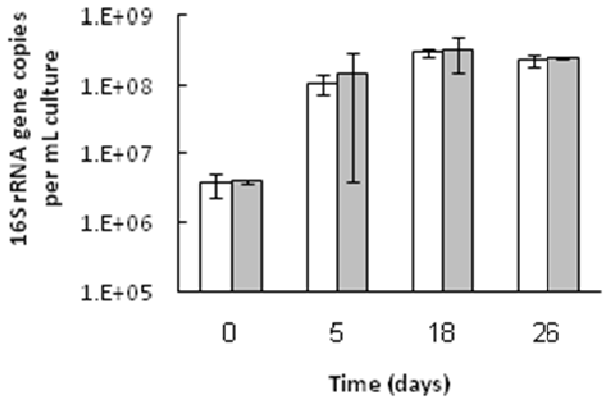

Figure 4.2. Comparison of 16S rRNA gene quantification with strain-specific probes and the genus-targeted TAna probe. White bars represent the sum of 16S rRNA gene copies enumerated with both strain-specific probes. Grey bars represent the copies enumerated with the TAna probe.

site materials. The multiplex tool successfully amplified DNA from enrichment cultures, microcosms and field samples including sediment, groundwater, and soil. The mqPCR tool demonstrated that *Anaeromyxobacter* strains were heterogeneously distributed at the Oak Ridge IFC site. In FeOOH enrichment cultures derived from Area 1 well FWB032 supplied with acetate, strain FRC-D1-like sequences accounted for approximately one third of the *Anaeromyxobacter* community and became dominant when lactate was supplied as electron donor. These findings suggest that FRC-D1-like organisms were present *in situ* in Area 1; however, analysis of three soil samples from Area 1 failed to yield any FRC-D1-like sequences indicating that these populations were present in numbers below the detection limit (i.e., no fluorescent signal in qPCR reactions) (Table 4.3). In contrast, FRC-W-like sequences were not detected in FeOOH enrichment cultures but ranged from $6.40 \times 10^2 \pm 3.5 \times 10^1$ to $3.5 \times 10^4 \pm 1.2 \times 10^4$ 16S rRNA gene copies per g of soil in Area 1 boreholes FB074 and FB089, respectively. TAna probe results from Area 1 samples indicated that total *Anaeromyxobacter* 16S rRNA gene copies ranged from $5.2 \times 10^2 \pm 2.2 \times 10^2$ to $1.13 \times 10^5 \pm 5.4 \times 10^4$ per g of soil in boreholes FB074 and FB089, respectively. Cell numbers for each target strain ranged from 13 ± 1 to 122 ± 36 % of the total *Anaeromyxobacter* community in all Area 1 site-derived materials (soil cores or enrichment cultures) (Table 4.3).

mqPCR results of sediment and groundwater samples from the Area 3 bioremediation pilot-scale treatment zone indicated that total *Anaeromyxobacter* cell numbers were elevated throughout the subsurface region influenced by ethanol biostimulation, as were total bacterial cell numbers (Figures 4.3A and B). The *Anaeromyxobacter* community increased from values which ranged from below the detection limit to $7.8 \times 10^4 \pm 2.8 \times 10^4$ 16S rRNA gene copies per g sediment outside the treatment zone to values as high as $3.5 \times 10^8 \pm 1.0 \times 10^8$ 16S rRNA gene copies per g of sediment near the injection well FW104 (Figure 4.3A and B and Table 4.4). Relative to total bacterial 16S rRNA gene copies, *Anaeromyxobacter* 16S rRNA gene copies increased from 0.0002 ± 0.0001% outside the treatment zone to 2.3 ± 0.8 % in the middle

Table 4.3. Geochemical characteristics and presence of *A. dehalogenans* strains FRC-D1 and FRC-W in Oak Ridge IFC site materials (Area 1).

	Site geochemistry					FRC-D1	FRC-W
	Uranium	Nitrate	Fe (II)	pH	Sample type	% of Total *Anaeromyxobacter*	
Area 1 location	(mg/L)	(mM)	(mM)		(Collection date)		
FB074	-- [a]	1.99 - 21.85 [b]	-- [a]	2.91 - 6.25 [b]	Soil core (18Oct04)	BDL [c]	77.4 ± 6.6 – 122 ± 36 [d]
FB089	< 0.015 [e]	62.42 [e]	< 0.587 [e]	5.48 [e]	Soil core (17May05)	BDL [c]	13 ± 1 – 31 ± 10 [d]
FB090	0.05 [e]	16.39 [e]	3.21 [e]	6.02 [e]	Soil core (17May05)	BDL [c]	31.2 ± 19.5 [f]
FWB032	1 [b]	11.8 [b]	-- [a]	5.4 [b]	FeOOH/Acetate microcosm [g], pH7	34 ± 14	BDL [c]
	1 [b]	11.8 [b]	-- [a]	5.4 [b]	FeOOH/Lactate microcosm [g], pH7	91 ± 21	BDL [c]

[a] --: No data available

[b] Values represent site data at the time of sample collection [(34); David Watson, personal communication].

[c] Below detection limit; indicates that no fluorescent signal was detected above background.

[d] Range of values represents samples from multiple homogenized soil core depth intervals for a single borehole.

[e] Value measured in groundwater collected from an adjacent monitoring well in 2004 (http://public.ornl.gov).

[f] Only a single depth interval contained a quantifiable number of *Anaeromyxobacter* 16S rRNA gene sequences.

[g] Microcosms established by Petrie et al., 2003 (34) from site materials collected in 2001.

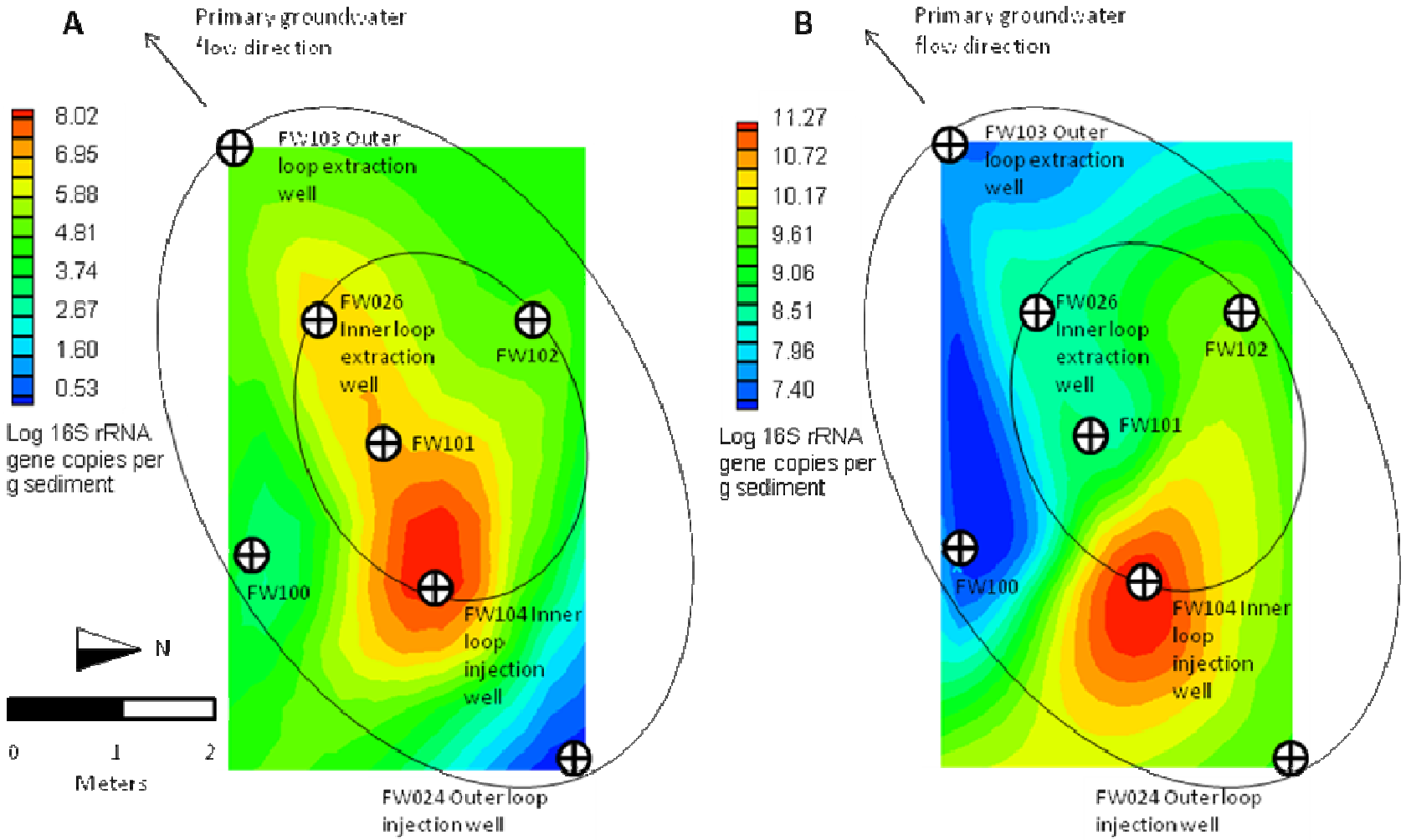

Figure 4.3. Spatial representation of *Anaeromyxobacter* (TAna probe) (A) and total Bacterial (B) 16S rRNA gene abundance at the Oak Ridge IFC site Area 3 based on qPCR analysis of samples from seven wells. Circles are schematically represent the inner and outer recirculation loops based on tracer studies and hydrologic models (29). FW100, FW101, and FW102 are multiport sampling wells.

Table 4.4. Comparison of *Anaeromyxobacter* 16S rRNA gene to total bacterial 16S rRNA gene copy numbers.

Location (well number)	Total *Anaeromyxobacter*	
	16S rRNA genes per g sediment	Proportion of total Bacteria (%)
FW105 (outside the treatment loops)	$7 \times 10^4 \pm 3 \times 10^4$	0.0002 ± 0.0001
FW104 (inner loop injection well)	$1.8 \times 10^8 \pm 5 \times 10^7$	0.06 ± 0.04
FW103 (outer loop extraction well)	$1.2 \times 10^5 \pm 2 \times 10^4$	0.13 ± 0.09
FW102-3 (multiport well in inner loop)	$1.3 \times 10^5 \pm 1 \times 10^4$	0.0020 ± 0.0019
FW-101-2 (multiport well in inner loop)	$1.4 \times 10^7 \pm 2 \times 10^6$	2.3 ± 0.8
FW100-2 (multiport well in outer loop)	$4.2 \times 10^3 \pm 8 \times 10^2$	0.016 ± 0.003
FW026 (inner loop extraction well)	$7.0 \times 10^6 \pm 7 \times 10^5$	1.2 ± 0.1
FW024 (outer loop injection well)	BDL	BDL

multiport well located downstream of the injection well (Table 4.4). Although mqPCR assessment of 33 Area 3 site samples (18 sediment and 15 groundwater samples) demonstrated *Anaeromyxobacter* presence in this subsurface region, neither strain FRC-D1 or FRC-W 16S rRNA gene sequences could be quantified in any tested sample from Area 3; however, FRC-W-like sequences were detected but not quantified (i.e., present below the quantification limit of 1.2 x 10^1 16S rRNA gene copies per reaction) in samples collected from wells FW100-3 and FW103 located outside of the ethanol stimulation loop.

4.4.3 Clone libraries from Area 3 site materials. To explore the *Anaeromyxobacter* 16S rRNA gene sequences dominant in Area 3, *Anaeromyxobacter* 16S rRNA gene, three clone libraries were established with DNA derived from samples of the ethanol injection well FW104. Restriction analysis of nearly complete 16S rRNA genes (1,410 bp) yielded identical patterns and 11 fragments were sequenced. Pairwise comparisons of evolutionary divergence among the 16S rRNA gene sequences recovered from Area 3 with the *A. dehalogenans* type strain 2CP-1 indicated sequence similarities between 93.3-94%. The 16S rRNA gene sequences from uncharacterized *Anaeromyxobacter* spp. in Area 3 were detected and quantified with the TAna probe but not with either of the strain-specific probes. Consistent with the qPCR results, the 16S rRNA gene target region (*E. coli* positions 474-490) of strains detected in Area 3 (Accession numbers CP000769 and FJ190063 – FJ190073) are not complementary to the FRC-W- and FRC-D1-specific minor groove-binding probes. Evolutionary distance analysis revealed that the *Anaeromyxobacter* strains detected in Area 1 and the available *Anaeromyxobacter* isolates are phylogenetically distinct from the dominant Area 3 *Anaeromyxobacter* population(s) (Figure 4.4). Bootstrap values reinforce that representatives of at least three distinct *Anaeromyxobacter* clusters, designated A, B, and C, exist at the Oak Ridge IFC site (Figure 4.4). Cluster A contains characterized *Anaeromyxobacter* isolates [17,18,29,45], including type strain 2CP-1 [29], as well as the Oak Ridge IFC site isolates targeted in this study (strains FRC-D1 and FRC-W). Cluster A

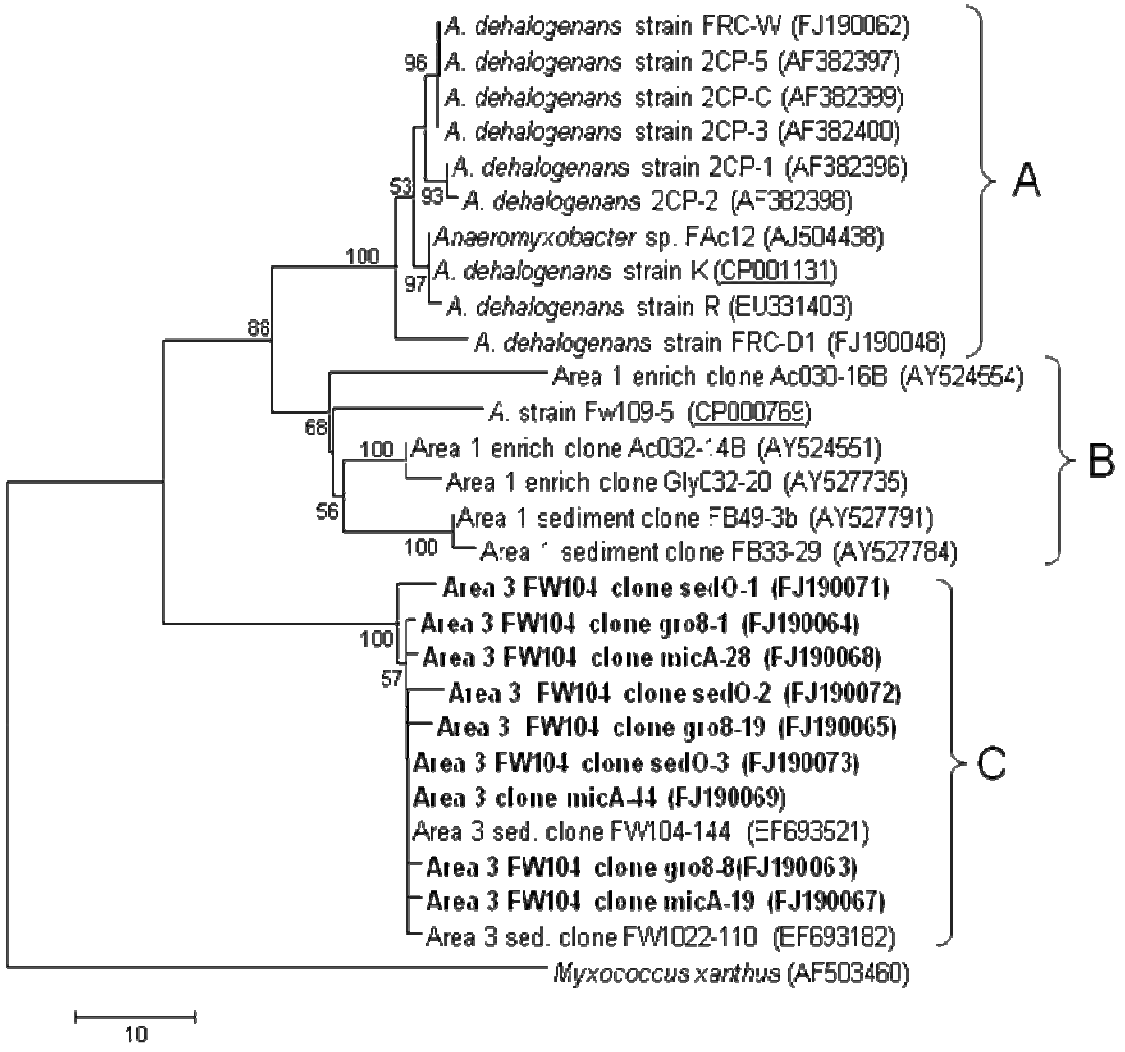

Figure 4.4. 16S rRNA gene-based phylogeny of characterized *Anaeromyxobacter* strains, Oak Ridge IFC site isolates, and environmental clone sequences. Area 3 sequences from cloned 16S rRNA gene fragments determined in this study are indicated in bold. The *Myxococcus xanthus* 16S rRNA gene sequence (AF503460) was used to root the tree. The scale bar represents the number of differences in the nucleotide sequence. Bootstrap values are based on 500 replications and are not shown at nodes with less than 50% bootstrap support. GenBank accession numbers of genomes (underlined) and 16S rRNA genes are indicated in parentheses. Distinct phylogenetic clusters are indicated with letters A, B and C.

sequences were detected in Area 1 but not in Area 3, whereas Cluster C sequences, which were greater than 99.4% similar to each other, were unique to Area 3.

4.5 Discussion

Consistent with previous community analyses [13,14,15], *Anaeromyxobacter* 16S rRNA gene sequences are present in uranium-contaminated Areas 1 and 3 at the Oak Ridge IFC site. The spatial analysis of samples across seven wells of Area 3 demonstrated that *Anaeromyxobacter* abundance correlated with the zone influenced by ethanol biostimulation and the zone of decreased dissolved U(VI) concentrations (Figure 4.3) [38,39]. *Anaeromyxobacter* spp. grow with a variety of electron acceptors including U(VI), nitrate, ferric iron, and manganese oxide [12,16,17]. Hence, respiratory substrates other than U(VI) may have supported *Anaeromyxobacter* growth, although nitrate concentrations in the treatment zone were generally low during active bioremediation [39], and nitrate was not detected in Area 3 groundwater samples collected concurrently with the Area 3 sediment samples used for this study [collected October 5, 2005; [13]]. Iron (0.01-0.03 mM) and manganese (0.06-0.08 mM) are present in Area 3 groundwater at the time of sampling [13] and respiration of these oxidized metals may have contributed to growth *in situ*. The spatial correlation between *Anaeromyxobacter* and the decreased soluble uranium concentrations is consistent with laboratory studies demonstrating that *Anaeromyxobacter* spp. respire U(VI) [11,12] and suggests that *Anaeromyxobacter* spp. grow with U(VI) as electron acceptor *in situ*. Interestingly, the mqPCR and clone library analyses demonstrated an uneven distribution of three distinct *Anaeromyxobacter* populations across Areas 1 and 3. Within the *Anaeromyxobacter* genus, only Cluster C 16S rRNA gene sequences were detected in the Area 3 biostimulation treatment zone. The samples examined in this study provided no evidence for the presence of Cluster A or Cluster B sequences in the Area 3 treatment zone although Cluster A and B representatives occur in Area 3. For example, strain Fw109-5 (Cluster B) was isolated from Area 3 site materials outside the treatment zone (Matthew

Fields, personal communication) and 16S rRNA gene sequences of strain FRC-W (Cluster A) were detected but not quantified (< 1.2 x 10^1 gene copies per reaction) just outside the treatment zone. Conversely, Cluster C sequences have not been detected in Area 1 and strain FRC-W (Cluster A) sequences were quantifiable in all Area 1 soil cores tested. Strain FRC-W uses amorphous ferric iron as electron acceptor (Thomas and Löffler, unpublished data) but Area 1 FeOOH enrichment cultures were dominated by FRC-D1 16S rRNA gene sequences. This was unexpected because FRC-D1-like 16S rRNA gene sequences were not detected in any Area 1 samples examined, suggesting that this strain is not abundant under *in situ* conditions but responds to laboratory enrichment with FeOOH. These findings demonstrate that strain differences affect field-scale processes, thus emphasizing the need for strain-specific monitoring tools. TaqMan probes with a conjugated minor-groove-binding tripeptide [25] discriminated strain FRC-W and strain FRC-D1 16S rRNA gene sequences with only two mismatches in the probe target sequence. TaqMan probes allow multiplex detection, which requires that primers and probes have similar melting characteristics, and the data obtained with different quencher and fluorophore combinations must be compared to singleplex quantification results [42]. Although mqPCR requires careful design and evaluation, the multiplex format reduces the cost of the analyses and eliminates one element of experimental uncertainty by utilizing a single aliquot of template for quantification of the gene targets.

Based on previous principles of microbial biogeography [1,3], the heterogeneous distribution of *Anaeromyxobacter* strains at the Oak Ridge IFC site may be a result of several factors. The level of metabolic diversity within the *Anaeromyxobacter* community is unclear due to a limited number of isolated representatives. Characterization of Cluster A *Anaeromyxobacter* pure cultures indicates that physiological differences exist between strains that share nearly identical 16S rRNA gene sequences (Thomas, unpublished data). Traits relevant for field-scale processes include metabolic versatility (i.e., metal and nitrate respiration), growth rates and tolerance to elevated concentrations of electron acceptors. The characterized Cluster A representatives share

the ability to reduce U(VI), but the rates can be quite variable (unpublished data). Another shared trait among characterized isolates is the ability to reduce nitrate but the tolerance to nitrate (and nitrite) varies between strains [17]. Several *Anaeromyxobacter* isolates were isolated based on their ability to perform reductive dechlorination but putative reductive dehalogenase genes are lacking on the strain FW109-5 genome (Accession number CP000769) and, in contrast to other strains, this isolate cannot grow aerobically (Matthew Fields, personal communication). The dominance of Cluster C representatives and the apparent absence of Cluster A and B representatives following ethanol biostimulation in Area 3 suggest that environmental conditions in Area 3 may exclude some *Anaeromyxobacter* strains [37,38,39]. Alternatively, Cluster C *Anaeromyxobacter* strains may be capable of using ethanol directly as an electron donor, and thus have a competitive advantage over strains that utilize only ethanol fermentation products (i.e., hydrogen and acetate) as electron donors [12,17]. Cluster C sequences share 99.4-100% sequence similarity recovered from Area 3 [this study; [13]], suggesting that one group of closely related strains dominate the *Anaeromyxobacter* community in this treatment zone.

Successful dispersal of organisms in the environment requires not only appropriate metabolic adaptations but also transport of organisms from one location to another [1]. In spite of cross-plane fracture connectivity between Areas 1 and 3, the heterogeneous distribution of *Anaeromyxobacter* strains may be based on hydrologic isolation between both areas. Groundwater flow through fractures along dipping bedding planes connects the two areas. However, flow in the dip direction is small relative to strike parallel flow through the high-conductivity transition zone between overlying unconsolidated saprolite and underlying less-weathered bedrock [9]. Thus, while Areas 1 and 3 may be connected for the purposes of contaminant transport, transport of bacterial cells may be subject to limitations that play a role in the observed heterogeneous distributions [5,9,33,34,53]. Tracer tests have been conducted in the Area 1 and Area 3 treatment zones [36,54], however, no analyses have been conducted to elucidate transport between the two treatment zones. Detailed studies that will explore chemical

and bacterial transport between Areas 1 and 3 are needed clarify this issue and contribute to scaled-up remediation efforts.

While the reasons and mechanisms for the observed heterogeneous distribution of *Anaeromyxobacter* populations at the Oak Ridge IFC site require further investigation, this study demonstrates that strain-specific monitoring provides valuable information about the microbiology contributing to U(VI) reduction. Apparently, Cluster C *Anaeromyxobacter* populations are involved in U(VI) reduction following ethanol biostimulation in Area 3 and future efforts should focus on the isolation and characterization of those strains that are major contributors to the process of interest under *in situ* conditions.

4.6 Acknowledgements

This research was supported by the Environmental Remediation Science Division (ERSD), Biological and Environmental Research (BER), U.S. Department of Energy and by NSF IGERT (Grant No. DGE 0114400) and NSF GK-12 (Grant No. 0338261) fellowships to S.H.T. E.P.-C. also acknowledges partial support through an NSF IGERT fellowship and is recipient of an NSF graduate research fellowship. We thank Joy Van Nostrand, Jizhong Zhou, Mary Beth Leigh, and Erick Cardenas for DNA samples extracted from the Area 3 treatment zone, Joel Kostka and Denise Akob for soil, DNA, and enrichment samples from Area 1, Qingzhong Wu for providing isolate FRC-W, and Youlboong Sung for providing DNA from Area 3 site samples and microcosms.

4.7 References

1. Ramette A, Tiedje JM (2007) Biogeography: An emerging cornerstone for understanding prokaryotic diversity, ecology, and evolution. Microbial Ecology 53: 197-207.

2. Green J, Bohannan BJM (2006) Spatial scaling of microbial biodiversity. Trends in Ecology & Evolution 21: 501-507.

3. Martiny JBH, Bohannan BJM, Brown JH, Colwell RK, Fuhrman JA, et al. (2006) Microbial biogeography: putting microorganisms on the map. Nature Reviews Microbiology 4: 102-112.

4. Ramette A, LiPuma JJ, Tiedje JM (2005) Species abundance and diversity of *Burkholderia cepacia* complex in the environment. Applied and Environmental Microbiology 71: 1193-1201.

5. Treves DS, Xia B, Zhou J, Tiedje JM (2003) A two-species test of the hypothesis that spatial isolation influences microbial diversity in soil. Microbial Ecology 45: 20-28.

6. Zhou JZ, Xia BC, Huang H, Palumbo AV, Tiedje JM (2004) Microbial diversity and heterogeneity in sandy subsurface soils. Applied and Environmental Microbiology 70: 1723-1734.

7. Carney KM, Matson PA, Bohannan BJM (2004) Diversity and composition of tropical soil nitrifiers across a plant diversity gradient and among land-use types. Ecology Letters 7: 684-694.

8. Cho JC, Tiedje JM (2000) Biogeography and degree of endemicity of fluorescent *Pseudomonas* strains in soil. Applied and Environmental Microbiology 66: 5448-5456.

9. Phillips DH, Watson DB, Roh Y, Mehlhorn TL, Moon JW, et al. (2006) Distribution of uranium contamination in weathered fractured saprolite/shale and ground water. Journal of Environmental Quality 35: 1715-1730.

10. Marshall MJ, Dohnalkova AC, Kennedy DW, Plymale AE, Thomas SH, et al. (2008) Electron donor-dependent radionuclide reduction and nanoparticle formation by *Anaeromyxobacter dehalogenans* strain 2CP-C. Environmental Microbiology 11: 534-543.

11. Sanford RA, Wu Q, Sung Y, Thomas SH, Amos BK, et al. (2007) Hexavalent uranium supports growth of *Anaeromyxobacter dehalogenans* and *Geobacter* spp. with lower than predicted biomass yields. Environmental Microbiology 9: 2885-2893.

12. Wu Q, Sanford RA, Löffler FE (2006) Uranium(VI) reduction by *Anaeromyxobacter dehalogenans* strain 2CP-C. Applied and Environmental Microbiology 72: 3608-3614.

13. Cardenas E, Wu WM, Leigh MB, Carley J, Carrol lS, et al. (2008) Microbial communities in contaminated sediments, associated with bioremediation of uranium to submicromolar levels. Applied and Environmental Microbiology 74: 3718-3729.

14. Petrie L, North NN, Dollhopf SL, Balkwill DL, Kostka JE (2003) Enumeration and characterization of iron(III)-reducing microbial communities from acidic subsurface sediments contaminated with uranium(VI). Applied and Environmental Microbiology 69: 7467-7479.

15. North NN, Dollhopf SL, Petrie L, Istok JD, Balkwill DL, et al. (2004) Change in bacterial community structure during *in situ* biostimulation of subsurface sediment cocontaminated with uranium and nitrate. Applied and Environmental Microbiology 70: 4911-4920.

16. He Q, Sanford RA (2003) Characterization of Fe(III) reduction by chlororespiring *Anaeromyxobacter dehalogenans*. Applied and Environmental Microbiology 69: 2712-2718.

17. Sanford RA, Cole JR, Tiedje JM (2002) Characterization and description of *Anaeromyxobacter dehalogenans* gen. nov., sp. nov., an aryl halorespiring facultative anaerobic Myxobacterium. Applied and Environmental Microbiology 68: 893-900.

18. Treude N, Rosencrantz D, Liesack W, Schnell S (2003) Strain FAc12, a dissimilatory iron-reducing member of the *Anaeromyxobacter* subgroup of Myxococcales. FEMS Microbiology Ecology 44: 261-269.

19. Konstantinidis KT, Tiedje JM (2005) Genomic insights that advance the species definition for prokaryotes. Proceedings of the National Academy of Sciences of the United States of America 102: 2567-2572.

20. Konstantinidis KT, Tiedje JM (2005) Towards a genome-based taxonomy for prokaryotes. Journal of Bacteriology 187: 6258-6264.

21. Felis GE, Dellaglio F (2007) On species descriptions based on a single strain: proposal to introduce the status species proponenda (sp pr.). International Journal of Systematic and Evolutionary Microbiology 57: 2185-2187.

22. Ritalahti KM, Amos BK, Sung Y, Wu QZ, Koenigsberg SS, et al. (2006) Quantitative PCR targeting 16S rRNA and reductive dehalogenase genes simultaneously

monitors multiple *Dehalococcoides* strains. Applied and Environmental Microbiology 72: 2765-2774.

23. Chakravorty S, Helb D, Burday M, Connell N, Alland D (2007) A detailed analysis of 16S ribosomal RNA gene segments for the diagnosis of pathogenic bacteria. Journal of Microbiological Methods 69: 330-339.

24. Mackay IM (2004) Real-time PCR in the microbiology laboratory. Clinical Microbiology and Infection 10: 190-212.

25. Afonina I, Zivarts M, Kutyavin I, Lukhtanov E, Gamper H, et al. (1997) Efficient priming of PCR with short oligonucleotides conjugated to a minor groove binder. Nucleic Acids Research 25: 2657-2660.

26. Liu D, Lawrence ML, Austin FW, Ainsworth AJ (2007) A multiplex PCR for species- and virulence-specific determination of *Listeria monocytogenes*. Journal of Microbiological Methods 71: 133-140.

27. Scott JC, Koylass MS, Stubberfield MR, Whatmore AM (2007) Multiplex assay based on single-nucleotide polymorphisms for rapid identification of *Brucella* isolates at the species level. Applied and Environmental Microbiology 73: 7331-7337.

28. Varma-Basil M, El-Hajj H, Marras SAE, Hazbon MH, Mann JM, et al. (2004) Molecular beacons for multiplex detection of four bacterial bioterrorism agents. Clinical Chemistry 50: 1060-1063.

29. Cole JR, Cascarelli AL, Mohn WW, Tiedje JM (1994) Isolation and characterization of a novel bacterium growing via reductive dehalogenation of 2-chlorophenol. Applied and Environmental Microbiology 60: 3536-3542.

30. Löffler FE, Sanford RA, Tiedje JM (1996) Initial characterization of a reductive dehalogenase from *Desulfitobacterium chlororespirans* Co23. Applied and Environmental Microbiology 62: 3809-3813.

31. Watson DB, Kostka JE, Fields MW, Jardine PM (2004) The Oak Ridge Field Research Center conceptual model. http://www.esd.ornl.gov/orifrc/: U.S. Department of Energy.

32. Brooks SC (2001) Waste characteristics of the former S-3 ponds and outline of uranium chemistry relevant to NABIR Field Research Center studies. Oak Ridge, TN: U.S. Department of Energy ORNL/TM-2001/27.

33. Jardine PM, Mehlhorn TL, Larsen IL, Bailey WB, Brooks SC, et al. (2002) Influence of hydrological and geochemical processes on the transport of chelated-metals

and chromate in fractured shale bedrock. Journal of Contaminant Hydrology 55: 137-159.

34. Jardine PM, Sanford WE, Gwo JP, Reedy OC, Hicks DS, et al. (1999) Quantifying diffusive mass transfer in fractured shale bedrock. Water Resources Research 35: 2015-2030.

35. Dreier RB, Solomon DK, Beaudoin CM (1987) Fracture characterization in the unsaturated zone of a shallow land burial facility. In: Evans DD, Nicholson TJ, editors. Flow and Transport Through Unsaturated Rock. Washington, D.C.: American Geophysical Union.

36. Istok JD, Senko JM, Krumholz LR, Watson D, Bogle MA, et al. (2004) In situ bioreduction of technetium and uranium in a nitrate-contaminated aquifer. Environmental Science & Technology 38: 468-475.

37. Wu W-M, Carley J, Fienen M, Mehlhorn T, Lowe K, et al. (2006) Pilot-scale *in situ* bioremediation of uranium in a highly contaminated aquifer. 1. Conditioning of a treatment zone. Environmental Science & Technology 40: 3978-3985.

38. Wu WM, Carley J, Gentry T, Ginder-Vogel MA, Fienen M, et al. (2006) Pilot-scale *in situ* bioremedation of uranium in a highly contaminated aquifer. 2. Reduction of U(VI) and geochemical control of U(VI) bioavailability. Environmental Science & Technology 40: 3986-3995.

39. Wu W-M, Carley J, Luo J, Ginder-Vogel MA, Cardenas E, et al. (2007) *In situ* bioreduction of uranium (VI) to submicromolar levels and reoxidation by dissolved oxygen. Environmental Science & Technology 41: 5716-5723.

40. Akob DM, Mills HJ, Kostka JE (2007) Metabolically active microbial communities in uranium-contaminated subsurface sediments. FEMS Microbiology Ecology 59: 95-107.

41. Amos BK, Sung Y, Fletcher KE, Gentry TJ, Wu WM, et al. (2007) Detection and quantification of *Geobacter lovleyi* strain SZ: Implications for bioremediation at tetrachloroethene- and uranium-impacted sites. Applied and Environmental Microbiology 73: 6898-6904.

42. ABI (2005) Applied Biosystems 7900HT Fast Real-Time PCR System and 7300/7500 Real-Time PCR Systems: Chemistry Guide 4348358 Rev. E.

43. Altschul SF, Gish W, Miller W, Myers EW, Lipman DJ (1990) Basic Local Alignment Search Tool. Journal of Molecular Biology 215: 403-410.

44. Pfaffl MW (2001) A new mathematical model for relative quantification in real-time RT-PCR. Nucleic Acids Research 29: 2002-2007.

45. Thomas SH, Wagner RD, Arakaki AK, Skolnick J, Kirby JR, et al. (2008) The mosaic genome of *Anaeromyxobacter dehalogenans* strain 2CP-C suggests an aerobic common ancestor to the delta-Proteobacteria. PLoS ONE 3: e2103.

46. Zhou J, Davey ME, Figueras JB, Rivkina E, Gilichinsky D, et al. (1997) Phylogenetic diversity of a bacterial community determined from Siberian Tundra soil. Microbiology 143: 3913-3919.

47. Cole JR, Chai B, Marsh TL, Farris RJ, Wang Q, et al. (2003) The Ribosomal Database Project (RDP-II): previewing a new autoaligner that allows regular updates and the new prokaryotic taxonomy. Nucleic Acids Research 31: 442-443.

48. Tamura K, Dudley J, Nei M, Kumar S (2007) MEGA4: Molecular Evolutionary Genetics Analysis (MEGA) software version 4.0 Molecular Biology and Evolution 24: 1596-1599.

49. Saitou N, Nei M (1987) The neighbor-joining method: A new method for reconstructing phylogenetic trees. Molecular Biology and Evolution 4: 406-425.

50. Felsenstein J (1985) Confidence limits on phylogenies: An approach using the bootstrap. Evolution 39: 783-791.

51. Tamura K, Nei M, Kumar S (2004) Prospects for inferring very large phylogenies by using the neighbor-joining method. Proceedings of the National Academy of Sciences 101: 11030-11035.

52. He JZ, Ritalahti KM, Aiello MR, Löffler FE (2003) Complete detoxification of vinyl chloride by an anaerobic enrichment culture and identification of the reductively dechlorinating population as a *Dehalococcoides* species. Applied and Environmental Microbiology 69: 996-1003.

53. Jiang HL, Maszenan AM, Tay JH (2007) Bioaugmentation and coexistence of two functionally similar bacterial strains in aerobic granules. Applied Microbiology and Biotechnology 75: 1191-1200.

54. Luo J, Cirpka OA, Fienen MN, Wu WM, Mehlhorn TL, et al. (2006) A parametric transfer function methodology for analyzing reactive transport in nonuniform flow. Journal of Contaminant Hydrology 83: 27-41.

55. Luo J, Weber F-A, Cirpka OA, Wu W-M, Nyman JL, et al. (2007) Modeling *in situ* uranium(VI) bioreduction by sulfate-reducing bacteria. Journal of Contaminant Hydrology 92 129–148.

CHAPTER 5: Evaluation of oxygen metabolism in *Anaeromyxobacter dehalogenans* strain 2CP-C reveals unique ecophysiology among U(VI)-reducing bacteria

5.1 Abstract

Versaphilic *Anaeromyxobacter* spp. respire soluble U(VI) species leading to the formation of insoluble uraninite, and are present at the uranium contaminated Oak Ridge Integrated Field Research Challenge (IFC) site. Pilot-scale *in situ* bioreduction of U(VI) has been accomplished in Area 3 of the Oak Ridge IFC site but the susceptibility of the reduced material to reoxidation by oxygen compromises long-term immobilization. Analysis of groundwater and sediment samples collected before and after oxygen intrusion measured an increase of the *Anaeromyxobacter* population in response to O_2. For example, in well FW101-2, attached *A. dehalogenans* cells increased about 5-fold from $2.2 \times 10^7 \pm 8.6 \times 10^6$ to $1.0 \times 10^8 \pm 2.2 \times 10^7$ cells per g sediment. In contrast, sediment associated cells of *Geobacter lovleyi,* a population native to Area 3 and also capable of U(VI) reduction, did not increase in response to oxygen. Planktonic *A. dehalogenans* cells captured via groundwater sampling were present in much lower numbers ($<1.3 \times 10^4 \pm 1.1 \times 10^4$ cells per L) than sediment-associated cells, suggesting that *A. dehalogenans* cells occur predominantly associated with soil particles. Laboratory studies confirmed aerobic growth of *A. dehalogenans* strain 2CP-C at initial oxygen partial pressures (pO_2) of 0.02, 0.03, 0.07, and 0.18 atm; however, a negative linear correlation ($k = -0.09*pO_2 + 0.051$; $R^2 = 0.923$) was observed between the growth rate constant k and pO_2 indicating that this organism should be classified as a microaerophile. Quantification of cells during aerobic growth revealed that the fraction of electrons released in electron donor oxidation and used for biomass production (f_s) decreased from 0.52 at a pO_2 of 0.02 atm to 0.19 at a pO_2 of 0.18 atm. Hence, the apparent fraction of

electrons utilized for energy (i.e., oxygen reduction) (f_e) increased from 0.48 to 0.81, respectively, suggesting that at high pO_2, oxygen is also consumed in a non-respiratory process. The ability to tolerate high oxygen concentrations, microaerophilic oxygen respiration and preferential association with soil particles represents an ecophysiology that distinguishes *A. dehalogenans* from other known U(VI)-reducing bacteria, and these features may play relevant roles for stabilizing immobilized radionuclides *in situ*.

5.2 Introduction

The U.S. Department of Energy (DOE) has initiated efforts to remediate 120 uranium-contaminated locations in 36 states and territories that have been impacted by former nuclear weapons production sites [1]. Several dissimilatory iron-reducing bacteria (DIRB) are capable of reducing soluble U(VI) to sparingly soluble U(IV), which precipitates as uraninite (UO_2) [2,3,4,5] and the feasibility of microbial U(VI) reduction and immobilization as a containment strategy has been successfully demonstrated at field sites [6,7]. A remaining challenge is controlling oxic/anoxic interface processes to ensure the long-term stability of the precipitated material because U(IV) is susceptible to re-oxidation by oxidants including oxygen [8,9,10]. The undesirable effects of U(IV) re-oxidation and mobilization have been observed at a bioremediation pilot plot at the DOE Integrated Field Research Challenge (IFC) site at the Oak Ridge National Laboratory as well as in column studies constructed from Oak Ridge IFC site materials [9,10,11]. Consequently, advancement of bioremediation treatment at uranium-contaminated sites requires not only an understanding of the processes contributing to U(VI) reduction but

also the processes that maintain conditions conducive to keeping uranium in its reduced form.

DIRB grow by coupling the oxidation of organic compounds or H_2 to the reduction of ferric iron, as well as other metals including manganese and uranium [2,12,13,14,15,16,17]. Metals reduced by DIRB under anoxic conditions undergo rapid cycling between reduced and oxidized states at oxic/anoxic transition zones due to fluctuating oxygen gradients [18]. As a result, many DIRB thrive near the oxic/anoxic interface where they take advantage of abundant electron acceptors (i.e., reduced iron and manganese oxyhydroxides). Organisms capable of consuming and respiring oxygen, as well as oxidized metals, are thus expected to be particularly good competitors in fluctuating redox environments, taking advantage of oxygen and oxidized metals as electron acceptors. Several DIRB have been shown to consume oxygen, ranging from facultative aerobes (e.g., *Shewanella* spp.) to those that reduce oxygen only when present at very low partial pressures (e.g., some *Desulfovibrio* spp. [19,20]).

Anaeromyxobacter spp. are common soil and subsurface delta-Proteobacteria with remarkable respiratory versatility in anoxic environments [13,17,21]. Recent studies demonstrated that *Anaeromyxobacter dehalogenans* strain 2CP-C reduces U(VI) and grows with U(VI) as electron acceptor [17,22], and *Anaeromyxobacter* 16S rRNA gene sequences were detected at uranium contaminated sites including the Oak Ridge IFC site [23,24,25]. A few studies have reported growth of *Anaeromyxobacter* spp. under aerobic conditions and the analysis of the *A. dehalogenans* strain 2CP-C genome supports that this organism is capable of oxygen utilization [21,26,27]; however, these studies did not

explore the physiological response of *Anaeromyxobacter* spp. to oxygen and no data for oxygen tolerance, growth yields and growth rates are available.

A. dehalogenans strain 2CP-C possesses genes coding for oxygen respiration and detoxification of reactive oxygen species (ROS) similar to other members of the myxobacteriales [28]. For example, strain 2CP-C carries genes encoding a cytochrome aa_3 oxidase with sequence similarities to genes of other members of the myxobacteriales and a superoxide dismutase that possesses sequence similarity to a gene in *Stigmatella aurantiaca* [28,29]. In addition to genes associated with oxygen metabolism, which are characteristic for aerobic organisms, strain 2CP-C possesses a cytochrome cbb_3 oxidase, an enzyme system with high oxygen affinity common among many anaerobes and microaerophiles [30,31,32]. The assembly of oxygen respiration and ROS genes suggest a fine-tuned response of *Anaeromyxobacter dehalogenans* to oxygen partial pressure (pO_2). The quantitative microbial analysis of Area 3 samples detected an increase (i.e., growth) of the *Anaeromyxobacter* population following oxygen intrusion. Detailed laboratory studies revealed *A. dehalogenans'* unique physiological adaptation to pO_2, which distinguishes it from other DIRB and has implications for uranium immobilization at field sites.

5.3 Materials and Methods

5.3.1 Samples from the Oak Ridge IFC site. Groundwater samples were collected by ORNL personnel from a pilot-scale uranium bioreduction pilot plot at the Oak Ridge IFC site in Area 3 [6,9,33]. Multiport sampling wells FW101 and FW102 were sampled before and after oxygen intrusion into the pilot plot area at screened intervals 2 (13.7 m

below ground surface [bgs]) and 3 (12.2 m bgs), respectively [9]. Both FW101 and FW102 are located in the inner circulation loop [34]. Oxygen intrusion occurred between days 806-884 and samples were taken during pilot plot operation on days 746, 754, 810, 887, and 901 (Figure S1) [9]. Area 3 sediment samples were collected by ORNL personnel using a well surging technique from wells FW101-2 and FW102-3 on day 774 during the phase of active biostimulation with ethanol (days 755-805) [23], which preceded oxygen intrusion (days 806-884) (Figure 5.1) [6,22,33]. Sediment samples were collected again on day 935 during weekly ethanol stimulation, about 7 weeks after termination of the 11-week introduction of un-reduced (i.e., aerobic) groundwater into the pilot plot (days 806-884) (Figure 5.1). Sediment/groundwater slurries were centrifuged and sediment pellets frozen at -80°C in 50-ml Falcon tubes, shipped on dry ice and stored at -80°C until DNA extraction [23].

5.3.2 DNA extraction. DNA from laboratory cultures was extracted using InstaGene Matrix (Bio-Rad Laboratories, Hercules, CA). Aliquots (0.5 mL) from laboratory cultures were transferred to 1.5 mL Eppendorf plastic tubes (Westbury, NY) and cells were collected by centrifugation at 16,000 x g for 3 minutes at room temperature. The supernatant was decanted and the pellets were frozen at -20ºC for at least 24 hours. Instagene Matrix solution (0.2 mL; Bio-Rad Laboratories, Hercules, CA) was added to each frozen pellet and DNA was prepared according to the manufacturer's specifications. The DNA was utilized immediately or stored at -20°C until qPCR analysis.

DNA extraction from Area 3 sediment samples used 500 mg aliquots of sediment and the FastDNA SPIN kit for soil (BIO 101, Vista, CA), and dry DNA aliquots (100 ng

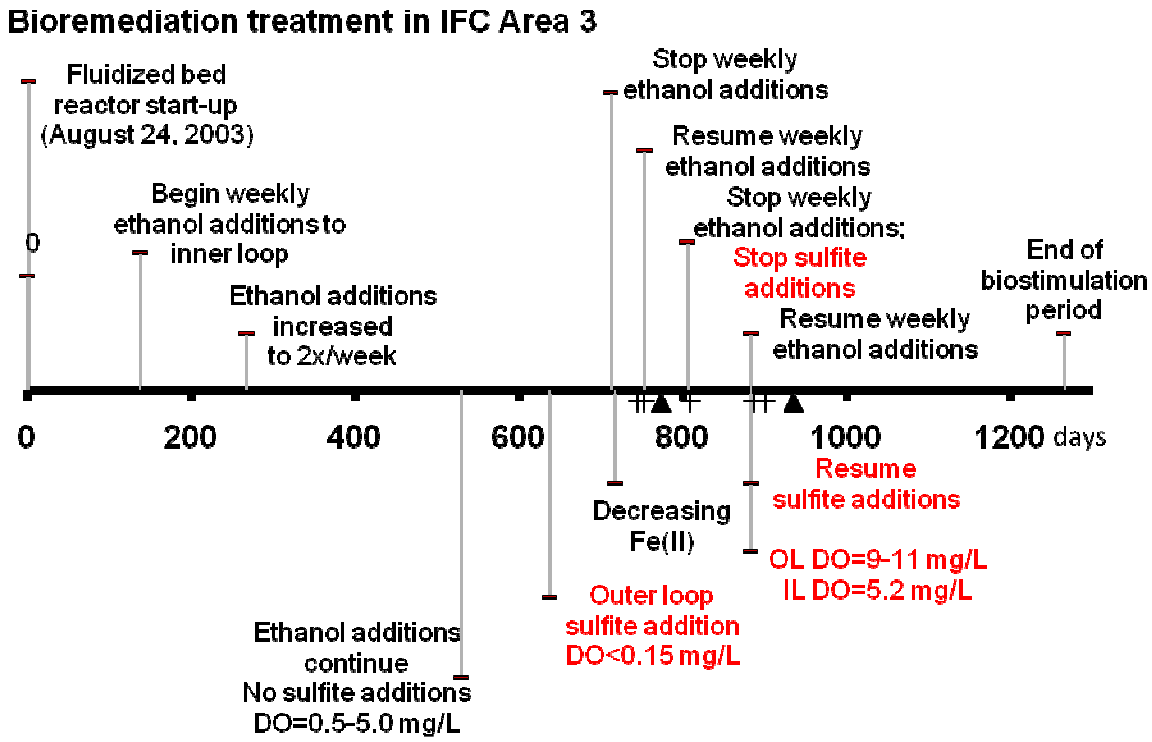

Figure 5.1. Timeline of operation of Area 3 pilot test plot. Day 0 indicates the start of the aboveground treatment (Wu et al., 2006b). Ethanol additions to the inner treatment loop began on day 138. Sulfite additions to the outer treatment loop began on day 637. The re-oxidation test study included four treatment phases: (1) ethanol addition to stimulate U(VI) reduction, (2) ethanol addition to the inner loop and sulfite addition to the outer loop, (3) sulfite addition only, (4) no additions. Groundwater sampling events are indicated with a plus and sediment sampling events are indicated with a triangle.

each) were shipped to Georgia Tech. The DNA was re-suspended in 100 µL of sterile, nuclease-free, deionized water to yield a homogeneous solution with a DNA concentration of 1 ng μL^{-1}. DNA from groundwater was extracted as described [35] and shipped to Georgia Tech by Joy Van Nostrand (University of Oklahoma).

5.3.3 Quantitative real-time PCR (qPCR) analysis. qPCR used both SYBR green and TaqMan detection chemistries. The SYBR green approach for quantifying organisms closely related to *Geobacter lovleyi* was performed as described [36]. TaqMan probes and primers specific to the *A. dehalogenans* strain 2CP-C 16S rRNA gene (genome GenBank accession CP000251) were designed using Primer Express software (Applied Biosystems, Foster City, CA) and utilized for laboratory culture analysis. Strain-specific qPCR reactions [37] were utilized in order to rule out contamination and verify that growth calculations were restricted to the strain of interest. Reactions targeting strain 2CP-C contained forward primer 5'-TCG CGA GGG ACG AAT AAG G- 3', reverse primer 5'-CGG TGC TTC CTC TCG AGG TA-3', and probe 5'-FAM-ACA GTC CGT TTC GAT GAC-NFQ-3' that utilized FAM as a reporter dye on the 5' end and a non-fluorescent quencher (NFQ) on the 3' end as described [37]. To quantify all *Anaeromyxobacter* 16S rRNA gene sequences in field samples, forward primer 5'-GCA ACG CCG CGT GTG T-3', reverse primer 5'-TCC CTC GCG ACA GTG CTT-3', and probe 5'-VIC-ATG AAG GTC TTC GGA TCG T-NFQ-3' were used as described [37]. The specificity of all probes and primers was tested using BLAST searching for short, nearly exact nucleotide sequence matches [38]. qPCR two-fold concentrated master mix (Applied Biosystems [ABI], Foster City, CA), 2.5 µM probe, and 5 µM of each primer were combined in sterile, nuclease-free water. Aliquots (18 µL) of the reaction mix were

dispensed into an ABI MicroAmp Fast Optical 96-Well Reaction Plate held on ice. Template DNA (2 μL) was added to each tube, and the tubes were sealed with an ABI Optical Adhesive Cover. Standard curves were prepared with purified plasmid DNA containing a 1.5-kb fragment of the *A. dehalogenans* strain 2CP-C 16S rRNA gene. 16S rRNA genes were amplified using universal primers [39,40] and cloned into plasmids using the Invitrogen TOPO TA Cloning kit (Carlsbad, CA). A 10-fold serial dilution series of purified plasmid (5×10^1 to 5×10^8 copies per reaction) was included in each qPCR run. The spectrofluorometric thermal cycler (ABI 7500 Real-Time PCR System) was used to detect FAM or SYBR green fluorescence. The quantification limit was considered to be the lowest standard in a linear standard curve that produced measurable fluorescence. The quantification limit for *Anaeromyxobacter* TaqMan qPCR reactions was 2 to 3 16S rRNA gene copies per reaction, which equates to about 2×10^2 16S rRNA gene copies/L of groundwater. Detection of *G. lovleyi* 16S rRNA genes used SYBR Green reactions and required 1×10^3 16S rRNA gene copies per reaction, or about 1×10^5 *G. lovleyi* 16S rRNA gene copies/L of groundwater to yield positive signals.

5.3.4 Bacterial strains and culture conditions. *A. dehalogenans* strain 2CP-C was routinely grown at 30°C without shaking in 60 mL (nominal capacity) glass serum bottles (Wheaton, Millville, NJ) containing 40 mL of reduced, 30 mM bicarbonate-buffered mineral salts medium with a N_2/CO_2 headspace (80:20, vol:vol) [41,42]. The bottles were sealed with butyl rubber stoppers (Geo-Microbial Technologies, Inc., Ochelata, OK) and aluminum crimp caps (Wheaton). Acetate (5 mM) (Sigma-Aldrich, St. Louis, MO) was provided as electron donor and 10 mM fumarate (Sigma-Aldrich) served as electron acceptor (unless indicated otherwise).

5.3.5 Oxygen growth experiments. For experiments with oxygen as electron acceptor, medium was prepared as described above except that 50 mM HEPES (4-[2-hydroxyethyl]-1-piperazine-ethanesulfonic acid), pH 7.2 (Sigma-Aldrich) replaced bicarbonate as the buffer system, the acetate concentration was increased to 10 mM, and fumarate was omitted. Medium (25 mL) was dispensed into 160-mL glass serum bottles, resulting in a headspace (N_2/CO_2; 80:20, vol:vol) of 135 mL. All cultures received 4% (vol:vol) inocula from stationary phase cultures grown on either fumarate or oxygen. Filter-sterilized (25 mm Acrodisc 0.2 μm membrane syringe filter, Pall Life Sciences, Ann Arbor, MI) gas mixtures containing 16, 30, and 60 mL air (i.e., 3.4, 6.3, and 13 mL oxygen) were added using a 60 mL syringe to achieve initial oxygen partial pressures (pO_2) of 0.02, 0.03, and 0.07 atm, respectively, and total pressures of 1.1 to 1.4 atm. In the case of the 0.032 atm O_2 treatment (30 mL air), nitrogen (1 atm) was added to the syringe to provide 60 mL of total gas added and to replicate the total pressure (1.4 atm) in the higher O_2 treatments. Closed control cultures did not receive oxygen, but instead received 60 mL of sterile nitrogen gas. In order to achieve the high initial pO_2 treatment, autoclaved serum bottles containing anaerobic medium, identical to the ones used for lower pO_2 treatments, were opened, loosely covered with sterile aluminum foil, shaken at 220 rpm, and re-sealed with sterile stoppers. The measured pO_2 in these bottles was 0.178 ± 0.008 atm after 3 hours of shaking. For analysis of growth at atmospheric pO_2, foam-stoppered 250-mL Erlenmeyer flasks were utilized, containing 25 mL medium and a 4% (vol:vol) stationary phase culture inoculum. No quantitative data are reported for atmospheric pO_2. All vessels were shaken at 220 rpm and incubated at 30°C in the dark.

Triplicate cultures were established for each pO_2 and samples were analyzed periodically for acetate, oxygen, and cell numbers via qPCR (see below).

5.3.6 Calculations. Oxygen partial pressure (pO_2) in microaerophilic culture vessels are reported in atmospheres (atm) and in total μmoles per bottle. Oxygen quantification used a 5-point calibration curve established by injecting samples from 160 ml bottles containing 25 ml of medium that contained 0, 16, 30, and 60 mL of air, and an ambient air sample. Detector response (i.e., peak area) was correlated to the amount of oxygen in the sample injected into the gas chromatograph. The peak areas were corrected for the method baseline response determined by injecting oxygen-free nitrogen gas. An ambient air sample was injected at every time point to correct for instrumental drift. Oxygen as μmoles per bottle were calculated according to the ideal gas law ($n/V = pO_2/RT$; where n equals the number of μmol, V equals the volume of the culture vessel [0.135 L], R is the ideal gas constant [0.082057 $L \cdot atm \cdot K^{-1} \cdot mol^{-1}$], and T is the room temperature in Kelvin). Thus, a pO_2 of 0.02 atm equates to 110 μmoles of oxygen per bottle. Due to oxygen's very low Henry's Law Constant (K_H) of 1.26×10^{-3} M/atm, dissolved oxygen did not significantly contribute to the total amount per bottle within the accuracy of the measurements (e.g., with 25 mL of aqueous medium in a 160 mL bottle and a pO_2 of 0.02 atm, less than 1% of the total amount of oxygen was dissolved in the aqueous phase).

5.3.7 Analytical methods. Organic acids were quantified using a Waters 1525 high performance liquid chromatography system equipped with an Aminex HPX-87H ion exclusion column and connected to a Waters 2487 dual wavelength absorbance detector

[43]. Oxygen was quantified using an Agilent Technologies Model 6890N gas chromatograph equipped with thermal conductivity detector as described [44].

5.3.8 Calculation of growth rate, growth yield, and f_e and f_s values. Growth rate values were determined using nonlinear regression analysis by plotting the number of 16S rRNA gene copies per mL of culture over time. Growth rate constants (k) were determined using the exponential growth equation $y=y_0*e^{kt}$ where y is the number of 16S rRNA gene copies at time t and y_0 is the number of 16S rRNA gene copies per mL at t=0. Triplicate cultures were used to determine growth rates at pO_2s of 0.02 atm, 0.03 atm, 0.07 atm, and 0.18 atm. Growth yields were determined based on initial and final 16S rRNA gene copies per mL of culture. The quantification of 16S rRNA gene copies was utilized as an approximation of cell numbers. The four sequenced *Anaeromyxobacter* genomes (GenBank Accession numbers CP001131, CP000769, CP000251, ABKC00000000) harbor duplicate rRNA operons [28] suggesting that members of the *Anaeromyxobacter* group contain two 16S rRNA gene copies per genome and cell. f_e and f_s were calculated from growth yields based on the electron balance of cell biosynthesis associated with oxygen reduction according to McCarty [45] and Criddle et al. [46].

5.3.9 Statistical analysis. Nonlinear and linear regression analyses, including significance tests for the regressions, were performed using GraphPad Prism version 5.00 (GraphPad software, San Diego, CA). For modeling exponential growth of strain 2CP-C, the growth rate constant (k) was constrained to less than 1, and default settings were used for all other analyses. To test for significance directly between averaged qPCR measurements, the Student's paired t-test (one-tailed distribution) was performed using Microsoft Excel.

5.4 Results

The comparative analysis of Area 3 sediment and groundwater samples collected before and after oxygen intrusion demonstrated changes in the *Anaeromyxobacter* population size (Figure 5.2). Mean *Anaeromyxobacter* 16S rRNA gene copies per g of sediment increased as much as five-fold in response to oxygen intrusion. For example, *Anaeromyxobacter* cell numbers increased from $2.2 \times 10^7 \pm 8.6 \times 10^6$ to $1.0 \times 10^8 \pm 2.2 \times 10^7$ cells per g of sediment collected from well FW101 (screened interval 2 [13.7 m bgs]). Student's paired t-test established statistical significance for the increase in *Anaeromyxobacter* 16S rRNA gene abundance per g of sediment after oxygen intrusion (p-values provided in Figure 5.2A). *Anaeromyxobacter* cell numbers in all of the groundwater samples collected from inner loop multi-level sampling wells were about four orders of magnitude lower (1×10^3 - 1×10^4 cells per L groundwater) than in sediments (1×10^7 - 1×10^8 cells per g sediment) suggesting that the majority of *Anaeromyxobacter* cells was attached to the soil matrix, rather than planktonic (Figure 5.2B). Groundwater DNA analysis also indicated that mean planktonic *Anaeromyxobacter* cell numbers either remained relatively constant (FW101-2) or significantly decreased (FW102-2 and -3) after oxygen intrusion (days 754-806) (Figures 5.2B and 5.1). Thus, the majority of the *Anaeromyxobacter* population resides with the solids, and the response of the *Anaeromyxobacter* population to oxygen differed remarkably in planktonic cells and solid-associated, attached cells. As a comparison to another U(VI)-reducing delta-Proteobacterium native to the Oak Ridge IFC Area 3,

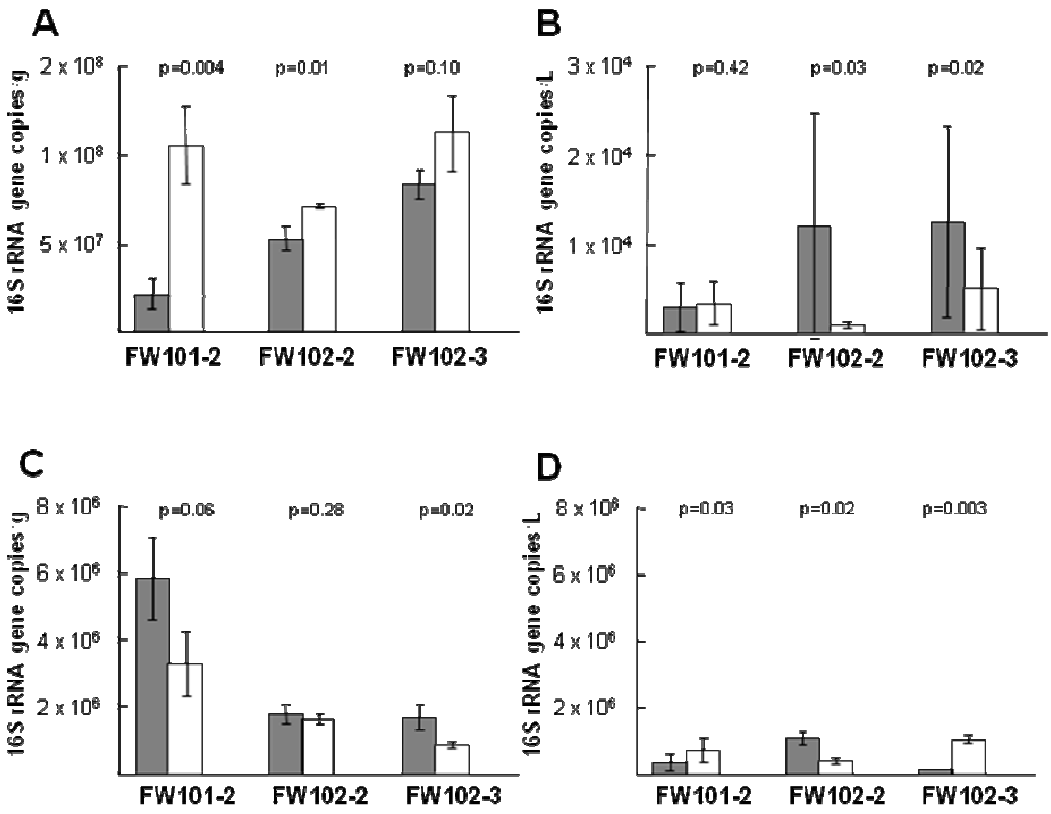

Figure 5.2. Oxygen effects on *Anaeromyxobacter dehalogenans* and *Geobacter lovleyi* populations native to the Oak Ridge IFC Area 3 U(VI)-reduction treatment zone. 16S rRNA genes of target organisms were monitored with qPCR in samples collected from multilevel sampling well FW101 at screened interval 2 (13.7 m bgs), and well FW102 at screened intervals 2 and 3 (12.2 m bgs). The top panels show the total population sizes indicated by 16S rRNA gene copy numbers of attached (A) and planktonic (B) *Anaeromyxobacter* spp. before (shaded bar) and after (white bar) oxygen intrusion. The bottom panels show quantitative data for the same samples for attached (C) and planktonic (D) *Geobacter lovleyi* strain SZ 16S rRNA gene copies, respectively. P-values from paired t-test are indicated above each set of bars. The p-value describes the probability that the difference between the two values is attributable to random variability. P-values less than 0.05 describe a statistically significant difference. Note y-axis scales are different.

samples were also analyzed for *G. lovleyi*-like organisms [36]. Data obtained for *G. lovleyi* contrast the observations made with *Anaeromyxobacter*. Comparative analysis of sediment samples taken on days 774 and 935 during active ethanol biostimulation prior to and after oxygen intrusion indicated that mean sediment-associated cell numbers of *G. lovleyi*-like bacteria decreased by as much as 50% following the intrusion of oxygenated groundwater (Figure 5.2C). Unlike *Anaeromyxobacter* cells, which occurred predominantly attached to solids, cell numbers of *G. lovleyi*-like organisms in groundwater and attached to solids were similar in all wells, under oxic or anoxic conditions, and ranged from 1.0×10^6 to 1.0×10^7 16S rRNA gene copies per g sediment or L of groundwater (Figure 5.2C and D). Following oxygen intrusion, the ratio of attached to planktonic *G. lovleyi* cells decreased in two of the three wells/screen intervals tested (FW101-2 and FW102-3) (Figure 5.2D).

5.4.1 Laboratory analysis of oxygen consumption. The field observations suggest *Anaeromyxobacter* spp. respond differently than *Geobacter* spp. to oxygen intrusion. Laboratory experiments were performed under precisely controlled conditions to study the different behaviors in more detail. Stationary phase strain 2CP-C cultures that were grown with 10 mM fumarate consumed oxygen and three consecutive additions of oxygen (each at a pO_2 of 0.02 atm) were reduced within 50 hours per addition (Figure 5.3A). Oxygen consumption coincided with acetate oxidation and no oxygen was reduced in uninoculated controls. No measurable net increase in biomass occurred while oxygen was reduced in stationary phase cultures as indicated by constant numbers of *A. dehalogenans* 16S rRNA gene copies (Figure 5.3A). The ability to consume oxygen in stationary phase cultures was not shared by *G. lovleyi* strain SZ. Under the conditions

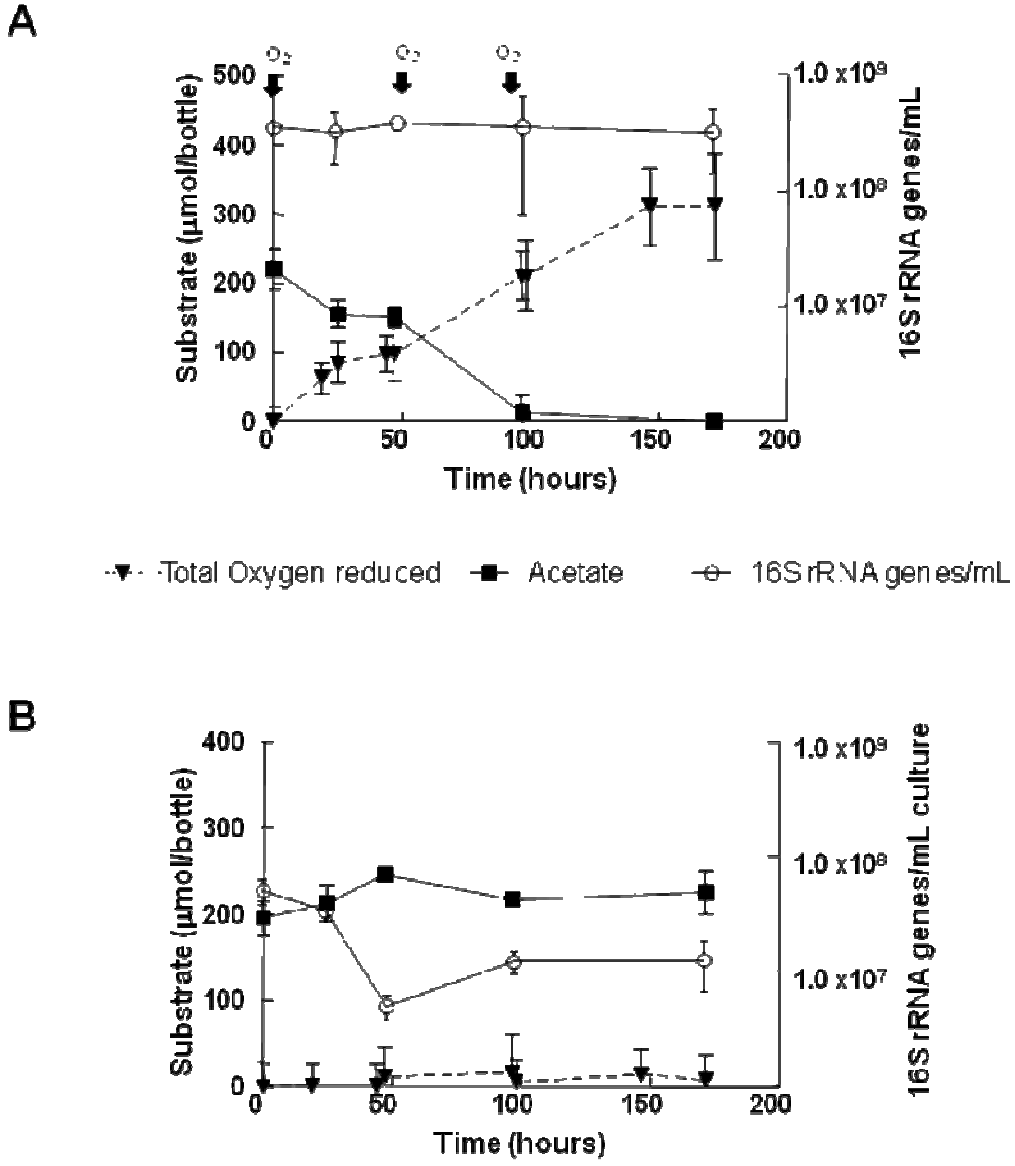

Figure 5.3. Response of *A. dehalogenans* strain 2CP-C and *G. lovleyi* to O_2. Stationary phase cultures of *A. dehalogenans* strain 2CP-C (A) and *G. lovleyi* (B) were exposed to an oxygen-containing headspace (initital pO_2 was 0.02 atm). Acetate (filled squares) and 16S rRNA gene copy numbers (open circles) were monitored over 10 days in cultures amended with 0.02 atm oxygen. The arrows indicate additional 0.02 atm oxygen amendments. Also shown is the total amount of oxygen reduced (filled inverted triangles). *G. lovleyi* strain SZ did not receive additional oxygen, since consumption was negligible.

tested, neither oxygen reduction nor acetate depletion were observed in cultures of *G. lovleyi* strain SZ and the cell numbers decreased by an order of magnitude (Figure 5.3B).

5.4.2 Microaerophilic growth by* A. dehalogenans *strain 2CP-C. Following confirmation of oxygen consumption in *A. dehalogenans* stationary-phase cultures, experiments were conducted to test for aerobic growth. While strain 2CP-C grew readily under anaerobic conditions, growth in liquid medium at atmospheric oxygen tension was unreliable and occurred in about one third of the cultures after long lag phases of 3 to 5 weeks. Shorter lag times and accelerated growth were observed when shaking was discontinued. To quantify oxygen depletion and to correlate oxygen consumption to biomass production, experiments in closed serum bottles were performed. At an initial pO_2 of 0.02 atm, oxygen consumption began after a 45-hour lag phase and 110 ± 29 µmoles of oxygen were consumed after 82 hours of incubation (Figure 5.4). Oxygen was not consumed in uninoculated control bottles (i.e., identical medium with no cells), indicating that strain 2CP-C cells were responsible for oxygen consumption. *A. dehalogenans* strain 2CP-C grew during oxygen reduction as indicated by increases in 16S rRNA gene copies from $2.66 \times 10^7 \pm 8.78 \times 10^6$ to $5.18 \times 10^8 \pm 7.20 \times 10^7$ per mL of culture suspension (Figure 5.3). In cultures without oxygen, the *A. dehalogenans* 16S rRNA gene copies decreased from $3.16 \times 10^7 \pm 9.16 \times 10^6$ to $6.48 \times 10^6 \pm 3.64 \times 10^6$ per mL of culture suspension over the 86 h incubation period, indicating that cell growth was attributable to oxygen. Oxygen consumption was linked to concomitant depletion of electron donor (i.e., acetate; Figure 5.4). No acetate consumption occurred in control cultures without oxygen and oxygen consumption ceased in bottles that had consumed all acetate (data not shown). Growth of *A. dehalogenans* was also observed at pO_2 of 0.03,

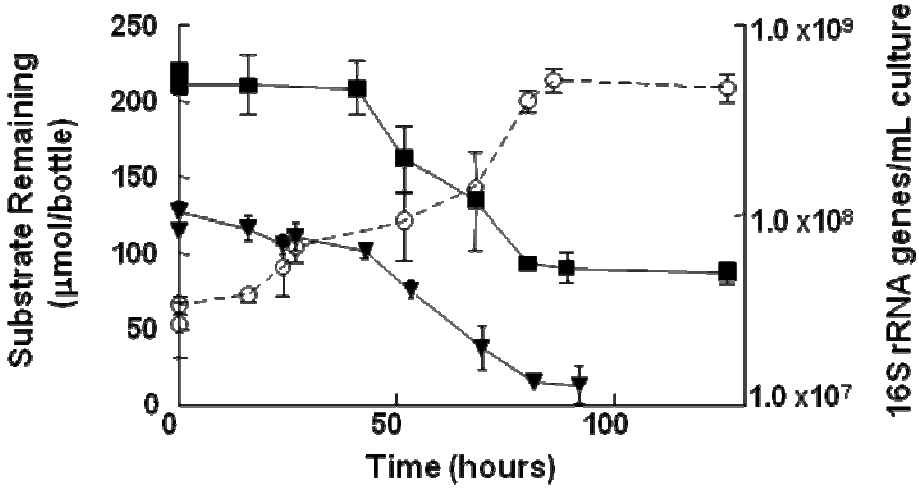

Figure 5.4. Growth of *A. dehalogenans* strain 2CP-C under aerobic conditions. Closed vessels containing defined mineral salts medium amended with acetate as electron donor received a 4% inoculum from a fumarate-grown culture and were incubated at 30°C. Initial pO_2 was 0.02 atm. Neither acetate consumption nor growth occurred in uninoculated controls. Inverted triangles and squares indicate oxygen and acetate, respectively (left y-axis). Open circles indicate 16S rRNA gene copies per mL culture (right y-axis).

0.07 and 0.18 atm with comparable lag times. When oxygen-grown cells were transferred to fresh medium, oxygen reduction and growth commenced with lag time of < 45 hours.

5.4.3 Effect of pO2 on growth. Interestingly, increasing pO_2 greatly affected growth rates of culture 2CP-C and the growth rate constant (k) decreased linearly (k = 0.09 *pO_2 + 0.051) from 0.051 ± 0.006 h^{-1} at a pO_2 of 0.02 atm to 0.034 ± 0.010 h^{-1} at a pO_2 of 0.18 atm (i.e., a 33% decrease) (Table 5.1; Figure 5.5). The slope of the k-pO_2 regression line was significantly non-zero ($P<0.05$). Doubling times of fumarate-grown and oxygen-grown (pO_2=0.02 atm) cultures were not statistically different, with 95% confidence intervals for the 10 to 19 hours and 12 to 16 hours growth periods, respectively (Table 5.1; Figure 5.5). In addition to growth rate, the O_2 utilization efficiency of *A. dehalogenans* strain 2CP-C decreased with increasing pO_2 (Table 5.2). The growth yield of strain 2CP-C at an initial pO_2 of 0.02 atm was 6 ± 2 g per mole electrons consumed, which is comparable to the growth yield with fumarate (5.7 g per mole electrons) (Table 5.2). When pO_2 was increased to 0.18 atm, the growth yield decreased by 78 % to 1.3 ± 0.5 g per mole electrons. The measurement of biomass produced in cultures amended with different amounts of oxygen revealed that the fraction of electrons used for cell growth (f_s) decreased from 0.52 to 0.19 at initial pO_2s of 0.02 and 0.18 atm, respectively. Accordingly, the fraction of electrons used for oxygen reduction (f_e) increased from 0.48 to 0.81 as the O_2 concentration increased from 0.02 atm to 0.18 atm, respectively (Table 5.2).

Table 5.1. *Anaeromyxobacter dehalogenans* strain 2CP-C growth rate parameters in mineral salts medium amended with acetate and different concentrations of O_2 at 30° C.

Nonlinear Regression of Growth Data ($y=y_0e^{-kt}$)[a]	**Initial pO_2 [atm]**				**Fumarate**
	0.18	**0.07**	**0.03**	**0.02**	**10 mM**
y_0 ($x10^6$)	5.1 ± 5.9	4.2 ± 2.5	3.9 ± 2.8	6.2 ± 3.3	11.1 ± 4.1
k (h^{-1})	0.034 ± 0.010	0.045 ± 0.006	0.045 ± 0.006	0.051 ± 0.006	0.058 ± 0.007
R^2 [b]	0.81	0.95	0.94	0.94	0.92
Doubling time (h)	22 ± 7	16 ± 2	16 ± 2	14 ± 2	12 ± 1

[a] Exponential equation used for fitting qPCR data (y_o=initial bacterial population, y=bacterial population at time t, k=growth rate constant)

[b] Regression fit

Table 5.2. *Anaeromyxobacter dehalogenans* strain 2CP-C growth yields and f_e values calculations for cells grown on different pO_2 and comparison to literature data for other electron acceptors.

	Electron Acceptor					
	Initial pO_2 [atm]				Fumarate [mM]	2-CP [mM]
	0.18	**0.07**	**0.03**	**0.02**	**10**[c]	**0.2**[d]
Cells per μmole e^- transferred to EA ($x10^7$)	3.5 ± 1.4	4.27 ± 0.72	13.1 ± 3.5	16.0 ± 5.8	14.9 ± 1.2	7.74
Cell yield[a] (dry weight) g per mole e^-	1.3 ± 0.5 [b]	1.6 ± 0.3 [b]	5 ± 1 [b]	6 ± 2 [b]	5.7 ± 0.6 [b]	2.9 [b]
Mole e^- cells per mole EA	0.23 ± 0.09	0.28 ± 0.05	0.88 ± 0.18	1.1 ± 0.35	1.0 ± 0.11	0.52
f_s	0.19	0.22	0.47	0.52	0.50	0.34
f_e	0.81	0.78	0.53	0.48	0.50	0.66

[a] Cell yield is reported per mole of electrons transferred to the electron acceptor based on oxygen reduction to water, 2-chlorophenol (2-CP) reduction to phenol, and fumarate reduction to succinate.

[b] Cell yield estimates are calculated by multiplying the number of cells per μmoles of electrons transferred to the electron acceptor times the dry weight of a single cell ($3.80 \pm 0.27 \times 10^{-14}$ g per cell) estimated previously (Sanford et al., 2007) for fumarate-grown cells.

[c] **(**Sanford et al., 2007)

[d] **(**He and Sanford, 2003)

[e] f_s is the fraction of electrons from the electron donor used for biomass synthesis

[f] f_e is the fraction of electrons from the electron donor transferred to the electron acceptor

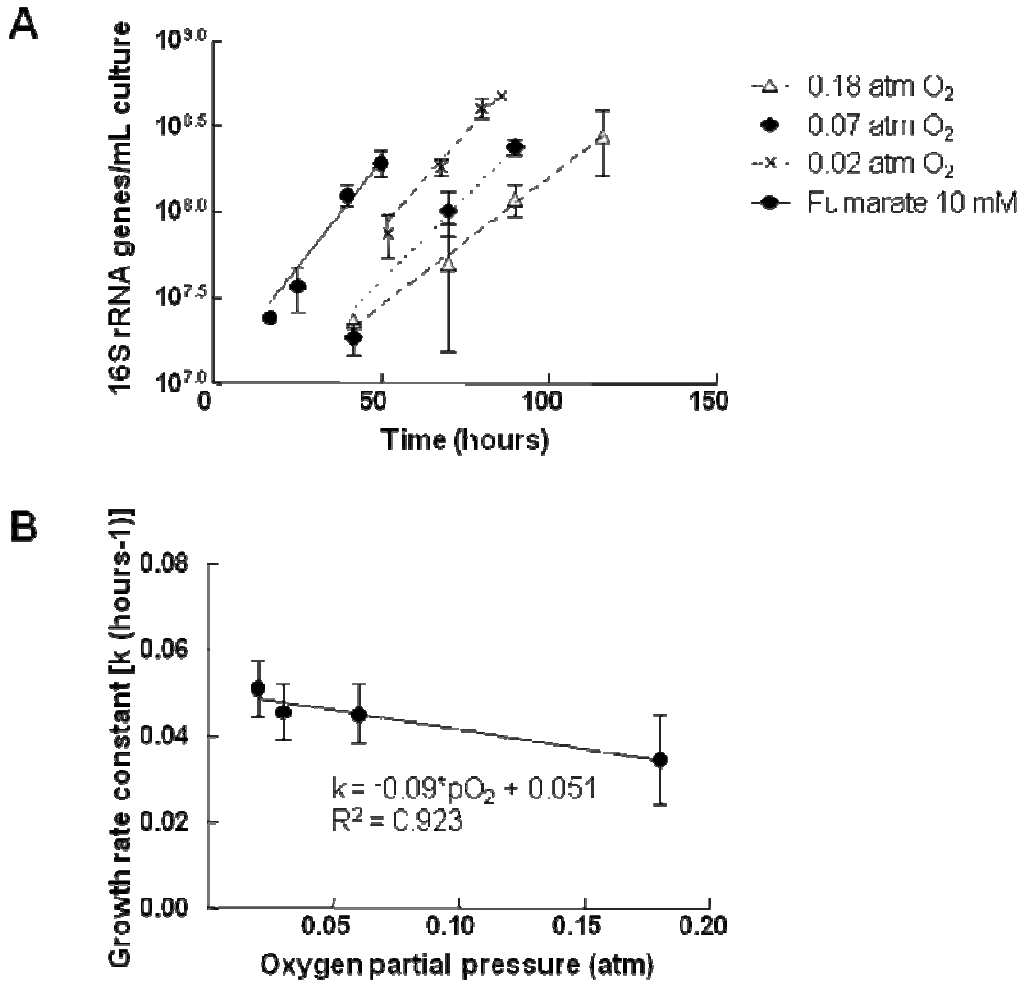

Figure 5.5. Growth characteristics of *A. dehalogenans* strain 2CP-C.

A. Graphical determination of growth rates at 30°C under aerobic and anaerobic conditions. Strain 2CP-C was grown in mineral salts medium anaerobically with acetate and fumarate (filled circles) or at initial pO_2s of 0.02 atm (crosses), 0.03 atm, 0.07 atm (filled diamonds), and 0.18 atm (open triangles). The 0.03 atm data have been omitted because of overlap with the 0.07 atm dataset.

B. Linear correlation between growth rate constant (k) and pO_2. Linear regression analysis of the growth rate data at varying pO_2 indicates an inverse linear correlation of k and pO_2.

5.5 Discussion

The observation of *in situ* growth of *Anaeromyxobacter* spp. following oxygen intrusion at the Oak Ridge IFC site motivated detailed laboratory studies of the oxygen metabolism of *A. dehalogenans* strain 2CP-C. These studies revealed specific adaptations of *Anaeromyxobacter* spp. to environments with fluctuating redox conditions. The genome analysis of *A. dehalogenans* strain 2CP-C suggested that two oxygen-reducing pathways exist; one that shares homology with anaerobes and microaerophiles and includes a cytochrome cbb_3 oxidase, and a second pathway characteristic for the phylogenetically closely related Myxobacteria that includes a cytochrome aa_3 oxidase [28]. Cytochrome oxidases can play roles in both respiratory (energy-yielding) and/or oxygen-detoxifying (non-energy yielding) reactions [30]. The alpha-Proteobacteria *Bradyrhizobium japonicum* and *Paracoccus dentrificans* both possess cytochrome aa_3 oxidases as well as cytochrome cbb_3 oxidases and are thought to maintain both protein complexes for quick response to changing pO_2 [47,48]. It is conceivable that one cytochrome oxidase is used for detoxification while a separate, respiratory cytochrome oxidase is involved in the organisms' energy metabolism at low pO_2. Oxygen reduction by fumarate-grown *A. dehalogenans* strain 2CP-C cells that had reached stationary phase suggests that an oxygen detoxification pathway may be constitutive, an adaptation beneficial for anaerobic or microaerophilic organisms near the oxic/anoxic interface.

Geobacter spp. represent another group of environmentally relevant metal reducers that are found at the oxic/anoxic interface, but whose relationship to oxygen remains unclear. *G. lovleyi* strain SZ failed to consume oxygen under the conditions tested but growth under aerobic conditions has been reported with *Geobacter sulfurreducens*.

Unlike for *A. dehalogenans*, oxygen reduction by *G. sulfurreducens* could not be recovered in transfer cultures without intermediate, anoxic cultivation with Fe(III) as electron acceptor [49]. Based on the existing genome annotation (CP001089), the electron transport chain of *G. lovleyi* strain SZ contains a cytochrome *bd*-type oxidase and not an aa_3-type, which is present in *G. sulfurreducens* [49] or the cbb_3-type present in *A. dehalogenans*. Therefore, differences in oxygen metabolism between *G. lovleyi* strain SZ and *G. sulfurreducens* would be expected.

Other members of the delta-Proteobacteria, including some *Desulfovibrio* spp., flourish at the oxic-anoxic interface and are capable of oxygen detoxification, although they were classically considered strict anaerobes [50]. Cultures of *D. desulfuricans* ATCC 27774 consumed oxygen, and the expression of catalase and superoxide dismutase increased when grown with nitrate under high pO_2 (up to 0.18 atm) [51]. Several transcriptomic and proteomic studies have been performed to identify the metabolic changes in response to oxygen adaptation by *Desulfovibrio* spp. [52,53,54,55]. Mukhopadhyay and colleagues demonstrated that sparging liquid cultures of sulfate-reducing *Desulfovibrio vulgaris* Hildenborough cultures with 0.1% oxygen caused only minor changes to the organism's transcriptome [56]. Conversely, air (21% oxygen) exposure caused down-regulation of central metabolic pathways, indicating that the organisms were dedicating less reducing power for biomass production at high pO_2 [56]. Growth measurements of *A. dehalogenans* strain 2CP-C indicated that the respiratory efficiency decreased at higher pO_2, resulting in less biomass synthesis (Table 2). Similar down-regulation of central metabolic pathways in response to high pO_2 could explain the decreasing biomass synthesis observed in *A. dehalogenans* strain 2CP-C cultures. Since

the genomes of four *Anaeromyxobacter* strains are available (Accession numbers CP001131, CP000769, CP000251, ABKC00000000), future transcriptomic and proteomic studies should elucidate pathway regulation and function of the different oxygen-reducing pathways in *Anaeromyxobacter* spp.

Laboratory experiments with *A. dehalogenans* strain 2CP-C confirmed aerobic growth but, remarkably, measured f_e and f_s values varied with changing initial pO_2 in cultures amended with acetate. The fraction of electrons released during electron donor oxidation and directed toward reduction of the terminal electron acceptor (f_e) indicates if the electron acceptor is used for energy generation (i.e., respiration) or if its reduction is uncoupled from growth (e.g., to achieve detoxification or to serve as a fortuitous electron sink). Previous studies have demonstrated that an organism's metabolic efficiency, as measured by f_e and f_s, is constant for a given set of substrates [45,46]. For example, characteristic f_e values for aerobic respiration range between 0.4 and 0.88 (depending on the electron donor) [57], and are governed by the energetics of the energy-generating redox reaction [45]. Studies comparing respiratory electron acceptors of *A. dehalogenans* strain 2CP-C with acetate provided as electron donor, reported f_e and f_s values for ferric iron reduction ($f_e = 0.80$ and $f_s = 0.22$) and chlororespiration ($f_e = 0.66$ and $f_s = 0.34$) [13]. Growth yield (f_s) and the efficiency of oxygen utilization (f_e) in *A. dehalogenans* strain 2CP-C at a pO_2 of 0.02 atm are comparable to those observed with fumarate or nitrate as electron acceptors. At a pO_2 of 0.18 atm, less biomass was produced and f_e and f_s values were in line with those measured for chlororespiration, an energetically less favorable process than aerobic respiration [58]. Growth experiments performed at atmospheric oxygen concentrations indicated oxygen toxicity, and detoxification is a likely

explanation for the observed shift in the cells' use of reducing power. The shift to detoxification does not change the energetics of oxygen reduction but electron transfer is decoupled from generating a proton motive force for energy capture. Thus, f_e under high pO_2 conditions reflects an apparent f_e in the sense that not all the free energy change associated with the redox reaction is coupled to growth, and the true f_e is only observed under low pO_2, when oxygen toxicity is absent. Hence, evaluation of f_e for an aerobic process should be determined at different pO_2s to ensure that a true, as opposed to an apparent f_e, is measured. This procedure is pertinent for organisms whose relationships to oxygen are unclear.

Metal-reducing *Geobacter* spp. use flagellar motility [59,60], and the quantitative analysis of Area 3 sediment and groundwater samples demonstrated that *Geobacter lovleyi* cells are planktonic at four orders of magnitude greater density than *Anaeromyxobacter* cells, which is consistent with *Anaeromyxobacter*'s classification as a Myxobacterium with surface motility [28]. The uneven distribution of metal-reducing organisms between solids and groundwater emphasizes the need for investigation of how organism-specific characteristics and environmental factors influence attached versus planktonic state. Obviously, the analysis of *Anaeromyxobacter* population dynamics based on groundwater sampling data alone will provide an incomplete picture of the true abundance of members of this group. It is also important to note that *G. lovleyi* cells increased in groundwater in response to oxygen intrusion. Since this result is inconsistent with laboratory results, which indicated that *G. lovleyi* does not respire oxygen, it is conceivable that *G. lovleyi* detaches in response to oxygen intrusion, shifting its population to a planktonic lifestyle. The detachment hypothesis is supported by the

observation that the decrease in attached *G. lovleyi* cell numbers in FW102-3 (-8.04 x 10^5 cells per g sediment) is approximately equal to the increase in planktonic *G. lovleyi* cell numbers (+8.96 x 10^5 cells per L groundwater).

Bioreduction and immobilization of uranium remains a promising treatment strategy but re-oxidation of mineralized U(IV) affects stability of the reduced material and long-term site management issues arise. In anaerobic subsurface environments, different metal-reducing populations coexist [23,25,61,62,63], and Area 3 harbors *Geobacter* spp., *Anaeromyxobacter* spp., and *Desulfovibrio* spp. Ecological exclusion theory predicts that organisms occupying the same ecological niche do not co-occur in the same environment [64]. Therefore, physiological features must distinguish the metal reducing populations present in Area 3, and a relevant distinguishing factor is their response to oxygen. Since oxidants like oxygen affect the stability of mineralized U(IV), future efforts should not only explore organisms that reduce U(VI) but also focus on the organisms' ecophysiology that may affect the long-term stability of reduced radionuclides.

5.6 Acknowledgements

This research was supported by the Environmental Remediation Science Division (ERSD), Biological and Environmental Research (BER), U.S. Department of Energy and by NSF IGERT (Grant No. DGE 0114400) and NSF GK-12 (Grant No. 0338261) fellowships to S.H.T. We acknowledge the help of Sue Carroll, Weimin Wu, Jack Carley, and Terry Gentry for providing field samples and Joy D. Van Nostrand for providing DNA from Oak Ridge IFC site groundwater samples. We are grateful to Guangxuan Zhu for help with analytical instrumentation and Ulas Tezel for assistance with the oxygen measurements.

5.7 References

1. Lloyd JR, Renshaw JC (2005) Bioremediation of radioactive waste: radionuclide-microbe interactions in laboratory and field-scale studies. Current Opinion in Biotechnology 16: 254-260.

2. Wall JD, Krumholz LR (2006) Uranium reduction. Annual Review of Microbiology 60: 149-166.

3. Nealson KH, Belz A, McKee B (2002) Breathing metals as a way of life: geobiology in action. Antonie Van Leeuwenhoek International Journal of General and Molecular Microbiology 81: 215-222.

4. Gadd GM (2004) Microbial influence on metal mobility and application for bioremediation. Geoderma 122: 109-119.

5. Gorby YA, Lovley DR (1991) Electron-Transport in the Dissimilatory Iron Reducer, Gs-15. Applied and Environmental Microbiology 57: 867-870.

6. Wu WM, Carley J, Gentry T, Ginder-Vogel MA, Fienen M, et al. (2006) Pilot-scale *in situ* bioremedation of uranium in a highly contaminated aquifer. 2. Reduction of U(VI) and geochemical control of U(VI) bioavailability. Environmental Science & Technology 40: 3986-3995.

7. Yabusaki SB, Fang Y, Long PE, Resch CT, Peacock AD, et al. (2007) Uranium removal from groundwater via *in situ* biostimulation: Field-scale modeling of transport and biological processes. Journal of Contaminant Hydrology 93: 216-235.

8. Langmuir D (1978) Uranium solution-mineral equilibria at low temperatures with applications to sedimentary ore deposits. Geochimica Et Cosmochimica Acta 42: 547-569.

9. Wu W-M, Carley J, Luo J, Ginder-Vogel MA, Cardenas E, et al. (2007) *In situ* bioreduction of uranium (VI) to submicromolar levels and reoxidation by dissolved oxygen. Environmental Science & Technology 41: 5716-5723.

10. Wan JM, Tokunaga TK, Brodie E, Wang ZM, Zheng ZP, et al. (2005) Reoxidation of bioreduced uranium under reducing conditions. Environmental Science & Technology 39: 6162-6169.

11. Komlos J, Mishra B, Lanzirotti A, Myneni SCB, Jaffe PR (2008) Real-time speciation of uranium during active bioremediation and U(IV) reoxidation. Journal of Environmental Engineering-Asce 134: 78-86.

12. Arnold RG, Hoffmann MR, Dichristina TJ, Picardal FW (1990) Regulation of dissimilatory Fe(III) reduction activity in *Shewanella putrefaciens*. Applied and Environmental Microbiology 56: 2811-2817.

13. He Q, Sanford RA (2003) Characterization of Fe(III) reduction by chlororespiring *Anaeromyxobacter dehalogenans*. Applied and Environmental Microbiology 69: 2712-2718.

14. Lovley DR, Giovannoni SJ, White DC, Champine JE, Phillips EJP, et al. (1993) *Geobacter metallireducens* gen nov sp nov, a microorganism capable of coupling the complete oxidation of organic-compounds to the reduction of iron and other metals. Archives of Microbiology 159: 336-344.

15. Lovley DR, Widman PK, Woodward JC, Phillips EJP (1993) Reduction of uranium by cytochrome-c(3) of *Desulfovibrio vulgaris*. Applied and Environmental Microbiology 59: 3572-3576.

16. Roden EE, Lovley DR (1993) Dissimilatory Fe(III) reduction by the marine microorganism *Desulfuromonas acetoxidans*. Applied and Environmental Microbiology 59: 734-742.

17. Sanford RA, Wu Q, Sung Y, Thomas SH, Amos BK, et al. (2007) Hexavalent uranium supports growth of *Anaeromyxobacter dehalogenans* and *Geobacter* spp. with lower than predicted biomass yields. Environmental Microbiology 9: 2885-2893.

18. Brune A, Frenzel P, Cypionka H (2000) Life at the oxic-anoxic interface: Microbial activities and adaptations. FEMS Microbiology Reviews 24: 691-710.

19. Johnson MS, Zhulin IB, Gapuzan M-ER, Taylor BL (1997) Oxygen-Dependent Growth of the Obligate Anaerobe *Desulfovibrio vulgaris* Hildenborough. Journal of Bacteriology 179: 5598-5601.

20. Lemos RS, Gomes CM, Santana M, LeGall J, Xavier AV, et al. (2001) The 'strict' anaerobe *Desulfovibrio gigas* contains a membrane-bound oxygen-reducing respiratory chain. FEBS Letters 496: 40-43.

21. Sanford RA, Cole JR, Tiedje JM (2002) Characterization and description of *Anaeromyxobacter dehalogenans* gen. nov., sp. nov., an aryl halorespiring facultative anaerobic Myxobacterium. Applied and Environmental Microbiology 68: 893-900.

22. Wu Q, Sanford RA, Löffler FE (2006) Uranium(VI) reduction by *Anaeromyxobacter dehalogenans* strain 2CP-C. Applied and Environmental Microbiology 72: 3608-3614.

23. Cardenas E, Wu WM, Leigh MB, Carley J, Carrol lS, et al. (2008) Microbial communities in contaminated sediments, associated with bioremediation of uranium to submicromolar levels. Applied and Environmental Microbiology 74: 3718-3729.

24. North NN, Dollhopf SL, Petrie L, Istok JD, Balkwill DL, et al. (2004) Change in bacterial community structure during *in situ* biostimulation of subsurface sediment cocontaminated with uranium and nitrate. Applied and Environmental Microbiology 70: 4911-4920.

25. Petrie L, North NN, Dollhopf SL, Balkwill DL, Kostka JE (2003) Enumeration and characterization of iron(III)-reducing microbial communities from acidic subsurface sediments contaminated with uranium(VI). Applied and Environmental Microbiology 69: 7467-7479.

26. Cole JR, Cascarelli AL, Mohn WW, Tiedje JM (1994) Isolation and characterization of a novel bacterium growing via reductive dehalogenation of 2-chlorophenol. Applied and Environmental Microbiology 60: 3536-3542.

27. Treude N, Rosencrantz D, Liesack W, Schnell S (2003) Strain FAc12, a dissimilatory iron-reducing member of the *Anaeromyxobacter* subgroup of Myxococcales. FEMS Microbiology Ecology 44: 261-269.

28. Thomas SH, Wagner RD, Arakaki AK, Skolnick J, Kirby JR, et al. (2008) The mosaic genome of *Anaeromyxobacter dehalogenans* strain 2CP-C suggests an aerobic common ancestor to the delta-Proteobacteria. PLoS ONE 3: e2103.

29. Goldman BS, Nierman WC, Kaiser D, Slater SC, Durkin AS, et al. (2006) Evolution of sensory complexity recorded in a myxobacterial genome. Proceedings of the National Academy of Sciences of the United States of America 103: 15200-15205.

30. Pitcher RS, Watmough NJ (2004) The bacterial cytochrome cbb_3 oxidases. Biochimica et Biophysica Acta 1655: 388-399.

31. Garcia-Horsman JA, Barquera B, Rumbley J, Ma JX, Gennis RB (1994) The superfamily of heme-copper respiratory oxidases. Journal of Bacteriology 176: 5587-5600.

32. Pitcher RS, Brittain T, Watmough NJ (2002) Cytochrome cbb_3 oxidase and bacterial microaerobic metabolism. Biochemical Society Transactions 30: 653-658.

33. Wu W-M, Carley J, Fienen M, Mehlhorn T, Lowe K, et al. (2006) Pilot-scale *in situ* bioremediation of uranium in a highly contaminated aquifer. 1. Conditioning of a treatment zone. Environmental Science & Technology 40: 3978-3985.

34. Luo J, Weber F-A, Cirpka OA, Wu W-M, Nyman JL, et al. (2007) Modeling *in situ* uranium(VI) bioreduction by sulfate-reducing bacteria. Journal of Contaminant Hydrology 92 129–148.

35. Zhou J, Bruns MA, Tiedje JM (1996) DNA recovery from soils of diverse composition. Applied and Environmental Microbiology 62: 316–322.

36. Amos BK, Sung Y, Fletcher KE, Gentry TJ, Wu WM, et al. (2007) Detection and quantification of *Geobacter lovleyi* strain SZ: Implications for bioremediation at tetrachloroethene- and uranium-impacted sites. Applied and Environmental Microbiology 73: 6898-6904.

37. Thomas SH, Pavlekovic M, Lee N, Marshall MJ, Kennedy DW, et al. (2006) Diversification in the subsurface: Strain variation of *Anaeromyxobacter dehalogenans* in a uranium and nitrate-contaminated subsurface environment. 11th International Symposium on Microbial Ecology.

38. Altschul SF, Gish W, Miller W, Myers EW, Lipman DJ (1990) Basic Local Alignment Search Tool. Journal of Molecular Biology 215: 403-410.

39. Zhou J, Fries MR, Chee-Sanford JC, Tiedje JM (1995) Phylogenetic analyses of a new group of denitrifiers capable of anaerobic growth on toluene and description of *Azoarcus tolulyticus* sp nov. Int J Syst Bacteriol 45: 500-506.

40. Weisburg WG, Barns SM, Pelletier DA, Lane DJ (1991) 16S ribosomal DNA amplification for phylogenetic study. Journal of Bacteriology 173: 697-703.

41. Cole JR, Fathepure BZ, Tiedje JM (1995) Tetrachloroethene and 3-chlorobenzoate dechlorination activities are co-induced in *Desulfomonile tiedjei* DCB-1. Biodegradation 6: 167-172.

42. Löffler FE, Sanford RA, Tiedje JM (1996) Initial characterization of a reductive dehalogenase from *Desulfitobacterium chlororespirans* Co23. Applied and Environmental Microbiology 62: 3809-3813.

43. He JZ, Ritalahti KM, Aiello MR, Löffler FE (2003) Complete detoxification of vinyl chloride by an anaerobic enrichment culture and identification of the reductively dechlorinating population as a *Dehalococcoides* species. Applied and Environmental Microbiology 69: 996-1003.

44. Okutman Tas D, Pavlostathis SG (2005) Microbial reductive transformation of pentachloronitrobenzene under methanogenic conditions. Environmental Science & Technology 39: 8264-8272.

45. McCarty PL (1971) Energetics and bacterial growth. In: Dekker M, editor. Organic Compounds in Aquatic Environments. New York: S.D. Faust and J.V. Hunter. pp. 495-531.

46. Criddle CS, Alvarez LA, McCarty PL (1991) Microbial processes in porous media. In: Bear J, Corapcioglu MY, editors. Transport Processes in Porous Media. the Netherlands: Kluwer Academic Publishers. pp. 639-691.

47. Baker SC, Ferguson SJ, Ludwig B, Page MD, Richter OMH, et al. (1998) Molecular genetics of the genus *Paracoccus*: Metabolically versatile bacteria with bioenergetic flexibility. Microbiology and Molecular Biology Reviews 62: 1046-1078.

48. Preisig O, Zufferey R, ThonyMeyer L, Appleby CA, Hennecke H (1996) A high-affinity cbb_3-type cytochrome oxidase terminates the symbiosis-specific respiratory chain of *Bradyrhizobium japonicum*. Journal of Bacteriology 178: 1532-1538.

49. Lin WC, Coppi MV, Lovley DR (2004) *Geobacter sulfurreducens* can grow with oxygen as a terminal electron acceptor. Applied and Environmental Microbiology 70: 2525-2528.

50. Krekeler D, Teske A, Cypionka H (1998) Strategies of sulfate-reducing bacteria to escape oxygen stress in a cyanobacterial mat. FEMS Microbiology Ecology 25: 89-96.

51. Lobo SAL, Melo AMP, Carita JN, Teixeira M, Saraiva LM (2007) The anaerobe *Desulfovibrio desulfuricans* ATCC 27774 grows at nearly atmospheric oxygen levels. FEBS Letters 581: 433-436.

52. Pereira PM, He Q, Xavier AV, Zhou JZ, Periera IAC, et al. (2008) Transcriptional response of *Desulfovibrio vulgaris* Hildenborough to oxidative stress mimicking environmental conditions. Archives of Microbiology 189: 451-461.

53. Fournier M, Aubert C, Dermoun Z, Durand MC, Moinier D, et al. (2006) Response of the anaerobe *Desulfovibrio vulgaris* Hildenborough to oxidative conditions: Proteome and transcript analysis. Biochimie 88: 85-94.

54. Santana M (2008) Presence and expression of terminal oxygen reductases in strictly anaerobic sulfate-reducing bacteria isolated from salt-marsh sediments. Anaerobe 14: 145-156.

55. Zhang WW, Culley DE, Hogan M, Vitiritti L, Brockman FJ (2006) Oxidative stress and heat-shock responses in *Desulfovibrio vulgaris* by genome-wide transcriptomic analysis. Antonie Van Leeuwenhoek International Journal of General and Molecular Microbiology 90: 41-55.

56. Mukhopadhyay A, Redding AM, Joachimiak MP, Arkin AP, Borglin SE, et al. (2007) Cell-wide responses to low-oxygen exposure in *Desulfovibrio vulgaris* Hildenborough. Journal of Bacteriology 189: 5996-6010.

57. McCarty PL (1988) Bioengineering Issues Related to In Situ Remediation of Contaminated Soils and Groundwater. In: Omenn GS, editor. Environmental Biotechnology: Reducing Risks from Environmental Chemicals through Biotechnology. New York and London: Plenum Press.

58. Löffler FE, Tiedje JM, Sanford RA (1999) Fraction of electrons consumed in electron acceptor reduction and hydrogen thresholds as indicators of halorepiratory physiology. Applied and Environmental Microbiology 65: 4049-4056.

59. Childers SE, Ciufo S, Lovley DR (2002) *Geobacter metallireducens* accesses insoluble Fe(III) oxide by chemotaxis. Nature 416: 767-769.

60. Sung Y, Fletcher KF, Ritalaliti KM, Apkarian RP, Ramos-Hernandez N, et al. (2006) *Geobacter lovleyi* sp nov strain SZ, a novel metal-reducing and tetrachloroethene-dechlorinating bacterium. Applied and Environmental Microbiology 72: 2775-2782.

61. Stein LY, La Duc MT, Grundl TJ, Nealson KH (2001) Bacterial and archaeal populations associated with freshwater ferromanganous micronodules and sediments. Environmental Microbiology 3: 10-18.

62. Cummings DE, Snoeyenbos-West OL, Newby DT, Niggemyer AM, Lovley DR, et al. (2003) Diversity of *Geobacteraceae* species inhabiting metal-polluted freshwater lake sediments ascertained by 16S rDNA analyses. Microbial Ecology 46: 257-269.

63. Weber KA, Urrutia MM, Churchill PF, Kukkadapu RK, Roden EE (2006) Anaerobic redox cycling of iron by freshwater sediment microorganisms. Environmental Microbiology 8: 100-113.

64. Hutchinson GE (1961) The paradox of the plankton. American Naturalist 95: 137-145.

CHAPTER 6: Changes in genotype, substrate usage, and growth rate among closely-related *Anaeromyxobacter* isolates from pristine and radionuclide-impacted soil environments

6.1 Abstract

Anaeromyxobacter dehalogenans isolates derived from a radionuclide-impacted subsurface were characterized, and compared to those derived from pristine agricultural and riverine samples. Culture-dependent and molecular analyses revealed genetic and metabolic diversity among closely related strains. The isolates shared >99% overall 16S rRNA gene sequence identity but clustered into five groups (clades A-E) based on a detailed analysis of the highly variable V3 region. A comparative analysis of genetic characteristics reflected the phylogenetic clustering.

At least two new genotypes of *A. dehalogenans* were isolated from the Oak Ridge Integrated Field-scale Research Challenge site, with one falling into an existing genotype, and two isolates that each described new genotypes. Additionally, the two new isolates from an agricultural soil and a riverine environment represent a distinct phylotype together. Culture-based techniques were utilized to compare growth rates and substrate utilization ranges, and determine optimal culturing conditions. Core physiological properties were not substantially different among phylogenetic clusters with average doubling times ranging between 12.5 and 16.5 hours and temperature and pH optima of 35°C and 7.0. Members of the cluster designated clade A demonstrated a particularly wide pH range (pH 5-8) and grew well at temperatures as high as 40°C. Loss of specific functions including reductive dehalogenation and nitrous oxide reduction was observed.

These data accentuate the importance of characterizing multiple isolates when describing bacterial clades and emphasize the need for cultured representatives to fully determine a species' physiological capabilities. In addition, this study contributes to the issue of speciation in bacteria.

6.2 Introduction

The phenotypic diversity within bacterial species (i.e., strain diversity) that inhabit soil, sediment and subsurface environments remains poorly understood. Studies with pathogenic bacterial species have demonstrated substantial phenotypic diversity patterns among closely related strains [1,2,3,4,5]. For example, clones of *S. aureus* have been found to harmlessly colonize the nose of 20% of the human population [6], but, since dramatic changes in infection phenotype occur over relatively short evolutionary time, potential for virulence can be difficult to determine genetically [7]. Intra-species variability among environmental purple nonsulfur bacterial isolates are an example of strain-level variation in a non-pathogenic organism [8]. Genomic fingerprinting divided *Rhodopseudomonas palustris* strains into four major genotypes, which were accompanied by phenotypic differences, including the absence of benzoate utilization in some strains [9]. Physiological changes like those observed among *S. aureus* and *R. palustris* strains can have substantial implications for environmental nutrient cycling, including contaminant degradation. For example, *Dehalococcoides* spp. are chlororespiring organisms with varying chloroethene-utilization patterns within a single species group that shares a single indistinguishable 16S rRNA gene sequences [10]. In addition, intra-specific metabolic variability has been explored in a thermophilic, metal-reducing

population and demonstrated different electron donor utilization patterns among *Thermoanaerobacter* strains [11]. *Anaeromyxobacter dehalogenans* strains have been implicated in metal and radionuclide reduction but the impact of strain variations on function (e.g., metal reduction and immobilization) has not been evaluated.

Anaeromyxobacter represents the first myxobacterial genus capable of anaerobic metabolism, and representatives of the genus have been identified in soil, sediment, and subsurface environments, many of which are characterized by fluctuating redox conditions; such as rice fields, wetland sediments, peat bogs and contaminated groundwater environments [12,13,14,15,16,17,18,19,20]. The *Anaeromyxobacter* genus comprises metabolically versatile microaerophilic soil bacteria that are capable of anaerobic respiration of several ortho-substituted mono-and dihalogenated phenols, nitrate, nitrite, nitrous oxide, fumarate, AQDS, managanese (IV), uranium (VI), technetium, and ferric iron ([21,22,23,24,25,26]; unpublished data). Respiratory versatility by *Anaeromyxobacter* spp. potentially influences nitrogen, carbon and metal cycling in the environment, including the conversion of soluble U(VI) and Tc(VII) to relatively insoluble U(IV) and Tc(IV), respectively [26] and the anaerobic biodegradation of halogenated phenolic compounds, including pesticides (this study). Three phylogenetically distinct representatives have been isolated within the genus *Anaeromyxobacter*, including the only described species *A. dehalogenans* [21] and isolates Myxobacterium KC [16], and *Anaeromyxobacter* st. Fw109-5 (Matthew Fields; personal communication), each of which represents a 16S rRNA gene sequence indicative of a new species.

Several different *A. dehalogenans* strains with slight variations in 16S rRNA gene sequence have been isolated and cultured from diverse environmental samples, mostly pristine environments [13,21,23]. Additional isolates were derived from agricultural soils and contaminated subsurface environments ([13]; this study). The role of environmental factors in shaping *Anaeromyxobacter* phenotypes is unclear. The Oak Ridge Integrated Field-scale Research Challenge (IFC) site is contaminated with high concentrations of nitrate and uranium and has been shown to contain *Anaeromyxobacter* spp. including *A. dehalogenans* [12,18,27,28]. As an organism which, based on previous characterizations, has the potential to play roles in nitrogen, carbon and metal-cycling at the Oak Ridge IFC site, the physiology of native *A. dehalogenans* strains has substantial implications. Molecular tools for monitoring *A. dehalogenans* have been designed and used but knowledge of strain diversity is crucial to draw meaningful conclusions [29]. The current study characterizes differences between closely related *Anaeromyxobacter dehalogenans* strains (based on 16S rRNA gene sequence identity) isolated from the Oak Ridge IFC, agricultural soils and pristine river sediments.

6.3 Materials and Methods

6.3.1 Source of* A. dehalogenans *isolates. Strains FRC-D1, D3, R5, and R8 were isolated from FeOOH-enrichments derived from microcosms established with material collected from the Oak Ridge Integrated Field-scale Research Challenge (IFC) site in Area 1 (wells FW030 and FW032). Soil cores for microcosm setup were collected prior to the onset of push-pull experiments and were not impacted by biostimulation treatment with electron donor [18]. Isolation of pure cultures from the FeOOH

enrichments proceeded through serial transfers of ferric iron-reducing cultures in mineral salts medium [30] amended with 5 mM acetate and 4 mM (nominal concentration) FeOOH followed by dilution to extinction in 0.6% (w/vol) low melting agarose medium amended with 5 mM acetate and 10 mM fumarate. Isolated colonies were recovered from these agar shakes using sterile syringes and needles following a described protocol [31] and transferred to fresh medium containing 5 mM acetate and 5 mM ferric citrate. The dilution-to-extinction procedure in semi-solid medium was repeated at least twice to obtain pure cultures.

Strain FRC-W was isolated from a 2-chlorophenol (2-CP) enrichment culture derived from sediment from well FW034 (Area 1 at the Oak Ridge IFC site). 2-CP-dechlorinating isolates were obtained by picking colonies from mineral salts agar shakes, amended with 5 mM acetate and 10 mM fumarate, and transferring them to liquid medium with 2-CP and acetate to verify dechlorination activity. Purity of 2-CP-dechlorinating cultures was established by three consecutive transfers of homogeneous colonies after anaerobic growth in acetate/fumarate-amended agar shakes.

Strains R and K were isolated from 2,6-dichlorophenol enrichment cultures seeded with Illinois agricultural soil and Korean river sediment, respectively. When reductive dechlorination was observed, enrichments were streaked onto Difco™ R2A agar (Becton, Dickinson, and Company, Sparks, MD) plates supplemented with 2 mM acetate and 10 mM fumarate. Plates were incubated anaerobically at 30° C. Individual red colonies, color associated with previous *Anaeromyxobacter* cultures [21], were picked from each plate when growth had been observed and transferred to anaerobic broth medium (see below) containing acetate and 2,6-DCP. Actively dechlorinating

cultures were subjected again to isolation via colony growth on R2A agar plus fumarate plates.

6.3.2 Growth conditions. *Anaeromyxobacter dehalogenans* strains FRC-D1, FRC-D3, FRC-R5, FRC-R8, FRC-W, K and R were routinely grown with 2-5 mM acetate and either 1 mM nitrate or 10 mM fumarate in 26-ml anaerobic culture tubes (Balch tubes) containing 15 ml of anoxic, bicarbonate-buffered mineral salts medium as described previously [30] except that concentration of ammonium was reduced from 5.61 mM to 2 mM and, in some cases, sulfide was omitted. The bottles were closed with butyl rubber stoppers and aluminum crimp caps. The headspace of culture vessels consisted of nitrogen gas balanced with carbon dioxide to adjust the pH to 7.1 (about 80:20 N_2:CO_2 [vol/vol]). Triplicate culture vessels were incubated at 30° or 35°C.

6.3.3 Phylogenetic analysis. Genomic DNA was obtained from Fe(III)/acetate- or nitrate/acetate-grown cultures and extracted with a QIAamp DNA mini kit (QIAGEN, Santa Clarita, CA). 16S rRNA genes were PCR-amplified using a universal bacterial primer pair (8F and 1525R) and 50 ng of genomic DNA as template, and sequenced as described [32,33]. Related 16S rRNA gene sequences from cultured organisms and environmental clone sequences were identified by NCBI Basic Local Alignment Search Tool (BLAST) [34] analysis and obtained from GenBank (http://www.ncbi.nlm.nih.gov/Genbank/index.html). Distance matrices and phylogenetic trees were generated following 16S rRNA gene sequence alignment using the MegAlign program of the Lasergene software package (DNA Star Inc., Madison, MI). Bootstrap values were calculated with the MEGA software program for 1,000 replicates [35]. The nearly complete 16S rRNA gene sequences (~1,470 bp) of the *Anaeromyxobacter*

dehalogenans strains have been deposited in GenBank under the following accession numbers: strain R — EU331403, strain K — (JGI genome ABHX00000000), strain FRC-D1 — FJ190048, strain FRC-D3 —FJ190049, strain FRC-R5 — FJ190057, strain FRC-R8 — FJ190060, strain FRC-W — FJ190062.

6.3.4 REP-PCR. Repetitive extragenic palindromic (REP)-PCR was applied to fingerprint and differentiate strains. DNA was extracted from 10 ml of fresh liquid cultures using the QIAGEN Genomic-tip 100/G (Valencia, CA). The REP-PCR and electrophoresis were performed as described [36]. REP primers REP1R-I, 5'-IIIICGICGICATCIGGC-3', and REP2-I, 5'-ICGICTTATCIGGCCTAC-3' were mixed with approximately 60 ng of purified DNA in PCR reactions containing 5 µl of 5X Gitschier Buffer, 0.2 µL of 20 mg mL^{-1} BSA, 2.5 µL of 100% DMSO (Sigma, Saint Louis, MO), 1.25 µL of 25 mM-Mix (1:1:1:1), volume of each primer stock to achieve final concentrations of 50 pmol μL^{-1}, 2 units of Taq polymerase, and water to bring the total volume to 25 µL. The PCR reactions were performed on a GeneAmp® PCR System 9700 (Applied Biosystems, Foster City, CA) under the following conditions: 95 °C for 2 min, 94 °C for 3 s, then 35 cycles of 92 °C for 30 s, 40 °C for 1 min and 65 °C for 8 min, with a final extension step of 65 °C for 8 min. A 12 µL aliquot of PCR products were resolved on a 2% agarose gel made with 1x TAE buffer and run for 2 hrs at 85 V. The 1Kb Plus DNA ladder (Invitrogen, CA) was used as marker for lane/size normalization. Gels were soaked in ethidium bromide solution (1µg mL^{-1}) and exposed to UV light. Images were captured using the Gel-Doc software (Bio-Rad, Hercules, CA).

6.3.5 Design and application of primers targeting functional genes. Primers for amplifying the *rdhA* gene in *A. dehalogenans* strain 2CP-C were designed using IDT

DNA Primer Quest primer selection tool (http://www.idtdna.com/Scitools/Applications/Primerquest/; Integrated DNA Technologies, Inc., Coralville, IA). Primer sequences were checked for specificity using BLAST. Degenerate primers were designed to amplify the *nosZ* gene of *A. dehalogenans* strain 2CP-C as well as other non-denitrifying organisms as described [37]. For the current study, degeneracies were eliminated and general primers were selected based on a gene alignment of *nosZ* gene sequences from all four *Anaeromyxobacter* spp. with sequenced genomes (Accession numbers: CP001131, CP000769, CP000251, ABKC00000000). Primers rtAn1F (5'-ACCTGAAGTACGTCATCCAGCTCT-3') and rtAn1R (3'-TCGATGTTCTCGTAGTTCATGCCG-5') targeting the *rdhA*1 gene of *Anaeromyxobacter dehalogenans* strain 2CP-C (Locus ID: Adeh_0331) were used with the following temperature program: 3:00 min at 95^{o}C followed by 30 cycles of (0:30 at 94^{o}C; 0:30 at 60.0^{o}C; 0:45 at 72^{o}C), and a final step of 3:00 at 72^{o}C. Primers 912F (5'-CGT CCC CGG CCT CGT GTA-3') and 1853R (5'-GAG CAG AAG TTC GTG CAG TAG TAG GG-3') targeting the *nosZ* gene of the four sequenced *Anaeromyxobacter dehalogenans* strains (Accession numbers: CP001131, CP000769, CP000251, ABKC00000000) were used in PCR as described previously [37]. The following temperature program was used: 5:00 min at 94°C, followed by 35 cycles of (0:30 at 94 °C, 0:45 at 60°C, and 2:00 at 72°C), and a final step of 10:00 at 72°C. PCR was performed in total reaction volumes of 20 µl with 2 µl of 10x reaction PCR buffer (Applied Biosystems), 250 µM of each deoxynucleoside triphosphate (Applied Biosystems), 100 nM concentration of each primer, 13 µg of bovine serum albumin (Boehringer Mannheim) and 1- 5 ng of template DNA. PCR was carried out in a

GeneAmp 9700 PCR system (Applied Biosystems). Fragments were resolved in 1-1.5% Metaphor agarose (FMC Bioproducts, Rockland, ME) gels using fresh TAE buffer (40 mM Tris base in 20 mM acetic acid, 1 mM EDTA, pH 8.5) at 4°C and stained with ethidium bromide (1 μg mL^{-1}).

6.3.6 Physiological characterization.

6.3.6.1 Growth rate. Growth rate of all strains was determined usingmineral salts medium, as described above, in 26 mL Balch tubes with 5 mM acetate as electron donor and 10 mM fumarate as electron acceptor. Growth was measured as optical density at 600 nm using a Spectronic 20D spectrophotometer (Milton Roy Company). Nonlinear regression analysis was performed using GraphPad Prism 5 software.

6.3.6.2 Electron donors. The ability of new isolates of *A. dehalogenans* to oxidize alternative substrates was determined with triplicate tubes amended with 1 mM nitrate and the following electron donors: formate (2 mM), lactate (2 mM), succinate (2 mM), pyruvate (2 mM), glucose (2 mM), and hydrogen (82 μmol). Electron donor oxidation was measured by its consumption and/or the reduction of nitrate to that of control cultures that received no electron donor. All culture tubes received 2% inoculum from acetate-nitrate-grown cultures that had consumed all acetate.

6.3.6.3 Electron acceptors. Electron acceptor utilization was evaluated in anaerobic medium containing 1-2 mM acetate (and/or 82 μmoles H_2). The following compounds were tested: nitrate (1 mM), nitrite (1 mM), O_2 (105 μmoles/tube; 0.160 atm), AQDS (0.5 mM), ferric citrate (5 mM), hydrous ferric oxide (HFO, 5 mM), lepidocrosite (5 mM), goethite (5 mM), MnO_2 (5 mM), uranyl carbonate (200 μM), 2-chlorophenol (100 μM), 2,6-dichlorophenol (100 μM), fumarate (10 mM), bromoxynil (50 μM), 2,4-

dichlorophenoxy acetic acid (2,4-D, 100μM), atrazine (50 μM), Dicamba (50 μM), and nitrous oxide (N_2O, 15 μmoles/tube). All culture tubes received 2% inocula from either an acetate-nitrate-grown culture that had consumed all nitrate and nitrite except for the herbicide-amended tubes, which were inoculated from a 2,6-DCP-grown culture. Electron acceptor reduction was measured by monitoring its consumption and/or the oxidation of acetate or H_2. Data were compared to those obtained with control cultures that received no electron acceptor.

6.3.6.4 Temperature and pH optima. To test effect of temperature on growth, triplicate culture vessels were incubated at 4, 9, 22, 30, 35, and 40°C. Effect of pH on growth was tested in mineral salts medium prepared with different buffer systems: 20 mM MES [2-(N-morpholino) ethanesulfonic acid] (pH 5, 6, and 6.5 adjusted with concentrated HCl or 10 M NaOH prior to inoculation), 20 mM bicarbonate (pH 7, 7.5, and 8). All vials were amended with 1 mM Acetate and 1 mM nitrate as substrates and received 2% (vol/vol) inocula from acetate/nitrate-grown cultures. Growth was monitored by optical density measurements at 600 nm using a Spectronic 20D spectrophotometer (Milton Roy Co. Rochester, NY).

6.3.7 Analytical procedures. The decrease of Mn(VI) was monitored spectrophotometrically as described [38]. U(VI) was determined by a modified laser-excitation spectrofluorescence method described [25]. Nitrate and nitrite were quantified with a Dionex ICS-3000 ion chromatograph (Dionex Corp., Sunnyvale, CA) equipped with a Dionex AS14 IonPac column. Fe(II) was analyzed using the ferrozine assay following HCl extraction [39,40,41]. Formate, lactate, succinate, succinate were monitored by HPLC with a Waters Breeze system equipped with a Waters 2487 dual-

wavelength absorbance detector set at 210 nm and a Waters 717 plus autosampler (20 µl injection volume) as described [42]. Halophenols and herbicides were measured using a Schimadzu HPLC with a Prevail C18 column. A methanol/phosphoric acid eluent was used as previously described. Nitrous oxide analyses were done using an SRI GC with a packed column and TCD detector with He as the carrier gas.

6.3.8 Statistical analysis. All significance tests, regression analyses, and 95% confidence intervals were performed using GraphPad Prism 5 with default settings. The average slope and y-intercept of each growth curve were determined by non-linear regression analysis. Non-linear regression analysis was used to determine whether the standard curves generated for the nine strains could be assigned global growth rate values. Samples for growth curve analysis were performed in triplicate. The symbols and error bars for growth curve analyses, thus, represent the averages of three data points and standard deviations of three replicate culture data points per time point.

6.4 Results

For all isolates described in this study, *A. dehalogenans* strains resulted from colonies identified based on their distinctive red color, when grown with fumarate as electron acceptor. Agricultural soil- and river sediment-derived dechlorinating cultures transferred to R2A plates amended with acetate and fumarate produced red colonies. Strain R and K cultures resulted from red colonies that were tested for dechlorination ability by transferring them to anaerobic broth medium with acetate and 2,6-DCP. Both strains showed stoichiometric reduction of DCP to phenol. Red colonies were also produced when iron and DCP-enrichments were derived from Oak Ridge IFC site

materials and incubated in fumarate-amended dilution series vials containing soft agar. These red colonies resumed iron-reduction and dechlorination activity when transferred back to liquid culture. In all cases, additional solid matrix (plates or soft agar vials) transfers produced additional red colonies.

6.4.1 Genetic analysis. Based on 16S rRNA gene sequence similarity alone, all *A. dehalogenans* isolate sequences included in this analysis shared greater than 99% identity, justifying inclusion in a single bacterial species (Figure 6.1). Alignment of nearly complete (1,470 bp) 16S rRNA genes supports phylogenetic distinctions between *A. dehalogenans* isolates derived from diverse environmental samples (Figure 6.1). The alignment-based clustering pattern is supported by comparisons between 16S rRNA gene sequences at the V3 hypervariable region between positions 460 and 479 (Figure 6.2). Additional genetic data corroborated the division of *A. dehalogenans* into five clades. REP-PCR genomic fingerprints of each strain are shown in Figure 6.3. Unique fingerprints were obtained for all nine isolates but similarities (i.e., DNA fragments of similar size) were shared among isolates of the same clade, as established by 16S rRNA gene sequence analysis. Clade A contains the new strains R and K, enriched with acetate and chlorophenol from agricultural soil and river sediment, respectively. These strains join the previously isolated strain FAc12 (enriched as an iron reducer from rice-paddy soil) [13]. Clade C includes the new strains FRC-D1 and FRC-D3, which were obtained from iron-reducing enrichment cultures derived from microcosms established with uranium and nitrate contaminated material. Under similar enrichment conditions, representatives of Clade D, strains FRC-R5 and FRC-R8, were obtained from Oak Ridge IFC Area 1 site materials. Clade E includes the previously characterized strains 2CP-C

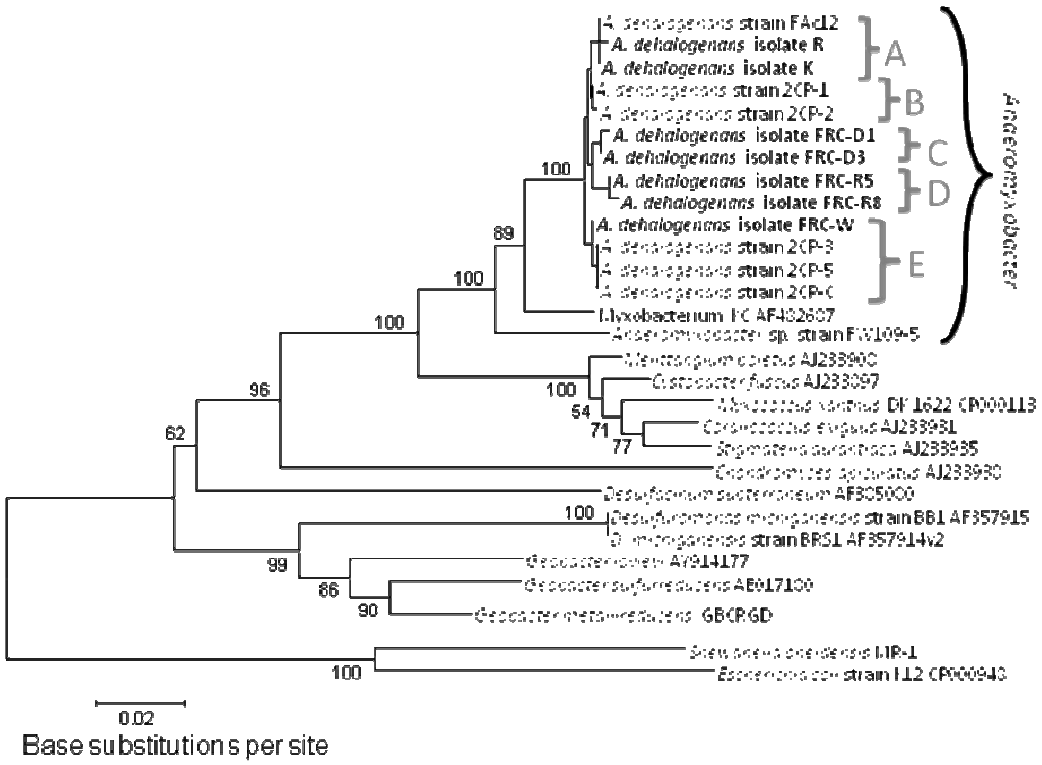

Figure 6.1. Phylogenetic tree of environmental isolates based on nearly complete alignment of 16S rRNA genes. *A. dehalogenans* strains described in this study are shown in bold print. Letters indicate *A. dehalogenans* clades differentiated based on 16S rRNA differences.

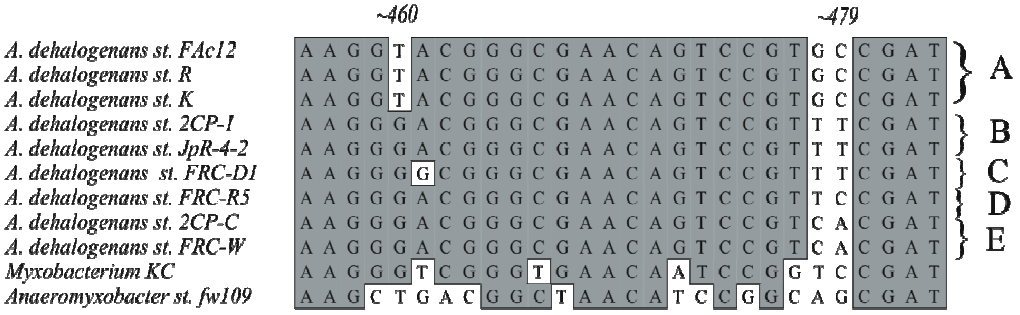

Figure 6.2. Highly variable region in 16S rRNA sequences of different *A. dehalogenans* isolates. Letters to the side of the rows indicate population clades of *A. dehalogenans* as designated in Figure 6.1. Each clade retains a signature sequence in this region.

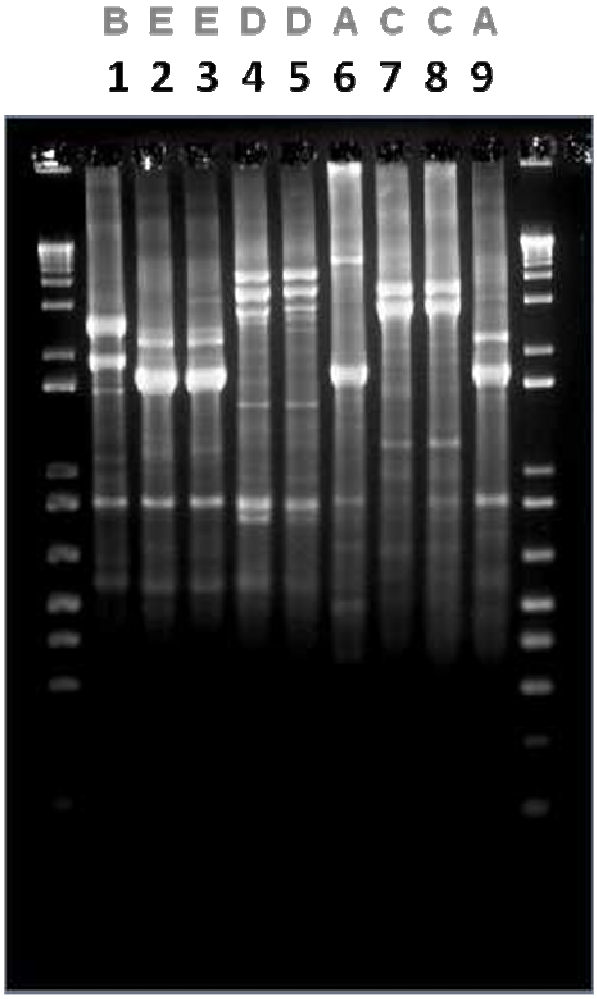

Figure 6.3. REP-PCR profiles of nine environmental *A. dehalogenans* isolates (lane 1. 2CP-1, lane 2. 2CP-C, lane 3. FRC-W, lane 4. FRC-R5, lane 5. FRC-R8, lane 6. R, lane 7. FRC-D3, lane 8. FRC-D1, lane 9. K). Letters above columns indicate population clades of *A. dehalogenans* as designated in Figure 6.1.

and 2CP-3, both enriched on acetate and chlorophenol, as well as strain FRC-W, which was also enriched on chlorophenol and isolated from the uranium and nitrate contaminated groundwater where members of Clade C and D were obtained.

Since the originally characterized *A. dehalogenans* strains 2CP-1 and 2CP-C respire halophenols, and a putative gene coding for reductive dehalogenation (*rdhA*) has been identified [43,44], investigation for a similar gene in the new isolates was conducted. Five out of seven analyzed strains (FRC-R5, FRC-R8, FRC-W, strain R, and strain K) contained a gene with sequence similarity to the *rdhA* gene in *A. dehalogenans* strain 2CP-C (Figure 6.4). The analysis of the strain K genome (AnaeK_0343; Genome accession number CP001131) confirmed the presence of this gene. No *rdhA* gene was detected in clade C representatives (strains FRC-D1 and FRC-D3). Physiological tests confirmed the lack of dechlorination activity in strains FRC-D1 and FRC-D3 (see below).

In probing the genome of *A. dehalogenans* strain 2CP-C, a novel nitrous oxide reductase gene (*nosZ*) was identified [37]. We have confirmed the ability of strain 2CP-C to reduce nitrous oxide and designed degenerate and non-degenerate PCR primers specific for detection of the *nosZ* in other related bacterial populations [37]. Results show that an *Anaeromyxobacter*-type *nosZ* homologous gene occurs in representatives of clades A, B, and E but not in either clades C or D (Figure 6.5). Physiological tests also confirmed the lack of nitrous oxide reduction activity in clade C and D representatives from (see below).

6.4.2 Physiological tests. Growth rate measurements suggested that optimal growth for all isolates, as indicated by the time to reach maximum optical density (absorbance at 600 nm = 0.18 ± 0.04), occurred at 35°C and pH 7, but, members of clade A grew equally

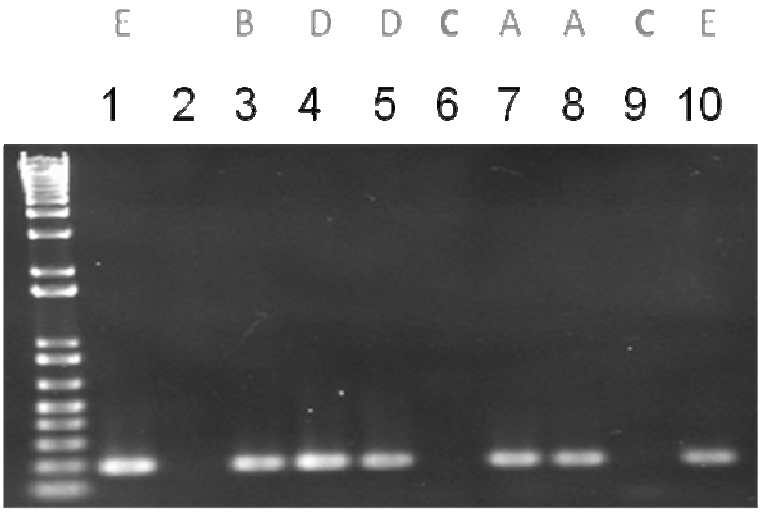

Figure 6.4. PCR detection of reductive dehalogenase (*rdhA1)* gene in new *A. dehalogenans* strains (lane 1. 2CP-C, lane 2. water, lane 3. 2CP-1, lane 4. FRC-R5, lane 5. FRC-R8, lane 6. FRC-D3, lane 7. R, lane 8. K, lane 9. FRC-D1, lane 10. FRC-W). Primers were designed based on the gene present in *A. dehalogenans* strain 2CP-C. Letters above columns indicate population clades of *A. dehalogenans* as designated in Figure 6.1.

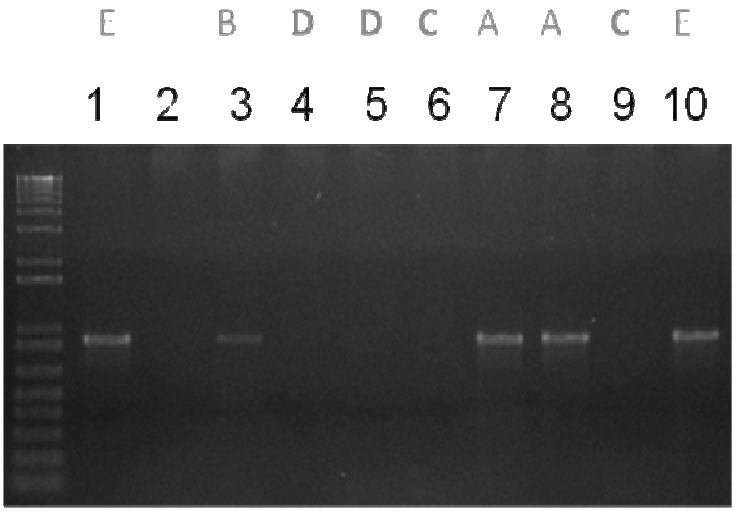

Figure 6.5. PCR detection of nitrous oxide reductase (nosZ) gene in new *A. dehalogenans* strains (lane 1. 2CP-C, lane 2. water, lane 3. 2CP-1, lane 4. FRC-R5, lane 5. FRC-R8, lane 6. FRC-D3, lane 7. R, lane 8. K, lane 9. FRC-D1, lane 10. FRC-W). Primers were designed based on the gene present in *A. dehalogenans* strains 2CP-C, 2CP-1, and K. Letters above columns indicate population clades of *A. dehalogenans* as designated in Figure 1.

well at 40°C (Tables 6.1 and 6.2). Growth occurred at 22° and 30°C (pH 7.0) in all clades while no growth occurred for any strain at 9° C or 4° C, even after 50 days of incubation (Table 6.2). pH range for growth at 35°C varies with different isolates (Table 6.1). Growth rates for clade A isolates were optimal between pH 7 and 8, reaching maximal optical density between 2 and 2.3 days, but growth was observed at pH 5 (between 23 and 50 days). The other clades tested exhibited little tolerance for pH variability and a narrower pH range of optimal growth (pH 7.0 – 7.5). A noticeable increase in the time to reach maximal density occurs from pH 7.5-8.0, increasing from 2.0 to 3.0 days in cultures representing narrow pH range clades. Nonlinear regressions calculated based on the exponential growth equation (Figure 6.6; $N = N_{0*}e^{kt}$) demonstrated that strains' doubling times all range between 12.3 and 13.9 hours except for strain 2CP-1, whose 15.3 hour doubling time is more than an hour greater than any other strain (Table 6.3). The fastest-growing strain, based on fumarate growth data, was strain K, but doubling times were not statistically different, based on 95% confidence intervals. All strains have statistically similar doubling times with a global growth rate constant (k) of 0.053 ± 0.001 and 95% confidence interval of doubling time between 12.7 and 13.6 hours (Table 6.3).

Substrate consumption analyses revealed few differences for electron donor utilization capacities. All isolates used acetate, formate, lactate, pyruvate, succinate, and H_2 as electron donors to reduce nitrate (Table 6.4). Nitrate reduction was also supported by glucose in cultures of isolates FRC-R5, FRC-R8, and FRC-W but not of isolates FRC-D1, FRC-D3, K and R. Fermentative glucose utilization in the absence of a suitable electron acceptor was not observed in any of the cultures.

Table 6.1. Days to reach maximal OD of *Anaeromyxobacter* strains at different pHs

	pH[a]					
Isolate (Clade)	**5**	**6**	**6.5**	**7**	**7.5**	**8**
strain K (A)	22	15	7.3	2	2.3	2.3
strain R (A)	50	15	7.3	2	2.3	2.3
FRC-D1 (C)	-[b]	21	15	2	2	3
FRC-D3 (C)	-	-	14	2	2	3
FRC-R5 (D)	-	30	14	2.1	2.1	3
FRC-R8 (D)	-	28	14	2	2	3
FRC-W (E)	-	21	11	2	2	3

[a] Tested with 1 mM nitrate and 5 mM acetate at 35ºC
[b] Represented no growth observed after 71 days of incubation

Table 6.2. Days to reach maximal OD of *Anaeromyxobacter* strains at different temperatures.

	Temperature (ºC)[a]					
Isolate	**4**	**9**	**22**	**30**	**35**	**40**
strain K (A)	-	-	7.1	3.3	2.1	2.1
strain R (A)	-	-	7.1	3	2.1	2.1
FRC-D1 (C)	-[b]	-	7.1	4	2.3	3.3
FRC-D3 (C)	-	-	7.1	4	2.3	3.3
FRC-R5 (D)	-	-	7.1	3.3	2.1	3.3
FRC-R8 (D)	-	-	7.1	3.3	2.1	3.3
FRC-W (E)	-	-	7.1	3	2	2.3

[a] Tested with 1 mM nitrate and 5 mM acetate at pH~7.2.
[b] Represents no growth observed after 50 days of incubation

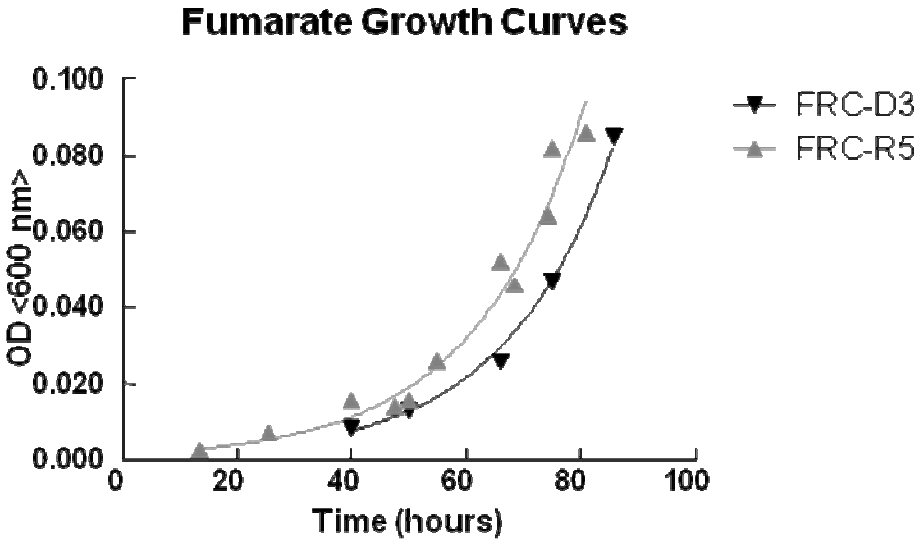

Figure 6.6. Fumarate growth curves for two representative strains. Exponential region of growth curves are shown for cultures grown on mineral salts medium amended with 5 mM acetate and 10 mM fumarate.

Table 6.3. Growth rate constant and doubling times of fumarate grown *A. dehalogenans* strains.

Isolate (Clade)	Growth rate constant (k)	Doubling Time (hours)[b]
strain R (A)	0.052	13.4 (11.3-16.5)
strain K (A)	0.054	12.8 (10.8-15.7)
2CP-1 (B)	0.042	16.5 (14.7 - 18.9)[c]
FRC-D1 (C)	0.051	13.7 (12.3-15.3)
FRC-D3 (C)	0.0553	12.5 (11.3-14.1)[c]
FRC-R5 (D)	0.048	14.5 (12.3-17.7)
FRC-R8 (D)	0.053	13.1 (12.2-14.3)[c]
FRC-W (E)	0.053	13.0 (11.2-15.5)
2CP-C (E)	0.047	14.7 (11.9-19.2)
Global[a]	**0.053**	**13.2 (12.7-13.6)**

[a] Global growth rate could be calculated for all 9 data sets (p=0.21).
[b] 95% confidence interval is given in parentheses for doubling time.
[c] Doubling time of strain 2CP-1 is significantly different from strains FRC-D3 and FRC-R8.

Table 6.4. Use of different electron donors by *A. dehalogenans* clades with nitrate (1 mM) as the electron acceptor.

Electron donor	Clade A (Strain K)	B (2CP-1)	C (FRC-D1)	D (FRC-R5)	E (FRC-W)
Acetate	+	+ [a]	+	+	+
Formate	+	+ [a]	-	-	+
Lactate	+	(+) [a]	+	+	+
Pyruvate	+	+ [a]	+	(+)	+
Succinate	+	+ [a]	+	+	+
H_2	+	+	+	+	+
Glucose	-	ND	-	+	+
AH_2QDS	ND	ND	-	-	ND

+ = Utilized for growth
(+) = Less growth than with other donors
- = No metabolic activity detected
ND = Not determined
[a] From (Sanford et al., 2002)

Of the experiments in this study, electron acceptor utilization experiments revealed the most diversity among strains. All isolates showed Mn(IV) and U(VI) reduction with acetate as electron donor, but reductive dehalogenation of 2-chlorophenol was not observed in cultures of FRC-D1 and FRC-D3 belonging to clade C (Table 6.5). This is consistent with PCR results indicating that strains FRC-D1 and FRC-D3 do not contain *rdhA*. In addition, only three of the five clades demonstrated reduction of nitrous oxide, consistent with PCR results indicating that representatives of Clades C and D did not possess a gene which can be amplified with *A. dehalogenans*-specific *nosZ*-targeted genes. All clades demonstrated microaerophilic oxygen reduction.

6.5 Discussion

Despite enriching and isolating from contaminated and pristine soil, sediment, and aquifer materials under either ferric iron- or halophenol-respiring conditions, the new *Anaeromyxobacter* strains obtained are remarkably similar phylogenetically (Figure 6.1). Agricultural soil isolates fell into three of the five clades (A, B and E), Oak Ridge IFC isolates fell into three of the five clades (C, D, and E), and river sediment isolates fell into two clades (A and B). No new members of Clade B were isolated, which contains the previously isolated strain 2CP-1 (*A. dehalogenans* type strain) and strain JpR-4-2 (Accession number EF067314). Clade designations suggest no clear correlation between geographical location and clade, which points toward the ecological speciation model, in which small-scale environmental heterogeneity and niche differentiation define species, as opposed to geographic barriers (i.e., allopatric speciation) [45]. Similarities among

Table 6.5. Use of different electron acceptors by *A. dehalogenans* clades with acetate (1-2 mM) as the electron donor.

Electron acceptor	Clade A (Strain K)	B (2CP-1)	C (FRC-D1)	D (FRC-R5)	E (FRC-W)
O_2	+	+	+	+	+
$N_2O \rightarrow N_2$	++	++	-	-	++
$NO_3^- \rightarrow NO_2^-$	+++	+++	+++	+++	+++
$NO_2^- \rightarrow NH_4^+$	+++	+++	+++	-	+++
Mn (IV)	+++	+++	++	+++	+++
AQDS	++	++	++	++	++
U (VI) [b]	++	++	++	++	++
Fumarate	++	++	++	++	++
Halophenols and Herbicides					
2-CP	++	++	-	++	++
2,6-DCP	++	++	-	++	++
2,4-D	-	-	ND	-	-
Bromoxynil	+/-	+/-	ND	+/-	+/-
Dicamba	-	-	ND	-	-
Atrazine	-	-	ND	-	-
Fe (III)					
Ferric citrate	+++	+++	+++	+++	+++
HFO	++	++	++	++	++
Lepidocrosite	++	++	++	++	++
Goethite	+	+	+	+	+

+++ = very fast reduction
++ = moderately fast reduction
+ = reduces electron acceptor
+/- = some reduction observed
- = no reduction
[a] Electron donor for U(VI) test was H_2 gas with acetate as a carbon source.

isolates could also be due to culturing biases other than the ones considered for these analyses (i.e., electron acceptor selection and redox state of the medium). Based on sequence variability in the variable V3 region of the 16S rRNA gene (positions 460-479) [46,47], five clades could be distinguished (Figure 6.2). In this, and other studies, the highly variable V3 region was useful for discriminating strains. The V2 (nucleotides 137-242), V3 (nucleotides 433-497), and V6 (nucleotides 986-1043) regions are most variable and therefore suitable for distinguishing among bacterial strains within the same species (i.e., provide maximum discriminatory power) [48]. Thus, further investigations seeking targets to discriminate bacterial strains in environmental samples may be able to focus on these regions for culture-independent methods involving the 16S rRNA gene but additional data is needed to determine the universality of variation in the V3 region. Genotype data derived from REP-PCR analysis of *A. dehalogenans* strains suggested that genome sequence variation corresponds to variation of the V3 region. The correlation between 16S rRNA gene sequence variability and apparent variability at the genome level is not surprising. Konstantinidis and Tiedje demonstrated that 16S rRNA gene sequence variance and the average amino acid identity, and therefore gene sequence similarity, are often strongly correlated [49]. In fact, the 16S rRNA gene sequence variability was shown to correlate to average nucleotide identity and DNA-DNA reassociation values as well, in most cases [50]. The authors of these studies also stress, that, in some cases, strains of the same species vary up to 30% in gene content. Therefore confirmation of the presence of key functions was important to support genetic data with physiological analyses.

Results from physiological comparisons between closely related *A. dehalogenans* strains indicated that this species possesses a wealth of respiratory capability and presence in a wide variety of environments with distinct geochemical conditions. Physiological comparisons of temperature and pH optima, electron donor utilization, electron acceptor utilization and growth rates revealed considerable similarity among *Anaeromyxobacter* strains (Tables 1-5). A few exceptions are noted. Most remarkably, genetic analyses of the *rdhA* gene in clade C and the *nosZ* gene in representatives of clades C and D corresponded to the inability of these strains to reduce chlorophenol and nitrous oxide, respectively. The correlation between the lack of nitrous oxide reduction and 2-CP dechlorination activity with the absence of a *nosZ* gene or a *rdhA* gene, respectively, suggests that gene deletions/acquisitions have occurred recently in *A. dehalogenans* strains and points to dramatic metabolic shifts that can occur due to small genetic changes. The sequenced genome of *Anaeromyxobacter* sp. FW109-5 (Accession number CP000769) is also missing a gene homologous to *rdhA1*, indicating that this organism also lacks the ability to dechlorinate and suggesting that the *rdhA* genes may be frequently lost in the absence of selective pressure to maintain dechlorination ability such as the abundant chlorinated phenol found in many agricultural soils. Although not confirmed genetically, clade D isolates were also unable to grow by dissimilatory nitrite reduction to ammonium, a characteristic shared by all members of other clades and suggesting that the nitrite reductase gene *nrfA* may be absent in clade D representatives. All electron acceptor analyses were performed with acetate as electron donor and all electron acceptor analyses were performed with nitrate as electron acceptor. Results could vary with different electron donor/acceptor combinations at different initial

concentrations. For example, in the case of uranium reduction, hydrogen is needed for growing cells [24,25], but acetate suffices in resting cell experiments [51]. While growth rates were similar among strains, strain 2CP-1 mean growth rate is lower than other *A. dehalogenans* strains and significantly lower than strains FRC-D3 and FRC-R8. Slower growth of strain 2CP-1 would not be unexpected since this strain only possesses one ribosomal RNA gene on its genome (Accession number ABKC00000000), while the other sequenced isolates have two copies (Accession numbers CP001131 and CP000251) [52]. Based on the growth rate similarities, it is likely that clades C and D also contain populations with two rRNA genes but further analyses is needed to confirm this assumption. Thus, while the presence of *A. dehalogenans* in a clone library may provide data about the possibilities for metabolic function, culturing and microcosm data are needed for definitive conclusions.

Population genetics studies have been useful for assessing strain variability among pathogenic strains but more studies are needed to determine the metabolic consequences of strain variability in free-living microorganisms. 16S rRNA gene sequence-based technologies have been used to implicate *A. dehalogenans* in nitrogen, carbon, and metal cycling at the Oak Ridge IFC site [12,18,27,28], but the data presented here indicate that 16S rRNA gene sequence data must be interpreted carefully since strain variability can result in substantial changes in metabolism. Previous analyses of the *Anaeromyxobacter* community involved in uranium bioremediation at the Oak Ridge IFC site suggest that different species may be responsible for uranium reduction in different areas [29]. Hence, the ecological role of the particular *Anaeromyxobacter* spp. present may change from area to area. Studies of variability in the genetics of closely-related

strains involved in bioremediation help to enhance the current methods for population monitoring and allow more meaningful interpretations of culture-independent data.

6.6 Description of *Anaeromyxobacter dehalogenans*. The original species definition of *A. dehalogenans* characterized five different strains as facultative aerobes with anaerobic utilization of low concentrations of nitrate, fumarate, 2-chlorophenol, 2-bromophenol, and 2,6-dichlorophenol [21]. Subsequent work expanded the range of respiratory electron acceptors to include metals and radionuclides [22,25]. Surface motility has since been characterized in strain 2CP-C [44] as well as oxygen tolerance and utilization [53]. Presence in soil, sediments, peat bogs and aquifer materials [12,13,14,15,16,17,18,19,20] suggest that *A. dehalogenans* strains are adapted to variable redox and no representatives have been identified in saltwater, suggesting that they are restricted to freshwater environments. The current study demonstrates that respiratory functions are variable among *A. dehalogenans* strains, including dechlorination, which is not present in all characterized strains. Thus, *A. dehalogenans* is thought to be a microaerophilic metal-reducing organism with changing additional anaerobic respiratory functions that allow strains to adapt to specific environmental conditions like those found in agricultural soils and contaminated aquifers.

6.7 Acknowledgements

This research was supported by the Environmental Remediation Science Division (ERSD), Biological and Environmental Research (BER), U.S. Department of Energy and by NSF IGERT (Grant No. DGE 0114400) and NSF GK-12 (Grant No. 0338261) fellowships to S.H.T. E.P.-C. also acknowledges partial support through an NSF IGERT

fellowship and is recipient of an NSF graduate research fellowship. We thank Joel Kostka and Denise Akob for soil, DNA, and enrichment samples from Oak Ridge IFC Area 1.

6.8 References

1. Holtfreter S, Grumann D, Schmudde M, Nguyen HTT, Eichler P, et al. (2007) Clonal distribution of superantigen genes in clinical *Staphylococcus aureus* isolates. Journal of Clinical Microbiology 45: 2669-2680.

2. Mathema B, Kurepina N, Fallows D, Kreiswirth BN (2008) Lessons from molecular epidemiology and comparative genomics. Seminars in Respiratory and Critical Care Medicine 29: 467-480.

3. Mahenthiralingam E, Baldwin A, Dowson CG (2008) *Burkholderia cepacia* complex bacteria: opportunistic pathogens with important natural biology. Journal of Applied Microbiology 104: 1539-1551.

4. Selander RK, Beltran P, Smith NH, Helmuth R, Rubin FA, et al. (1990) Evolutionary Genetic Relationships of Clones of *Salmonella* Serovars That Cause Human Typhoid and Other Enteric Fevers. Infection and Immunity 58: 2262-2275.

5. Yang HH, Vinopal RT, Grasso D, Smets BF (2004) High diversity among environmental *Escherichia coli* isolates from a bovine feedlot. Applied and Environmental Microbiology 70: 1528-1536.

6. Wertheim HFL, Melles DC, Vos MC, van Leeuwen W, van Belkum A, et al. (2005) The role of nasal carriage in Staphylococcus aureus infections. Lancet Infectious Diseases 5: 751-762.

7. Melles DC, Gorkink RFJ, Boelens HAM, Snijders SV, Peeters JK, et al. (2004) Natural population dynamics and expansion of pathogenic clones of *Staphylococcus aureus*. Journal of Clinical Investigation 114: 1732-1740.

8. Oda Y, Wanders W, Huisman LA, Meijer WG, Gottschal JC, et al. (2002) Genotypic and phenotypic diversity within species of purple nonsulfur bacteria isolated from aquatic sediments. Applied and Environmental Microbiology 68: 3467-3477.

9. Oda Y, Star B, Huisman LA, Gottschal JC, Forney LJ (2003) Biogeography of the purple nonsulfur bacterium *Rhodopseudomonas palustris*. Applied and Environmental Microbiology 69: 5186-5191.

10. Ritalahti KM, Amos BK, Sung Y, Wu QZ, Koenigsberg SS, et al. (2006) Quantitative PCR targeting 16S rRNA and reductive dehalogenase genes simultaneously monitors multiple *Dehalococcoides* strains. Applied and Environmental Microbiology 72: 2765-2774.

11. Roh Y, Liu SV, Li G, Huang H, Phelps TJ, et al. (2002) Isolation and characterization of metal-reducing *Thermoanaerobacter* strains from deep subsurface environments of the Piceance Basin, Colorado. Applied and Environmental Microbiology 68: 6013-6020.

12. North NN, Dollhopf SL, Petrie L, Istok JD, Balkwill DL, et al. (2004) Change in bacterial community structure during *in situ* biostimulation of subsurface sediment cocontaminated with uranium and nitrate. Applied and Environmental Microbiology 70: 4911-4920.

13. Treude N, Rosencrantz D, Liesack W, Schnell S (2003) Strain FAc12, a dissimilatory iron-reducing member of the *Anaeromyxobacter* subgroup of Myxococcales. FEMS Microbiology Ecology 44: 261-269.

14. Brofft JE, McArthur JV, Shimkets LJ (2002) Recovery of novel bacterial diversity from a forested wetland impacted by reject coal. Environmental Microbiology 4: 764-769.

15. Borneman J, Triplett EW (1997) Molecular microbial diversity in soils from eastern Amazonia: Evidence for unusual microorganisms and microbial population shifts associated with deforestation. Applied and Environmental Microbiology 63: 2647-2653.

16. Coates JD, Cole KA, Chakraborty R, O'Connor SM, Achenbach LA (2002) Diversity and ubiquity of bacteria capable of utilizing humic substances as electron donors for anaerobic respiration. Applied and Environmental Microbiology 68: 2445-2452.

17. Lueders T, Wagner B, Claus P, Friedrich MW (2004) Stable isotope probing of rRNA and DNA reveals a dynamic methylotroph community and trophic interactions with fungi and protozoa in oxic rice field soil. Environmental Microbiology 6: 60-72.

18. Petrie L, North NN, Dollhopf SL, Balkwill DL, Kostka JE (2003) Enumeration and characterization of iron(III)-reducing microbial communities from acidic subsurface sediments contaminated with uranium(VI). Applied and Environmental Microbiology 69: 7467-7479.

19. Michalsen MM, Peacock AD, Spain AM, Smithgal AN, White DC, et al. (2007) Changes in microbial community composition and geochemistry during uranium and technetium bioimmobilization. Applied and Environmental Microbiology 73: 5885-5896.

20. Dedysh SN, Pankratov TA, Belova SE, Kulichevskaya IS, Liesack W (2006) Phylogenetic Analysis and *In Situ* Identification of Bacteria Community

Composition in an Acidic Sphagnum Peat Bog. Applied and Environmental Microbiology 72: 2110-2117.

21. Sanford RA, Cole JR, Tiedje JM (2002) Characterization and description of *Anaeromyxobacter dehalogenans* gen. nov., sp. nov., an aryl halorespiring facultative anaerobic Myxobacterium. Applied and Environmental Microbiology 68: 893-900.

22. He Q, Sanford RA (2003) Characterization of Fe(III) reduction by chlororespiring *Anaeromyxobacter dehalogenans*. Applied and Environmental Microbiology 69: 2712-2718.

23. Cole JR, Cascarelli AL, Mohn WW, Tiedje JM (1994) Isolation and characterization of a novel bacterium growing via reductive dehalogenation of 2-chlorophenol. Applied and Environmental Microbiology 60: 3536-3542.

24. Sanford RA, Wu Q, Sung Y, Thomas SH, Amos BK, et al. (2007) Hexavalent uranium supports growth of *Anaeromyxobacter dehalogenans* and *Geobacter* spp. with lower than predicted biomass yields. Environmental Microbiology 9: 2885-2893.

25. Wu Q, Sanford RA, Löffler FE (2006) Uranium(VI) reduction by *Anaeromyxobacter dehalogenans* strain 2CP-C. Applied and Environmental Microbiology 72: 3608-3614.

26. Marshall MJ, Dohnalkova AC, Kennedy DW, Plymale AE, Thomas SH, et al. (2008) Electron donor-dependent radionuclide reduction and nanoparticle formation by *Anaeromyxobacter dehalogenans* strain 2CP-C. Environmental Microbiology doi: 10.1111/j.1462-2920.2008.01795.x.

27. Cardenas E, Wu WM, Leigh MB, Carley J, Carrol lS, et al. (2008) Microbial communities in contaminated sediments, associated with bioremediation of uranium to submicromolar levels. Applied and Environmental Microbiology 74: 3718-3729.

28. Thomas SH, Pavlekovic M, Lee N, Marshall MJ, Kennedy DW, et al. (2006) Diversification in the subsurface: Strain variation of *Anaeromyxobacter dehalogenans* in a uranium and nitrate-contaminated subsurface environment. 11th International Symposium on Microbial Ecology.

29. Thomas SH, Crespo EP, Jardine PM, Sanford RA, Löffler FE Strain-specific probing reveals strain diversity and heterogeneous distribution of U(VI)-reducing *Anaeromyxobacter* spp. in a subsurface environment with nonuniform flow. Applied and Environmental Microbiology In review.

30. Löffler FE, Sanford RA, Tiedje JM (1996) Initial characterization of a reductive dehalogenase from *Desulfitobacterium chlororespirans* Co23. Applied and Environmental Microbiology 62: 3809-3813.

31. Löffler FE, Sanford RA, Ritalahti KM (2005) Enrichment, cultivation, and detection of reductively dechlorinating bacteria. Methods in Enzymology. pp. 77-111.

32. Löffler FE, Sun Q, Li JR, Tiedje JM (2000) 16S rRNA gene-based detection of tetrachloroethene-dechlorinating *Desulfuromonas* and *Dehalococcoides* species. Applied and Environmental Microbiology 66: 1369-1374.

33. Ritalahti KM, Loffler FE (2004) Populations implicated in anaerobic reductive dechlorination of 1,2-dichloropropane in highly enriched bacterial communities. Applied and Environmental Microbiology 70: 4088-4095.

34. Altschul SF, Gish W, Miller W, Myers EW, Lipman DJ (1990) Basic Local Alignment Search Tool. Journal of Molecular Biology 215: 403-410.

35. Tamura K, Dudley J, Nei M, Kumar S (2007) MEGA4: Molecular Evolutionary Genetics Analysis (MEGA) software version 4.0 Molecular Biology and Evolution 24: 1596-1599.

36. Debruijn FJ (1992) Use of Repetitive (Repetitive Extragenic Palindromic and Enterobacterial Repetitive Intergeneric Consensus) Sequences and the Polymerase Chain-Reaction to Fingerprint the Genomes of Rhizobium-Meliloti Isolates and Other Soil Bacteria. Applied and Environmental Microbiology 58: 2180-2187.

37. Rodríguez-Castaño GP (2008) Sequence diversity and expression of novel bacterial nitrous oxide reductase (*nosZ*) genes in tropical environments. Mayagüez, Puerto Rico University of Puerto Rico.

38. Burnes BS, Mulberry MJ, DiChristina TJ (1998) Design and application of two rapid screening techniques for isolation of Mn(IV) reduction-deficient mutants of *Shewanella putrefaciens*. Applied and Environmental Microbiology 64: 2716-2720.

39. Stookey LL (1970) Ferrozine - a New Spectrophotometric Reagent for Iron. Analytical Chemistry 42: 779-&.

40. Lovley DR, Phillips EJP (1986) Organic-Matter Mineralization with Reduction of Ferric Iron in Anaerobic Sediments. Applied and Environmental Microbiology 51: 683-689.

41. Lovley DR, Phillips EJP (1988) Novel Mode of Microbial Energy-Metabolism - Organic-Carbon Oxidation Coupled to Dissimilatory Reduction of Iron or Manganese. Applied and Environmental Microbiology 54: 1472-1480.

42. He JZ, Ritalahti KM, Aiello MR, Löffler FE (2003) Complete detoxification of vinyl chloride by an anaerobic enrichment culture and identification of the reductively dechlorinating population as a *Dehalococcoides* species. Applied and Environmental Microbiology 69: 996-1003.

43. Krajmalnik-Brown R (2005) Genetic identification of reductive dehalogenase genes in *Dehalococcoides*. Georgia Institute of Technology School of Civil and Environmental Engineering Doctor of Philosophy.

44. Thomas SH, Wagner RD, Arakaki AK, Skolnick J, Kirby JR, et al. (2008) The mosaic genome of *Anaeromyxobacter dehalogenans* strain 2CP-C suggests an aerobic common ancestor to the delta-Proteobacteria. PLoS ONE 3: e2103.

45. Whitaker RJ (2006) Allopatric origins of microbial species. Philosophical Transactions of the Royal Society B-Biological Sciences 361: 1975-1984.

46. Smit S, Widmann J, Knight R (2007) Evolutionary rates vary among rRNA structural elements. Nucleic Acids Research 35: 3339-3354.

47. Van de Peer Y, Chapelle S, De Wachter R (1996) A quantitative map of nucleotide substitution rates in bacterial rRNA. Nucleic Acids Research 24: 3381-3391.

48. Chakravorty S, Helb D, Burday M, Connell N, Alland D (2007) A detailed analysis of 16S ribosomal RNA gene segments for the diagnosis of pathogenic bacteria. Journal of Microbiological Methods 69: 330-339.

49. Konstantinidis KT, Tiedje JM (2005) Towards a genome-based taxonomy for prokaryotes. Journal of Bacteriology 187: 6258-6264.

50. Konstantinidis KT, Tiedje JM (2005) Genomic insights that advance the species definition for prokaryotes. Proceedings of the National Academy of Sciences of the United States of America 102: 2567-2572.

51. Marshall MJ, Dohnalkova AC, Kennedy DW, Plymale AE, Thomas SH, et al. (2008) Electron donor-dependent radionuclide reduction and nanoparticle formation by *Anaeromyxobacter dehalogenans* strain 2CP-C. Environmental Microbiology 11: 534-543.

52. Nomura M, Morgan EA (1977) Genetics of bacterial ribosomes. Annual Review of Genetics 11: 297-347.

53. Thomas SH, Sanford RA, Leigh MB, Cardenas E, Löffler FE *Anaeromyxobacter dehalogenans* microaerophilism reveals a novel niche among metal reducing organisms at an uranium-contaminated field site. In Preparation.

CHAPTER 7: Conclusions and recommendations

In order to clarify the relevance of *Anaeromyxobacter* populations for uranium-contaminated environments and to help to define separate niches for divergent metal- and radionuclide-reducing organisms; genetic, physiological, and environmental distribution studies were conducted using computational and molecular methods and anaerobic culturing techniques. Analyses of strain variability in an environmentally relevant organism, potentially involved in many biogeochemical cycles globally, advance the science of biogeography and microbial population genetics.

Comparative genomics, which combined comparisons to organisms within the same phylogenetic context with comparisons to organisms bearing metabolic similarities, provided insight into the evolution of respiratory versatility in *A. dehalogenans*. Aerobic and predatory enzymes on the *A. dehalogenans* genome confirm its phylogenetic classification as a myxobacterium, as well as genes for surface motility. Both surface motility and aerobic metabolism were confirmed experimentally. In order to further elucidate the metabolic and physiological implications of the *A. dehalogenans* genome, comparisons were made to *G. sulfurreducens*, another sequenced metal-reducing organism. Commonalities between *A. dehalogenans* and *G. sulfurreducens* include genes encoding large multi-heme cytochromes and flagellar motility. Flagellar motility was not observed experimentally.

In addition to genomic evidence for aerobic respiration, *Anaeromyxobacter* spp. are prolific at the Oak Ridge IFC, though groundwater conditions are frequently aerobic. In order to elucidate the oxygen-reduction and respiratory capacity of *A. dehalogenans*, strain 2CP-C was utilized in experiments with variable oxygen partial pressure (pO_2).

Careful measurements of substrate utilization and biomass accumulation revealed that *A. dehalogenans* strain 2CP-C is capable of aerobic respiration at low to medium pO_2 but, interestingly, as pO_2 increased, growth rate and biomass production per decreased. This is the first description of a metabolic shift which changes f_e with changing substrate concentration, in response to toxicity. Additionally, samples were analyzed from an oxygen intrusion study in the Oak Ridge IFC subsurface. Data suggest that *Anaeromyxobacter* spp. increase in response to oxygen intrusion *in situ*.

Several novel strains of *A. dehalogenans* were isolated from uranium-contaminated environments. The Fe-reducing Oak Ridge IFC strains were compared to strains derived from agricultural soil and river sediment. Five clades of *A. dehalogenans* strains were defined. In order to evaluate the distribution of the *Anaeromyxobacter* strains in uranium-contaminated environments, and to elucidate the strains potentially relevant for *in situ* uranium reduction, a multiplex qPCR technique was utilized to analyze site materials from the Oak Ridge IFC. Probes and primers were designed targeting the highly variable V3 region, and drawing on minor groove binding technologyto distinguish among strains which bear > 99% 16S rRNA gene sequence similarity. Microcosms and sediments from Oak Ridge IFC treatment Area 1 confirmed the *in situ* presence of *A. dehalogenans* strains that had been isolated from those sediments but clone library sequences were needed to identify the dominant strain in Oak Ridge IFC treatment Area 3.

The research presented here elucidated the ecophysiology of a relevant uranium-reducing microorganism and explored its distribution and activity at a uranium-contaminated site. Future directions include further efforts toward niche description,

additional isolation of strains from uranium-contaminated environments, and exploration of the implications of these findings on uranium reduction. Specific research activities to follow up on the research presented here include:

- The genome of *A. dehalogenans* was compared to only one metal-reducing organism and was done based on the highest gene sequence similarity. Subtractive analysis of genomes belonging to many metal-reducing organisms, based on enzyme functional analysis may identify a core group of genes which are necessary for dissimilatory metal reduction.
- Experiments elucidating *A. dehalogenans* ecophysiology were primarily conducted in pure culture. Competition studies using other metal-reducing organisms may help to elucidate the environmental factors that determine the composition of metal-reducing communities.
- Few strain variability studies have been conducted. Strain variability may play a role in *Geobacter* and *Shewanella* ecology, as well as in *Anaeromyxobacter* ecology. The relevant variations among strains may elucidate differences that help to describe the evolution of extant metal reduction.
- The work presented here implies that aerobic metabolism by metal reducing organisms may play a role in stabilizing reduced uranium in the environment. Microcosm and *in situ* studies may be conducted to verify this assertion.

APPENDIX A: LABORATORY PROTOCOLS

A.1 Preparation of poorly crystalline Fe (III) oxyhydroxide: α-FeOOH

Protocol

1. Dissolve $FeCl_3 \times 6H_2O$ in Filtered E-pure water to provide 0.4 M concentration (108 g/L).
2. Stir continually while SLOWLY adjusting the pH to 7.0 dropwise with 10 N NaOH. This will require about 75 mL NaOH/L $FeCl_3$ solution. I use a peristaltic pump set to a very slow rotation (0.016-0.16 mL/min). It is extremely important not to let the pH go beyond 7.0 even momentarily during the neutralization step because this will result in a Fe (III) oxide that is less available for microbial reduction. The pH will stay around 1.5-1.6 for a long time. When it starts to move above 2.0 SLOW DOWN. The pH changes from 2.0 to 7.0 VERY QUICKLY. Stop the titration at pH 5.0-6.0 and stir for an hour to give pH time to go up. Then add base very very slowly using very tiny drops and stirring for a long long time in between. This stage is EXTREMELY sensitive.
3. Continue to stir for at least 30 min once pH 7.0 is reached and recheck pH to be sure it has stabilized at pH 7.0.
4. To remove dissolved chloride, centrifuge the suspension at 5000 rpm for 15 min 3-6 times. Discard supernatant, resuspend Fe (III) oxide (tapped with spanner). Make the same final volume that you use to make 0.4 M initially (e.g, dissolve 10.8128 g of $FeCl_3 \times 6H_2O$ in 100 ml, after centrifuge make sure you make all suspension in 100 ml volume).
5. Fill ~50 ml FeOOH solution to sterile 160 ml bottle and microwave until it boils for a few seconds
6. Make anoxic FeOOH solution using hungate

FYI

Hematite is dehydrated forms of FeOOH
Most Lovley's paper, they use Iron Oxide but this is the same with FeOOH
To form β-FeOOH (akaganeite), use 0.5 M $FeCl_3 \times 6H_2O$

Cf.

Iron Oxide from Kelly Nevin U of Mass, Amherst (Lovley group)

Add 108 g of Fe(III)Cl heptahydrate to 1L of water
Slowly pH to 7 with 10N NaOH (~75 mL) will take a few hours
allow to stir one hour, will be very thick
spin at 5K for 20 min
pour off supernatant
wash 6 times with milliQ water (resuspend and respin)
resuspend in ~150 mL of water
do a 1:2500 diution and measure iron with hydroxylamine

By Youlboong Sung Jan-2004
Revised by Sara Thomas September 2006

A.2 Preparation of ferric citrate

Protocol
Here is the recipe to make up 0.5 M Iron Citrate.

24.48 g Ferric Citrate / 200 ml water

SLOWLY pH adjust to 7.0 or 7.2 or whatever your final media pH will be. This process will take time and it is better to take time with it. After adding the FeCit to the water, let it stir for a minute with a big strong magnet and then add 1 ml 10 N NaOH, Then check the pH and slowly add NaOH and try to keep the pH in the 6.5 to 7.0 range for a while, then walk away and let it stir for 10-15 minutes and again adjust the pH to where you need it and walk away for 5 minutes, repeat this process until it seems as though the pH is stable.

pH 7.0 will require ~10-20 ml 10N NaOH.

It should be a very dark (almost black looking) solution, but it should also be a clear solution with no solid particles visible (or very little precipitate on the bottom).

You can autoclave or filter sterilize.

I normally use it in 5 mM to 50 mM concentrations for culture growth (1 ml per 100 ml of 0.5 M FeCit is 5 mM). At 5 mM there is a nice medium orange color which can be checked for reduction visually or you can measure Fe 2+ using the ferrozine method, but you have to do it immediately because there is no good way to preserve the sample so that the Fe 2+ does not oxidize. You will also need to do a time zero point because FeCit is actually a mix of Fe3+ and Fe2+.
Also, try to use as little reductant as possible. I think DTT is ok, but use it in as little concentration as you feel is safe because it might be able to reduce the Fe, I am not sure of that yet. I am sure sulfide and other things will reduce or beind to the Fe at high concentrations.

(from Mike Dollhopf)

A.3 Ferrozine method for determination of Fe(II) and total Fe

Stookey, 1970, Analytical Chem, 42:779-781
Kostka and Luther, 1994, Geochem.Cosmochem.Acta. 58:1701-1710
Kostka et al., 1996, Env.Sci.Tech, 44:522-529

Solutions
0.5 M HCL solution
Ferrozine buffer: 0.2g ferrozine, 12.0g HEPES buffer in 1L water
Hydroxylamine ferrozine buffer: 1g hydroxylamine in 100 ml Ferrozine buffer

Protocol

HCl extractable Fe(II). This is the total Fe(II) and the most common Fe(II) analysis.

1:10 dilution of the sample is extracted in 0.5 M HCl , Incubate for 30 minutes (the dilution may vary, but must be 1:10 or more dilute). I usually do a 100 µl sample to 900 µl HCl dilution.

1:10 or greater dilution into Ferrozine buffer (this is where the dilution to attain a proper absorbance range is usually made, but you should use the same dilution for all samples and standards). Again I usually take 100 µl of HCL extract and dilute into 900 µl buffer. Incubate for 10-15 minutes.

Measure absorbance @ 562 nm. If there are visible particulates, you can filter the sample before measuring absorbance.

Total Iron

Use the same method as above, but use the Hydroxylamine buffer instead of the plain Ferrozine buffer.

Dissolved Fe(II)

Filter the sample through a 0.2 µm filter before the HCl extraction

Standards

Standards can be prepared by first making a 100mM Fe(II) stock using throughly N2 purged water with a small HCl addition (100 µl per 100ml of concentrated HCl). Ferrous Ammonium Sulfate is a common Fe(II) source.

Standards are then made using stopper closed vials containing a known amount of water. These must be thoroughly N2 purged also prior to the addition of stock Fe(II)

A.4 Low Melting Agarose Dilution Series Protocol

1) Prepare anaerobic media (about 200mL)
2) Prepare twenty 20mL vials (10 for liquid media dilution, 10 for agarose dilution)
3) Add 0.5 %Sea Plaque Low Melting Agarose to 10 vials (0.05g in 10 ml total culture volume)
4) Dispense Liquid media:

Inside glove box

- Bring media, pipette, septa, and vials (make sure all agar containing vials are wrapped with plastic wrap to prevent blow off inside cycle chamber)
- Dispense 9 ml of media to all 20 vials (10 for liquid media dilution vials, 10 for agarose containing vials and close with gray septa
- All vials will automatically contain some hydrogen (2-5%)

At Hungate station

- Flush headspace of both prepared media bottle and vials while dispensing 9 ml media to each vial
- DO NOT BLOW INTO VIALS CONTAINING AGAROSE!
- Add a couple of drops of media to make agar wet before flushing
- After inserting N_2-line, add remaining liquid media for a total of 9mL
- Flush for ~30 seconds
- Close with septum, holding N_2-line out of the vial while you add the first couple of drops to the next vial.
- Repeat for each of the 10 vials containing LMA

5) Crimp all vials
6) Autoclave
7) Let liquid media cool. Solid media should be held in a 45°C water bath until immediately before inoculation.
8) INOCULATION: This is performed in the clean hood. Begin by making an ice bath. All agar-containing vials should remain in the water bath.
    a. Add Wolin vitamins and e^- acceptor/donor to liquid dilution media
    b. Perform serial dilutions from 1ml culture
        i. You will have 10^{-1}, 10^{-2}, 10^{-3}, …10^{-10}
        ii. Change needle and syringe every 3 transfers
    c. Remove 1-3 agarose containing vials from water bath and move quickly to the clean hood to add Wolin and e^- acceptor/donor. (if you want to use chlorinated compound as an electron acceptor, add after procedure h.)
    d. Replace vials in water bath, repeat this step for all 10 agarose- containing vials
    e. Retrieve one vial of LMA from bath
    f. Inoculate 1 ml from most (10^{-10}) to least (10^{-1}) diluted liquid culture. Inject very gently and roll gently to mix inoculum throughout the agarose-containing culture. Use new needle and syringe every 3 transfers.
        i. Each solid culture will be 10^{-1} the dilution of the liquid cultures giving you 10^{-11}, 10^{-10}, 10^{-9}…10^{-2}
    g. Submerge agar culture in ice bath right side up.

h. After solidification (~10 minutes) incubate upside down.
i. Make clear labels for all vials

Sara Henry and Youlboong Sung
Jan-2004

A.5 Preparation of uranyl carbonate

1. Sterilize 60 mL serum bottles and black butyl rubber stoppers.
2. Prepare 30 mM bicarbonate buffer (pH 8.4) in serum bottle(s).
    a. $NaHCO_3$ FW=84.01. 30 mM = 0.25 g / 100 mL
3. Purge buffer with nitrogen gas at Hungate station.
4. Meanwhile, weigh out uranyl acetate to make 30 mM uranyl stock.
    a. U(VI) FW=424.15. 30 mM = 0.51 g / 40 mL
5. Go into glove box to dissolve/dispense into bottles. Take sterile syringe/filters.
6. In glove box, add uranyl acetate solid to bicarbonate buffer in non-sterile container, add stopper, and shake until dissolved.
7. Put stock into syringe and push through filter into sterile serum bottle.
8. Stopper bottle(s) and remove from glove box.
9. Crimp bottles and over-pressurize with filter-sterilized nitrogen.

A.6 Preparation of Ferric NTA

According to http://water.usgs.gov/nrp/microbiology/link_feiiimedia.html:

1. Dissolve 1.64 g sodium bicarbonate in 100 mL
2. Add 2.56 g Nitrilotiacetic acid (trisodium salt)
3. Add 2.70 g $FeCl_3$
4. Purge the mixture with N_2/CO_2 (80:20)
5. Filter sterilize into a sterile, sealed, anaerobic 100mL bottle. (Final pH is ~7)
6. Overpressurize using filter-sterilized N_2/CO_2 (80:20)
7. Add from sterile stock into sterilized media (1:9).

It is possible to make a 1M stock for use with larger volumes of media. (But difficult to filter). Some organisms will not tolerate more than 10mM Fe(III)-NTA.

APPENDIX B: Enrichment and isolation efforts

B.1 Sources of cultures. Sediment slurry samples were collected in December 2006 from five sites along the Columbia River in areas that have been impacted by the Department of Energy Hanford site near Richland, WA. Samples were shipped on ice to the Löffler laboratory by Matthew Marshall and Jim Fredrickson (Pacific Northwest National Laboratory).

Duplicate 15 x 10 cm peat core samples were collected in September 2006 from two different elevations (i.e., hummock, hollow) in Mer Bleue Conservation Area east of Ottawa in eastern Ontario, Canada. The cores were taken by cutting into the peat, starting at the water table, which was at a depth of about 40 cm in the hummock and 15 cm in the hollow. The top of the water table is subject to periodic draining and, hence, variable oxygen concentrations. About 1 kg of peat was included in each core. Water chemistry data for the Mer Bleue Conservation Area has been reported previously [2,4]. The pH for samples included in this study is estimated at 4.0, while Fe^{3+} is expected to be between 0 and 5 μmol/L and Fe^{2+} between 10 and 40 μmol/L. NO_3 in Mer Bleue peat cores is expected to be about 0.1 mg/L, NH_4 about 0.6 mg/L, and H_2S about 1-2 μmol/L. Dissolved organic carbon has been estimated at about 4-7 μmol/L.

B.2 Microcosms, enrichment, and isolation. In all cases, microcosms were established inside an anoxic chamber (Coy Manufacturing, Ann Arbor, MI) filled with a mixture of 97% (vol/vol) N_2 and 3% (vol/vol) H_2. Microcosms which demonstrated reduction of electron acceptor were sequentially transferred to 60-mL vials containing mineral salts medium amended with acetate. Microcosms and each set of enrichment

cultures were each sampled with a 25-gauge, 7/8-inch needle and 1 mL syringe (BD, Franklin Lakes, NJ) for organic acids, iron, and qPCR analyses. Specific culturing approaches and enrichment strategies were different for Columbia River sediments and Peat Bog core samples due to differences in source material and, thus, expected physiological differences among microbial populations. Culturing approaches are described below.

Homogenized Columbia River sediment slurry (2 mL) was transferred to 20-mL vials and 9 mL of reduced mineral salts medium [5] was added to each vial. All of the vials were amended with 5 mM lactate and sealed with black butyl rubber stoppers. Upon removal from the anoxic chamber, two vials from each of the five sampling sites were amended with a single electron acceptor. Electron acceptors utilized for enrichment included ferric citrate (5 mM) and amorphous ferric oxyhydroxide (FeOOH, 4 mM) [as well as perchloroethene (PCE), carbon tetrachloride, and nitrous oxide which demonstrated no activity]. Columbia River microcosms which demonstrated reduction of electron acceptor were sequentially transferred to 60-mL vials containing mineral salts medium amended with acetate. Microcosms and the first transfer of each set of enrichment cultures were each sampled with a 25-gauge, 7/8-inch needle and 1 mL syringe (BD, Franklin Lakes, NJ) after 7 days of incubation at room temperature. After sediment-free iron-reducing cultures were obtained, further enrichment was achieved by preparing dilution-to-extinction series in 20-mL vials containing 10 mL of mineral salts medium amended with 5 mM acetate and 5 mM ferric citrate or 10 mM fumarate. Pure cultures were obtained from dilution-to-extinction soft agar cultures (0.5% wt/vol low-melting-point agarose) prepared in 10 mL of bicarbonate-buffered mineral salts medium

amended with 5 mM acetate and 10 mM fumarate. All vials were incubated in the inverted position. Red colonies were picked using a 21-gauge, 2-inch needle and 1 mL syringe, since they are indicative of *Anaeromyxobacter* spp. [6]. After picking, colonies were resuspended in mineral salts medium and cultures were monitored for Fe-reduction activity. Aerobic plating was used, in addition to anaerobic methods, to achieve pure culture in Columbia River enrichments. Plates were made using tryptic soy broth (TSB) and 1.5% agar. A serial dilution was generated from previously anoxic culture and 100 µL of each dilution was spread on plates and incubated at room temperature. Colonies were picked, resuspended in mineral salts medium, and injected into stoppered 60-mL bottles containing reduced medium. Cultures were monitored for iron-reduction activity.

About 10 g of peat bog material was added to each of 18 autoclaved 160-mL serum bottles and covered by pouring 100 mL of sterile medium into the bottle. Due to the low ionic strength of source materials, Peat Bog microcosms were established using 1/10 and 1/50 dilutions of the typical mineral salts medium amended with 3 mM acetate [5]. For Peat Bog microcosms, pH of 5.5 (mimicking *in situ* conditions) was achieved using 5 mM bicarbonate buffered medium bubbled with CO_2. Bottles were capped with autoclaved black butyl rubber stoppers and crimp caps and incubated in the dark at room temperature without shaking. One of two sources of 1 mM ferric iron (ferric citrate or amorphous FeOOH) were provided as acceptor, for medium of each ionic strength (1/10 or 1/50 diluted salts). Triplicate no-acceptor cultures were also established for medium of each ionic strength.

B.3 Primer design. Specific PCR primers targeting conserved regions of the 16S rRNA gene of *Shewanella* spp. were designed based on nearly complete 16S rRNA gene

sequences available in GenBank. The 16S rRNA gene sequences were aligned using the MegAlign program of the Lasergene software package (DNA Star Inc., Madison, Wisconsin). The forward primer She112F was selected based on a region of the 16S rRNA gene specific to *Shewanella* spp. and BLAST analysis against the NCBI non-redundant database suggested primer specificity (Table 7.1). The reverse primer She220R is the reverse complement of She211f designed by Todorova et al. [7]. The expected size of the She112F/She220R amplicons is 108 bp. Probes and primers for were applied as described for quantification of total Eubacteria [8], *Geobacteraceae* [9], and *Anaeromyxobacter* [10] (Table 7.1).

B.4 DNA extraction, qPCR analysis, and PCR amplification of 16S rRNA genes. DNA was extracted from 10 mL Columbia River sediment slurry using the MoBio PowerSoil™ DNA Isolation Kit (MoBio Laboratories, Inc.). Resulting DNA sample concentrations ranged from 10 to 120 ng/μL. DNA was extracted from 1 mL of each microcosm or enrichment culture (Columbia River and Peat Bog cultures) using InstaGene Matrix (Bio-Rad Laboratories, Hercules, CA).

Table B.1. Primer pairs for qPCR analysis.

Target Group	qPCR Chemistry	Primer/Probe Name	Sequence	Ref.
Anaeromyxobacter spp.	SYBR Green	60F 461R	5'-CGA GAA AGC CCG CAA GGG T-3' 5'-ATT CGT CCC TCG CGA CAG T-3'	(2)
Anaeromyxobacter spp.	SYBR Green	Ade399 Fwd Ade466 Rev	5'-GCA ACG CCG CGT GTG T-3' 5'-TCC CTC GCG ACA GTG CTT-3'	(4)
Geobacteraceae	SYBR Green	Geo564F Geo840R	5'-AAGCGTTGTTCGGAWTTAT-3' 5'-GGCACTGCAGGGGTCAATA-3'	(1)
Shewanella spp.	SYBR Green	She 120F She 220R	5'-GCCTAGGGATCTGCCCAGTCG-3' 5'-CTAGGTTCATCCAATCGCG-3'	(5)
Eubacteria	TaqMan	Bac1055YF Bac1392R Bac1115Probe	5'-ATGGYTGTCGTCAGCT-3' 5'-ACGGGCGGTGTGTAC-3' 5'-FAM-CAACGAGCGCAACCC-TAMRA-3'	(3)

B.5 Quantitative real-time PCR. Quantitative real-time PCR (qPCR) approaches used both TaqMan and SYBR Green detection chemistries. For SYBR Green, qPCR twofold concentrated master mix (Applied Biosystems, Foster City, CA) and 300 nM primers were combined in sterile, nuclease-free water prior to addition of DNA template. The optimal probe and primer concentrations were determined experimentally by using the protocol provided with the master mix. Aliquots (18 μL) of the reaction mix were dispensed into an Applied Biosystems MicroAmp™ Fast Optical 96-Well Reaction Plate held on ice. Template DNA (2μL) was added to each well and the entire plate was sealed with an Applied Biosystems Optical Adhesive Cover. Standard curves were generated using tenfold diluted plasmid DNA (pCR®2.1-TOPO) containing a single 16S rRNA gene fragment from *Shewanella oneidensis* strain MR-1, *Geobacter lovleyi* strain SZ, or *Anaeromyxobacter dehalogenans* strain 2CP-C. The spectrofluorimetric thermal cycler (Applied Biosystems 7500 Real-Time PCR System) was used to detect SYBR Green fluorescence. The PCR temperature program was as follows: 2 min at 50ºC, 10 min at 95 ºC followed by 40 cycles of 15 sec and 95 ºC and 1 min at 60 ºC. Melting curve analysis was performed with the default settings of the ABI software from 67 ºC to 95 ºC following the completion of each qPCR. TaqMan reactions to quantify total bacteria were performed as described previously [8,10].

B.6 16S rRNA gene sequencing and phylogenetic analysis. Genomic DNA was obtained from fumarate-grown cultures in order to minimize inhibitory compounds (i.e., solids, NTA). Individual genomic DNA was extracted with a QIAamp DNA mini kit (QIAGEN, Santa Clarita, CA). 16S rRNA genes were PCR amplified using a universal bacterial primer pair (8F and 1525R) and 50 ng of genomic DNA as the template and

sequenced as described previously [11,12]. Related 16S rRNA gene sequences from cultured organisms and environmental clones were identified by BLAST analysis and obtained from GenBank. Distance matrices, bootstrap values and phylogenetic trees were generated following sequence alignment using the MEGA software program [13].

B.7 Characterization of substrate utilization and growth conditions. Three different Fe(III) species were utilized for enrichment and characterization of isolates. FeOOH, Fe citrate, and FeNTA were synthesized as described previously (Appendix A). Each substrate has a different advantage since FeOOH is insoluble, Fe citrate is soluble and widely accessible to microorganisms, and FeNTA is soluble but does not carry a fermentable substrate as its complexing agent. The ferrozine assay (Appendix A) was used to confirm Fe(III) reduction to Fe(II). Standard curves were generated using Ammonium ferrous sulfate. Organic acids were quantified using a Waters 1525 high performance liquid chromatography system equipped with an Aminex® HPX-87H ion exclusion column and connected to a Waters 2487 dual wavelength absorbance detector [14].

B.8 Columbia river enrichments and isolate CR2-9

B.8.1 qPCR Analysis. Three known genera of metal-reducing organisms were quantified in order to determine the genus which would be most relevant to metal reduction in Columbia River sediments. Interestingly, all three of the 16S rRNA gene sequences queried via qPCR analysis were present in DNA extracted from Columbia River sediment slurries (Figure 7.2; Table 7.2). In four out of five Columbia River sediment samples, mean 16S rRNA gene sequences of *Anaeromyxobacter* spp. were

higher than either *Geobacteraceae* or *Shewanellae* under conditions tested, ranging from $2.1 \times 10^4 \pm 1.8 \times 10^4$ to $5.1 \times 10^5 \pm 3.4 \times 10^5$ 16S rRNA gene copies per mL sediment slurry. Inferred *Geobacteraceae* cell titers were close to those of *Anaeromyxobacter* spp., with a range between $1.3 \times 10^4 \pm 7 \times 10^3$ and $4 \times 10^5 \pm 2 \times 10^5$ 16S rRNA gene copies per mL sediment slurry. *Shewanellae* were the least abundant of the metal-reducing bacteria tested, ranging from values detectable but below the quantitation limit ($\leq 3.8 \times 10^2 \pm 9 \times 10^1$ 16S rRNA gene copies per mL sediment) to $3 \times 10^4 \pm 1 \times 10^4$ 16S rRNA gene copies per mL sediment (Figure 7.2).

In order to determine the success of *Anaeromyxobacter* enrichment strategies, qPCR was utilized to examine iron-enriched cultures derived from Columbia River microcosms. The ferric citrate enrichment derived from sampling site 2 (Figure 7.1) was targeted for further isolation attempts due to high *Anaeromyxobacter* spp. values determined by qPCR (Figure 7.3).

B.8.2 Enrichment and Isolation. Microcosms established with Columbia River sediment amended with acetate and H_2 precipitated FeS (insoluble, black) from both Fe citrate (soluble, yellow) and FeOOH (insoluble, orange) after 2 weeks. A sediment-free culture was obtained after sequential transfers (1% [vol/vol]) to completely synthetic, defined bicarbonate-buffered medium, with acetate as the electron donor and Fe citrate as the electron acceptor. A single red colony, picked from the 10^{-9} dilution of Fe-reducing culture, continued to reduce Fe substrates when re-inoculated to anaerobic culture, including Fe-NTA. 16S rRNA gene sequence analysis indicated that the dominant organisms in these Fe-reducing cultures were most closely related to *Enterobacter*

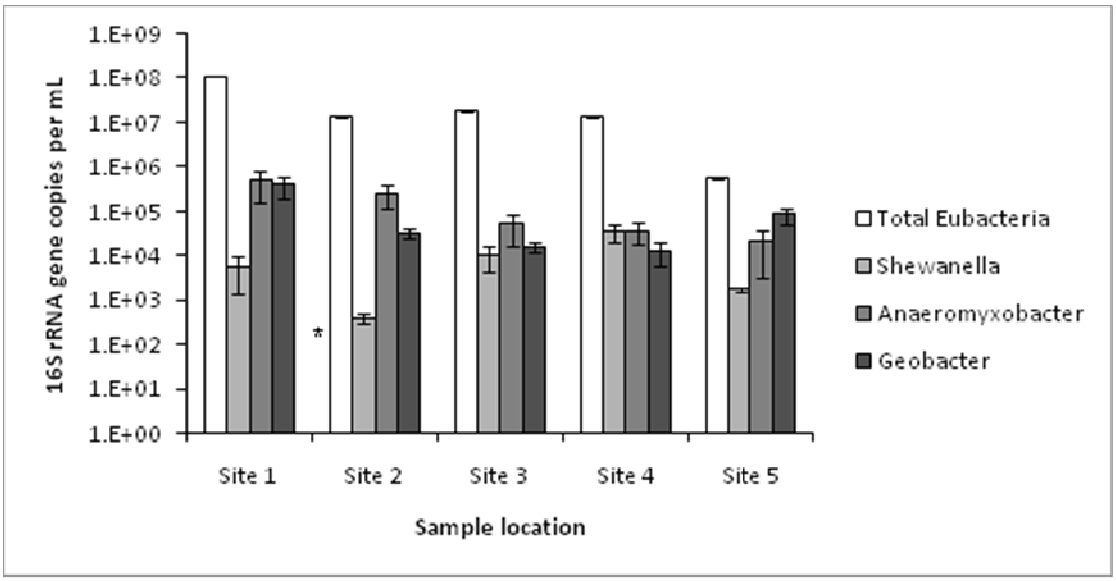

Figure B.1. qPCR analysis of three known metal-reducing genera in Columbia River sediments.
*Shewanellae cell titers were detectable but below the quantitation limit ($\leq 3.8 \times 10^2 \pm 9 \times 10^1$ 16S rRNA gene copies per mL sediment) in sediment slurries from Site 2.

Table B.2. Percent of total bacteria in Columbia River sediment slurry samples of three metal-reducing genera.

	Percent (%) of Total Eubacteria		
	Shewanellae	***Anaeromyxobacter***	***Geobacteraceae***
Site 1	0.005 ± 0.004	0.5 ± 0.3	0.4 ± 0.2
Site 2	0.003 ± 0.002	2.0 ± 1.9	0.25 ± 0.21
Site 3	0.06 ± 0.04	0.3 ± 0.2	0.09 ± 0.03
Site 4	0.3 ± 0.1	0.3 ± 0.2	0.09 ± 0.06
Site 5	0.31 ± 0.07	3.8 ± 3.3	15 ± 7

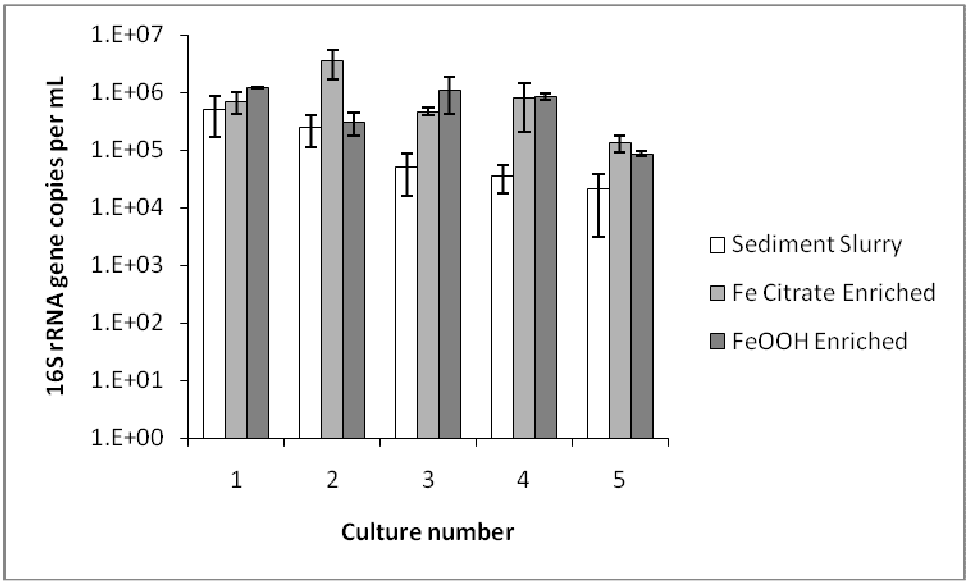

Figure B.2. qPCR analysis of three Anaeromyxobacter spp. in Columbia River enrichment cultures.

amnigenus p412 (Figure 7.4). Hence, aerobic plating was used for isolation. Plating on aerobic TSB resulted in visible colonies after 1-2 days of incubation at room temperature. However, colonies re-suspended from agar plates demonstrated no Fe-reduction, although precipitate formed in Fe-citrate cultures. The culture fermented citrate completely in Fe-citrate cultures but iron was not reduced.

Isolation of Fe-reducing organisms, designated strains CR2-9a and CR2-9b, were achieved through sequential transfers of the culture derived from agarose suspensions with Fe-NTA as electron acceptor, followed by a dilution-to-extinction series in semisolid medium. Since NTA is not a fermentable substrate, transfers with Fe-NTA selected against the *Enterobacter/Pantoea*-like strain which had existed in co-culture with strains CR2-9a and CR2-9b when grown with Fe citrate. Ellipsoid, reddish colonies developed down to the 10^{-9} dilution with fumarate as the electron acceptor. Isolated colonies grown with fumarate were transferred to liquid medium with Fe-NTA, and Fe(III)-to-Fe(II) reduction activity was recovered during incubation at room temperature.

B.8.3 Phylogeny and taxonomy of Columbia River isolates. Analysis of 16S rRNA gene sequences from strains CR2-9a and CR2-9b indicated an affiliation with the species *Anaeromyxobacter dehalogenans* (Figure 7.4). The closest relatives, *A. dehalogenans* strains 2CP-C, 2CP-3, and 2CP-5 (identical 16S rRNA genes) share 99.69-99.93% similar 16S rRNA gene sequences with the CR2-9a and CR2-9b isolates, with 1300/1304 and 1496/1497 identities, respectively. Phenotypic characteristics and their novel area of origination support classifying isolates CR2-9a and CR2-9b as distinct strains within the *Anaeromyxobacter dehalogenans* cluster since this is the first known isolate of *A. dehalogenans* which reduces iron complexed with NTA.

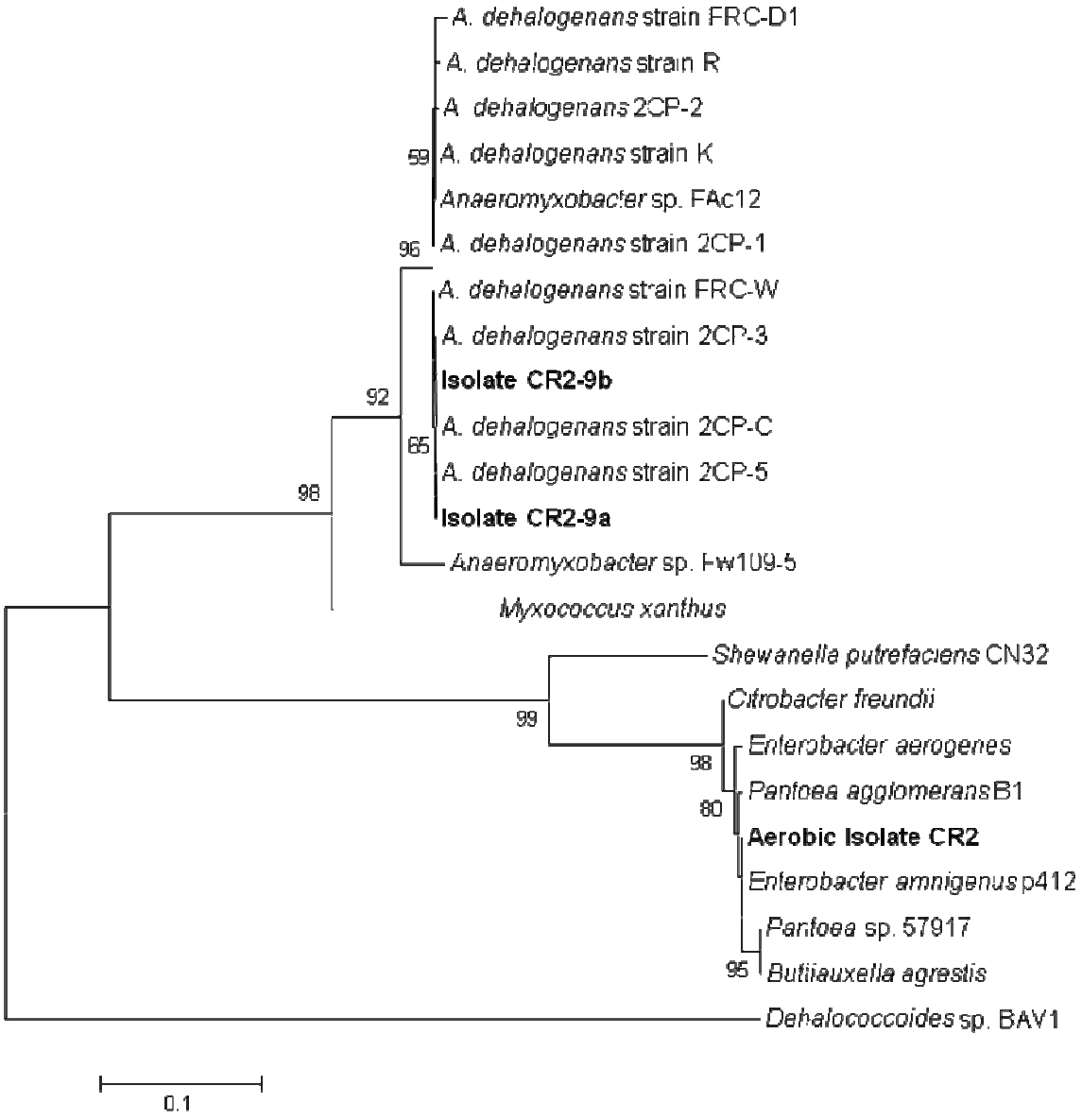

Figure B.3. Phylogenetic tree of 16S rRNA gene sequences of organisms isolated from Columbia River sediments. Outgroup is Dehalococcoides sp. BAV1. Bootstrap values are based on 500 replicates and values less than 50 have been removed.

The aerobic isolate derived from a metal-reducing co-culture with *Anaeromyxobacter* is most closely related to organisms in the genus *Pantoea*/*Enterobacter*. A metal-reducing *Pantoea* has been isolated previously [15]. In addition, sequences belonging to organisms from the genus *Pantoea* have been identified in clone libraries that were derived from Oak Ridge IFC site materials and Fe(III)-reducing enrichment cultures [16,17]. In fact, in Oak Ridge IFC site Area 1 enrichments established with glycerol as a carbon source, 86% of cloned sequences fell within the *Geobacteraceae* family with the remaining sequences all closely related to *Pantoea agglomerans*. Clearly, *Pantoea* spp. are affiliated with Fe(III)-reducing communities. However, since aerobic colonies were unable to reduce iron when re-introduced to anaerobic cultures, it is unlikely that the Columbia River *Pantoea* isolate presented here is capable of metal-reduction. Metal-reduction in Columbia River enrichments is thus attributed to the anaerobic component of the culture (strain CR2-9) that was derived from the same mixed colony picked from agarose suspensions.

B.9 Peat bog enrichments

Iron reduction was observed, either visually or analytically (Figure 7.5), in Peat Bog microcosms after 30 days. Electron donor depletion was difficult to measure, particularly in citrate-containing enrichments. Acetate appeared quite high in citrate enrichments and, since citrate is not detected, fermentation of citrate to acetate is likely. *Anaeromyxobacter*-like 16S rRNA gene sequences were quantified at $1.5 \times 10^6 \pm 9.6 \times 10^5$ (enrichment A) to $2.3 \times 10^6 \pm 1.6 \times 10^6$ (enrichment C) 16S rRNA genes per mL culture in enrichments after four 1% transfers in acetate/Fe(II) medium (about 250 days after initiation of microcosms). Total bacteria in the same culture ranged from 10^8 to 10^{10}

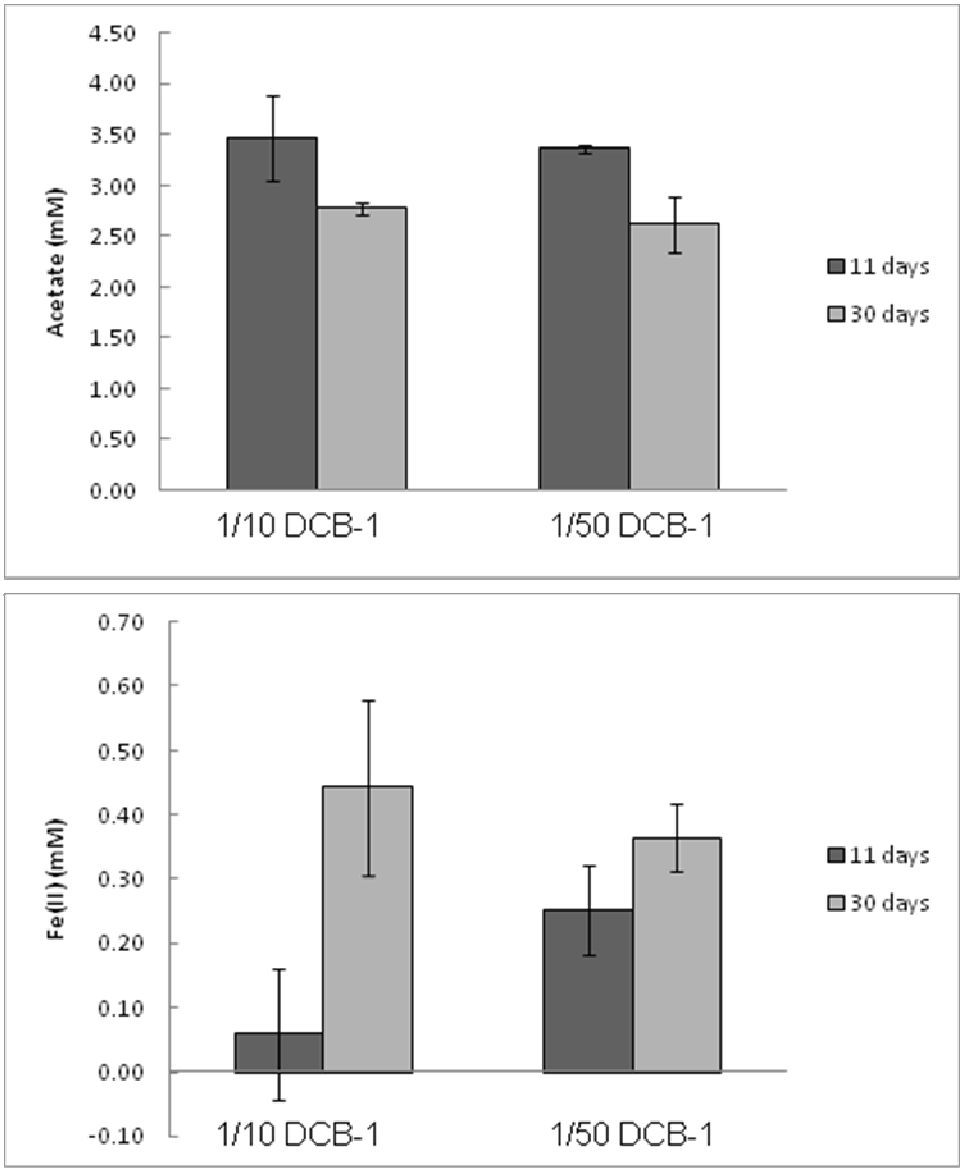

Figure B.4. Substrate analyses for FeOOH enrichments derived from Peat Bog core samples. (A) Electron donor utilization. (B) Fe(II) Accumulation.

16S rRNA gene copies per mL culture, indicating that *Anaeromyxobacter* is not the dominant strain in peat bog enrichments at the most recent analysis. When enrichments were transferred to acetate/fumarate medium, *Anaeromyxobacter* sequences were no longer detected. *Geobacter* spp. were not detected in peat bog enrichment cultures. Peat bog enrichments continue to be promising sources of new *Anaeromyxobacter* isolates and other DMRBs.

B.10 References

1. Riley RG, Zachara JM, Wobber FJ (1992) Chemical Contaminants on DOE Lands and Selection of Contaminant Mixtures for Subsurface Science Research. DOE/ER-0547T, US Department of Energy, Washington, DC.

2. Blodau C, Roehm CL, Moore TR (2002) Iron, sulfur, and dissolved carbon dynamics in a northern peatland. Archiv Fur Hydrobiologie 154: 561-583.

3. Moore T, Blodau C, Turunen J, Roulet N, Richard PJH (2005) Patterns of nitrogen and sulfur accumulation and retention in ombrotrophic bogs, eastern Canada. Global Change Biology 11: 356-367.

4. Blodau C, Basiliko N, Mayer B, Moore TR (2006) The fate of experimentally deposited nitrogen in mesocosms from two Canadian peatlands. Science of the Total Environment 364: 215-228.

5. Löffler FE, Sanford RA, Tiedje JM (1996) Initial characterization of a reductive dehalogenase from *Desulfitobacterium chlororespirans* Co23. Applied and Environmental Microbiology 62: 3809-3813.

6. Sanford RA, Cole JR, Tiedje JM (2002) Characterization and description of *Anaeromyxobacter dehalogenans* gen. nov., sp. nov., an aryl halorespiring facultative anaerobic Myxobacterium. Applied and Environmental Microbiology 68: 893-900.

7. Todorova SG, Costello AM (2006) Design of *Shewanella*-specific 16S rRNA primers and application to analysis of *Shewanella* in a minerotrophic wetland. Environmental Microbiology 8: 426–432.

8. Ritalahti KM, Amos BK, Sung Y, Wu QZ, Koenigsberg SS, et al. (2006) Quantitative PCR targeting 16S rRNA and reductive dehalogenase genes simultaneously monitors multiple *Dehalococcoides* strains. Applied and Environmental Microbiology 72: 2765-2774.

9. Cummings DE, Snoeyenbos-West OL, Newby DT, Niggemyer AM, Lovley DR, et al. (2003) Diversity of *Geobacteraceae* species inhabiting metal-polluted freshwater lake sediments ascertained by 16S rDNA analyses. Microbial Ecology 46: 257-269.

10. Thomas SH, Padilla-Crespo E, Jardine PM, Sanford RA, Löffler FE Strain-specific probing reveals strain diversity and heterogeneous distribution of U(VI)-reducing Anaeromyxobacter spp. in a subsurface environment with nonuniform flow. Submitted.

11. Löffler FE, Sun Q, Li JR, Tiedje JM (2000) 16S rRNA gene-based detection of tetrachloroethene-dechlorinating *Desulfuromonas* and *Dehalococcoides* species. Applied and Environmental Microbiology 66: 1369-1374.

12. Ritalahti KM, Loffler FE (2004) Populations implicated in anaerobic reductive dechlorination of 1,2-dichloropropane in highly enriched bacterial communities. Applied and Environmental Microbiology 70: 4088-4095.

13. Tamura K, Dudley J, Nei M, Kumar S (2007) MEGA4: Molecular Evolutionary Genetics Analysis (MEGA) software version 4.0 Molecular Biology and Evolution 24: 1596-1599.

14. He JZ, Ritalahti KM, Aiello MR, Löffler FE (2003) Complete detoxification of vinyl chloride by an anaerobic enrichment culture and identification of the reductively dechlorinating population as a *Dehalococcoides* species. Applied and Environmental Microbiology 69: 996-1003.

15. Francis CA, Obraztsova AY, Tebo BM (2000) Dissimilatory Metal Reduction by the Facultative Anaerobe *Pantoea agglomerans* SP1. Applied and Environmental Microbiology 66: 543-548.

16. North NN, Dollhopf SL, Petrie L, Istok JD, Balkwill DL, et al. (2004) Change in bacterial community structure during in situ biostimulation of subsurface sediment cocontaminated with uranium and nitrate. Applied and Environmental Microbiology 70: 4911-4920.

17. Petrie L, North NN, Dollhopf SL, Balkwill DL, Kostka JE (2003) Enumeration and characterization of iron(III)-reducing microbial communities from acidic subsurface sediments contaminated with uranium(VI). Applied and Environmental Microbiology 69: 7467-7479.